

Charles University in Prague
Faculty of Pharmacy in Hradec Králové
Department of Inorganic and Organic Chemistry

Mgr. Eva Vavříková

**DESIGN OF NEW ANTIBACTERIAL
ACTIVE MOLECULES**

Doctoral Thesis

Hradec Králové

July 2010

Univerzita Karlova v Praze
Farmaceutická fakulta v Hradec Králové
Katedra anorganické a organické chemie

Mgr. Eva Vavříková

**DESIGN NOVÝCH ANTIBAKTERIÁLNĚ
AKTIVNÍCH MOLEKUL**

Dizertační práce

Hradec Králové

Červenec 2010

Acknowledgements

Firstly, I would like to thank my supervisor Assoc. Professor RNDr. Jarmila Vinšová, Ph.D. for her valuable advices and constant support throughout my study.

Secondly, I would like to thank my family for their encouragement during these years.

I would especially like to thank the research group of Assoc. Prof. Vinšová for friendly atmosphere and pleasant environment in the lab.

My special thanks to Professor Dr. Slovenko Polanc from Faculty of Chemistry and Chemical Technology in Ljubljana for his co-supervisory and fruitful collaboration during my stay in Slovenia.

I am very thankful to Assoc. Prof. Szilvia Bösze, PhD. from Eötvös Lóránd University, Research Group of Peptide Chemistry, Hungarian Academy of Science in Budapest for allowing me to make some biological measurement in their laboratory and for contributive and helpful co-operation.

Thanks to all my friends and colleagues at the Department of organic and inorganic chemistry.

I would like thanks for the significant financial support of Grant agency (GAUK 76807/2007, FRVŠ 92/2009 G6) and specific university research grant (SVV-2010-261-001).

Finally, my thanks are also given to Assoc. Prof. PharmDr. Jiří Kuneš, Ph.D. for NMR spectra measurement, Mrs. Iva Vencovská who measured of IR spectra and Mrs. Dana Cardová who recorded UV spectra.

The work described in this thesis is my own original research that I have worked up by myself. All literature and other sources, which I used, are listed in the references and work properly cited.

Abstract

The main task of the thesis was a design and synthesis of new potential antimycobacterial active molecules. Presently, the appearance of MDR-TB strains is alarming and the development of new therapeutical agents is necessary. The work is divided into two parts; first one is related to aminopolysaccharide chitosan and its connection with appropriate antimycobacterial drugs or dyes, second part is concerned with modifications of current antituberculotics.

Due to the structure and physico-chemical properties, chitosan has been found as an interesting drug carrier in biomedical chemistry. It is used in drug delivery system with control release of the drug in the target cells or tissues. The component of the first part of the thesis was to review molecular modelling of chitosan, especially its usage as a prodrug or carrier in a field of antibacterial, antitumor and antioxidant activity. Derivatives of chitosan linked with the first or second line antituberculotics were prepared for the purpose of decreasing hepatotoxicity of used drugs. Their antimycobacterial activity against *M. tbc.*, *M. avium* and *M. kansasii* was 125 µg/mL for all strains. Unexpectedly, *O*-carboxymethyl chitosan as an intermediate showed better MIC against *M. tbc.* and *M. avium*. It means that biological activity of chitosan derivatives is based on the inhibitory effect of linked antituberculotics and the degree of deacetylation of chitosan. All tested derivatives did not exhibit cytotoxic effect on PBMC and Hep G2 cells. Chitosan was able to reduce cytotoxicity of antimycobacterial drugs.

Chitosan has been found as a convenient carrier for photoantimicrobial activity in wound healing treatment. Nanofibres of chitosan with rose bengal were prepared, but finally, they had not a sufficient quality for following usage.

Fluorescent labelled chitosan was used for uptake studies by flow cytometer assay. Phagocytosis of chitosan was observed on macrophages and monocytes which are hosts for mycobacteria during a long-time treatment and latent TB.

The aim of the second part of the thesis was a connection of two active molecules by an easily released methine bridge. In first series, PAS, CPX, NFX, PZA were linked with fluorinated hydrazones of benzoic acid. They have shown higher activity against MDR-TB (0.5 µg/mL) than isoniazid and exhibited no decomposition at neutral pH and also in rat plasma more than 48 hours which could improve the bioavailability to target site.

Second series of hydrazones included isoniazid connected with electron acceptor substituted anilines through the methine bridge showed similar biological activity as the parent compound INH. Lipophilicity of these derivatives is higher than INH, it signifies more effective transport of the molecule through cellular membranes.

Abstrakt

Hlavním cílem práce je design a syntéza nových antimykobakteriálně aktivních molekul. Vzhledem k vzrůstajícímu výskytu MDR-TB kmenů je v současné době výzkum nových léčiv proti tuberkulóze velmi aktuální. Předkládaná dizertační práce je rozdělena do dvou částí; první se týká aminopolysacharidu chitosanu a možnosti jeho spojení s vhodnými antituberkulotiky a barvivou, druhá část se zabývá obměnami molekul současných antituberkulotik.

Díky jedinečné struktuře a fyzikálně-chemickým vlastnostem má chitosan široké uplatnění. Používá se jako nosič léčiv s kontrolovaným uvolněním aktivní látky v místě účinku. Úvodní část práce podává přehled molekulárních modifikací chitosanu jako proléčiva s antibakteriální, protinádorovou a antioxidační aktivitou. Za účelem snížení hepatotoxicity antimykobakteriálních léčiv byly připraveny deriváty chitosanu ve spojení s antituberkulotiky první nebo druhé řady. Látky vykazovaly MIC 125 $\mu\text{g/mL}$ proti *M. tbc.*, *M. avium* a *M. kansasii*, což je v souladu s procentem navázaného léčiva. Je zajímavé, že meziprodukt *O*-karboxymethyl chitosan prokázal dokonce lepší MIC proti *M. tbc.* a *M. avium*. Z toho lze usuzovat, že biologická aktivita derivátů chitosanu je založena jak na inhibičním efektu použitých antituberkulotik tak na stupni deacetylce chitosanu. U všech testovaných derivátů se neprojevil cytotoxický účinek na PBMC krevní buňky ani na Hep G2 buněčnou linii, což znamená, že chitosan má schopnost snížit cytotoxicitu antimykobakteriálních léčiv.

Chitosan byl dále použit jako vhodný nosič fotosenzitivních barviv za účelem fotoantibakteriální aktivity při léčbě a hojení ran. Bohužel kvalita nanovláken vyrobených z derivátu chitosanu a bengálské červeně nebyla dostačující pro další použití.

Pomocí průtokového cytometru byla provedena studie fagocytózy fluorescenčně značeného chitosanu. Podle očekávání projevily fagocytární aktivitu imunitní buňky monocyty a makrofágy, které hrají důležitou roli jako hostitelé mykobakterií při latentní tuberkulóze.

Druhá část práce byla zaměřena na spojení dvou aktivních molekul snadno hydrolyzovatelným methinovým můstkem. Jako první série byly syntetizovány fluorované hydrazony benzoové kyseliny v kombinaci s PAS, CPX, NFX, PZA. Jejich antimykobakteriální aktivita proti MDR-TB (MIC = 0.5 $\mu\text{g/mL}$) byla vyšší než u INH. Pomocí studie měření stability bylo zjištěno, že ani po 48 hodinách při neutrálním pH a také v krevní plasmě získané z potkanů nedocházelo k rozkladu látek. Tento fakt může být využit pro zlepšení biodostupnosti léčiva v místě účinku.

Druhá série hydrazonů, které obsahovaly isoniazid spojený s aniliny s elektron-akceptorními substituenty přes methinový můstek, vykazovala podobnou biologickou aktivitu jako standard INH. Lipofilita těchto derivátů je vyšší než u isoniazidu, což by mohlo vést k efektivnějšímu transportu aktivní molekuly přes buněčné membrány.

List of publications

This thesis is based on the following publications, which are referred to in the text by the Roman numerals I. – V.

I. Recent advances in drugs and prodrugs design of chitosan

Jarmila Vinšová, **Eva Vavříková**

Current Pharmaceutical Design. 2008, vol 14, p 1311-1326. (IF₂₀₀₈ 4.399)

II. Chitosan a jeho farmaceutické aplikace

Eva Vavříková, Jarmila Vinšová

Chemické Listy. 2009, vol 103, p 56-65. (IF₂₀₀₉ 0.717)

III. Cytotoxicity decreasing effect and antimycobacterial activity of chitosan conjugated with antituberculous drugs

Eva Vavříková, Jana Mandíková, František Trejtnar, Kata Horváti, Szilvia Bösze, Jiřina Stolaříková, Jarmila Vinšová

Carbohydrate Polymer. 2010, under revision

IV. New fluorinated hydrazones as potential antitubercular drugs

Eva Vavříková, Slovenko Polanc, Marijan Kočevar, Kata Horváti, Szilvia Bösze, Jiřina Stolaříková, Kateřina Vávrová, Jarmila Vinšová

Bioorganic Medicinal Chemistry. 2010, under revision

V. Salicylanilide carbamates: Promising antitubercular agents active against multidrug resistant *Mycobacterium tuberculosis* strains.

Juana Monreal Ferriz, Kateřina Vávrová, Filip Kunc, Aleš Imramovský, Jiřina Stolaříková, **Eva Vavříková**, Jarmila Vinšová

Bioorganic Medicinal Chemistry. 2010, vol 18, p 1054-1061. (IF₂₀₀₉ 2.822)

Content

List of Abbreviations	1
1. Introduction	3
1.1. Tuberculosis	3
1.2. Treatment of tuberculosis	4
2. Aim of the thesis	5
3. Chitosan as a prodrug	6
3.1. General information (Paper I)	6
3.2. Pharmaceutical applications of chitosan (Paper II)	8
3.3. Antimicrobial activity	9
3.3.1. Mechanism of activity	9
3.3.2. Antibacterial activity of chitosan derivatives	11
3.4. Antitumor activity	19
3.4.1. Antitumor activity of nano-size particles	19
3.4.2. Antitumor activity of chitosan derivatives	20
3.5. Antioxidant activity	25
3.5.1. Reactive oxygen species and chitosan as antioxidant	25
3.5.2. Antioxidant activity of chitosan derivatives	27
3.5. Chitosan connected with antituberculosics	29
3.5.1. Chitosan conjugated with INH, PZA and ETA (Paper III)	29
3.5.2. Chitosan conjugated with second line antituberculosic drugs	32
3.5.2.1. Determination of degree of deacetylation	37
3.5.2.2. Determination of molecular weight	37
3.5.2.3. Determination of degree of substitution	38
3.5.2.4. Experimental part	39

3.6. Chitosan connected with dyes	46
3.6.1. Chitosan connected with photosensitizer dyes	46
3.6.1.1. Experimental part	49
3.6.2. Chitosan connected with fluorescein isothiocyanate	50
3.6.2.1. Experimental part	53
3.7. Conclusion of first part of thesis	54
4. Modifications of antimycobacterial drugs	56
4.1. Introduction	56
4.2. Derivatives of fluorine-containing hydrazones (Paper IV)	56
4.3. Derivatives of isoniazid	61
4.3.1 Experimental part	67
4.3.1.1. General	67
4.3.1.2. Biological evaluation	67
4.3.1.3. Lipophilicity determination	69
4.3.2. Experimental results	70
4.4. Conclusion of second part of thesis	80
5. Biological testing of prepared compounds	81
5.1. Cytotoxicity determination by MTT assay	81
5.1.1. Antituberculosis drug-induced hepatotoxicity	82
5.1.2. Immune response to <i>Mycobacterium tuberculosis</i>	83
5.2. Flow cytometry	83
6. References	85
7. Appendix	

List of Abbreviations

AK	Amikacin
CPX	Ciprofloxacin
CS	D-cycloserin
DD	Degree of deacetylation
DOX	Doxorubicin
DS	Degree of substitution
DTX	Docetaxel
<i>E. coli</i>	Escherichia coli
EDC	<i>N</i> -(3-dimethylaminopropyl)- <i>N'</i> -ethylcarbodiimide
EMB	Ethambutol
ENX	Enoxacin
EPR effect	Enhanced permeability and retention effect
FITC	Fluorescein isothiocyanate
G ⁺ /G ⁻	Grampositive/Gramnegative bacteria
GluN	D-glucosamine
GluNAc	<i>N</i> -acetyl-D-glucosamine
HIV	Human immunodeficiency virus
INH	Isoniazid
LMX	Lomefloxacin
LVX	Levofloxacin
MIC	Minimum inhibition concentration
MDR-TB	Multidrug-resistant tuberculosis
<i>M. tbc.</i>	<i>Mycobacterium tuberculosis</i>
MW	Molecular weight
NFX	Norfloxacin
NSCS	<i>N</i> -succinyl chitosan

OCMC	<i>O</i> -carboxymethyl chitosan
OFX	Ofloxacin
PAS	<i>para</i> -Amino-salicylic acid
PDT	Photodynamic therapy
PTX	Paclitaxel
PZA	Pyrazinamide
RB	Rose bengal
RMP	Rifampin
ROS	Reactive oxygen species
<i>S. aureus</i>	Staphylococcus aureus
SI	Selectivity index
SPX	Sparfloxacin
STM	Streptomycin
TEM	Transmission electron microscopy
TPPC4	<i>meso</i> -Tetra(4-carboxyphenyl)porphin
TB	Tuberculosis
WHO	World Health Organization
XDR-TB	Extensively drug-resistant tuberculosis

1. Introduction

1.1. Tuberculosis

Tuberculosis is an infectious disease caused by *Mycobacterium tuberculosis* which has uncommon properties: slow-growing, hydrophobic cell wall, acid, alkali and alcohol resistance. Cell wall of *M. tbc.* is primarily composed of mycolic acids and allows the bacillus to lie dormant for many years. The important property of mycobacteria is intracellular parasitisation in macrophages of its host and the elimination of their immune system response. Other key features of *M. tuberculosis* are an easy transmission from person to person by aerosol and the low infective dose.¹ The consequence of these extreme abilities is long duration of TB treatment, development of resistant strains for some antituberculous drugs and latent infection. Due to these remarkable factors, TB still remains as one of the most dangerous and lethal diseases in the world. In 2008, there were estimated 9.4 million new TB cases and 1.3 million deaths.² One-third of the world's population is primarily infected by TB and becomes potential reservoir of *Mycobacterium tuberculosis* for future. Globally, the resurgence of tuberculosis has been attributed to the emergence of drug-resistant strains of TB, the prevalence of co-infection with HIV and social and economic developments affecting access to medical care.³

Twenty years ago, MDR-TB strain was defined as resistant to at least two most effective anti-TB drugs, isoniazid and rifampicin (first-line anti-TB drugs). XDR-TB was identified as resistant to any fluoroquinolone and to at least one of three injectable drugs capreomycin, kanamycin or amikacin that are called second-line anti-TB drugs, in addition to MDR-TB. Nontuberculous mycobacterial strains are opportunistic pathogens with a relative resistance to a wide range of antibiotics.⁴ The mechanism of resistance to the first-line anti-TB drugs has been linked to mutations at least 10 genes⁵, followed by drug inactivating enzymes or decreased level of activating enzymes. 13.3 % of all TB cases showed resistance to INH and 5.3 % of all TB cases were indicated as MDR-TB resistant.⁶ Currently, research of novel MDR potential drugs is intended to main goals of the development of new agents with two months or less duration therapy, development of new mechanism of potential agent⁷ without cross-resistance and improvement of treatment of latent TB.⁸

1.2. Treatment of tuberculosis

Recommended contemporary chemotherapy of TB is an administration of a mixture at least five anti-TB drugs. INH, PZA, RMP and EMB present first-line agents, they are followed by injectable drugs as STM, kanamycin, amikacin, capreomycin and tuberactinomycin A, B, N, O.⁹ Fluoroquinolones (OFX, LFX, moxifloxacin and CPX) are considered as a supported treatment because of their accumulation in *M. tbc.* and good affinity for the target enzyme.¹⁰ Long-duration treatment is necessary for complete sterilization of *M. tbc.* Ordinary cure contains two months of administration of INH, PZA, RMP and EMB, or INH, PZA, RMP and STM. Next four months INH, RIF and/or PZA should be administered due to existence of latent infection. Negative effect of long TB treatment leads to the serious side effects, mainly drug-induced hepatotoxicity with prevalence of TB patients which is 3 – 11 %.^{11,12}

Alarming statistical data of the TB incidence were main motive for the establishment of rules supporting TB eradication. The first project of WHO named DOTS (directly observed treatment, short course) which was associated legislation, case detection, standardized treatment and monitoring of TB.¹³ In 2006, WHO decided to increase the support for TB treatment and established a document named The Stop TB Strategy. Its goal is dramatically reduce global burden of TB by 2015 by the basic rules which increase quality of diagnosis and treatment, protect vulnerable population from TB and support development of new tool for TB treatment.^{14,15}

2. Aim of the thesis

Submitted work is divided into two parts; first one is related to aminopolysaccharide chitosan and its connection with appropriate antimycobacterial drugs or dyes, second part is concerned with modifications of antimycobacterial drugs with methine bridge. The overall aim of this thesis was to investigate the synthesis, antimycobacterial evaluation and cytotoxicity determination.

The specific objectives of this study were:

- Literary review of chitosan (Paper I, II).
- The synthesis of chitosan conjugates with antituberculotics or dyes and biological evaluation of the synthesized compounds (Paper III).
- The modification of antimycobacterial drugs by connection of two active molecules through easily released methine bridge, structure activity relationship and biological evaluation of the synthesized compounds (Paper IV).
- Biological studies of prepared compounds

3. Chitosan as a prodrug

3.1. General information (Paper I)

The interest of polymeric materials enhances every year. Chitosan is very attractive compound, its usage involves wide range of pharmaceutical, biomedical, industrial and agricultural fields. Chitosan as a main topic appears in many different scientific articles, the amount of accepted papers increases every year. The popularity of this polysaccharide has started from requested properties which are biocompatibility, biodegradability, lack of toxicity and hypoallergic reaction. The proper utilization depends on many factors that can be changed. Molecule weight (MW), degree of deacetylation (DD), degree of substitution, length and position of a substituent in glucosamine units of chitosan and pH of chitosan solution can play an important role on a final biological activity. Chitosan is a linear polysaccharide, derived from naturally abundant chitin, composed from D-glucosamine and *N*-acetyl-D-glucosamine units bonded by β -1,4-glycosidic linkages. It is a product of alkaline deacetylation of chitin and its structure contains less than 50 % of *N*-acetylglucosamine units. Long chains of chitosan are formed of four crystalline polymorphic forms, three hydrated and one anhydrous.¹⁶ Reactivity of chitosan is done by three types of reactive functional groups, an amino group as well as both primary and secondary hydroxyl groups at the C2, C3 and C6. Numerous useful derivatives for specific application can be synthesized by chemical modifications of these groups. The most frequent chemical modifications include quaternization, acylation, tosylation, Schiff base formation, *O*-carboxymethylation, *N*-carboxyalkylation, *N*-succinylation and graft copolymerization. Original chitosan is insoluble in neutral and alkaline pH conditions. In pH < 7, free amino groups are protonated and the polysaccharide becomes soluble. Chemical modification improves the solubility of chitosan over a wide pH range.

Chitosan and its derivatives possess special properties for use in pharmaceutical and biomedical applications.¹⁷ Chitosan itself has antimicrobial properties and an inhibition effect depends on the concentration, molecular weight and kind of bacteria.¹⁸ Antitumor activity is resulted from a simple change of chemical structure, low molecular weight, water-solubility and degree of deacetylation.¹⁹ Similarly, mainly low molecular weight and degree of deacetylation, have influence on the antioxidant activity.²⁰ Mucoadhesion and absorption-enhancing properties of

chitosan have been utilized for delivery of therapeutic proteins and antigen particularly via mucosal routes to cells, and induction of antibodies after mucosal vaccination (immunoadjuvant effect).^{21,22} Other facility of chitosan is support of vascularization and angiogenesis without secretion of inflammatory cytokines from endothelial cells. Chitosan – alginate membrane is compatible with endothelial cells and has no effect to their activated status.²³ The wound healing has been another emphasis of chitosan–based application. Collagenase activity and the amount of activated fibroblasts which are important in reparations of injured tissues depend on MW and DD.²⁴ Chitosan connected with polyphosphate and silver has exhibited acceleration of blood clotting, platelet adhesion and thrombin generation. The incorporation of silver was also effective in reducing mortality compared to standard treatment.²⁵ Polyelectrolyte complexes are able to reduce the risk of dehydration of wounds and make easy removing of chitosan modulus from the wound surface without damaging the newly regenerated tissue. Chitosan as a cationic polyelectrolyte and γ -poly (glutamic acid) as an anionic polyelectrolyte²⁶ or poly(vinylalcohol)/water-soluble chitosan/glycerol hydrogel²⁷ are novel stripped polyelectrolyte complexes with good mechanical properties potentially applied as a wound dressing materials. Further utilization is in industrial and environmental fields. Due to free amino groups, chitosan and its derivatives have chelating ability to bind heavy and toxic metal ions.²⁸ The great attention is focused on non-viral gene therapy. Nucleic acid-chitosan complexes are studied for their high transfection efficiency and lack of toxicity. MW and stability of complexes are crucial factors for investigation of gene delivery.^{29,30} Chitosan and its nanoparticles have potential to form polyelectrolyte complex with nucleic acids, enhancing cellular uptake and provide effective unpacking of the complexes in the cytoplasmatic compartment. There are two types of the carrying system, DNA or RNA entrapping system which is advantageous for nucleic acid protection.³¹

All these applications are used as various kinds of drug carriers for the controlled release. Common requirements for drug delivery system are optimization of drug application, minimization of the undesirable drug properties and improving of drug efficiency. Other advantages of polymeric molecules are the slow release of effective components as depot forms, the improving of membrane permeability and solubility. Targeting components are able to precisely recognize and specifically interact with receptors on the targeted tissue. Procedure

of the production of drug conjugates is an encapsulation into nano-sized particles that have the ability to reach the target size.³² Release of loading drugs from conjugates can be occurred by diffusion, chemical/environmental stimulation or enzyme-specific stimulation. The facility of drug loading depends on hydrophilicity and/or charges of active drugs and their carriers.³³ Amphiphilic derivatives are prepared for simpler drug release³⁴. Nanomicelles based on glycol chitosan with alkyl chains exhibited higher drug-loading capacity and high drug-loading efficiency.³⁵ Priorities as biocompatibility and sterility explain the utility of chitosan as potential material for various biomedical applications.

3.2. Pharmaceutical applications of chitosan (Paper II)

In both reviews (**Paper I, II**) there are summarized main physical properties important for design of structure and pharmaceutical applications of chitosan in three main fields of medical branches – antimicrobial, antitumor and antioxidant. Chitosan has low solubility in water at pH 7, therefore, it is necessary to proceed chemical modification of its skeleton. The most common chitosan modification which increases water solubility and antimicrobial activity is quarternisation of amino group. Quarternisation by methyl iodide led also to better activity against fungi. *N,N*-Diethyl-*N*-methylchitosan has received attention as an oral drug delivery vehicle. Chitosan-*N*-2-hydroxypropyltrimethylammonium chloride enhances biocidal activity on Grampositive bacteria. Guanidinylated chitosan associates with the cell surface and shows higher antibacterial activity of Gramnegative bacteria. Antitumor activity of chitosan depends on the molecular size, solubility and partial acetylation. *N*-Succinyl chitosan connected with mitomycin C was prepared for the treatment of leukemia P388 and melanom B16. 5-Fluorouracil was conjugated with the partly acetylated *O*-carboxymethyl chitosan through tetrapeptide spacer Gly-Phe-Leu-Gly which ensure specific drug release in tumor tissue. Antioxidant activity of chitosan depends on molecular weight as well as on the degree of deacetylation. Low molecular weight partly deacetylated chitosan is possible to consider as a natural antioxidant. Even if the exact mechanism of activity is unknown, it is assumed that amino group and hydroxyl groups bonded on C2, C3 and C6 position react with unstable free radicals to form more stable macromolecular radicals. Both papers present data collected till 2008. Following chapters 3.3. – 3.6. bring current findings of the last two years.

3.3. Antimicrobial activity

3.3.1. Mechanism of activity

It is known that the chitosan itself has an inhibition effect against bacteria and fungi. However, the exact mechanism of antibacterial activity of chitosan is not yet completely known, several mechanisms that may contribute to the antimicrobial action have been suggested. Process of antibacterial activity is caused by changes in the bacterial membrane permeability, breakdown of the cytoplasmatic membrane barrier or blocking the transport of nutrients, resulting cell lysis.

Generally, the mechanism of inhibition activity differs from MW, DD, the type of bacterium, pH and concentration of active compound connected to chitosan as well as different substituent.

MW: Chitosan with high MW cannot pass through the microbial membrane and hence remains on the cell surface, forms a film which blocks nutrients transport to the microbial cell membrane, while chitosan with low MW can pass through the cell wall. Owing to their small size and being water soluble, polysaccharide can traverse through the microbial membrane and regulate DNA transcription.³⁶ The exposure of chitosan with different MW and concentration was studied on *S. aureus* (G^+) and *E. coli* (G^-). The antibacterial effect on gram positive bacteria was enhanced with the increasing concentration and increasing MW, against gram negative bacteria as the molecular weight decreased the effect was enhanced. The lower MW allows to enter the mycobacterial cell more easily and disturbs the metabolism in the cell. 100 % Inhibition for both strains was reached with 1 % concentration of chitosan.¹⁸

DD: Antibacterial activity enhances with increasing DD of chitosan. It means that the amino group as the active functional group was found to be essential for the antibacterial activity of chitosan.³⁷ The phenomenon might be explicated by different amount of $-NH_2$ groups contained in chitosan polymer. Amino groups can chelate divalent cations³⁸ which stabilize the G^- outer membranes.

Type of bacteria: Chitosan and its derivatives have great influence on cell wall destruction of G^- bacteria (*E. coli*) then to G^+ bacteria (*S. aureus*).^{37,39} The reason is different constitution of their cell wall, consequently, mechanism of the interaction is diverse for G^- and G^+ .

Cell wall of G^- bacteria is made up of a thin membrane of peptidoglycan. An outer cytoplasmic membrane is composed from lipopolysaccharide, lipoprotein and phospholipids stabilized by divalent cations, such as Mg^{2+} and Ca^{2+} . If chitosan is protonated and the carboxyl and phosphate groups of the bacterial surface are anionic, it offers potential sites for electrostatic binding of lower MW chitosan. The cell wall permeability is changed and the osmotic stability is decreased. Complex disrupted the barrier properties of the cytoplasmic membrane, entered to the cell and disturbed the physiological activities of the bacteria or the leakage of enzymes and nucleotides from bacteria. The confirmation of this mechanism was performed by the observation of escaping of enzymes during the treatment of *S. aureus* and *E. coli*. With increasing contact time between the chitosan and both bacterial strains, the leakage of enzymes from the cells increased gradually and the treatment had stronger impact to G^- than to G^+ bacteria. Polymyxin B and EDTA were used for understanding the antibacterial mechanism of chitosan on *E. coli*. Polymyxin B, cationic antibiotic, reacts with anionic phosphate groups in the cell membrane, thereby destroys the cell membrane structure. EDTA chelates Mg^{2+} and Ca^{2+} which are presented in the cell wall and affecting its permeability. The leakage of nucleotides from bacterial cells increased with increasing contact time and concentration of polymyxin B, EDTA and chitosan. The inactivation of *E. coli* by chitosan happened through a two-phase sequential mechanism, affecting the cell wall and the cell membrane.³⁷ Other study consider also with the interaction of chitosan with *E. coli* cell membrane. Chitosan 50 kDa was the most effective in damaging of the integrity of cell membrane, intracellular proteins were almost fully released. The experiment with alizarin red documented that chitosan rapidly increased permeability of cytoplasmic membrane, the presumable mechanism consist in a binding of polycationic molecule of chitosan with the negatively charged *O*-specific oligosaccharide units of lipoproteins of *E. coli* cytoplasmic membrane. It led to the disruption of the integrity of membrane and depletion of the nutrients. Interaction of chitosan with phospholipid membrane was simulated by connection with phosphatidylcholine liposomes. IR spectra demonstrated that there were carbonyl and phosphoryl groups in phosphatidylcholine that participated in the interaction with amino groups of chitosan.³⁶

G⁺ bacterium has cell wall composed mainly from peptidoglycan, which does not allow the formation of a surface layer. Presumable dominant mechanism for G⁺ is based on higher MW chitosan forming a polymer membrane on the surface of the cell which obstructs nutrients entering to the cell.¹⁸ Prodrugs can stop the entering of nutrients to the cell or leak them from the cells which describe principle of the first mechanism. The second mechanism is based on the binding of lower MW (< 5000 kDa) chitosan to DNA and inhibition of mRNA synthesis through penetration to the nuclei and interferes with the synthesis of mRNA and proteins.

3.3.2. Antibacterial activity of chitosan derivatives

Majority of experimental studies have used *E. coli* and *S. aureus* as representative bacterial models.

MW of polymers plays important role in their biological properties. Low molecular weight chitosan (LMWC) products were prepared by chitinase, lysozyme and cellulase. Chitinase was the best choice for producing LMWC (13.5 – 8.5 kDa) and also inhibition of *E. coli* was efficient (50 µg/mL). Compared with it, lysozyme-catalysed LMWC was less soluble due to higher range of MW but more effective against *E. coli* (40 µg/mL). Cellulase-catalysed chitosan has lost its antibacterial activity due to extensive hydrolysis.⁴⁰ Chitosan, carboxymethylated chitosan and chitosan sulfates were connected with 5-chloro-4-hydroxybenzene-1,3-disulfonyl dichloride or 5-chloro-2-hydroxybenzene-1,3-disulfonyl dichloride (Fig. 1).³⁹ All derivatives exhibited roughly the same inhibition effect to five crop-threatening pathogenic fungi (the maximum inhibitory index was 65.98 % to 50.50 %) and *S. aureus*, *Sarcina*, *E. coli* and *Pseudomonas aeruginosa* (31.25 – 249.98 µg/mL). The antibacterial activity of derivatives enhanced with the decreasing MW.

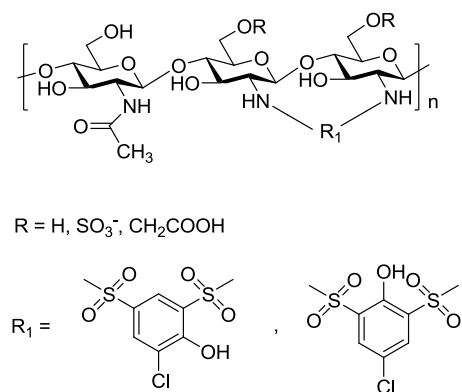


Fig. 1 Structures of hydroxybenzenedisulfonamides

Di-quaternary group can contribute to the antibacterial activity. The highest inhibition against G⁺ strains *S. aureus* and *Staphylococcus pneumoniae* showed chitosan derivative with *N*-[1-carboxymethyl-2-(1,4,4-trimethylpiperazine-1,4-dium)] substituent which was generally more active at pH 7.2 than at pH 5.5 (Fig. 2).⁴¹

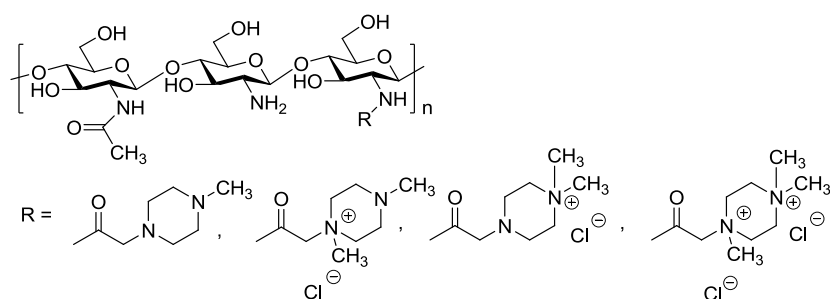


Fig. 2 Chitosan substituted by piperazine moiety

N-substituted chitosan was quaternized using *N*-(3-chloro-2-hydroxypropyl)trimethylammonium chloride (Fig. 3) for increasing water solubility. MIC was carried out on *E. coli* and *S. aureus* in order to explore the impact of the extent of *N*-substitution (ES) on their biological activities. If ES is higher than 20 %, MIC values were higher. Antibacterial activities ranged from 8 to 64 μg/ml for *S. aureus* and from 16 to 64 μg/mL for *E. coli*.⁴²

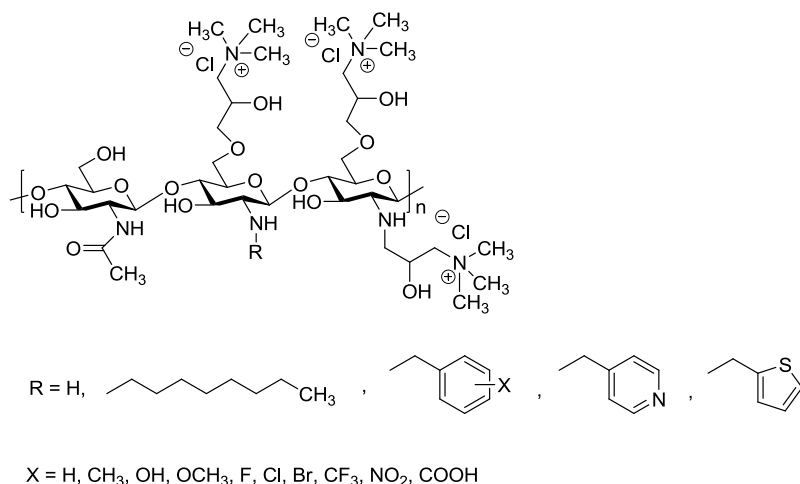


Fig. 3 *N*-substituted chitosan quaternized derivatives

Other study from the same research group presents *N*-methylation of *N*-arylated chitosan derivatives containing *N,N*-dimethyl-1-aminotolyl and pyridyl substituents which produced quaternary ammonium salts in presence of sodium iodide and iodomethan (Fig. 4). The methylated products were water soluble over all range of pH and displayed antibacterial activity against *S. aureus* and *E. coli*. Their MIC values were in the range of 32 – 128 $\mu\text{g}/\text{mL}$ against both bacteria.⁴³

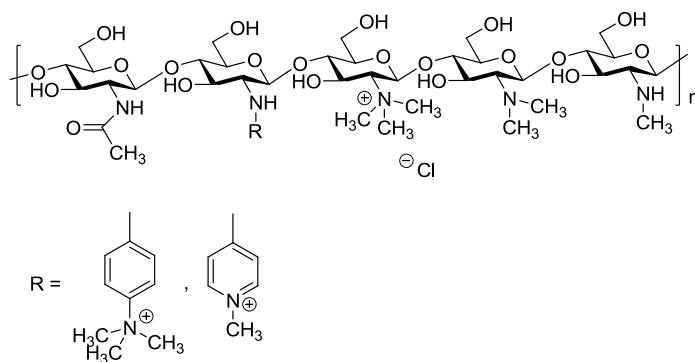


Fig. 4 *N*-methylation of *N*-arylchitosan containing *N,N,N*-trimethylbenzenaminium and *N*-methylpyridinium substituents of chitosan

N-alkylated photo-polymerizable chitosan derivative was synthesized by Michael reaction of chitosan and polyethylene glycol diacrylate (PEGDA) (Fig.5). PEGDA-chitosan exhibited good water solubility and significant antimicrobial activity against *E. coli*, but inhibition was

appreciably weaker than activity of chitosan alone. Polymerization and solidification was initiated by UV irradiation. Photopolymerization is used in many industrial applications, doesn't need solvent and requires less energy than thermal curing.⁴⁴

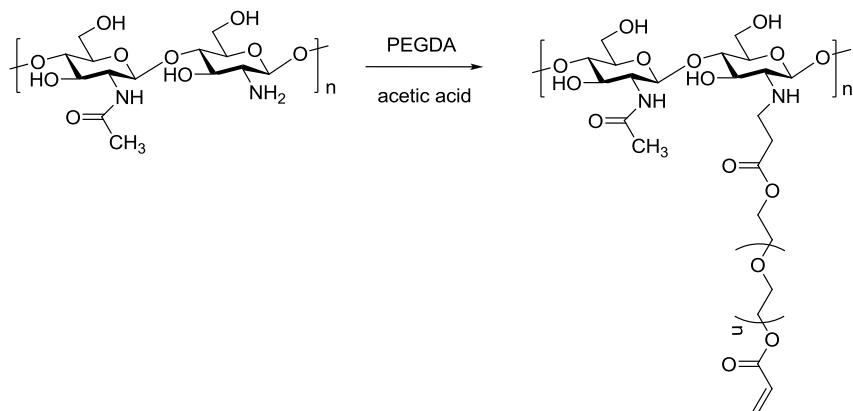


Fig.5 Michael reaction of chitosan and polyethylene glycol diacrylate.

Schiff base of chitosan was synthesized by the reaction of chitosan with citral under high-intensity ultrasound (Fig. 6).⁴⁵ The antimicrobial activities were investigated against *E. coli* (0.1 w/v), *S. aureus* (0.1 w/v) and *A. niger* (0.5 w/v) and inhibition activities increased with increasing concentration of chitosan and Schiff base and are stronger than that of chitosan.

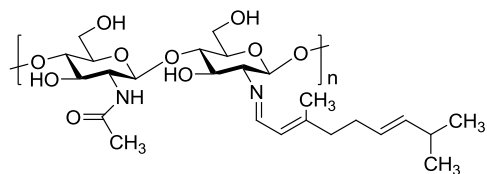


Fig. 6 Schiff base of chitosan

Hydrophobic effect of oleoyl chitosan (OC) was studied.⁴⁶ The fluorescence experiments indicated that OC interacted with proteins on the cell membrane of *E. coli*. Scanning electron microscopy photographs showed *E. coli* adhered to the surface of the chitosan microspheres and provided evidences for the disruption of cells, while the bacterium conglomerated on the surface of the OC. The chitosan microspheres changed the permeability of membrane and caused cellular leakage. Antibacterial activity of OC was poorer than chitosan alone.

Other chemical chitosan modification was a conjugation with arginine, that gave two different forms of arginine functionalized chitosan (6% and 30% arginine) like more soluble forms at physiological pH. Interactions of polycations in outer cell membrane specifically increased the cell membrane permeability.³⁹ 6 %-Substituted chitosan-arginine was more effective than the 30 %-substituted chitosan-arginine in inhibition of *Pseudomonas fluorescense* and *E. coli* growth. 30 %-Substituted chitosan-arginine, which was less viscous, appeared to be more effective in permeabilizing the cell membranes of both bacteria. It proves that the initial site of action of chitosan-arginine is the bacterial outer membrane. Cell aggregation for both bacteria was observed immediately after addition of the conjugate, which might have contributed to growth inhibition.

Preparation of blend chitosan films is frequent because of its ability to show good miscibility and homogeneity. *O*-hydroxyethyl chitosan xanthate (HECS) was synthesised and blended with cellulose xanthate. 3 % HECS showed significant inhibition effect against *E. coli*, the moisture absorption and antistatic property were enhanced.⁴⁷ The electrospun ultrathin-structured systems of zein/chitosan bioblends were prepared and carried out against *S. aureus*. Relatively low amount of chitosan (5 mg) in blend (100 mg) was able to provide an efficient biocide effect.⁴⁸

Using of carboxymethylated chitosan for different chemical modifications is very common. Carboxymethyl chitosan has been grafted by poly(*N*-vinyl imidazole) in aqueous solution using potassium persulfate as an initiator. Antimicrobial activity was enhanced by grafted products. The highest inhibition effect was shown by carboxymethylated copolymer against *E. coli* (97.6 % inhibition), *S. aureus* (53.3 %), *Fusarium oxysporum* (63.3 %) and *Aspergillus fumigatus* (54 %).⁴⁹ *O*-carboxymethyl and *N,O*-carboxymethyl chitosan nanoparticles were synthesized by simple cross-linkage using sodium triphosphate.⁵⁰ Antibacterial activity was measured against *S. aureus* by MIC method for three different concentrations. Chitosan nanoparticles showed less antibacterial activity compared to *O*-CMC and *N,O*-CMC. Antibacterial effect increased with increasing concentration. The highest concentration of *O*-CMC killed all bacteria and for *N,O*-CMC all three concentrations inhibited all colonies.

Chitosan is able to show antibacterial activity also in connection with inorganic compound. Chitosan-clay nanocomposites were prepared by an ion exchange reaction between chitosan and sodium montmorillonite with the cationic exchange capacity and exhibited inhibition effect against *S. aureus* and *E. coli*. The highly dispersed chitosan molecules in the nanocomposites through layer-by-layer stacking structure play an important role in enhancing of antimicrobial activity. Potential application of chitosan-clay nanocomposites could be in the development of natural biopolymer-based biodegradable packaging materials.⁵¹ Silver is well-known for its antimicrobial potential. Chitosan Ag-nanoparticles showed antibacterial activity against *E. coli*. Scanning electron microscope of *E. coli* cell detected complete lysis of cells after 4 hours.⁵² Other silver nanoparticles dispersing in chitosan solution during γ -ray irradiation exhibited antimicrobial activities against *E. coli* and *S. aureus*. Antimicrobial activity of the film increased with increasing silver nanoparticle content. Silver nanoparticles showed stronger inhibitory effect against *E. coli* than *S. aureus*.⁵³

Further study has developed crosslinked chitosan coated Ag-loading nano-SiO₂ composite (CCTS-SLS) which exhibited MIC against *E. coli* and *S. aureus* 250 $\mu\text{g/mL}$ and 300 $\mu\text{g/mL}$. Activities were much higher than separately used chitosan or silver-loading nano SiO₂.⁵⁴ Stronger antibacterial effect of *E. coli* can be explained by the structural difference between thicker G⁺ cellular cell wall of *S. aureus* than G⁻ cell wall of *E. coli*.

Chitosan is usefull as biomaterial for wound care due to its biocompatibility and intrinsic hemostatic properties. Anionic polyphosphate polymer and silver ions were added to chitosan for more potent haemostatic agent. The presence of Ag had significantly faster and more potent bactericidal action than chitosan-polyphosphate. Chitosan-polyphosphate-Ag was effective in reducing mortality compared to standard gauze treatment contaminated with high levels of *Pseudomonas aeruginosa*.⁵⁵

Biocompatibility and antibacterial properties are very important in implant removal and revision surgery. Chitosan is a good candidate for usage as a scaffold for bone tissue engineering and as a prevention of orthopaedic implant-associated infection. Chitosan-*N*-2-hydroxy-*N,N,N*-trimethylpropan-1-amonium chloride (HACC) was prepared with different degrees of substitution (Fig. 7). Antibacterial activity against *S. aureus*, *Methiciline-resistant S.*

aureus and *Staphylococcus epidermidis* of HACC 18 % and 44 % of substitution was significantly higher than others. HACC 18% was non-cytotoxic to L-929 cells and enhanced the proliferation as well as osteogenic differentiation; it had good biocompatibility with bone cells.²⁵

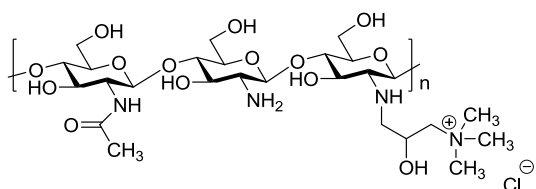


Fig. 7 Structure of chitosan-*N*-2-hydroxy-*N,N,N*-trimethylpropan-1-amonium chloride

Chitosan is able to inhibit growth of different strains of fungi and yeasts. Antimicrobial activity of three acyl thiourea derivatives of chitosan (Fig. 8) was evaluated. In general, antibacterial activities of derivatives were better than that of chitosan.⁵⁶ MIC value against *E. coli* was 15.62 $\mu\text{g/mL}$ and *Pseudomonas aeruginosa* 15.62 or 62.49 $\mu\text{g/mL}$. MIC values for two G^+ bacteria *S. aureus* and *Sarcina* were 62.46 $\mu\text{g/mL}$. Antifungal activities were measured against *Alternaria solani*, *Fusarium oxysporum f. sp. vasinfectum*, *Colletotrichum gloeosporioides (Penz.) Saec.*, and *Phyllisticta zingiberi*. Range of inhibitory values was from 31.23 % to 66.67 % at 500 $\mu\text{g/mL}$ for all fungi.

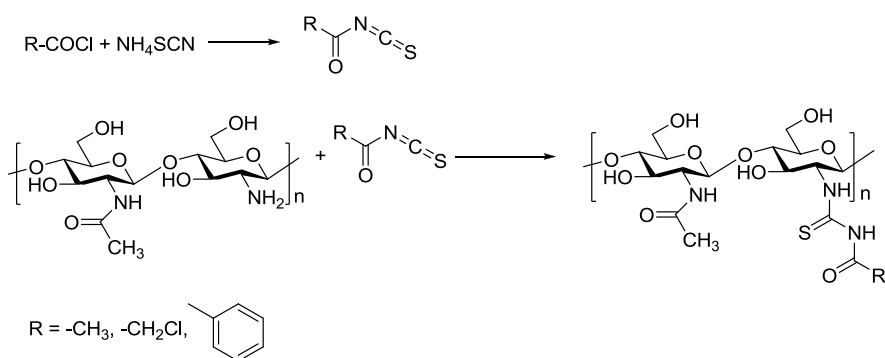


Fig. 8 Acyl thiourea derivatives

Antimicrobial effect of MW of chitosan was investigated also against fungi. Quaternized chitosan was synthesized in two averages of MW – LMW 7600 and HMW 700000.⁵⁷ Derivatives gave stronger antifungal activities than chitosan alone. LMW chitosan showed

stronger inhibitory index (25 %) than HMW chitosan (19.6 %) against *Botrytis cinerea* Pers. (*B. cinerea* pers.) and *Colletotrichum lagenarium* (Pass) Ell.et halst (*C. lagenarium* (Pass) Ell.et halst). Quaternized derivatives exhibit higher antifungal activity with HMW. When the concentration of individual target material was raised to 1000 µg/mL, the growth of both fungi was completely inhibited. Next experiment compared influence of MW to fungal growing. Low molecular weight chitosan (17 kDa) was more effective to inhibition of mycelian growth of *Rhizopus stolonifer* (Ehrenb.:Fr.) Vuill while the high molecular weight chitosan (30 kDa) affected spore shape, sporulation and germination.⁵⁸

Antibacterial properties of chitosan are used in many branches. Antimicrobial properties of chitosan and its derivatives are important also in textile industry. Wool fabric coated with chitosan - henna dye exhibited antibacterial activity against *E. coli* and *S. aureus*. Chitosan significantly enhanced antimicrobial activity of the dye. The positive side effect of chitosan application is improving the dye uptake of wool fabric and improving fastness properties of fabric.⁵⁹ The second textile study, considered in jute fabric, tested chitosan-metal complex linked in the surface of a fabric against *S. aureus* and *Candida albicans*. For the same metal salt concentration (0.15 %), the antibacterial and antifungal properties follow the order: chitosan-Zn > chitosan-Zr > chitosan-Ag > chitosan.⁶⁰

Addition of chitosan can improve properties of a paper. Polysaccharide was linked with polyhexamethylene guanidine hydrochloride (PHGH) or PHGH in the presence of sodium tripolyphosphate as a crosslinking agent (PHGHE).⁶¹ MIC values of PHGH and PHGHE against *E. coli* were 5.2 and 10.4 µg/mL. These chitosan complexes were used as functional additives for papers. Papers blended with PHGH and PHGHE showed a remarkable inhibition effect against *E. coli* and *S. aureus*. Atomic force microscopy images indicate that the antimicrobial mechanism of the complexes was likely due to membrane damage.

Antimicrobial packaging has attracted attention the food industry because of the increase in consumer demand for minimally processed and preservative products. Experimental chitosan/methyl cellulose film incorporating vanillin was applied on fresh-cut cantaloupe and pineapple and their effects on microbial control and fruit quality were investigated. After eight days of storage both fruits covered with experimental film had no colonies of *E. coli* and

significantly lower number of *Saccharomyces cerevisiae* than fruits without wrapping.⁶² Other work in food packaging was engaged in development and characterization of biological properties of renewable blend of chitosan with gliadin, protein isolated from gluten. The renewable blend indicated significant antimicrobial effect against *S. aureus* which increased with increasing concentration of the amount of chitosan in blend.⁶³

3.4. Antitumor activity

3.4.1. Antitumor activity of nano-size particles

The regulation of mitosis can be changed by various mechanisms. These defects are usually induced by mutations of genes which code signal proteins, transcription factors, or proteins regulating cell adhesion or apoptosis. It can lead to uncontrolled division of cells, escape from normal tissue, dissemination and growing in other tissues. Two main strategies of chemotherapy are observed for killing the tumor, one is apoptosis induction and the other is necrosis induction. Specific modes of apoptosis and necrosis are recognized by characteristic patterns of morphological and biochemical changes.⁶⁴

Polymeric nano-sized carriers have shown a high tumor targeting ability at tumor tissue and are minimally found at sites of normal tissue. Accumulation of them in tumor is explained by enhanced permeability and retention (EPR) effect which is caused by the disorganized vascularization of tumor. Nano-size drug delivery systems have outstanding advantages such as passing through the smallest capillary vessels because of their ultra-tiny volume, avoiding rapid clearance by phagocytes, penetrating cells and tissue gap to arrive at target organs. Recently, polymeric micelles or nanoparticles have attraction as passive targeting of drugs, with solubilisation of water insoluble drugs, prevention of side effects and long drug circulation time. Physicochemical characteristics as particle size, chemistry on the surface of nanoparticles or stability of nanoparticles can effectively enhanced EPR effect.⁶⁵ Colloidal delivery systems can fulfil the requirements of an ideal and versatile drug carrier. Polymeric micelles are formed by self-assembly in an aqueous environment and possess a core-shell structure.

Chitosan-base nanoparticles were known to be very stable due to its specific structure and physicochemical properties. In general, particles up to about 100 – 200 nm can be internalized

by receptor-mediated endocytosis, while larger particles have to be taken up by phagocytosis.⁶⁵ Chitosan mostly supports antitumor activities of its substituents, mechanism of anticancer effect depends on them. The drug-loading capacity and stability of chitosan nanoparticles are significantly affected by the degree of substitution.

3.4.2. Antitumor activity of chitosan derivatives

Carboxymethyl chitosan can be applied also in cancer therapy. Hydrogel nanoparticles were prepared by using linoleic acid modified carboxymethyl chitosan after the sonification (Fig. 9). Self-aggregated nanoparticles exhibited increase of loading capacity and loading efficiency. *In vitro* anticancer activity of hydrogel against HeLa cells was comparable to the activity of free doxorubicin as standard. Free nanoparticles showed almost no effect on the cytotoxicity of cells.⁶⁶

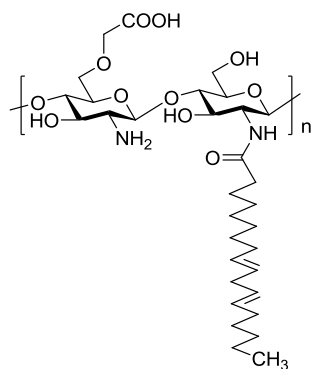


Fig. 9 The structure of carboxymethyl chitosan conjugated with linoleic acid

N-succinyl chitosan (NSCS) is well known as a drug carrier with low toxicity and a long circulating effect in the body.⁶⁷ Recently *N*-succinyl chitosan became a main component of micelles or nanoparticles used for delivery system in anticancer therapy. Antitumor effect of *N*-succinyl chitosan nanoparticles was investigated on K562 cells. Nanoparticles inhibited the proliferation of K562 with IC_{50} of 14.26 $\mu\text{g/mL}$. Cytomorphology studies as TEM, fluorescent assay and DNA fragmentation analysis revealed characteristics of apoptosis and necrosis, indicating that the antitumor effect was achieved by both.⁶⁴

Hydrophobically modified polysaccharides are able to self-aggregate by their intra- and/or intermolecular hydrophobic interactions in aqueous media to form nanoparticles with

hydrophobic core and hydrophilic shell. This is suitable for doxorubicin and taxol.⁶⁶ Doxorubicin (DOX) is a member of anthracycline antitumor drugs and is widely used in chemotherapy for various tumors. Its mechanism of action is incorporation to DNA, including inhibition of topoisomerase II and RNA polymerase. Methoxy poly(ethylene glycol)-grafted carboxymethyl chitosan was prepared as nanoparticles with DOX (Fig. 10) by ion complex formation and the particle size < 300 nm. Releasing of DOX was faster in acidic pH. Nanoparticles showed increasing cytotoxicity in DOX-resistant C6 glioma cells compared with DOX alone. Nanoparticles could penetrate into cells, it was observed by fluorescence assay, and can effectively inhibit cell proliferation.⁶⁸

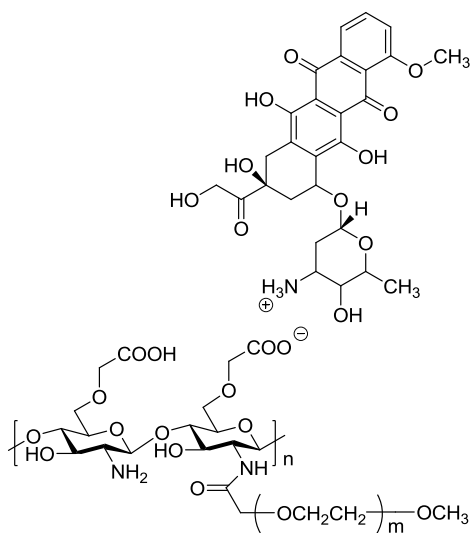


Fig. 10 Methoxy poly(ethylene glycol)-grafted carboxymethyl chitosan with DOX

DOX hydrochloride was loaded into oleoyl-chitosan (OCH) nanoparticles (Fig. 11) with different MW. Loading efficiency and DOX release rate increased with decreasing of MW. OCH nanoparticles alone based on low MW (5 kDa) chitosan had higher drug loading efficiency, release rate and antitumor activity than those based on high MW (300 kDa). The inhibitory effect of DOX-loaded OCH nanoparticles to human lung cancer cell line A549 was higher than DOX solution without chitosan.⁶⁵

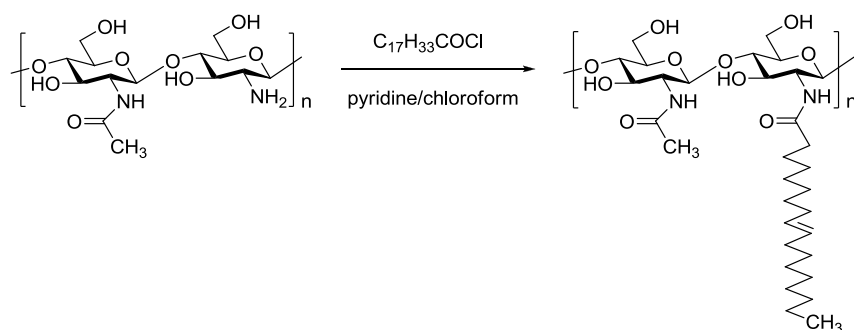


Fig. 11 Synthesis of oleoyl-chitosan

Chitosan-DOX conjugate was connected with Pluronic [poly(ethylene glycol)-block-poly(propylene glycol)-block-poly(ethylene glycol)], injectable depot system for clinical purpose, and acrylated with glycidyl methacrylate. *In vitro* cytotoxicity of degradable chitosan-DOX hydrogel was comparable to free DOX in human lung adenocarcinoma cell line A549. Chitosan-DOX hydrogel and DOX alone showed similar incidence to *in vivo* test in athymic nude mice bearing human lung adenocarcinoma. Values of cytotoxicities were comparable and the tumor volume was significantly reduced. Inconvenient property of prepared hydrogel was able to reduce burst release, which is advantageous in anticancer therapy because it further increased local concentration of anticancer drugs at the injection site.⁶⁹

Chitosan oligosaccharide was grafted by stearic acid and DOX (size of micelles 30 – 110 nm). Release rate of DOX from grafted copolymer increased with decreasing pH, from 7.2 to 5.0 which might be advantageous for the targeting delivery of antitumor drugs because of the lower pH of tumor tissue (pH 5 – 6). *In vitro* cytotoxicity was performed on human breast carcinoma cell line MCF-7 and MCF-7/Adr (multi-drug resistant variant). IC₅₀ values of both cell lines were similar (1.27 – 7.70 µg/mL) and effectively suppressed the tumor growth.⁷⁰

Glycol chitosan was modified with hydrophobic 5β-cholanic acid (Fig. 12) and cisplatin was easily encapsulated into chitosan nanoparticles (300 – 500 nm) by dialysis method. Nanoparticles were successfully accumulated in tumor tissues in tumor-bearing mice because of the prolonged circulation and EPR effect. Encapsulated nanoparticles showed lower toxicity compared to free cisplatin.⁷¹

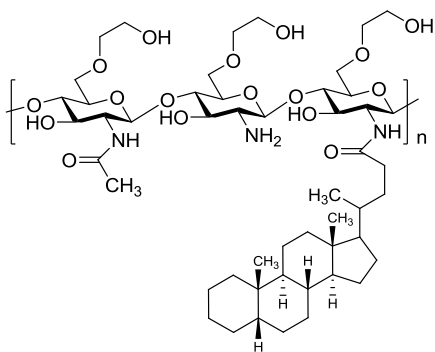


Fig. 12 Glycol chitosan acylated with hydrophobic cholanolic acid

Paclitaxel (PTX), clinical water insoluble anticancer drug promoting microtubulin polymerization, is used against a variety of cancer types, especially breast and ovarian cancer. To enhance its solubility, PTX was aggregated with cyclodextrin, liposomes or different polymeric micelles which increased EPR effect of PTX and decreased high toxicity of PTX. Nanomicelles based on glycol chitosan linked with alkyl chains exhibited low toxicity and high biocompatibility. PTX was loaded to nanomicelles by using dialysis method. Enhanced degree of substitution of alkyl chains increased drug-loading capacity, drug-loading efficiency and long-term stability in aqueous solution (5 days).⁷²

Another study containing PTX probed hydrotropic oligomer-glycol chitosan which was synthesized by conjugation with *N,N*-diethylnicotinamide-based oligomer. PTX was encapsulated to nanoparticles (300 nm) with high quantity of 20 wt %. Biodistribution was investigated by fluorescence labelled nanoparticles which showed excellent tumor specificity in SCC7 tumor-bearing mice, due to enhanced EPR effect.⁷³

Zhang et al.³⁵ developed *N*-octyl-*O*-sulphate chitosan micelles as the delivery system for PTX. Micelles showed high drug-loading capacity and entrapment efficiency. Biodistribution study indicated that most of the PTX were distributed in liver, kidney, spleen and lung, the longest retention effect was observed in the lung. Antitumor effect of micelles and free PTX was observed at dose 10 mg/kg in *in vivo* antitumor mice model inoculated with sarcoma 180, enrich solid carcinoma, hepatoma solidity, Lewis lung cancer cells and A-549 human lung cancer cells.

Docetaxel (DTX), as well as PTX, have influence on cell mitosis and are able to induce apoptosis of cancer cells. DTX was covalently attached to the low MW chitosan via succinyl bond (Fig. 13). Half-life in blood of conjugate was 3.8 – 6.2 times higher in comparison with the intravenously injected DTX. The orally administered conjugate showed comparable antitumor effect as the same dose of DTX administered intravenously (10 mg/kg) which was evaluated in nude mice bearing human non-small cell lung carcinoma and glioblastoma.⁷⁴

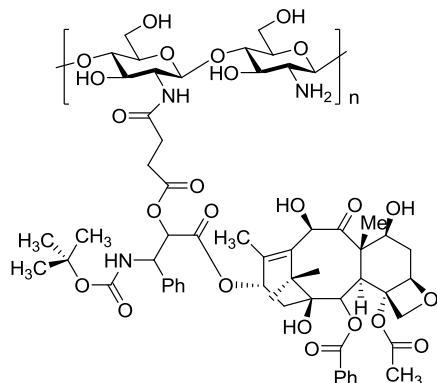


Fig. 13 Chemical structure of chitosan-DTX conjugate

Hydrophobic modified glycol chitosan conjugate with 5 β -cholanic acid (Fig. 12) was used as a drug carrier for DTX. Nanoparticles formed spontaneously self-assembled aggregates (350 nm) and showed *in vivo* reasonable stability in the blood stream. Nanoparticles exhibited higher tumor efficiency such as reduced tumor volume and increased survival rate in A549 lung cancer cells-bearing mice. Anticancer drug toxicity was strongly reduced, compared to that of free DTX in tumor-bearing mice.⁷⁵

Norcantharidin is a new chemotherapy agent which is effective against primary carcinoma of the liver as an inhibitor of protein phosphatase 1 and protein phosphatase 2A. Lactosaminated *N*-succinyl chitosan is known as a liver-specific drug carrier.⁷⁶ Asialoglycoprotein receptor is located on the hepatocellular carcinoma cell membrane. It can specifically recognize β -D-galactose. For this reason, the asialoglycoprotein receptor can be exploited as a hepatocyte specific targeting marker for drug delivery. Galactosylated chitosan was prepared with norcantharidin as a drug carrier for anti-hepatocarcinoma medicine (Fig. 14). Nanoparticles demonstrated satisfactory compatibility with hepatoma cells and strong cytotoxicity against

hepatocellular carcinoma cells SMMC-7721 (31.44 $\mu\text{g/mL}$) and HepG2 (57.88 $\mu\text{g/mL}$). Nanoparticles displayed better tumor inhibition effect in *in vivo* mice bearing H22 liver tumor comparing free norcarditin.⁷⁷

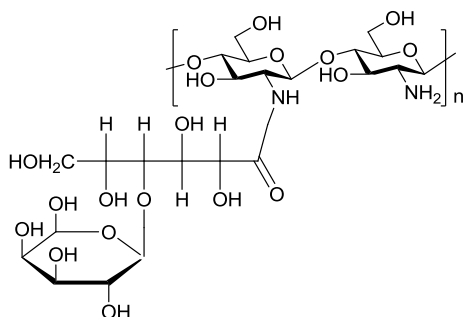


Fig. 14 Scheme of galactosylated chitosan

3.5. Antioxidant activity

3.5.1. Reactive oxygen species and chitosan as antioxidant

Reactive oxygen species (ROS), including superoxide anion radicals ($\text{O}_2^{\bullet-}$), hydroxyl radicals ($\bullet\text{OH}$), and hydrogen peroxide (H_2O_2) etc., are often generated as the oxidation products of biological reactions or exogenous factors. ROS are able to react with most biomolecules as lipids, proteins, amines, lipoproteins, carbohydrates, and DNA. ROS are generally unstable and can highly activate one or more unpaired electrons in the body. The attack of ROS against proteins can produce protein carbonyls and other modifications in some amino acid residues, resulting in impairing the function of the protein. Lipid peroxidation is known due to membrane lipid destruction caused by ROS. It leads to reduction of membrane fluidity, enhancing of membrane permeability and damage of membrane proteins. ROS are able to induce all forms of oxidative DNA damage, including bases modifications, base-free sites and DNA-protein cross-link.⁷⁸ The antioxidant activity of compounds has been attributed to various mechanisms as a prevention of chain initiation, a binding of transition metal ion catalysts, a decomposition of peroxides, reductive capacity and radical scavenging.

Scavenging activity of chitosan is due to strong hydrogen-donating ability of chitosan. ROS can react with active hydrogen atoms in hydroxyl or amino groups of chitosan to form a most stable macromolecular radical. Chitosan has high metal bonding capacity due to free amino groups.

As well as in previous parts of this review, MW and concentration have influence on the antioxidant activity of chitosan. Low MW and higher concentration showed the most antioxidative effect. Conversely, higher MW was the most effective in reducing lipid oxidation. The antioxidant effect of different MW of chitosan is attributed to the chelation of metal ions. The high MW of chitosan should have lower mobility than the lower MW chitosan which can increase the possibility of inter- and intramolecular bonding among the high MW chitosan. This could be responsible for less chelation by high MW chitosan.^{79,80}

In several studies, chitosan alone was investigated as potential antioxidant agent. Scavenging of hydroxyl radicals by chitosan inhibited the lipid peroxidation of phosphatidylcholine and linoleate liposomes.⁸⁰ Similar work realized an experiment with using linoleic acid peroxidation. Degradation of suitable MW of chains was made by irradiation. MW of chitosan decreased with increasing irradiation dose. Different MW of chitosan showed inhibition of linoleic acid peroxidation in the linoleic acid model system. Significant scavenging of superoxide radicals (74.2 %) exhibited low MW chitosan (2.1 kDa) at 0.1 mg/mL. Scavenging percentage of high MW chitosan (210 kDa) and low MW chitosan against hydroxyl radicals was 16.6 % and 63.8 %.⁸¹

Yen et al.⁸² studied antioxidant properties of chitosan from crab shells with different DD. All chitosans showed relatively high antioxidant activities 58.3 – 70.2 % at 1 mg/mL and 79.9. – 85.2 % at 10 mg/mL. Scavenging activities of hydroxyl radicals were in the range of 88.7 – 94.1 %. At 1 mg/mL, chelating abilities of all chitosans on ferrous ions were 82.9 – 96.5 %. Chelating abilities are important in food industry for preservation of flavor and taste of food. Transition metal ions can initiate lipid peroxidation, start a chain reaction and deteriorate quality of food. High chelating property of chitosan can be beneficial as food supplement.

Human serum albumin (HSA) is the major target of oxidative stress in uremia and other vascular disorders. The result of oxidative stress is increasing levels of HSA carbonyl derivatives. Low MW chitosan was able to prevent formation of carbonyl and hydroperoxide groups in HSA exposed to peroxy radical. It was also a potent inhibitor of conformational changes in protein.²⁰ Treatment with chitosan for four weeks decreased the ratio of oxidized albumin and increased total plasma antioxidant activity.⁸³

3.5.2. Antioxidant activity of chitosan derivatives

N-carboxymethyl chitosan oligosaccharides were prepared with different degrees of substitution. The scavenging activity of 1,1-diphenyl-2-picrylhydrazyl (DPPH) radicals was measured. The antioxidant effect decreased with increasing degree of substitution. Lower degree of substitution has resulted in more active amino groups that could donate more hydrogens to the reaction with DPPH radicals.⁸⁴

ROS are involved in the progression of tumor-induced angiogenesis because they can positively activate several kinds of matrix metalloproteinases (MMPs). MMPs significantly play a substantial role in the pathogenesis of various chronic diseases, because they are secreted by some cancer cells and other various types of cells. Especially, MMP-2 and MMP-9 degrade components of the basement membrane are responsible for tumor invasion and metastasis. Carboxymethylated chitosan was studied as an inhibitor of the expression of MMP-2 and MMP-9 in HT1080 human fibrosarcoma cells. In accordance with gelatin zymographic analysis, carboxymethylated chitosan down-regulated expression of both MMPs without any cytotoxic influence. Carboxymethylated chitosan showed also high inhibition of membrane protein oxidation and membrane lipid oxidation.⁷⁸

Antioxidant activities of high and low MW chitosan-*N*-2-hydroxy-*N,N,N*-trimethylpropan-1-amonium chloride were compared (Fig. 7). Scavenging rates enhanced with increasing concentrations. Low MW form had stronger scavenging effect on $O_2^{\cdot-}$ (87 % at 0.8 mg/mL) and $\bullet OH$ (45 % at 3.0 mg/mL) also reducing power was more pronounced than high MW quaternary chitosan. The chelating effect of ferrous ion of both molecules was not concentration dependent. Chelating potency increased at 0.1 mg/mL (53 %) and decreased afterwards with increasing concentrations (5 %).⁸⁵

Quaternized carboxymethyl chitosan derivatives were prepared with degree of quaternization in the range of 34.3 – 59.5 %. All derivatives showed better scavenging activity against hydroxyl radicals than chitosan. Scavenging activity increased with increasing degree of quaternization, it signified the influence of the positive charge on the scavenging activity against $\bullet OH$.⁸⁶

Zhong et al.⁸⁷ reported enhanced scavenging effect on $O_2^{\cdot-}$ (80 - 90 % at 0.4 mg/mL) and $\bullet OH$ (55 - 75 % at 0.7 mg/mL), and also reducing power of chitosan connected with 5-chloro-4-hydroxybenzene-1,3-disulphonyl dichloride or 5-chloro-2-hydroxybenzene-1,3-disulphonyl dichloride. Hydroxyl and amino groups of chitosan and hydroxyl group of disulfonamides reacted with hydroxyl radical to form stable macromolecular radicals.

The same collective determined antioxidant activity of 2-phenylhydrazinecarbothioamide chitosan or hydrazinecarbothioamide chitosan (Fig. 15). Two different MW and two substituents were studied. Better scavenging effect on $O_2^{\cdot-}$ (80 - 90 % at 0.4 mg/mL) and $\bullet OH$ (70 - 90 % at 1.4 mg/mL), and also reducing power in range 1.0 - 1.5 mg/mL were exhibited by both low MW products. $-NH-$ and $C=S$ groups were able to react with free radicals and increased the antioxidant activity of chitosan.⁸⁸

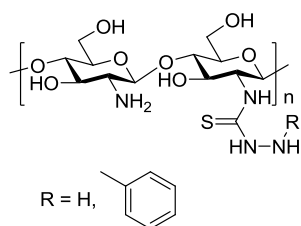


Fig. 15 Structure of 2-phenylhydrazinecarbothioamide chitosan and hydrazinecarbothioamide chitosan

Natural compounds with antioxidant activity obtained from plants are used for improving antioxidant effect of polymers. Natural phenolic antioxidant gallic acid was connected to chitosan in presence of *N*-(3-dimethylaminopropyl)-*N'*-ethylcarbodiimide (Fig. 16). Significant activities showed chitosan derivative with degree of substitution 15.62 %. The galloyl group could effectively transfer a hydrogen atom, forming stable semiquinone radicals, which was observed in electron paramagnetic resonance spectrum of chitosan gallate.⁸⁹ DPPH scavenging capacity was 87.3 % at concentration 1200 μM . Scavenging activity of carbon-centered radical $R\bullet$, which is one of the representative oxidized products in lipid membranes and lipoproteins, needed 200 μM for 60 %. Chitosan galloyl amide, with only a certain amount of gallate groups, showed antioxidant activity on $\bullet OH$ close to the pure gallic acid. This result could be due to

synergistic effect in $\bullet\text{OH}$ scavenging of both components of the complex chitosan gallyl amide.⁹⁰

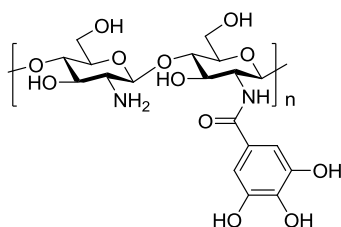


Fig. 16 Structure of chitosan gallyl amide

For their strong antioxidant effect, polyphenolic structures were tried to enhance antioxidant activity of chitosan. Green tea extract was incorporated to chitosan film. Green tea is a good source of polyphenolic compounds having strong antioxidant properties, especially the ability to scavenge reactive oxygen and nitrogen species. DPPH scavenging assay showed presumable synergistic effect of chitosan and extract which enhanced antioxidant activity of film (51 % at 20 % of incorporated amount). Extract also improved mechanical and water vapor barrier properties of chitosan film.⁹¹

Chitosan fibres were grafted with chemically different flavonoids – flavanols, flavonol, flavone, flavanone, isoflavone. Tyrosinase was used to produce reactive *o*-semiquinones that were covalently bonded to the amino group of chitosan. Generally, flavanols exhibited the highest values in the range of 69 – 88 % in DPPH free radical scavenging assay, superoxide anion scavenging activity and also total antioxidant activity.⁹²

3.5. Chitosan connected with antituberculotics

3.5.1. Chitosan conjugated with INH, PZA and ETA (**Paper III**)

Chemical modifications of chitosan improve water solubility and inhibition effect against bacteria. To the best of our knowledge no studies aimed to the antimycobacterial activity of chitosan or chitosan derivatives against *M. tbc.* complex or other strains of mycobacteria have not been published yet. *O*-carboxymethyl (OCMC, **1**) or *N*-succinyl (NSCS, **4**) chitosan was linked with INH, PZA and ETA (**3a - 3c**, **6a - 6c**) (Scheme 1, 2). The prepared chitosan derivatives were tested *in vitro* for antimycobacterial activity against *M. tbc.* 331/88 and some

non-TB strains such as *M. avium* (330/88) and *M. kansasii* (235/80 and 6509/96) (Table 1). Compounds **3a** - **3c** and **6a** - **6c** have shown the same MIC of 125 µg/mL. *O*-carboxymethyl chitosan **1** (without substitution of antituberculosic drug) showed minimum inhibitory concentration 62.5 µg/mL against *M. tbc.*, 31.25 and 62.5 µg/mL against *M. avium*. *N*-succinyl chitosan **4** has considerably lower activity (500 µg/mL) against these strains. **4** Exhibited good activity against *M. kansasii* after 7 days (62.5 µg/mL).

In general, it seems that there are two factors influencing the activity of compounds. Firstly, presence of the first or second line antituberculosic drugs (INH, PZA, ETA) which is important in the inhibition of mycobacteria. Although, the degree of substitution is not high, products **3a** - **3c** and **6a** - **6c** have exhibited very good antimycobacterial activity. The second factor is probably an antibacterial activity of original chitosan structure which corresponds with the inhibition values against *M. tuberculosis* and *M. avium* of **1** and probably contribute to mycobacterial growth inhibition. The explication of this activity could be high degree of deacetylation of chitosan. It means that the amino group as the active functional group (chelating divalent cation) was found to be essential for the antibacterial activity of chitosan. MIC values of **3a** - **3c** and **6a** - **6c** are equal for all tested strains, this implies that amount of free amino groups in chitosan derivatives should be the same.

Table 1. Values of antimycobacterial activity and *in vitro* cytotoxicity

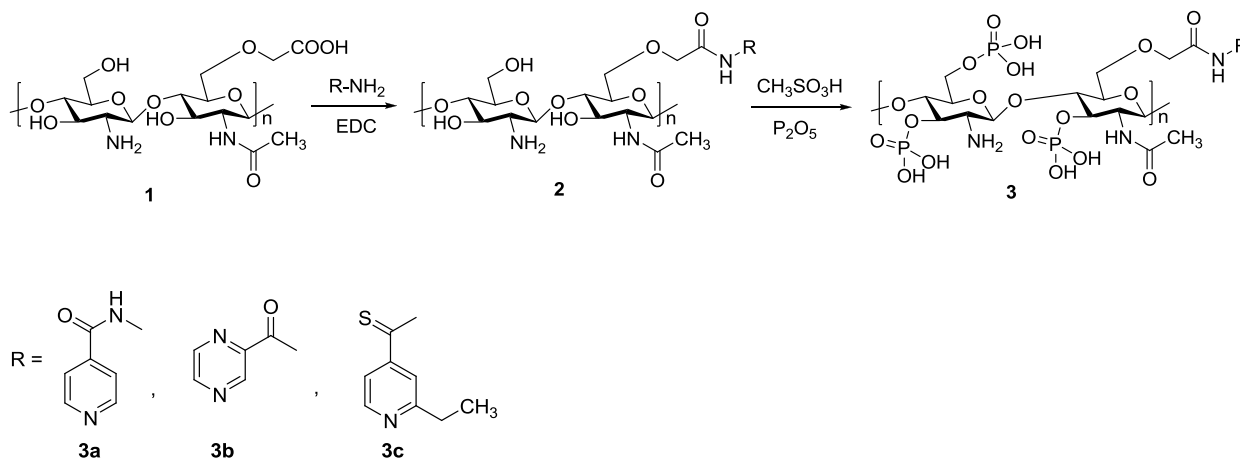
	MIC [µg/mL]										[mg/mL]	
	<i>M. tbc</i>		<i>M. avium</i>		<i>M. kansasii</i>			<i>M. kansasii</i>			HepG2 IC ₅₀	PBMC IC ₅₀
	331/88	330/88	235/80	6509/96	7 d	14 d	21 d	7 d	14 d	21 d		
OCMC	62.5	62.5	31.25	62.5	125	125	125	125	125	125	2.83	> 1.67
NSCS	>500	>500	500	>500	62.5	500	>500	250	>500	>500	> 3	NT
3a	125	125	125	125	125	125	125	125	125	125	2.13	> 1.78
3b	125	125	125	125	125	125	125	125	125	125	> 3	> 9.35
3c	125	125	125	125	125	125	125	125	125	125	2.32	NT
6a	125	125	125	125	125	125	125	125	125	125	> 3	> 3.54
6b	125	125	125	125	125	125	125	125	125	125	2.72	> 8.86

6c	125	125	125	125	125	125	125	125	125	125	2.96	NT
----	-----	-----	-----	-----	-----	-----	-----	-----	-----	-----	------	----

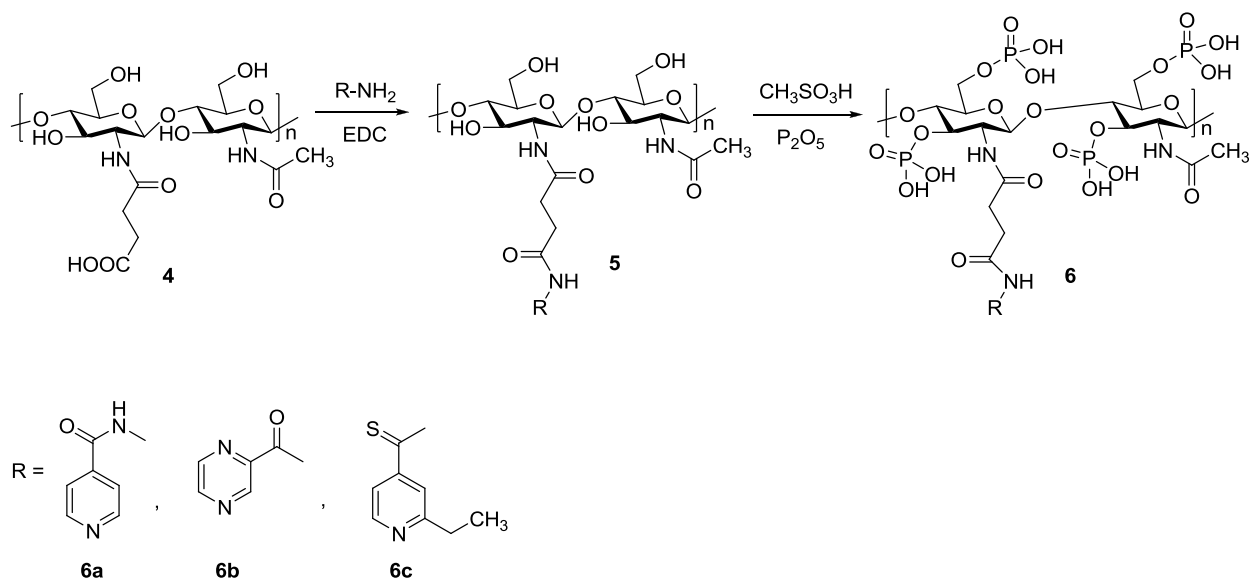
NT = not tested

The conjugation of chitosan and antituberculotics was aimed to decrease of the toxic effect of drugs on hepatocytes. Cytotoxicity test was evaluated on human liver cell line Hep G2. Cytotoxicity of prepared compounds was tested also on human peripheral blood mononuclear cells (PBMC) which contain macrophages and monocytes. Immune system plays important role during a long-time treatment and latent TB. All tested compounds in examination range of concentrations have not exhibited obvious cytotoxic effect on PBMC (higher than 1.67 – 9.35 mg/mL) and Hep G2 cells (Table 1). Compounds **4**, **3b** and **6a** showed values of IC_{50} higher than 3 mg/mL. Chitosan has exhibit possibility to compensate cytotoxic effect of antituberculotic drugs.

Briefly, *O*-carboxymethyl (OCMC) or *N*-succinyl (NSCS) chitosan was linked with INH, PZA and ETA in presence of equimolar amount of EDC at 0 - 5 °C. Water solubility of prepared conjugates was improved by phosphorylation (Scheme 1, Scheme 2). All prepared compounds were characterized by IR spectra and 1H NMR spectra.



Scheme 1. Conjugation of OCMC and antituberculotic drugs



Scheme 2. Conjugation of NSCS and antituberculosic drugs

DD of chitosan was found out by elemental analysis and calculation from ratio C/N. Chitosan had DD 20.04 %. MW was determined by measurement of viscosity and calculated according to the Mark – Houwink equation formula⁹³ which is recommended for polymers. Original chitosan had MW 29972 Da, prepared intermediates and derivatives had significantly lower MW 13 – 17 kDa. Half values of molecule weights were probably caused by synthetic procedure. Degree of substitution (DS) was determined using UV spectrophotometric technique on the base of calibration curves. Percentages of a content of antituberculosic drugs were low, around 1 %.

3.5.2. Chitosan conjugated with second line antituberculosic drugs

Results presented in the Paper III led us to continue in the synthesis of chitosan derivatives linkage with some second line and quinolone antituberculosics.

D-Cycloserin (CS) ((*R*)-4-aminoisoxazolidin-3-one) inhibits D-alanine racemase and D-alanine-D-alanine synthetase. Enzymes are essential for synthesis of peptidoglycan, subsequently synthesis of cell wall and their maintenance. CS is more effective against G⁺ than against G⁻ bacteria. Toxicity of CS is associated with effective dosage; nevertheless, due to MDR TB strains CS is still used as a second line antituberculosic drug.⁹⁴ Administration of high doses of CS (1g/day) led to the symptoms of neurotoxicity, on the other side, CS exhibits

anticonvulsant properties in experimental epilepsy models.⁹⁵ *In vitro* activity of CS against *M. tbc.* is in wide range 1.5 - 30 µg/mL depending on the medium.⁹⁶

The structure of *p*-aminosalicylic acid (4-amino-2-hydroxybenzoic acid) (PAS) is similar to sulphonamides. The mechanism of action was interpreted as the competitive inhibition of *p*-aminobenzoic acid which is necessary for a synthesis of dihydrofolic acid. More probable mechanism consists in chelation of extracellular ferric cations. Fe²⁺ and Fe³⁺ are important for a transport into mycobacteria, ferric cations are essential for them. Current data showed that PAS is able to effectively chelate manganese concentration during manganese intoxication.⁹⁷ PAS is a bacteriostatic drug that is primarily active against *M. tbc* with MIC of 0.5 – 2 µg/mL.⁹⁶

Fluoroquinolones are a group of synthetic wide spread antimicrobial agents used in daily medicine practice. They are divided into four generations with strong inhibition effect against G⁺, G⁻ and some of anaerobic bacteria. Generally, main side effects are neurotoxicity and gastrointestinal symptoms. They are responsible for binding of prokaryotic DNA gyrase and bacterial topoisomerase IV, belonging to the group of II-topoisomerase enzymes. Mechanism of action is based on the 1-alkyl-1,4-dihydro-4-oxoquinoline-3-carboxylic acid skeleton of fluoroquinolones. Two coplanar carbonyl groups are bonding sites for DNA gyrase. 6-Fluoro and 7-piperazinyl groups are responsible for the broad spectrum of antibacterial activities. Chemical modifications at C7 are suitable for controlling the pharmacokinetic properties.⁹⁸ Resistance to quinolones is often induced by mutations of replication genes and segregation of chromosomal DNA. Several types of mutation are determined by region of *gyrA* which encodes the DNA gyrase subunit A. They are associated with high level of fluoroquinolones resistance in *M. tbc.*⁹⁹

Quinolones which were used for connection with chitosan belong to second and third generations. Quinolones of II. generation: 1) Norfloxacin (NFX) is effective against Enterobacteriaceae. Efficiency to G⁺ and mycobacteria is weak. Usually NFX is prescribed to urinary infections. 2) Ciprofloxacin (CPX) has inhibition effect against most of G⁻, *S. aureus*, *M. tbc.* (4 µg/mL)¹⁰⁰, *Mycobacterium fortuitum* and *Mycobacterium kansasii*. CPX is prescribed to urinary infections and enterocolitis. Administration of CPX is intravenous or per oral due to high bio-availability (85 %).¹⁰¹ 3) Ofloxacin (OFX) is used in similar cases as CPX.

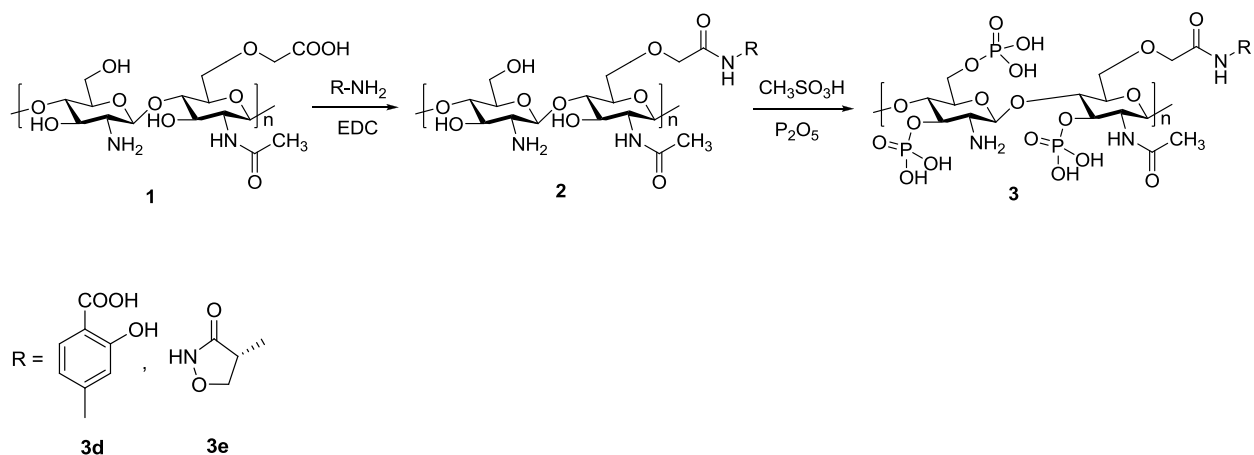
Antimicrobial activity is weaker against *Pseudomonas aeruginosa*. *In vitro* activity against *M. tbc.* is 2 µg/mL.¹⁰⁰ 4) Levofloxacin (LVX) is *S*-isomer of OFX and ten times more efficient than *R*-isomer. LFX exhibits the same properties as OFX, LFX shows significant effect against penicillin resistant *Streptococcus pneumoniae*.¹⁰² *In vitro* activity against *M. tbc.* is 1 µg/mL.¹⁰⁰

Quinolones of III. generation: 1) Enoxacin (ENX) has very broad spectrum on G⁻ bacteria, staphylococci and aminoglycoside-resistant microorganism. ENX demonstrates high penetration into kidney and 94.7 % long-term eradication rate against *E. coli*.¹⁰³ 2) Lomefloxacin (LMX) has been used in clinical trials and is approved in several countries for the treatment of infections caused by a variety of organisms, particularly G⁻ (including *Pseudomonas spp.*, *Klebsiella spp.*, *E. coli*, and *Haemophilus influenzae*).¹⁰⁴ 3) Sparfloxacin (SPX) is characterized by excellent activity against G⁺ (*Streptococcus pneumoniae*) and selected activity against anaerobes and atypical pathogens. Metal complexes of SPX (Fe²⁺-SPX and Cd²⁺-SPX) exhibited significantly higher antibacterial and antifungal activity than free SPX.¹⁰⁵

Principle of the synthesis of chitosan compounds was similar as in the Paper III. Three approaches of synthesis were developed. *O*-carboxymethyl or *N*-succinyl chitosan exhibited good water solubility and were used for the connection with second line antituberculous drugs. Third possibility of linkage was a direct bond between chitosan and drugs. This synthetic way was utilized for fluoroquinolones. NFX, CPX, ENX, LMX and SPX have free secondary amino group in piperazinyl ring which was primarily protected by acetylation. Following step was ordinary reaction with primary amino group of free chitosan and free carboxylic group of protected fluoroquinolones. Phosphorylation as a final step proceeded with presence of methanesulfonic acid and phosphorus pentoxide. Acetylated amino group in piperazinyl ring was deprotected during this reaction due to low pH. Generally, phosphorylation enhanced solubility of aqueous solutions.

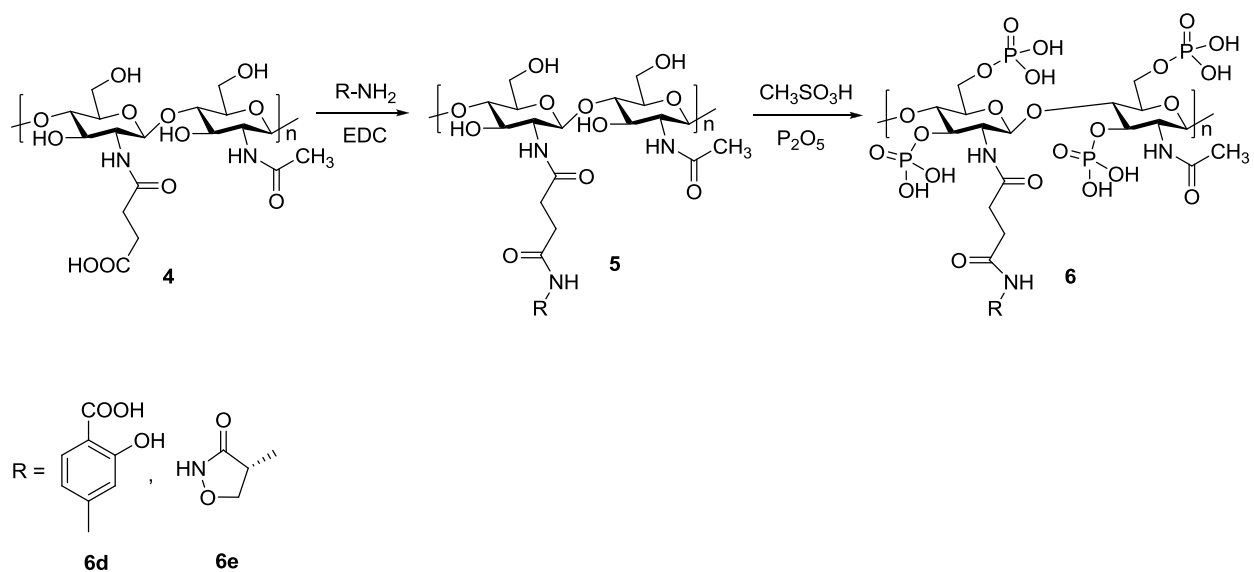
O-carboxymethyl chitosan was connected with PAS or CS through an activation of carboxylic groups by EDC (Scheme 3). The reaction of PAS has two possibilities of linkage: first covalent bond can connect carboxylic group of OCMC and amino group of PAS; second linkage can exist between amino group of OCMC and carboxylic group of PAS. In the second step of

synthesis, derivatives were phosphorylated by methanesulfonic acid and phosphorus pentoxide. Finally, both compounds were dissolved in 10 % solution of NaOH.



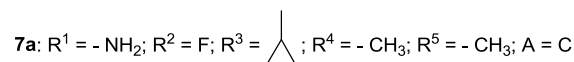
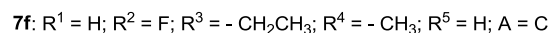
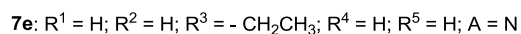
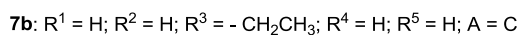
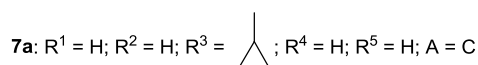
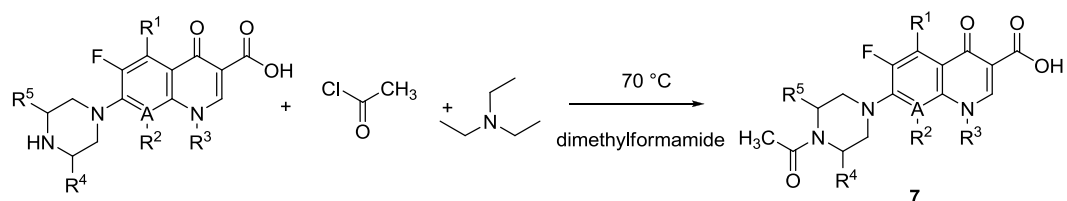
Scheme 3. Conjugation of OCMC and antituberculosic drugs

Second approach of synthesis was based on the connection of *N*-succinyl chitosan with PAS or CS with activation of carboxylic groups by EDC. For increasing water solubility, derivatives were phosphorylated by methanesulfonic acid and phosphorus pentoxide (Scheme 4). Compound **6d** was completely dissolved in water, compound **6e** was dissolved in 10 % solution of NaOH.



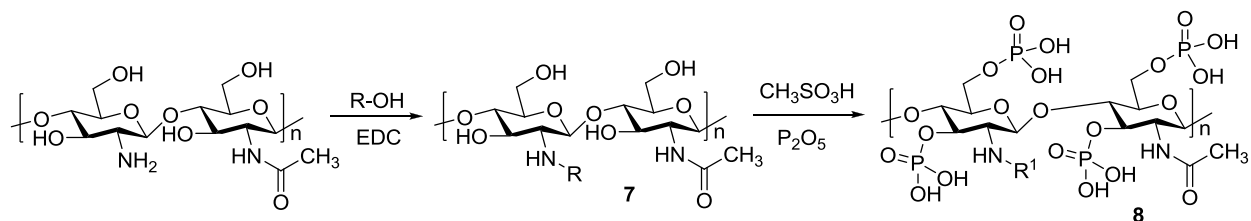
Scheme 4. Conjugation of NSCS and antituberculosic drugs

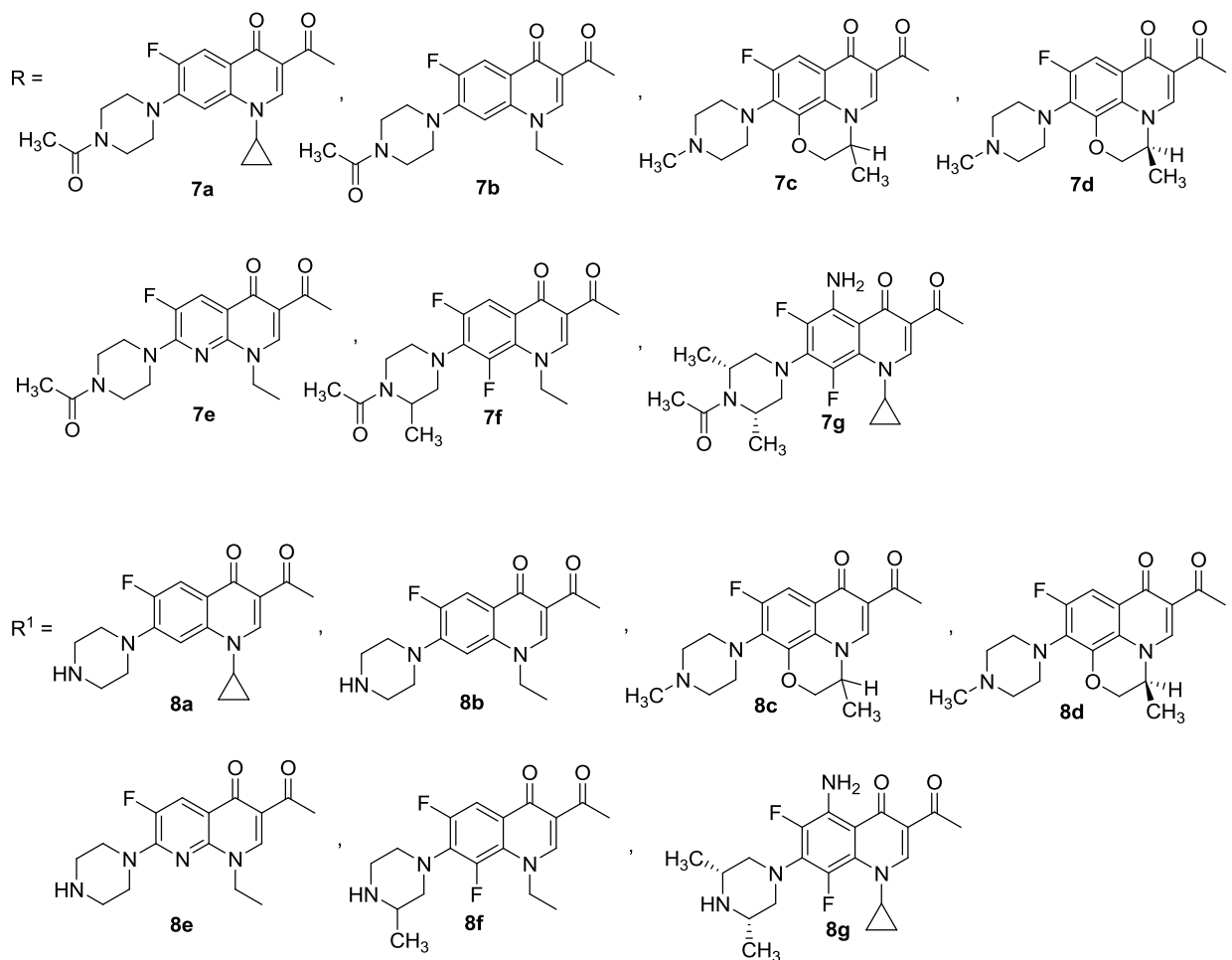
Secondary amino groups of piperazinyl ring were protected by acetylation which is common procedure for blocking of amino group. *N*-acetylation has been performed at 70 °C in the presence of acetyl chloride and triethylamine in solution of dimethylformamide¹⁰⁶ (Scheme 5). Products were purified by column chromatography, as a mobile phase was used chloroform-ethanol 8:2. Yields of acetylated quinolones were in the range of 34 – 57 %.



Scheme 5. Synthesis of acetylated fluoroquinolones

Third approach of synthesis was covalent linkage between amino group of chitosan and protected fluoroquinolones with activation of carboxylic groups by EDC (Scheme 6). Following steps are similar as in the previous procedures (Scheme 1, 2). All compound **8a-8g** were slightly dissolved in water and showed low solubility in 10 % solution of NaOH.





Scheme 6. Conjugation of chitosan and antitubercular drugs

3.5.2.1. Determination of degree of deacetylation

Degree of deacetylation of chitosan was calculated from ratio C/N of chitosan. Data from elemental analysis were used and degree of acetylation was calculated by the formula: $DA = ((C/N) - 5.145) / (6.861 - 5.145) \times 100$. Number 5.145 corresponds to complete *N*-deacetylated chitosan and 6.861 exhibits fully acetylated chitosan. Resulting degree of deacetylation for origin chitosan is 20.04% which is in accordance with the information from Sigma-Aldrich.

3.5.2.2. Determination of molecular weight

Molecular weight (MW) of products was calculated from viscosity measurement. As an aqueous solution system 0.3 M acetic acid/0.2 M sodium acetate at 25 °C was chosen. Stock

solutions were prepared from all synthesized compounds. The Mark – Houwink equation formula was used for calculation of MW: $[\eta] = K \cdot M^a$; $[\eta]$ is intrinsic viscosity, M is molecular weight, K and a are viscometric constants depending on the degree of deacetylation of chitosan. Values for constants were $K = 0.074 \text{ cm}^3 \text{ g}^{-1}$ and $a = 0.76$. Resulting MW are summarized in Fig. 17. Original chitosan had MW 29972 Da but the synthetic procedure resulted in the significant degradation of the polymer backbone.

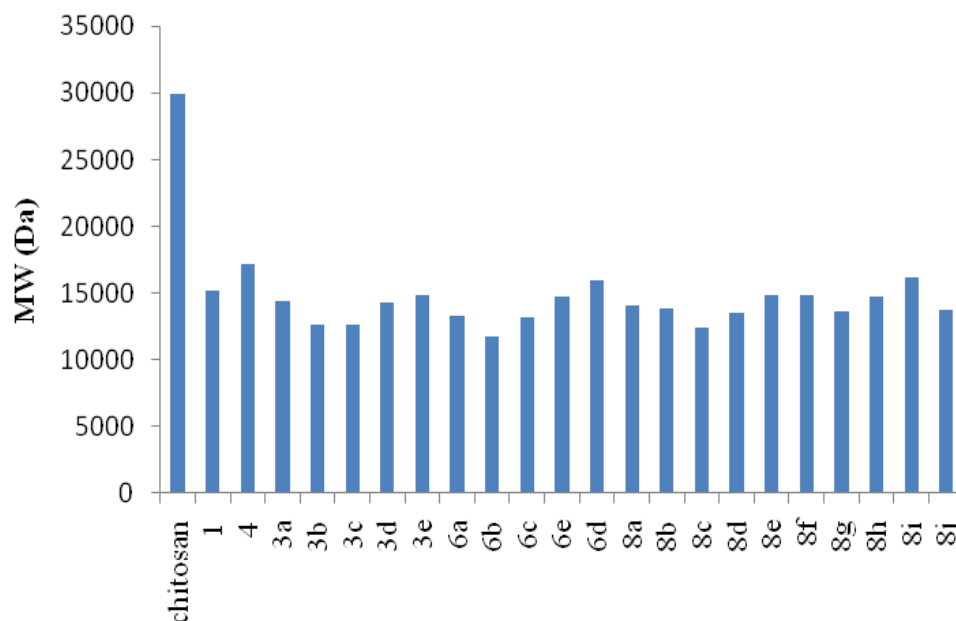


Fig. 17 Molecular weights of chitosan and prepared compounds

3.5.2.3. Determination of degree of substitution

Degree of drug substitution on prepared compounds was determined by UV spectrophotometric technique on the base of calibration curve method. Calibration curve was expressed for CS, PAS and CPX. Degree of substitution was calculated as a percentage of drug from whole polymeric molecule of product. Calibration solutions of CS and PAS were dissolved in water, calibration solutions of CPX were dissolved in 1 % CH_3COOH . Samples of products were dissolved in water (**3d**) or 10 % NaOH (**3e**, **6d**, **6e**, **8a-8g**). Fig. 18 summarizes degree of substitution of each prepared compound. In general, percentage of a content of antituberculosic drugs was low which is in accordance with the Paper III. The highest values of substitution

exhibited compounds **3d** (4.24 %), **6d** (5.60 %) and **6e** (5.95 %). The reason of high degree of substitution of **3d** can be reaction of amino and carboxylic groups of OCMC and amino and carboxylic groups of PAS. Final product is double substituted. This idea is supported by half degree of substitution of **6d**. Both CS derivatives **6d**, **6e** have degree of substitution higher than 5 %. Degrees of substitution of other prepared compounds **3e**, **8a-8g** are between 0.5 – 2.3 %.

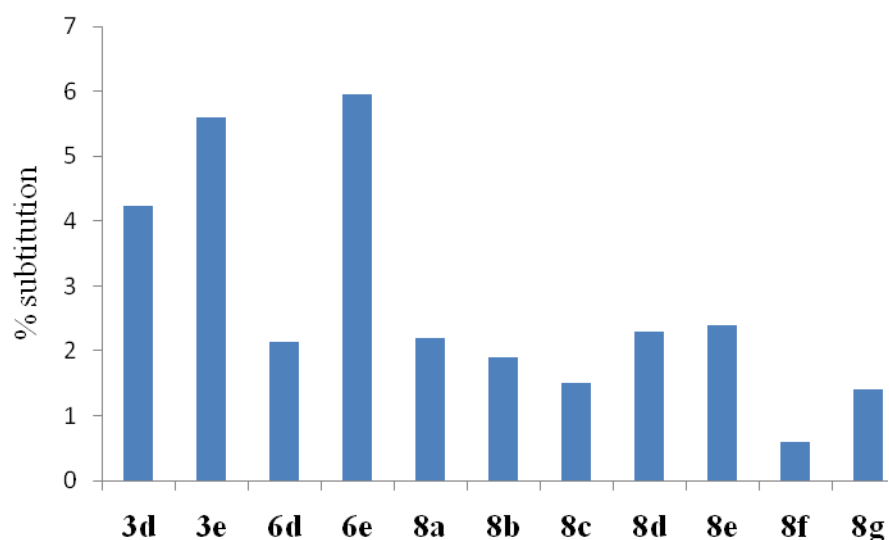


Fig. 18 Degree of substitution of prepared compounds

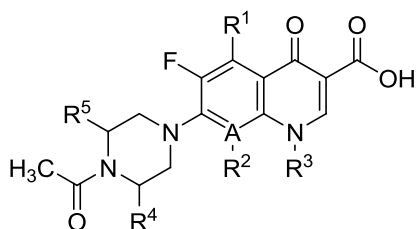
3.5.2.4. Experimental part

All chemicals were obtained from Sigma-Aldrich Co. Melting points were determined on the Büchi Melting Point B-540. Elemental analyses (C, H, N) were performed with a Perkin-Elmer 2400 CHNS/O analyzer. Infrared spectra were recorded on a Bio-Rad FTS 3000 MX spectrometer in ATR. NMR spectra were measured in DMSO-*d*₆ or D₂O solutions on a Bruker Avance 300 (300 MHz for ¹H and 75.5 MHz for ¹³C). The chemical shifts, δ , are given in ppm, related to tetramethylsilane (TMS) as an internal standard. The coupling constants (*J*) are reported in Hz. The reactions were monitored and the purity of the products was checked by TLC (Fluka silica gel/TLC cards 60 PF₂₅₄). The plates were visualized using UV light. Names of compounds were generated and structures were drawn with ChemBioDraw Ultra 11.0 and are formatted as ACS Document 1996.

General procedure of the synthesis of acetylated fluoroquinolones

Fluoroquinolone (1 mmol) was dissolved in dimethyl formamide (60 ml) at 70 °C. One molar equivalent of triethylamine and one molar equivalent of acetyl chloride were added. The mixture was stirred at 70 °C for 2 hours. The mixture was cooled to room temperature, excess of solvent was evaporated in vacuum and the residue was dissolved in dichloromethane (2x25 mL) and filtered. Column chromatography was used for cleaning the product (mobile phase: chloroform - ethanol 8:2).

Data of acetylated fluoroquinolones (**7a**, **7b**, **7e – 7g**)



General structure

7-(4-acetylpiperazin-1-yl)-1-cyclopropyl-6-fluoro-4-oxo-1,4-dihydroquinoline-3-carboxylic acid (**7a**) Yield 34.54 %; mp 250-252 °C. IR (ATR): 2920, 2849, 1733, 1668 (CO-NH), 1622, 1497, 1440, 1381 (CH₃), 1337, 1246, 1213, 1143, 1025, 999, 972, 885, 831, 804, 780, 748 cm⁻¹. ¹H NMR (DMSO-*d*₆, 300 MHz): δ 8.64 (s, 1H), 7.88 (d, *J* = 13.2 Hz, 1H), 7.55 (d, *J* = 7.4 Hz, 1H), 3.79 (m, 1H), 3.65 (m, 4H, CH₂), 3.29 (m, 4H, CH₂), 2.06 (s, 3H), 1.38 (m, 2H), 1.17 (m, 2H). ¹³C NMR (DMSO-*d*₆, 75 MHz): 176.5, 168.6, 166.1, 161.2, 154.8, 148.2, 145.2, 139.3, 119.0, 111.1, 106.9, 49.8, 45.5, 36.1, 21.4, 7.8. Anal. Calcd for C₁₉H₂₀FN₃O₄ (373.38): C, 61.12; H, 5.40; N, 11.25. Found: C, 59.81; H, 5.63; N, 10.94.

7-(4-acetylpiperazin-1-yl)-1-ethyl-6-fluoro-4-oxo-1,4-dihydroquinoline-3-carboxylic acid (**7b**) Yield 49.00 %; mp 232-234 °C. IR (ATR): 2836, 1727, 1698 (CO-NH), 1626, 1479, 1458, 1377 (CH₃), 1301, 1243, 1213, 1144, 1124, 1103, 1034, 987, 932, 887, 827, 805, 749 cm⁻¹. ¹H NMR (DMSO-*d*₆, 300 MHz): 8.96 (s, 1H), 7.94 (d, *J* = 13.2 Hz, 1H), 7.24 (d, *J* = 7.2 Hz, 1H), 4.61 (q, *J* = 6.9 Hz, 2H), 3.53 (d, *J* = 4.9 Hz, 4H, CH₂), 3.40 (d, *J* = 4.6 Hz, 4H, CH₂), 2.42 (s, 3H), 1.44 (t, *J* = 7.0 Hz, 3H, CH₃). ¹³C NMR (DMSO-*d*₆, 75 MHz): 176.4, 166.2, 158.5, 153.9, 152.0, 148.9, 144.6, 137.3, 120.1, 111.5, 107.3, 106.7, 49.3, 46.8, 42.8, 14.6. Anal.

Calcd for C₁₈H₂₀FN₃O₄ (361.37): C, 59.83; H, 5.58; N, 11.63. Found: C, 60.11; H, 5.25; N, 11.41.

7-(4-acetylpiperazin-1-yl)-1-ethyl-6-fluoro-4-oxo-1,4-dihydro-1,8-naphthyridine-3-carboxylic acid (**7e**) Yield 57.20 %; mp 218-220 °C. IR (ATR): 2891, 2554, 1723, 1658 (CO-NH), 1626, 1579, 1471, 1443, 1403, 1366, 1342, 1271, 1173, 1159, 1107, 1036, 942, 919, 827, 790, 731 cm⁻¹. ¹H NMR (DMSO-*d*₆, 300 MHz): 8.97 (s, 1H), 7.97 (d, *J* = 6.3 Hz, 1H), 4.42 (m, 2H), 3.68 (m, 4H, CH₂), 2.82 (m, 4H, CH₂), 2.43 (s, 3H), 1.38 (t, *J* = 7.3 Hz, 3H, CH₃). ¹³C NMR (DMSO-*d*₆, 75 MHz): 176.4, 166.1, 150.1, 148.1, 147.8, 146.0, 145.1, 119.4, 112.5, 108.2, 48.5, 47.4, 45.8, 40.2, 14.9. Anal. Calcd for C₁₇H₁₉FN₄O₄ (362.36): C, 56.35; H, 5.29; N, 15.46. Found: C, 56.74; H, 5.46; N, 15.82.

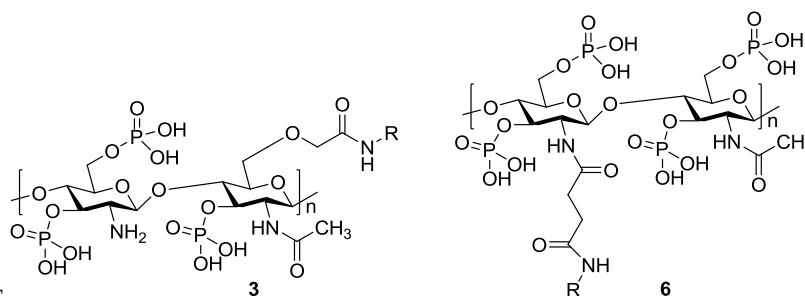
7-(4-acetyl-3-methylpiperazin-1-yl)-1-ethyl-6,8-difluoro-4-oxo-1,4-dihydroquinoline-3-carboxylic acid (**7f**) Yield 44.80 %; mp 235-237 °C. IR (ATR): 2697, 2456, 1722, 1690 (CO-NH), 1613, 1542, 1542.4, 1492, 1473, 1450, 1393 (CH₃), 1329, 1300, 1254, 1206, 1115, 1042, 1007, 979, 933, 892, 808, 757 cm⁻¹. ¹H NMR (DMSO-*d*₆, 300 MHz): 9.31 (s, 1H, COOH), 8.98 (s, 1H), 7.94 (d, *J* = 4.8 Hz, 1H), 4.59 (m, 2H), 3.71 (m, 4H, CH₂), 3.32 (m, 4H, CH₂), 2.46 (s, 3H), 1.44 (t, *J* = 6.4 Hz, 3H, CH₃), 1.23 (s, 3H, CH₃). ¹³C NMR (DMSO-*d*₆, 75 MHz): 176.7, 166.1, 160.2, 152.5, 147.6, 142.9, 138.5, 120.6, 111.3, 107.1, 106.9, 49.2, 46.5, 42.9, 17.5, 15.4. Anal. Calcd for C₁₉H₂₁F₂N₃O₄ (393.38): C, 58.01; H, 5.38; N, 10.68. Found: C, 58.26; H, 5.62; N, 10.29.

7-((3*R*,5*S*)-4-acetyl-3,5-dimethylpiperazin-1-yl)-5-amino-1-cyclopropyl-6,8-difluoro-4-oxo-1,4-dihydroquinoline-3-carboxylic acid (**7g**) Yield 54.80 %; mp 261-263 °C. IR (ATR): 2962, 2841, 1712, 1684 (CO-NH), 1641, 1585, 1530, 1440, 1395 (CH₃), 1332, 1292, 1185, 1150, 1084, 1029, 997, 963, 911, 808, 759 cm⁻¹. ¹H NMR (DMSO-*d*₆, 300 MHz): 8.50 (s, 1H), 7.30 (s, 2H, NH₂), 3.26 (m, 4H, CH₂), 2.88 (s, 2H, CH), 2.49 (m, 1H, CH), 2.05 (s, 3H, CH₃), 1.34 (s, 6H, CH₃), 1.03 (d, *J* = 5.9 Hz, 4H, CH₂). ¹³C NMR (DMSO-*d*₆, 75 MHz): 180.4, 169.0, 165.6, 162.2, 150.4, 136.5, 134.3, 128.1, 105.7, 57.5, 55.6, 51.0, 36.0, 30.9, 21.6, 19.2, 8.6. Anal. Calcd for C₂₁H₂₄F₂N₄O₄ (434.44): C, 58.06; H, 5.57; N, 12.90. Found: C, 57.82; H, 5.69; N, 13.27.

General procedure of the synthesis of compounds **3d**, **3e**, **6d**, **6e**

500 mg of *O*-carboxymethyl (**1**) or *N*-succinyl chitosan (**4**) was dissolved in water and 200 mg of appropriate drug (CS or PAS) was added. The mixture was cooled at 0 - 5 °C. The carboxylic group was activated with 220 mg of *N*-(3-dimethylaminopropyl)-*N'*-ethylcarbodiimide and the reaction mixture was stirred at 0 - 5 °C for 3 hours, then the temperature gradually increased to the room temperature. After 24 hours without isolation 2 ml of methanesulfonic acid and 300 mg of phosphorus pentoxide was added to the mixture. The reaction was stirred at 0 - 5 °C for 3 hours. The mixture was cooled overnight in a freezer and then products **3** or **6** were precipitated with acetone.

Data of compounds **3d**, **3e**, **6d**, **6e**



General structures

GluN and GluNAc are abbreviations which occur at the interpretations of ¹H NMR for units of chitosan D-glucosamine and N-acetyl-D-glucosamine.

OCMC conjugated with PAS (**3d**) Yield 82.15 %. IR (ATR): large peak 1633 (ν (CO-NH)), large peak 1434 (ν (COO⁻)), sharp peak 1246 (ν (P=O)), sharp intensive peak 1198 (δ (N-H)), strong peak 1061 (δ (sec. OH)), 788 (δ (C-H arom. ring)) cm⁻¹. ¹H NMR (DMSO-*d*₆, 300 MHz): 6.65 (s, 1H, H5'), 6.13 (m, 1H, H6'), 5.42 (s, 1H, H2'), 4.60 (s, 1H, H1 (GluN)), 4.40 (s, 1H, H1 (GluNAc)), 4.34 (s, 1H, NH), 3.15-2.80 (4H, H3, H4, H5, H6), 3.34 (s, 2H, CH₂), 2.94 (m, 1H, H2 (GluNAc)), 2.22 (s, 1H, H2 (GluN)), 1.59 (m, 3H, CH₃).

OCMC conjugated with CS (**3e**) Yield 87.26 %. IR (ATR): large peak 1658 (ν (CO-NH)), thin band 1577 (ν (CO-NH II.); δ (NH₂)), thin band 1414 (δ (CH₂, CH₃)), sharp peak 1249 (ν (P=O)), sharp intensive peak 1189 (δ (N-H)), strong peak 1060 (δ (sec. OH)), 991, 788 cm⁻¹. ¹H NMR (DMSO-*d*₆, 300 MHz): 6.14 (s, 1H, NH), 4.67 (s, 1H, H1 (GluN)), 4.33 (s, 1H, H1 (GluNAc)), 3.99 (s, 1H, NH), 3.83 (m, 2H, CH₂), 3.34 (m, 1H, CH), 3.26 (m, 2H, CH₂), 3.10-

2.85 (4H, H3, H4, H5, H6), 2.72 (s, 1H, H2 (GluNAc)), 2.21 (s, 1H, H2 (GluN)), 1.59 (m, 3H, CH₃).

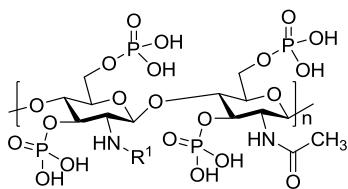
NSCS conjugated with PAS (**6d**) Yield 91.11 %. IR (ATR): large peak 1647 (ν (CO-NH)), thin band 1597 (ν (CO-NH II.); δ (NH₂)), thin band 1438 (δ (CH₂, CH₃)), sharp peak 1263 (ν (P=O)), sharp intensive peak 1184 (δ (N-H)), strong peak 1051 (δ (sec. OH)), 786 (δ (C-H arom. ring)) cm⁻¹. ¹H NMR (DMSO-*d*₆, 300 MHz): 8.34 (s, 1H, OH), 7.09 (s, 1H, H5'), 5.86 (m, 1H, H6'), 5.82 (s, 1H, H2'), 4.98 (s, 1H, H1 (GluN)), 4.82 (s, 1H, H1 (GluNAc)), 4.71 (s, 1H, NH), 3.58-3.25 (4H, H3, H4, H5, H6), 3.17 (s, 4H, -CH₂-CH₂-), 2.64 (m, 1H, H2 (GluNAc)), 2.21 (s, 1H, H2 (GluN)), 2.02 (m, 3H, CH₃).

NSCS conjugated with CS (**6e**) Yield 93.20 %. IR (ATR): large peak 1659 (ν (CO-NH)), large peak 1642 (ν (CO-NH I.)), thin band 1549 (ν (CO-NH II.); δ (NH₂)), large band 1441 (δ (CH₂, CH₃)), sharp peak 1249 (ν (P=O)), sharp intensive peak 1191 (δ (N-H)), small peak 1061 (δ (sec. OH)), 1012, 868, 788 cm⁻¹. ¹H NMR (DMSO-*d*₆, 300 MHz): 6.14 (s, 1H, NH), 4.80 (s, 1H, H1 (GluN)), 4.35 (s, 1H, H1 (GluNAc)), 3.92 (s, 1H, NH), 3.80 (m, 2H, CH₂), 3.30 (m, 1H, CH), 3.16-2.75 (4H, H3, H4, H5, H6), 2.44 (s, 4H, -CH₂-CH₂-), 2.22 (s, 1H, H2 (GluNAc)), 1.78 (s, 1H, H2 (GluN)), 1.59 (m, 3H, CH₃).

General procedure of the synthesis of compounds **8a** – **8g**

500 mg of chitosan was dissolved in water and 100 mg of appropriate fluoroquinolones or acetylated forms (OFX, LFX, **7a**, **7b**, **7e**, **7f** and **7g**) were added. The mixture was cooled at 0 - 5 °C. The carboxylic group of quinolones was activated with 120 mg of *N*-(3-dimethylaminopropyl)-*N'*-ethylcarbodiimide and the reaction mixture was stirred at 0 - 5 °C for 3 hours, then the temperature gradually increased to the room temperature. After 24 hours without isolation 2 ml of methanesulfonic acid and 300 mg of phosphorus pentoxide was added to the mixture. The reaction was stirred at 0 - 5 °C for 3 hours. The mixture was cooled overnight in a freezer and then products **8a-8g** were precipitated with acetone.

Data of compounds **8a** – **8g**



General structure

Chitosan conjugated with CPX (**8a**) Yield 82.97 %. IR (ATR): large peak 1665 (ν (CO-NH)), large peak 1619 (ν (CO-NH I.)), thin band 1581 (ν (CO-NH II.); δ (NH₂)), thin band 1487 (δ (CH₂, CH₃)), sharp peak 1262 (ν (P=O)), sharp intensive peak 1107 (δ (C-N)), small peak 1063 (δ (sec. OH)), 979 (ν (P-O-R)), 850, 750 cm⁻¹. ¹H NMR (DMSO-*d*₆, 300 MHz): 7.93 (s, 1H, arom. H), 7.81 (s, 1H, arom. H), 6.14 (s, 1H, arom. H), 4.60 (s, 1H, H1 (GluN)), 4.34 (s, 1H, H1 (GluNAc)), 4.27 (s, 1H, NH), 3.35 (m, 4H, CH₂), 3.33 (m, 4H, CH₂), 3.06-2.83 (4H, H3, H4, H5, H6), 2.71 (s, 1H, H2 (GluNAc)), 2.22 (s, 1H, H2 (GluN)), 1.59 (m, 3H, CH₃), 1.31 (m, 4H, CH₂).

Chitosan conjugated with NFX (**8b**) Yield 91.20 %. IR (ATR): large peak 1665 (ν (CO-NH)), large peak 1630 (ν (CO-NH I.)), thin band 1584 (ν (CO-NH II.); δ (NH₂)), thin band 1482 (δ (CH₂, CH₃)), sharp peak 1268 (ν (P=O)), sharp intensive peak 1105 (δ (C-N)), small peak 1068 (δ (sec. OH)), 982 (ν (P-O-R)), 853, 748 cm⁻¹. ¹H NMR (DMSO-*d*₆, 300 MHz): 7.86 (s, 1H, arom. H), 7.55 (s, 1H, arom. H), 6.23 (s, 1H, arom. H), 4.59 (s, 1H, H1 (GluN)), 4.28 (s, 1H, H1 (GluNAc)), 4.11 (s, 1H, NH), 3.29 (m, 4H, CH₂), 3.14 (m, 4H, CH₂), 3.16-2.87 (4H, H3, H4, H5, H6), 2.74 (s, 1H, H2 (GluNAc)), 2.21 (s, 1H, H2 (GluN)), 1.59 (m, 3H, CH₃), 1.32 (m, 2H, CH₂), 0.48 (t, 3H, CH₃).

Chitosan conjugated with OFX (**8c**) Yield 85.42 %. IR (ATR): large peak 1659 (ν (CO-NH)), large peak 1626 (ν (CO-NH I.)), thin band 1581 (ν (CO-NH II.); δ (NH₂)), thin band 1413 (δ (CH₂, CH₃)), sharp peak 1264 (ν (P=O)), 1192, sharp intensive peak 1107 (δ (C-N)), small peak 1062 (δ (sec. OH)), 990 (ν (P-O-R)), 924, 788 cm⁻¹. ¹H NMR (DMSO-*d*₆, 300 MHz): 6.78 (s, 1H, arom. H), 5.00 (s, 1H, H1 (GluN)), 4.65 (s, 1H, H1 (GluNAc)), 4.53 (s, 1H, NH), 3.71 (m, 4H, CH₂), 3.66 (m, 4H, CH₂), 3.46-3.29 (4H, H3, H4, H5, H6), 2.80 (s, 1H, H2 (GluNAc)), 2.22 (s, 1H, H2 (GluN)), 2.01 (m, 3H, CH₃), 1.90 (m, 3H, CH₃), 1.69 (m, 3H, CH₃).

Chitosan conjugated with LFX (**8d**) Yield 89.36 %. IR (ATR): large peak 1668 (ν (CO-NH)), large peak 1619 (ν (CO-NH I.)), thin band 1580 (ν (CO-NH II.); δ (NH₂)), thin band 1414 (δ

(CH₂, CH₃), sharp peak 1262 (ν (P=O)), sharp intensive peak 1107 (δ (C-N)), 980 (ν (P-O-R)), 890, 750 cm⁻¹. ¹H NMR (DMSO-*d*₆, 300 MHz): 6.77 (s, 1H, arom. H), 5.00 (s, 1H, H1 (GluN)), 4.65 (s, 1H, H1 (GluNAc)), 4.53 (s, 1H, NH), 3.70 (m, 4H, CH₂), 3.68 (m, 4H, CH₂), 3.46-3.31 (4H, H3, H4, H5, H6), 2.80 (s, 1H, H2 (GluNAc)), 2.20 (s, 1H, H2 (GluN)), 2.01 (m, 3H, CH₃), 1.90 (m, 3H, CH₃), 1.70 (m, 3H, CH₃).

Chitosan conjugated with ENX (**8e**) Yield 90.80 %. IR (ATR): large peak 1665 (ν (CO-NH)), large peak 1619 (ν (CO-NH I.)), thin band 1581 (ν (CO-NH II.); δ (NH₂)), thin band 1487 (δ (CH₂, CH₃)), sharp peak 1262 (ν (P=O)), sharp intensive peak 1107 (δ (C-N)), small peak 1063 (δ (sec. OH)), 979 (ν (P-O-R)), 850, 750 cm⁻¹. ¹H NMR (DMSO-*d*₆, 300 MHz): 7.82 (s, 1H, arom. H), 7.41 (s, 1H, arom. H), 4.68 (s, 1H, H1 (GluN)), 4.31 (s, 1H, H1 (GluNAc)), 3.82 (s, 1H, NH), 3.21 (m, 4H, CH₂), 3.10 (m, 4H, CH₂), 3.04-2.80 (4H, H3, H4, H5, H6), 2.73 (s, 1H, H2 (GluNAc)), 2.21 (s, 1H, H2 (GluN)), 1.59 (m, 3H, CH₃), 1.33 (m, 2H, CH₂), 0.45 (t, 3H, CH₃).

Chitosan conjugated with LMX (**8f**) Yield 84.36 %. IR (ATR): large peak 1659 (ν (CO-NH)), large peak 1619 (ν (CO-NH I.)), thin band 1580 (ν (CO-NH II.); δ (NH₂)), thin band 1414 (δ (CH₂, CH₃)), sharp peak 1263 (ν (P=O)), sharp intensive peak 1108 (δ (C-N)), 979 (ν (P-O-R)), 889, 750 cm⁻¹. ¹H NMR (DMSO-*d*₆, 300 MHz): 7.85 (s, 1H, arom. H), 7.39 (s, 1H, arom. H), 4.61 (s, 1H, H1 (GluN)), 4.38 (s, 1H, H1 (GluNAc)), 3.83 (s, 1H, NH), 3.26 (m, 4H, CH₂), 3.09 (m, 4H, CH₂), 3.06-2.80 (4H, H3, H4, H5, H6), 2.70 (s, 1H, H2 (GluNAc)), 2.20 (s, 1H, H2 (GluN)), 1.58 (m, 3H, CH₃), 1.30 (m, 2H, CH₂), 0.43 (t, 3H, CH₃).

Chitosan conjugated with SPX (**8g**) Yield 86.25 %. IR (ATR): large peak 1665 (ν (CO-NH)), large peak 1619 (ν (CO-NH I.)), thin band 1581 (ν (CO-NH II.); δ (NH₂)), thin band 1487 (δ (CH₂, CH₃)), sharp peak 1262 (ν (P=O)), sharp intensive peak 1107 (δ (C-N)), small peak 1063 (δ (sec. OH)), 979 (ν (P-O-R)), 850, 750 cm⁻¹. ¹H NMR (DMSO-*d*₆, 300 MHz): 7.83 (s, 1H, arom. H), 4.67 (s, 1H, H1 (GluN)), 4.41 (s, 1H, H1 (GluNAc)), 4.09 (s, 1H, NH), 3.38 (m, 4H, CH₂), 3.09 (m, 4H, CH₂), 3.01-2.76 (4H, H3, H4, H5, H6), 2.73 (s, 1H, H2 (GluNAc)), 2.59 (m, 2H, NH₂), 2.50 (m, 1H, CH), 2.22 (s, 1H, H2 (GluN)), 1.60 (m, 3H, CH₃), 1.30 (m, 4H, CH₂), 0.42 (t, 6H, CH₃).

^{13}C NMR spectra were not measured because the compounds were not soluble in water. Antibacterial activity and evaluation of cytotoxicity are under investigation.

3.6. Chitosan connected with dyes

3.6.1. Chitosan connected with photosensitizer dyes

The idea of connection of chitosan with photosensitizing agents was initiated by a co-operation with the Institute of Inorganic Chemistry, Academy of Science of the Czech Republic. Water soluble polymers containing photoactive group are studied as potential photosensitizers in photodynamic therapy (PDT). Lately, PDT has been studied as one of therapeutic possibilities in cancer, atherosclerosis, or in inactivation of bacteria¹⁰⁷ and viruses. Chitosan with advantageous biological properties has shown considerable attention as a suitable carrier for photosensitizers.

PDT combines therapeutic usage of drugs (photosensitizers) with a specific type of light which is able to activate them. PDT is based on photodynamic effects resulted in the oxidative damage of biological material by reactive forms of oxygen generated by sensitized reactions. The main photodynamical active species is singlet oxygen $^1\text{O}_2(^1\Delta_g)$ generated *in situ* by energy transfer from an excited sensitizer to oxygen molecule.¹⁰⁸ $^1\text{O}_2$ is a metastable excited state of basic state of molecular oxygen $^3\text{O}_2$.

In cancer therapy, the photodynamic effect is intensively studied. The sensitizer can be administered to the active site by intravenous injection. The high affinity of sensitizer to active site is given by different morphology and metabolism of fast growing tissue, where is accumulated and irradiated by the light with wavelength 600 - 900 nm. This light (laser, LED diodes) is able to excite the sensitizer. Excited sensitizer transfers the energy to free dissolved oxygen in tissues. Singlet oxygen and other reactive particles can destroy tumor cells.¹⁰⁹

High amount of dyes, aromatic and heterocyclic organic compounds and metal complexes are used for their ability to produce singlet oxygen. Sensitizers acceptable for PDT must have specific requirements: maximum absorption 600 - 800 nm, minimum absorption 400 - 600 nm, quantum yields of $^1\text{O}_2$ in a range of 0.3 - 0.8, stability against photodegradation and against

oxidation by $^1\text{O}_2$ or other reactive oxygen species generated *in situ*, non-toxicity, phototoxicity, specific retention in the malignant tissue and solubility.¹⁰⁸

Two photosensitizers, *meso*-tetra(4-carboxyphenyl)porphin (TPPC4)¹¹⁰ and rose bengal (RB)¹¹¹, were chosen for reactions with chitosan. Both molecules are sensitizers with type (π,π^*), excited electron comes from π orbital, resulting generation of $^1\text{O}_2$. TPPC4 belongs to porphyrinoid sensitizers, which are mostly used for this purpose because of their inherent similarity to natural porphyrins and competent physicochemical and photochemical properties. Porphyrins have a strong blue absorption band. Synthetic porphyrins are often substituted in the *meso*-position and they are applied as free ligands (non-metallated). Other porphyrinoid sensitizers can be complexed with Al, Zn, Mg, Ga, Si, Ge or Sn as central ions. The approximately planar porphyrinoid sensitizers tend to form stacked dimers (aggregates) held together by π - π interactions of the aromatic rings and by hydrophobic interactions.¹¹²

Rose bengal (4,5,6,7-tetrachloro-3',6'-dihydroxy-2',4',5',7'-tetraiodo-3*H*-spiro[isobenzofuran-1,9'-xanthen]-3-one, RB) is a water soluble photosensitizing dye, its structure is related to xanthene. It exhibits long live triplet state in high quantum yields. RB has a tendency to aggregation in high concentrated solutions which is undesirable property, because it impairs photochemical response.¹¹³ RB has an affinity to the surface of the nonviable cell and after light exposition, membrane damage and eventual cell lysis are induced, therefore RB is used to evaluate ocular surface diseases.¹¹⁴ RB has minimal side effects and is used in breast and melanoma cancer therapy. It is able to involve the induction of cell death by death receptor-mediated pathway and mitochondrial apoptotic pathway.¹¹⁵

The purpose of connection of chitosan with sensitizers was photoantimicrobial activity in wound healing treatment.¹¹⁶ The production of nanofibres was tried from the acidic solution of prepared compound chitosan with RB. The solubility of compound was not complete; nevertheless many experiments with different setting of machine were performed. In Fig. 19, there are nanofibres of chitosan with RB. Unluckily, prepared nanofibres had not an appropriate quality. Experiments are still under investigation.

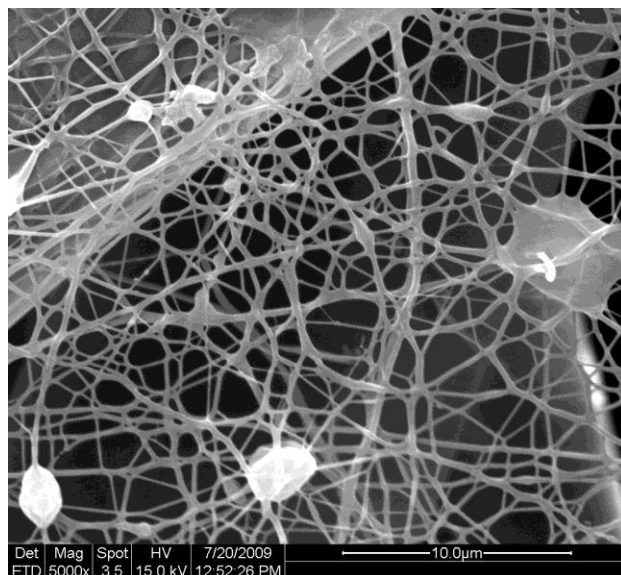
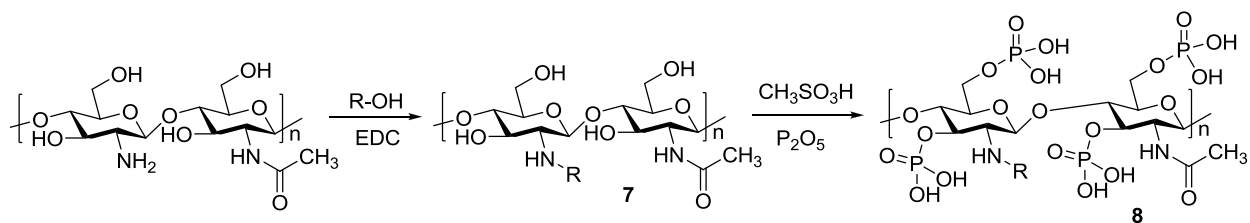
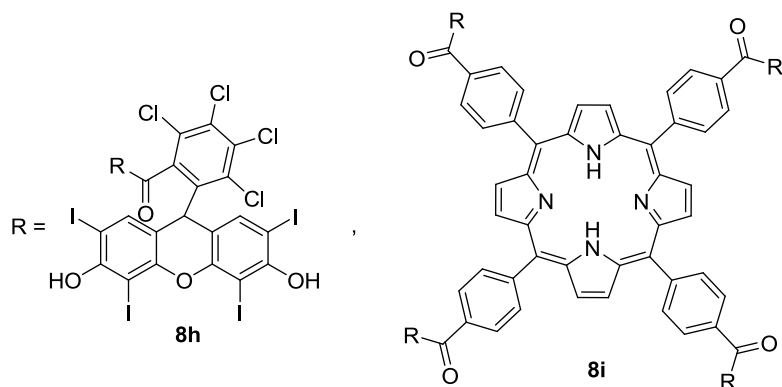


Fig. 19. Scanning electron microscopy image of the resulting nanofibres of chitosan connected with RB.

Nanofibrous layers were produced using the NanospiderTM electrospinning technology. A cylindrical-shape spinning electrode connected with a high voltage source rotated in a polymer solution. A highly charged thin layer of the solution on the electrode surface was then transformed into nanofibres, which were collected on a linearly moving grounded polypropylene textile.¹¹⁷

Covalent linkage between amino group of chitosan and carboxylic groups of TPPC4 or RB was prepared (Scheme 7). EDC was used for activation of carboxylic acid. Without further precipitation, phosphorylation was realized. The structure of TPPC4 allows reaction of all carboxylic groups and connected chains of chitosan together. Both compound **8h-8i** were slightly dissolved in water and acidic acid.





Scheme 7 Conjugation of chitosan and photosensitising drugs

3.6.1.1. Experimental part

General procedure of the synthesis of compounds **8h** and **8i**

500 mg of chitosan was dissolved in water and 100 mg of RB or TPPC4 was added. The mixture was cooled at 0 - 5 °C. The carboxylic groups of dyes were activated with 120 mg of *N*-(3-dimethylaminopropyl)-*N'*-ethylcarbodiimide and the reaction mixture was stirred at 0 - 5 °C for 3 hours, then the temperature gradually increased to the room temperature. After 24 hours without isolation 2 ml of methanesulfonic acid and 300 mg of phosphorus pentoxide was added to the mixture. The reaction was stirred at 0 - 5 °C for 3 hours. The mixture was cooled overnight in a freezer and then products **8h** and **8i** were precipitated with acetone.

Data of compounds **8h** and **8i**

Chitosan conjugated with RB (**8h**) Yield 62.87 %. IR (ATR): large peak 1663 (ν (CO-NH)), large peak 1617 (ν (CO-NH I.)), thin band 1581 (ν (CO-NH II.); δ (NH₂)), thin band 1485 (δ (CH₂, CH₃)), sharp peak 1263 (ν (P=O)), sharp intensive peak 1107 (δ (C-N)), small peak 1062 (δ (sec. OH)), 992 (ν (P-O-R)), 919, 751 cm⁻¹. ¹H NMR (DMSO-*d*₆, 300 MHz): 7.85 (s, 1H, arom. H), 4.91 (s, 1H, CH), 4.62 (s, 1H, H1 (GluN)), 4.38 (s, 1H, H1 (GluNAc)), 3.83 (s, 1H, NH), 3.30 (s, 2H, NH₂), 3.15-2.80 (4H, H3, H4, H5, H6), 2.74 (s, 1H, H2 (GluNAc)), 2.21 (s, 1H, H2 (GluN)), 1.60 (m, 3H, CH₃).

Chitosan conjugated with TPPC4 (**8i**) Yield 53.90 %. IR (ATR): large peak 1663 (ν (CO-NH)), large peak 1617 (ν (CO-NH I.)), thin band 1485 (δ (CH₂, CH₃)), sharp peak 1264 (ν (P=O)),

sharp intensive peak 1195 (δ (N-H)), sharp intensive peak 1107 (δ (C-N)), small peak 1061 (δ (sec. OH)), 993 (ν (P-O-R)), 919, 750 cm^{-1} . ^1H NMR (DMSO- d_6 , 300 MHz): 9.58 (s, 1H, arom. H), 7.82 (s, 1H, arom. H), 4.62 (s, 1H, H1 (GluN)), 4.38 (s, 1H, H1 (GluNAc)), 3.81 (s, 1H, NH), 3.30 (s, 2H, NH_2), 3.11-2.79 (4H, H3, H4, H5, H6), 2.71 (s, 1H, H2 (GluNAc)), 2.20 (s, 1H, H2 (GluN)), 1.60 (m, 3H, CH_3).

3.6.2. Chitosan connected with fluorescein isothiocyanate

The co-operation with Department of Pharmacology and Toxicology, Pharmaceutical faculty, Charles University in Prague has started determination of cytotoxicity of chitosan derivatives by fluorescent method. Chitosan alone was not detectable by this method (as described in Paper III), it was necessary to synthesize chitosan connected with fluorescent dye. Fluorescein isothiocyanate (3',6'-dihydroxy-5-isothiocyanato-3*H*-spiro[isobenzofuran-1,9'-xanthen]-3-one, FITC) is fluorescent label used in wide range of applications, including flow cytometry, fluorescence *in situ* hybridisation or immunohistochemical techniques which are based on labeling targeted structure (antibody, receptor).

Co-operation with Eötvös Lóránd University, Research Group of Peptide Chemistry, Hungarian Academy of Science in Budapest led us to determine uptake studies of chitosan connected with FITC. Firstly, prepared compound was used under fluorescent microscope (Fig. 20a, 20b) for an evaluation uptake on PBMC cells. Unfortunately, the solubility of compound in media RPMI-1640 medium without phenol red was not high and the active time for uptake was probably short (3 hours). In Fig. 20a and 20b chitosan connected with FITC seems to be aggregated in solution but no uptake is observed. This study is still under investigation.

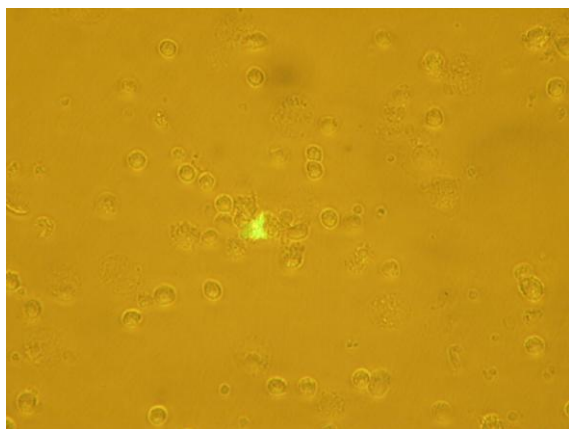


Fig. 20a Insoluble particle of chitosan connected with FITC under fluorescent microscope, no cellular uptake was observed

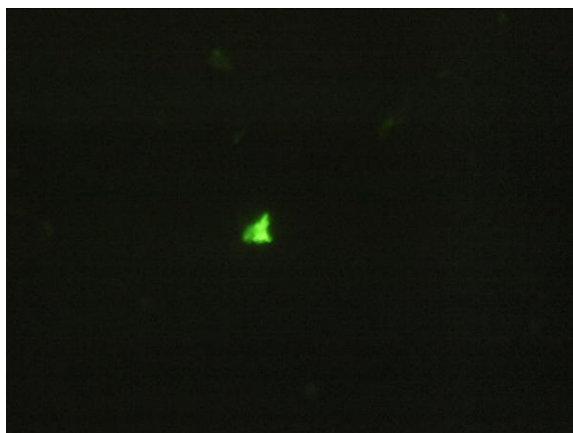


Fig. 20b Insoluble particle of chitosan connected with FITC under fluorescent microscope

Second study was the fluorescence uptake experiment evaluated on flow cytometer on the same sample of chitosan connected with FITC in range of concentration on PBMC cells (Fig. 21). Relatively high cellular uptake was observed on macrophages and monocytes due to their strong ability of phagocytoses. Lymphocytes showed very low uptake which is in accordance with their biological function.

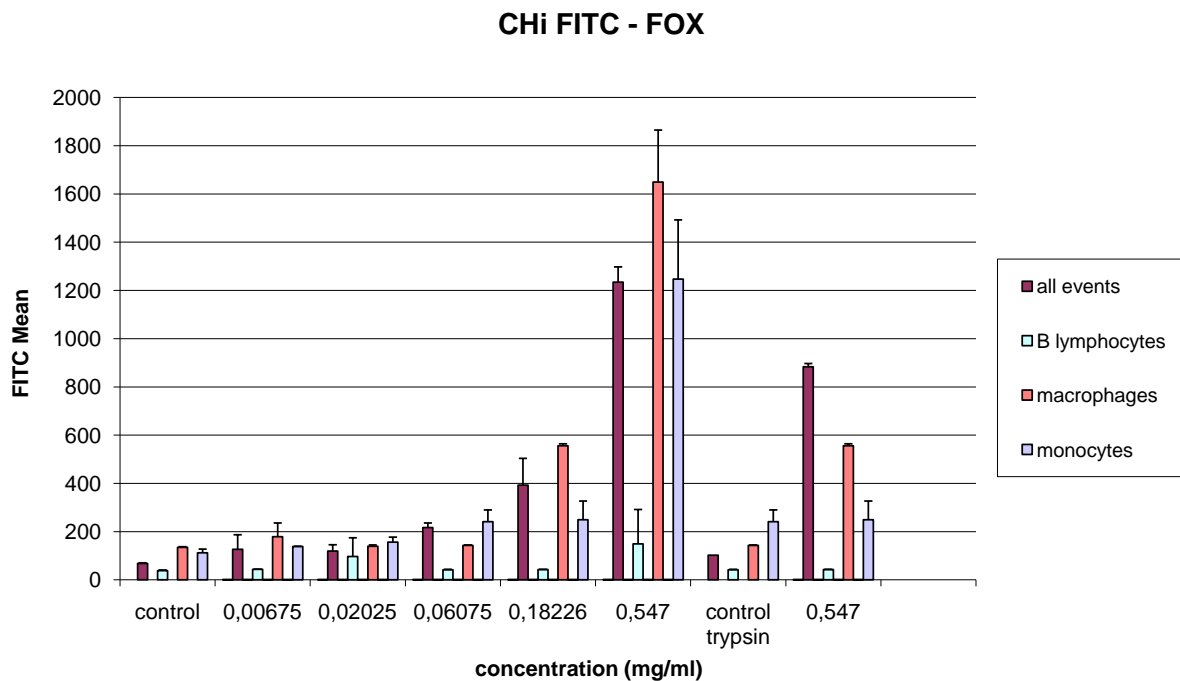
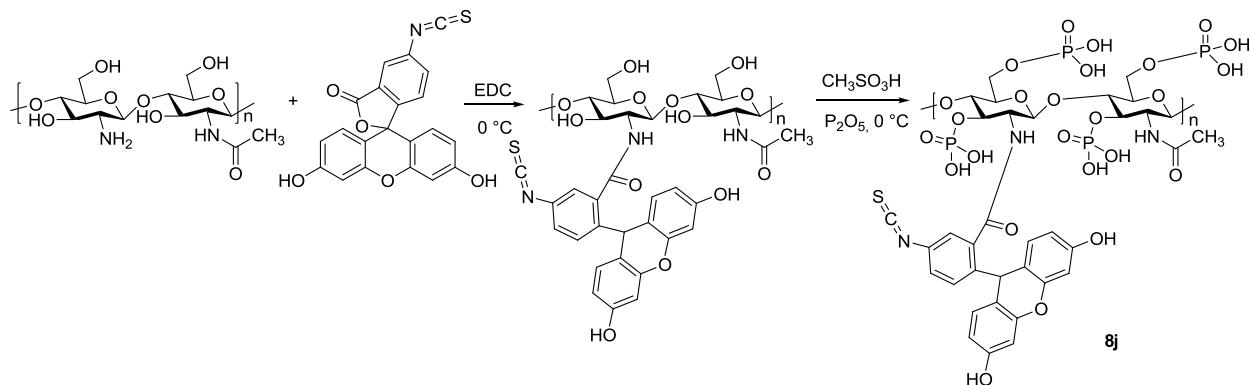


Fig. 21 Fluorescence uptake experiment evaluated on flow cytometer on sample of chitosan connected with FITC in the range of concentration on PBMC cells

Synthesis of chitosan connected with FITC is similar with previous procedures. EDC was used for activation of carboxylic group. Without further precipitation, phosphorylation was realized. Lactone ring of FITC was opened in water environment during the first step of synthesis, thereby, free carboxylic group could participate in connection. **8j** was completely soluble in 10 % NaOH solution.



Scheme 8 Conjugation of chitosan and FITC

3.6.2.1. Experimental part

General procedure of the synthesis of the compound **8j**

500 mg of chitosan was dissolved in water and 100 mg of FITC was added. The mixture was cooled at 0 - 5 °C. The carboxylic group of FITC was activated with 120 mg of *N*-(3-dimethylaminopropyl)-*N'*-ethylcarbodiimide and the reaction mixture was stirred at 0 - 5 °C for 3 hours, then the temperature gradually increased to the room temperature. After 24 hours without isolation 2 ml of methanesulfonic acid and 300 mg of phosphorus pentoxide was added to the mixture. The reaction was stirred at 0 - 5 °C for 3 hours. The mixture was cooled overnight in a freezer and then product **8j** was precipitated with acetone.

Data of compound **8j**

Chitosan conjugated with FITC (**8j**) Yield 71.67 %. IR (ATR): small peak 2075 (ν (N=C=S)), large peak 1653 (ν (CO-NH)), large peak 1617 (ν (CO-NH I.)), thin band 1588 (ν (CO-NH II.); δ (NH₂)), thin band 1485 (δ (CH₂, CH₃)), sharp peak 1248 (ν (P=O)), sharp intensive peak 1197 (δ (N-H)), sharp intensive peak 1116 (δ (C-N)), 932, 866, 788 cm⁻¹. ¹H NMR (DMSO-*d*₆, 300 MHz): 7.78 (s, 1H, arom. H), 4.91 (s, 1H, CH), 4.59 (s, 1H, H1 (GluN)), 4.35 (s, 1H, H1 (GluNAc)), 3.87 (s, 1H, NH), 3.31 (s, 2H, NH₂), 3.10-2.78 (4H, H3, H4, H5, H6), 2.74 (s, 1H, H2 (GluNAc)), 2.21 (s, 1H, H2 (GluN)), 1.60 (m, 3H, CH₃).

3.7. Conclusion of the first part of thesis

The outcomes of a literary search were published as two survey articles about chitosan and its structure, physico-chemical properties and pharmaceutical applications (Paper I, II). Chitosan has been found as an interesting aminopolysaccharide with manifold applications in biomedical chemistry. Low molecular weight and high degree of deacetylation of chitosan appear to be very important for antitumor, antioxidative and antibacterial activity. Both review articles summarize the findings published till 2008, the latest publications (2009 – 2010) are presented separately.

Seventeen derivatives of chitosan linked with the first or second line antituberculotics were prepared for the purpose of decreasing cytotoxicity of used drugs. Chitosan derivatives connected with INH, PZA and ETA (**3a-3c**, **6a-6c**) were tested for antimycobacterial activity against *M. tbc.*, *M. avium* and *M. kansasii*, their MIC were 125 µg/mL for all strains. Unexpectedly, *O*-carboxymethyl chitosan as intermediate showed better inhibition effect against *M. tbc.*, and *M. avium*. This fact can be explained by high degree of amino groups with chelating activity. Consequently, antimycobacterial activity of chitosan derivatives with antituberculotics depends on the presence of the first or second line antituberculosic drugs and the degree of deacetylation of chitosan. In addition, all tested derivatives did not exhibit obvious cytotoxic effect on PBMC and Hep G2 cells. It was found that chitosan is able to reduce cytotoxicity of antituberculosic drugs. (Paper III). Antimycobacterial activities of other synthesised chitosan derivatives connected with PAS, CS and fluoroquinolones (**3d**, **3e**, **6d**, **6e**, **8a-8g**) are currently processed.

Co-operations with the Institute of Inorganic Chemistry, Academy of Science of the Czech Republic; Department of Pharmacology and Toxicology, Pharmaceutical faculty and Eötvös Lóránd University, Research Group of Peptide Chemistry, Hungarian Academy of Science in Budapest led us to synthesized derivatives of chitosan with dyes (*meso*-tetra(4-carboxyphenyl)porphin, rose bengal, fluorescein isothiocyanate).

Chitosan has been found as a convenient carrier for photosensitising therapy, in our case the carrier with photoantimicrobial activity in wound healing treatment. Chitosan was linked with photosensitizer *meso*-tetra(4-carboxyphenyl)porphin and rose bengal. Unfortunately, the

solubility of the derivative with the first dye was not appropriate. Nanofibres were prepared from derivative of chitosan connected with rose bengal, but finally, nanofibres had not a sufficient quality for following usage.

Fluorescent labelled chitosan was used for uptake studies. Particles of chitosan connected with FITC were found not completely dissolved in medium under fluorescent microscope, thus no cellular uptake could be studied. Better results were received from the flow cytometer assay. Expected cellular uptake was observed on macrophages and monocytes.

4. Modifications of antimycobacterial drugs

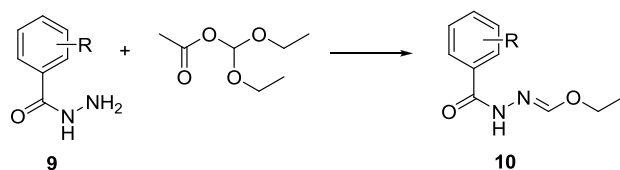
4.1. Introduction

Connection of two active molecules is one of the common approaches in drug design that is used as a prodrug form which reduces an emergence of resistance. Substituted carbohydrazone moiety has been found as a good pharmacophore group for many antituberculosic active molecules. In previous study of our research group¹¹⁸, two molecules with anti-tuberculosis activity were connected through the methine bridge which was gradually hydrolyzed. Probable synergic effect of both components with prolonged release was determined. C₁ fragment of hydrazones¹¹⁹ is useful for formation of C-N bond with appropriate amines as nucleophiles.

4.2. Derivatives of fluorine-containing hydrazones (Paper IV)

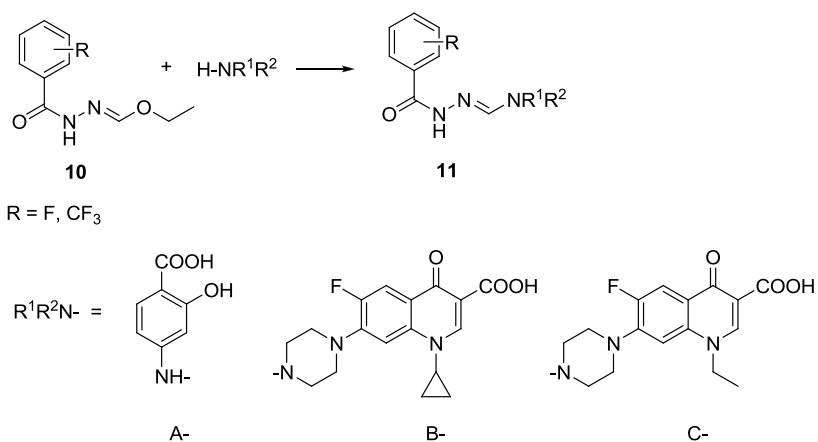
New derivatives containing fluorinated hydrazides of benzoic acid and first or second line antituberculosic drugs connected by methine bridge were prepared. Involvement of fluoroquinolones as second line antituberculosics to potential active molecule seems to be promising. Antimycobacterial activity of ciprofloxacin or norfloxacin connected with another drug was proved advantageous. Implementation of fluorine atoms to the molecule was found to increase its antimycobacterial activity as well as the lipophilicity.

Synthesis of new potential antitubercular drugs contains two steps. Primarily hydrazide of substituted benzoic acid (**9**) was activated by diethoxymethyl acetate in acetonitrile (Scheme 9). Starting hydrazides were substituted by fluoro or trifluoromethyl group on benzene ring. Ethyl benzoylformohydrazone (**10**) was condensed with *N*-nucleophile in the following step (Scheme 10). *N*-nucleophile was selected from the first or second lines of antituberculosics (*p*-aminosalicylic acid, ciprofloxacin and norfloxacin).



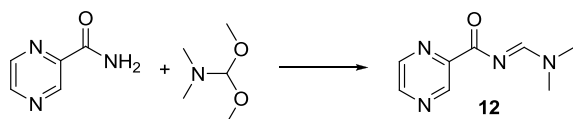
R = F, CF₃

Scheme 9 Synthesis of ethyl benzoylformohydrazone

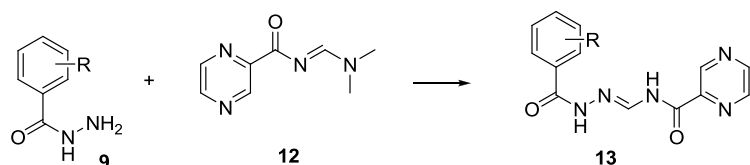


Scheme 10 Synthesis of PAS-, CPX- and NFX-derivatives

Slightly different approach was used for the synthesis of pyrazinecarboxamide (PZA) compounds. First step was the preparation of an activated molecule of PZA¹¹⁸ (**12**) (Scheme 11), which reacted with molecule of appropriate hydrazide (Scheme 12) to form *N*-(2-benzoylhydrazonomethyl)pyrazine-2-carboxamides (**13**).



Scheme 11 Synthesis of *N*-((dimethylamino)methylene)pyrazine-2-carboxamide



Scheme 12 PZA-derivatives preparation

In vitro antimycobacterial activity was evaluated against *M. tuberculosis* H₃₇Rv and MDR-TB strain *M. tuberculosis* A8 241 which is resistant to isoniazid and rifampicin (Table 2), *M. kansasii* My 235/80, *M. kansasii* 6509/96 and *M. avium* 330/88 (Table 3). All evaluated

compounds **11a-11l** have shown higher activity against MDR-TB (0.5 µg/mL). Minimal inhibitory concentration of compounds **11f** and **11g** (contained trifluoromethyl group and CPX) was found as the lowest against both strains of *Mycobacterium kansasii* as compared to other compounds as well as the standard INH.

Values of selectivity index (SI) indicate the rate between IC₅₀ of HepG2 cytotoxicity and MIC *M. tuberculosis*. Values of compound SI ≥ 10 are considered for further screening¹²⁰. Selectivity index calculated for MDR-TB *M. tuberculosis* for compounds **11d-11i** exhibit high values (Table 2).

Table 2. Values of antimycobacterial activity against *M. tbc.* strains

	R	R ¹ R ² N	MIC [µg/mL]		SI for <i>M. tbc.</i>	
			<i>M. tbc.</i>	<i>M. tbc.</i>	SI for <i>M. tbc.</i>	SI for <i>M. tbc.</i>
			H ₃₇ Rv (ATCC:27294)	A8 241 MDR-TB	H ₃₇ Rv	A8 241 MDR-TB
11a	4-CF ₃	A	4	0.5	NT	NT
11b	3-CF ₃	A	4	0.5	NT	NT
11c	4-F	A	4	0.5	NT	NT
11d	3-F	A	2	0.5	148.25	592.64
11e	2-F	A	2	0.5	192.06	767.77
11f	4-CF ₃	B	1	0.5	189.21	378.41
11g	3-CF ₃	B	2	0.5	87.79	351.15
11h	4-F	B	1	0.5	634.29	1268.58
11i	3-F	B	1	0.5	402.38	804.76
11j	4-CF ₃	C	5	5	3.98	3.98
11k	4-F	C	NT	NT	NT	NT
11l	3-F	C	6	5	31.67	38
13a	4-CF ₃	D	NT	NT	NT	NT
13b	3-F	D	NT	NT	NT	NT
INH	-	-	0.01	1	NT	NT

CPX	-	-	0.5	NT	NT	NT
NFX	-	-	5	NT	NT	NT

NT – not tested

Table 3. Values of antimycobacterial activity against non-tuberculous strains

	R	R ¹ R ² N	MIC [μmol/L]							
			<i>M. avium</i>		<i>M. kansasii</i>			<i>M. kansasii</i>		
			330/88		235/80		6509/96			
			14 d	21 d	7 d	14 d	21 d	7 d	14 d	21 d
11a	4-CF ₃	A	32	125	62.5	125	250	62.5	62.5	125
11b	3-CF ₃	A	250	500	32	125	125	62.5	62.5	62.5
11c	4-F	A	32	125	32	62.5	62.5	32	32	32
11d	3-F	A	32	62.5	32	62.5	62.5	32	32	32
11e	2-F	A	32	62.5	32	32	62.5	32	62.5	62.5
11f	4-CF ₃	B	32	62.5	2	2	4	1	1	2
11g	3-CF ₃	B	250	250	2	2	4	1	1	2
11h	4-F	B	62.5	125	4	4	8	8	8	16
11i	3-F	B	125	250	4	4	8	4	4	4
11j	4-CF ₃	C	500	500	2	4	8	2	4	8
11k	4-F	C	125	250	16	32	62.5	32	62.5	62.5
11l	3-F	C	125	250	16	32	62.5	16	16	32
13a	4-CF ₃	D	>1000	>1000	250	250	250	250	500	500
13b	3-F	D	>500	>500	250	250	>500	250	>500	>500
INH	-	-	>250	>250	>250	>250	>250	2	4	4
CPX	-	-	62.5	62.5	1	2	2	1	1	2
NFX	-	-	125	250	8	16	16	2	8	8
PAS	-	-	32	125	125	1000	>1000	32	125	500
PZA	-	-	500	>1000	500	>1000	>1000	125	1000	1000

NT – not tested

IC₅₀ values in mmol/L are presented in Table 4. IC₅₀ of tested compounds are low, in the range of 0,0373-1,21 mmol/L, that means they are nearly non-toxic. Cytotoxicity of the most active compounds was determined on human hepatocellular liver carcinoma cells HepG2, PBMC (Peripheral Blood Mononuclear Cells) and human SH-Sy5y neuroblastoma cells by MTT assay for cellular toxicity. Prepared compounds are non toxic in MIC concentrations.

Table 4. Values of *in vitro* cytotoxicity

	R	R ¹ R ² N	HepG2 IC ₅₀	PBMC IC ₅₀	Sy5y IC ₅₀
			[mmol/L]		
11a	4-CF ₃	A	NT	NT	NT
11b	3-CF ₃	A	NT	NT	NT
11c	4-F	A	NT	NT	NT
11d	3-F	A	0.934	0.934	NT
11e	2-F	A	1.210	1.210	NT
11f	4-CF ₃	B	0.347	0.347	NT
11g	3-CF ₃	B	> 0.322	> 0.322	NT
11h	4-F	B	> 1.280	> 0.763	NT
11i	3-F	B	> 0.812	> 0.305	NT
11j	4-CF ₃	C	> 0.0373	0.262	0.107
11k	4-F	C	> 0.797	> 0.331	NT
11l	3-F	C	> 0.393	> 0.393	> 0.430
13a	4-CF ₃	D	> 0.624	NT	NT
13b	3-F	D	> 0.130	> 0.305	NT
INH	NT	NT	NT	NT	NT

NT – not tested

Compound **11h** showed the highest value of SI, thus was chosen for stability measurement. The stability was evaluated on HPLC at different pH values which are shown in the Figure 22. At pH 7.4, the compound was stable; no significant decomposition was observed during 48 hours experiment. At both acidic buffers, the concentration of **11h** decreased, accompanied by a

proportional increase in the concentration of ciprofloxacin. No formylciprofloxacin was detected in the samples. There was not observed any statistically significant enzymatic decomposition of **11h** in rat plasma.

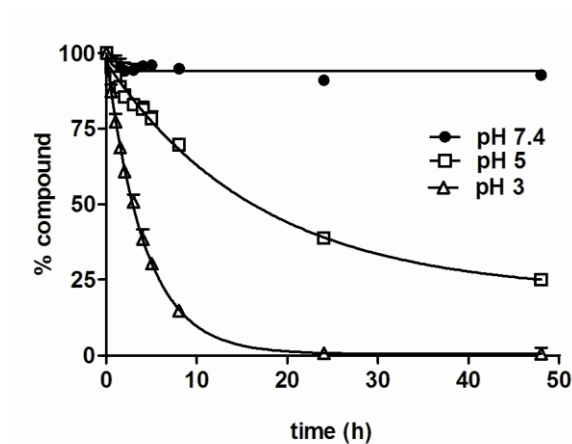


Fig. 22 Stability of **11h** in aqueous buffers at pH 7.4, 5 and 3. Data are presented as means \pm S.D, n = 3.

4.3. Derivatives of isoniazid

Isoniazid (isonicotinic acid hydrazide, INH) is still considered as the first line drug for chemotherapy of TB. INH is highly active against *M. tbc.* with MIC in the range of 0.02 – 0.2 $\mu\text{g}/\text{mL}$.¹²¹ In the bacteria cells (Fig. 23), INH is activated by KatG protein (catalase–peroxidase) or Mn^{2+} action with appearance of ROS.¹²² Activated INH has two possible actions. Firstly, INH and ROS may defect DNA, proteins and other macromolecules. Secondly, INH inhibits InhA (enoyl-acyl carrier protein reductase)¹²³ and AcpM-KasA (mycobacterial acyl carrier synthase – β -ketoacyl synthase) complex. Both enzymes are involved in the biosynthetic way for fatty acid production. Mycobacteria have two fatty acid synthases (FAS). Function of FAS I is in the synthesis of mycolic acid of the length C_{16} to $\text{C}_{24/26}$ which are substrates for synthetic complex FAS II. FAS II system contains a series of independent enzymes, including InhA and AcpM-KasA¹²⁴ responsible for elongation of the FAS I products.¹²² Chromosomal mutations of different genes, including *katG*, *inhA*, *ahpC* and other genes, cause resistance of *M. tbc.* to INH. Mutations of *katG* result in diminished or altered catalase-peroxidase activity. The most frequent substitution results in the replacement of the naturally-occurring serine with

threonine (S315T). This mutation occurs in the range between 30 and 60% of all INH resistant isolates.¹²⁵ The over expression of *inhA* led to low level of isoniazid resistance in *M. smegmatis* and was accompanied by cross-resistance to the second line antituberculosic drug ethionamide.¹²⁶

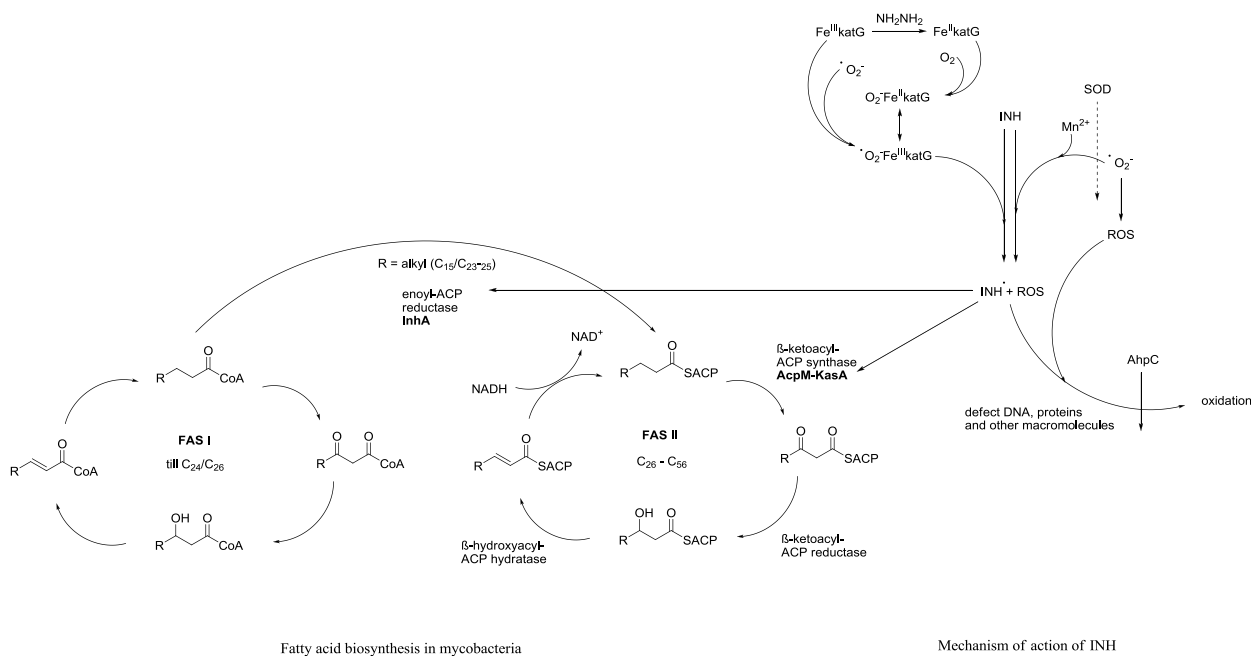
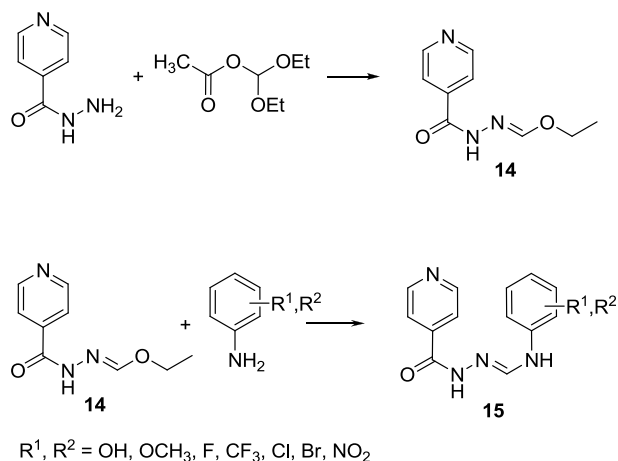


Fig. 23 Mechanism of INH activation and mycobacterial fatty acid biosynthesis

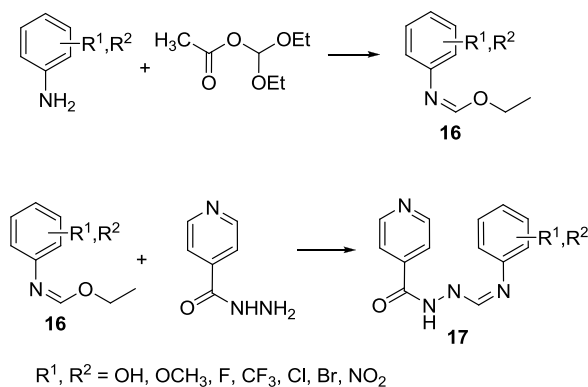
The aim of this part of research was enhanced antimycobacterial activity of INH by connection of electron-acceptor substituents. Potential increasing biological effect of substituents was calculated from QSAR studies.¹²² Isoniazid (INH) was linked with monosubstituted or disubstituted anilines by the CH fragment.¹²⁷ Two similar reactions were used for the preparation of INH derivatives.

The first synthetic approach of new antituberculosic drugs contains two steps. Isoniazid was treated with diethoxymethyl acetate to obtain isonicotinoylethoxymethylene hydrazone (**14**) in acetonitrile (Scheme 13). Its ethoxy group was substituted with appropriate aniline, as *N*-nucleophile, resulted in the formation of the corresponding isonicotinoylformohydrazonamides (**15**).



Scheme 13 Synthesis of isonicotinoylformohydrazone and corresponding isonicotinoylformohydrazone derivatives

Second approach is based on two steps. Activated substituted aniline (**16**) was prepared using diethoxymethyl acetate (Scheme 14). Ethoxy group of the compound **16** was condensed with INH to get products **17** *N'*-(iminomethyl)isonicotinoylhydrazide.



Scheme 14 Synthesis of *N'*-(iminomethyl)isonicotinoylhydrazide

Prepared INH derivatives **15**, **17** differ in the position of double bond. Compounds **15a** – **15o** contain formohydrazone bond and compounds **17a** – **17n** have formimidohydrazone as middle part of molecule. Their biological activities and values of lipophilicity were compared. *In vitro* antimycobacterial activity was evaluated against *Mycobacterium tuberculosis* CNTC My 331/88, *Mycobacterium kansasii* CNTC My 235/80, *M. kansasii* 6509/96 and *Mycobacterium avium* CNTC 330/88. Results are presented in Table 5. Several synthesized

compounds showed similar activity as a standard INH. Compounds **15f**, **15i**, **17c**, **17d**, **17f-17h**, **17n** exhibited same inhibitory effect as INH against *M. tbc*. In general, derivatives with halogenated substituents exhibited lower MIC values. Compound **17n** was the most active for all tested strains. Paralel derivatives (with the same substituents) showed similar activities. The best MIC values are highlighted in Table 5.

Table 5. Antimycobacterial evaluation of compounds **15** and **17**

	R ¹	R ²	MIC [μ mol/L]									
			<i>M. tbc</i>		<i>M. avium</i>		<i>M. kansasii</i>			<i>M. kansasii</i>		
			331/88		330/88		235/80			6509/96		
			14 d	21 d	14 d	21 d	7 d	14 d	21 d	7 d	14 d	21 d
15a	3-OH	-	2	2	500	500	250	1000	>1000	16	32	32
15b	4-OH	-	8	8	500	1000	250	500	1000	62.5	62.5	62.5
15c	3-OCH ₃	-	2	2	500	500	250	500	1000	16	16	16
15d	4-OCH ₃	-	2	4	500	500	250	500	1000	16	16	32
15e	4-CF ₃	-	2	2	500	1000	250	500	1000	32	32	32
15f	3-F	-	1	1	500	1000	250	1000	>1000	16	16	16
15g	4-F	-	2	4	1000	>1000	250	1000	>1000	32	62.5	62.5
15h	3-Cl	-	2	2	500	1000	250	1000	1000	16	32	32
15i	3-Br	-	1	1	250	500	250	1000	1000	8	8	16
15j	4-Cl	2-OH	2	4	250	500	250	500	500	16	16	32
15k	5-Cl	2-OH	2	2	500	500	125	250	250	8	16	32
15l	3-Cl	4-Cl	1	2	250	250	500	>500	>500	8	16	16
15m	3-F	4-F	4	4	250	500	250	500	1000	8	16	32
15n	3-Cl	4-F	1	2	250	500	250	1000	>1000	16	32	32
15o	4-Br	3-F	1	4	500	1000	250	500	1000	16	16	32
17a	3-OH	-	2	2	500	500	250	1000	1000	16	32	32
17b	4-OH	-	4	8	500	500	500	500	500	32	62.5	125

17c	3-CF ₃	-	1	1	500	1000	125	250	1000	16	16	32
17d	3-F	-	1	1	500	1000	125	1000	>1000	16	16	32
17e	4-F	-	1	2	250	500	250	1000	>1000	8	8	8
17f	3-Cl	-	1	1	1000	1000	125	500	500	16	16	16
17g	4-Cl	-	1	1	500	1000	125	250	1000	16	32	32
17h	3-Br	-	1	1	250	500	500	1000	>1000	8	8	16
17i	4-Br	-	2	4	500	500	125	250	500	32	32	32
17j	3-NO ₂	-	2	2	250	500	125	250	500	8	16	16
17k	3-Cl	4-Cl	1	2	500	500	250	500	500	16	16	32
17l	3-F	4-F	2	2	250	250	500	1000	1000	16	32	62.5
17m	3-Cl	4-F	2	4	1000	1000	250	500	500	16	16	32
17n	4-Br	3-F	1	1	250	250	62.5	250	250	8	8	16
INH	-	-	1	1	>250	>250	>250	>250	>250	2	4	4

Cytotoxicity of the most active compounds was determined on human hepatocellular liver carcinoma cells HepG2 and PBMC (Peripheral Blood Mononuclear Cells) by MTT assay for cellular toxicity. IC₅₀ values in mmol/L are presented in Table 6 as well as selectivity index (SI). Values of SI indicate the rate between IC₅₀ of HepG2 cytotoxicity and MIC *M. tuberculosis*. IC₅₀ of tested compounds are between 0.0218 - 0.326 mmol/L. Selectivity index calculated for *M. tuberculosis* for compound **17n** exhibit high value.

Table 6. Cytotoxicity evaluation of compounds **15k** and **17n**

	R ¹	R ²	HepG2 IC ₅₀	PBMC IC ₅₀	SI for <i>M. tbc.</i>
			[mmol/L]		331/88
15k	5-Cl	2-OH	0.0218	0.075	10.9
17n	4-Br	3-F	0.162	0.326	162

The purity and values of lipophilicity are presented in Table 7. The purity of compounds was measured by HPLC and the range was 92.77 - 99.98 %. The lipophilicity, as the capacity factor $\log k$, was determined by RP-HPLC and the results were compared by employing two commercially available programs. Values of lipophilicity of all prepared compounds were higher than INH, it signifies more effective transport of the molecule through cellular membranes.

Table 7. Experimental and calculated values of lipophilicity factor of compounds **15** and **17**

Compound	R ¹	R ²	Purity (%)	$\log k$	$\log P$	$\log P/\text{Clog } P$
					ACD/ $\log P$	ChemOffice
15a	3-OH	-	99.53	0.2681	1.32±0.57	0.99/0.409
15b	4-OH	-	98.90	0.2702	0.93±0.57	0.99/0.409
15c	3-OCH ₃	-	99.20	0.2412	1.93±0.57	1.25/0.995
15d	4-OCH ₃	-	98.19	0.2546	1.62±0.57	1.25/0.995
15e	4-CF ₃	-	99.62	0.3073	2.68±0.59	2.30/1.959
15f	3-F	-	98.74	0.3041	2.16±0.61	1.53/1.219
15g	4-F	-	98.49	0.3049	2.53±0.58	1.53/1.219
15h	3-Cl	-	98.86	0.3051	2.70±0.57	1.93/1.789
15i	3-Br	-	98.49	0.3068	2.88±0.61	2.20/1.939
15j	4-Cl	2-OH	99.75	0.3053	2.62±0.58	1.54/1.4188
15k	5-Cl	2-OH	93.76	0.3044	2.69±0.58	1.54/1.4188
15l	3-Cl	4-Cl	95.80	0.3134	3.57±0.58	2.49/2.382
15m	3-F	4-F	97.73	0.3047	2.52±0.64	1.69/1.292
15n	3-Cl	4-F	99.98	0.3058	3.06±0.62	2.09/1.932
15o	4-Br	3-F	99.65	0.3131	3.24±0.64	2.36/2.082
17a	3-OH	-	99.72	0.2453	1.28±0.57	0.92/0.225
17b	4-OH	-	99.44	0.2477	1.09±0.57	0.92/0.225
17c	3-CF ₃	-	98.86	0.3048	3.04±0.60	2.23/1.775
17d	3-F	-	97.89	0.3044	2.33±0.60	1.47/1.035

17e	4-F	-	98.25	0.3089	2.52±0.59	1.47/1.035
17f	3-Cl	-	97.66	0.3093	2.57±0.63	1.87/1.605
17g	4-Cl	-	98.90	0.3059	2.51±0.57	1.87/1.605
17h	3-Br	-	98.67	0.3069	2.68±0.61	2.14/1.755
17i	4-Br	-	99.15	0.3078	2.69±0.60	2.14/1.755
17j	3-NO ₂	-	99.75	0.2638	1.58±0.57	0.33/0.635
17k	3-Cl	4-Cl	97.51	0.3096	3.10±0.58	2.43/2.198
17l	3-F	4-F	97.64	0.3008	2.05±0.64	1.63/1.108
17m	3-Cl	4-F	92.77	0.3028	2.60±0.61	2.03/1.1748
17n	4-Br	3-F	93.28	0.3088	2.77±0.64	2.30/1.898
INH	-	-	-	-0.668	-0.89±0.24	-0.60/-0.668

4.3.1 Experimental part

4.3.1.1. General

All chemicals were obtained from Sigma-Aldrich Co. Melting points were determined on the Büchi Melting Point B-540. Elemental analyses (C, H, N) were performed with a Perkin-Elmer 2400 CHNS/O analyzer. Infrared spectra were recorded on a Bio-Rad FTS 3000 MX spectrometer in KBr pellets. NMR spectra were measured in DMSO-*d*₆ solutions on a Bruker Avance 300 (300 MHz for ¹H and 75.5 MHz for ¹³C). The chemical shifts, δ , are given in ppm, related to tetramethylsilane (TMS) as an internal standard. The coupling constants (*J*) are reported in Hz. The reactions were monitored and the purity of the products was checked by TLC (Fluka silica gel/TLC cards 60 PF₂₅₄). The plates were visualized using UV light. Names of compounds were generated and structures were drawn with ChemBioDraw Ultra 11.0 and are formatted as ACS Document 1996.

4.3.1.2. Biological evaluation

In vitro Antimycobacterial activity made in National Reference Laboratory

In vitro antimycobacterial activity was evaluated against *Mycobacterium tuberculosis* CNTC

My 331/88 (dilution of strains was 10^{-3} $\mu\text{mol/L}$), *Mycobacterium kansasii* CNTC My 235/80 (dilution of strains was 10^{-5} $\mu\text{mol/L}$), *M. kansasii* 6509/96 (dilution of strains was 10^{-4} $\mu\text{mol/L}$) and *Mycobacterium avium* CNTC 330/88 (dilution of strains was 10^{-4} $\mu\text{mol/L}$). All strains were obtained from Czech National Collection of Type Cultures (CNCTC) with exception of *M. kansasii* 6509/96, which is a clinical isolate. Antimycobacterial activity was measured in Sula's semisynthetic medium (SEVAC, Prague) at 37 °C. Compounds were dissolved in dimethyl sulfoxide solution (max 5% DMSO in water) and applied into the medium in concentration range 250, 125, 62, 31, 16, 8, 4, 2 and 1 $\mu\text{mol/L}$. Minimal inhibitory concentration (MIC) is determined after incubation at 37 °C for 7, 14 and 21 days. The MIC is the lowest concentration of a substance at which the inhibition of the growth of mycobacterium occurs.

In vitro Cytotoxicity of compounds by MTT assay

HepG2 human hepatoma cells (ATCC HB-8065) and human PBMC (peripheral blood mononuclear cells)¹²⁸ were cultured in RPMI-1640 medium without phenol red supplemented with 10% FCS, 2 mM L-glutamine and 160 $\mu\text{g/ml}$ gentamycin. Cell cultures were maintained at 37 °C, 5% CO₂ in water-saturated atmosphere. Cells were plated into 96-well plate with initial cell number of 5×10^3 per well (PBMC 2.0×10^5 cells/well). After 24 h of incubation at 37 °C prior to the experiment, cells were treated with compounds in 100 μL serum free medium overnight. Control cells were treated with serum free medium. Four parallel measurements were performed in all cases.

After overnight incubation at 37 °C, the cell viability was determined by 3-(4,5-dimethylthiazol-2-yl)-2,5-diphenyltetrazolium bromide (MTT)-assay.^{129,130} 45 μL MTT-solution (2 mg/mL) was added to each well. The respiratory chain and other electron transport systems¹³¹ reduce MTT and thereby form non-water-soluble violet formazan crystals within the cell.¹³² The amount of these crystals can be determined spectrophotometrically and serves as an estimate for the number of mitochondria and hence the number of living cells in the well.¹³³ After 4 hours of incubation cells were centrifuged for 5 min (2000 rpm) and supernatant was removed. The obtained formazan crystals were dissolved in 50 or 100 μL DMSO and optical density (OD) of the samples was measured at $\lambda = 540$ and 620 nm using ELISA Reader (iEMS Reader, Labsystems, Finland). OD₆₂₀ values were subtracted from OD₅₄₀ values. The percent of

cytotoxicity was calculated using the following equation: Cytotoxicity (%) = $[1 - (OD_{\text{treated}}/OD_{\text{control}})] \times 100$; where OD_{treated} and OD_{control} correspond to the optical densities of the treated and the control cells, respectively. In each case two independent experiments were carried out with 4–8 parallel measurements. The 50% inhibitory concentration (IC_{50}) values were determined from the dose-response curves. The curves were defined using Microcal™ Origin1 (version 6.0) software.

4.3.1.3. Lipophilicity determination

The purity of compounds was checked by HPLC. The detection wavelength 210 nm was chosen. Peaks in the chromatogram of the solvent (blank) were deducted from peaks in the chromatogram of the sample solution. A purity of the individual compounds was determined from area peaks in the chromatogram of the sample solution.

UV spectra (λ , nm) were determined on a Waters Photodiode Array Detector 2996 (Waters Corp., Milford, MA, U.S.A.) in ca $5 \cdot 10^{-4}$ M methanolic solution. $\log \epsilon$ (the logarithm of molar absorption coefficient ϵ) was calculated for the absolute maximum λ_{max} of the individual compounds.

The HPLC separation module Waters Alliance 2695 XE and Waters Photodiode Array Detector 2996 (Waters Corp., Milford, MA, U.S.A.) were used. The chromatographic column Symmetry® C₁₈ 5 μm , 4.6×250 mm, Part No. WAT054275, (Waters Corp., Milford, MA, U.S.A.) was used. The HPLC separation process was monitored by Millennium32® Chromatography Manager Software, Waters 2004 (Waters Corp., Milford, MA, U.S.A.). The mixture of MeOH p.a. (40.0%) and H₂O-HPLC – Mili-Q Grade (60.0%) was used as a mobile phase. The total flow of the column was 0.9 mL/min, injection 30 μL , column temperature 45 °C and sample temperature 10 °C. The detection wavelength 210 nm was chosen. The KI methanolic solution was used for the dead time (t_D) determination. Retention times (t_R) were measured in minutes.

The capacity factors k were calculated using the Millennium32® Chromatography Manager Software according to the formula $k = (t_R - t_D) / t_D$, where t_R is the retention time of the solute, whereas T_D denotes the dead time obtained via an unretained analyte. $\log k$, calculated from

the capacity factor k , is used as the lipophilicity index converted to $\log P$ scale. The $\log k$ values of the individual compounds are shown in Table 7.

$\log P$, *i. e.* the logarithm of the partition coefficient for *n*-octanol/water, was calculated using the programs CS ChemOffice Ultra ver. 9.0 (CambridgeSoft, Cambridge, MA, U.S.A.) and ACD/Log P ver. 1.0 (Advanced Chemistry Development Inc., Toronto, Canada). $\log P$ values (the logarithm of *n*-octanol/water partition coefficient based on established chemical interactions) were generated by means of CS ChemOffice Ultra ver. 7.0 (CambridgeSoft, Cambridge, MA, U.S.A.) software. The results are shown in Table 7.

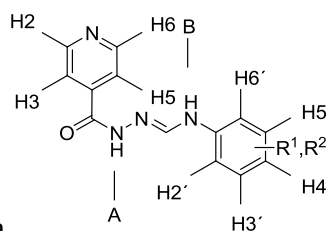
4.3.2. Experimental results

General procedure of the synthesis of compounds **15a** – **15o**

Diethoxymethyl acetate (15 mmol) was added to a stirred solution of isoniazid (10 mmol) in acetonitrile (100 mL) at 55 °C. The reaction mixture was stirred for 30 minutes at the same temperature. The solvent was evaporated in vacuo and the crude product was washed with diethyl ether (2x20 mL). The product ethyl isonicotinoylhydrazonoformate **14** was dried in the air, recrystallized from acetonitrile.

A solution of substituted aniline (1 mmol) in ethanol (1 mL) was added to a stirred solution of ethyl isonicotinoylhydrazonoformate **14** (1 mmol) in ethanol (10 mL) at 55 °C. The mixture was stirred for 6 hours at the same temperature and for 20 hours at room temperature. The product **15** was collected by filtration and recrystallized from appropriate solvent.

Data of compounds **15a** – **15o**



General structure for NMR evaluation

N-(3-hydroxyphenyl)-*N'*-isonicotinoylformohydrazoneamide (**15a**) Yield 56.90 %; mp 190-192 °C (ethanol). IR (KBr): 3226, 3085, 3030, 2871, 2601, 2488, 1669, 1631, 1599, 1544, 1497,

1445, 1414, 1366, 1306, 1247, 1164, 1062, 1003, 964, 909, 849, 764, 697, 688 cm^{-1} . ^1H NMR (DMSO- d_6 , 300 MHz): δ 11.17 (s, 1H, NH(A)), 9.47 (s, 1H, NH(B)), 8.70 (d, $J = 4.53$ Hz, 2H, H2, H6), 8.45 (s, 1H, CH), 7.85 (s, 1H, OH), 7.73 (d, $J = 5.51$ Hz, 2H, H3, H5), 7.62 (m, 1H), 7.54 (t, $J = 7.99$ Hz, 1H), 7.30 (m, 1H), 7.15 (d, $J = 7.88$ Hz, 1H). ^{13}C NMR (DMSO- d_6 , 75 MHz): 160.2, 158.4, 150.4 (2C), 147.7, 142.2, 141.5, 130.1, 121.4 (2C), 108.7, 106.9, 103.3. Anal. Calcd for $\text{C}_{13}\text{H}_{12}\text{N}_4\text{O}_2$ (256.26): C, 60.93; H, 4.72; N, 22.86. Found: C, 61.08; H, 5.02; N, 21.98.

N-(4-hydroxyphenyl)-*N'*-isonicotinoylformohydrazoneamide (**15b**) Yield 53.75 %; mp 190-192 $^{\circ}\text{C}$ (ethanol). IR (KBr): 3212, 3150, 3069, 2610, 1668, 1634, 1601, 1676, 1549, 1519, 1458, 1412, 1366, 1314, 1247, 1170, 1105, 1059, 1005, 1067, 909, 826, 755, 690 cm^{-1} . ^1H NMR (DMSO- d_6 , 300 MHz): δ 11.06 (s, 1H, NH(A)), 9.12 (s, 1H, NH(B)), 8.71 (d, $J = 4.91$ Hz, 2H, H2, H6), 8.26 (s, 1H, CH), 7.79 (d, $J = 5.06$ Hz, 2H, H3, H5), 7.45 (s, 1H, OH), 7.19 (d, $J = 7.73$ Hz, 2H, H2', H6'), 6.70 (d, $J = 8.06$ Hz, 2H, H3', H5'). ^{13}C NMR (DMSO- d_6 , 75 MHz): 160.2, 152.3, 150.3 (2C), 148.4, 141.7, 132.9, 121.4 (2C), 118.4 (2C), 115.8 (2C). Anal. Calcd for $\text{C}_{13}\text{H}_{12}\text{N}_4\text{O}_2$ (256.26): C, 60.93; H, 4.72; N, 21.86. Found: C, 60.81; H, 5.15; N, 21.41.

N-(3-methoxyphenyl)-*N'*-isonicotinoylformohydrazoneamide (**15c**) Yield 55.38 %; mp 164-166 $^{\circ}\text{C}$ (ethanol). IR (KBr): 3041, 2360, 1671, 1645, 1634, 1621, 1600, 1549, 1500, 1474, 1464, 1410, 1360, 1317, 1288, 1230, 1159, 1047, 968, 907, 840, 776, 755, 689 cm^{-1} . ^1H NMR (DMSO- d_6 , 300 MHz): δ 11.16 (s, 1H, NH(A)), 9.47 (s, 1H, NH(B)), 8.73 (d, $J = 5.78$ Hz, 2H, H2, H6), 8.47 (d, $J = 4.91$ Hz, 1H, CH), 7.77 (d, $J = 5.63$ Hz, 2H, H3, H5), 7.16 (t, $J = 8.14$ Hz, 1H), 6.93 (s, 1H), 6.78 (d, $J = 7.92$ Hz, 1H), 6.49 (d, $J = 8.13$ Hz, 1H), 3.36 (s, CH_3). ^{13}C NMR (DMSO- d_6 , 75 MHz): 160.3, 150.4 (2C), 147.5, 142.2, 141.5, 130.2, 121.9, 121.4 (2C), 108.7, 106.7, 102.3, 55.2. Anal. Calcd for $\text{C}_{14}\text{H}_{14}\text{N}_4\text{O}_2$ (270.36): C, 62.21; H, 5.22; N, 20.73. Found: C, 62.14; H, 5.46; N, 20.92.

N-(4-methoxyphenyl)-*N'*-isonicotinoylformohydrazoneamide (**15d**) Yield 28.58 %; mp 170-172 $^{\circ}\text{C}$ (ethanol). IR (KBr): 3421, 3208, 2836, 1667, 1620, 1549, 1535, 1515, 1466, 1365, 1319, 1308, 1290, 1247, 1179, 1035, 828, 685, 670 cm^{-1} . ^1H NMR (DMSO- d_6 , 300 MHz): δ 11.13 (s, 1H, NH(A)), 9.27 (s, 1H, NH(B)), 8.71 (d, $J = 5.65$ Hz, 2H, H2, H6), 8.35 (s, 1H, CH), 7.78 (d, $J = 5.53$ Hz, 2H, H3, H5), 7.29 (d, $J = 7.65$ Hz, 2H, H2', H6'), 6.85 (d, $J = 7.96$ Hz, 2H, H3',

H5'), 3.70 (s, CH₃). ¹³C NMR (DMSO-*d*₆, 75 MHz): 160.1, 154.2, 150.4 (2C), 148.1, 141.6, 134.3, 121.4 (2C), 118.1 (2C), 114.6 (2C). Anal. Calcd for C₁₄H₁₄N₄O₂ (270.36): C, 62.21; H, 5.22; N, 20.73. Found: C, 62.40; H, 5.51; N, 20.82.

N-(4-(trifluoromethyl)phenyl)-*N'*-isonicotinoylformohydrazoneamide (**15e**) Yield 42.40 %; mp 191-193 °C (acetonitrile). IR (KBr): 3424, 3234, 3051, 2360, 1651, 1635, 1615, 1549, 1530, 1491, 1458, 1412, 1328, 1270, 1194, 1164, 1115, 1068, 1014, 834, 753, 669 cm⁻¹. ¹H NMR (DMSO-*d*₆, 300 MHz): δ 11.09 (s, 1H, NH(A)), 8.71 (d, *J* = 4.5 Hz, 3H, NH(B), H₂, H₆), 8.32 (s, 1H, CH), 7.78 (m, 2H, H₃, H₅), 7.30 (d, *J* = 8.03 Hz, 2H, H₂', H₆'), 6.87 (d, *J* = 8.19 Hz, 2H, H₃', H₅'). ¹³C NMR (DMSO-*d*₆, 75 MHz): 160.1, 154.2 (2C), 150.3, 148.0, 141.6, 134.3, 121.9, 121.4 (2C), 118.1 (2C), 114.6 (2C). Anal. Calcd for C₁₄H₁₁F₃N₄O (308.27): C, 54.55; H, 3.60; N, 18.18. Found: C, 54.81; H, 3.93; N, 18.44.

N-(3-fluorophenyl)-*N'*-isonicotinoylformohydrazoneamide (**15f**) Yield 62.14 %; mp 180-182 °C (ethanol). IR (KBr): 3208, 1693, 1651, 1614, 1596, 1548, 1549, 1496, 1463, 1408, 1366, 1320, 1267, 1218, 1152, 1060, 1001, 970, 908, 845, 776, 682 cm⁻¹. ¹H NMR (DMSO-*d*₆, 300 MHz): δ 11.22 (s, 1H, NH(A)), 9.62 (s, 1H, NH(B)), 8.79 (d, *J* = 4.23 Hz, 2H, H₂, H₆), 8.42 (s, 1H, CH), 7.73 (d, *J* = 5.12 Hz, 2H, H₃, H₅), 7.30 (m, 2H), 7.03 (d, *J* = 6.73 Hz, 1H), 6.71 (t, *J* = 5.86 Hz, 1H). ¹³C NMR (DMSO-*d*₆, 75 MHz): 164.5, 160.4, 150.4 (2C), 147.1, 142.9, 141.4, 130.9, 121.4 (2C), 112.5, 107.5 (q), 103.4 (q). Anal. Calcd for C₁₃H₁₁FN₄O (258.25): C, 60.46; H, 4.29; N, 21.69. Found: C, 60.29; H, 4.06; N, 21.31.

N-(4-fluorophenyl)-*N'*-isonicotinoylformohydrazoneamide (**15g**) Yield 39.48 %; mp 191-193 °C (ethanol). IR (KBr): 3213, 3128, 3068, 2830, 1667, 1621, 1549, 1539, 1515, 1410, 1358, 1296, 1222, 1155, 1005, 965, 830, 754, 671 cm⁻¹. ¹H NMR (DMSO-*d*₆, 300 MHz): δ 11.15 (s, 1H, NH(A)), 9.03 (s, 1H, NH(B)), 8.69 (d, *J* = 4.62 Hz, 2H, H₂, H₆), 8.38 (s, 1H, CH), 7.76 (d, *J* = 5.03 Hz, 2H, H₃, H₅), 7.38 (d, *J* = 6.43 Hz, 2H, H₂', H₆'), 7.12 (d, *J* = 6.89 Hz, 2H, H₃', H₅'). ¹³C NMR (DMSO-*d*₆, 75 MHz): 160.3, 158.77, 150.3 (2C), 147.7, 141.5, 137.4, 121.4 (2C), 118.2 (2C), 115.7 (q, 2C). Anal. Calcd for C₁₃H₁₁FN₄O (258.25): C, 60.46; H, 4.29; N, 21.69. Found: C, 60.76; H, 4.05; N, 21.39.

N-(3-(chlorophenyl)-*N'*-isonicotinoylformohydrazoneamide (**15h**) Yield 53.96 %; mp 176-178 °C (ethanol). IR (KBr): 3208, 1692, 1650, 1616, 1593, 1548, 1549, 1502, 1463, 1403, 1366,

1320, 1265, 1218, 1154, 1060, 1006, 970, 908, 845, 759, 682 cm^{-1} . ^1H NMR (DMSO- d_6 , 300 MHz): δ 11.21 (s, 1H, NH(A)), 9.56 (s, 1H, NH(B)), 8.77 (d, $J = 5.06$ Hz, 2H, H2, H6), 8.46 (s, 1H, CH), 7.71 (d, $J = 5.62$ Hz, 2H, H3, H5), 7.36 (m, 2H), 7.03 (d, $J = 7.09$ Hz, 1H), 6.92 (m, 1H). ^{13}C NMR (DMSO- d_6 , 75 MHz): 160.1, 150.2 (2C), 147.1, 142.8, 141.4, 130.9, 123.7, 122.3, 121.4 (2C), 118.2, 115.4. Anal. Calcd for $\text{C}_{13}\text{H}_{11}\text{ClN}_4\text{O}$ (274.71): C, 56.84; H, 4.04; N, 20.40. Found: C, 56.62; H, 4.36; N, 20.26.

N-(3-(bromophenyl)-*N'*-isonicotinoylformohydrazoneamide (**15i**) Yield 59.92 %; mp 178-180 °C (ethanol). IR (KBr): 3201, 3050, 2892, 1673, 1632, 1593, 1548, 1481, 1408, 1378, 1314, 1283, 1219, 1070, 992, 908, 839, 763, 701, 681 cm^{-1} . ^1H NMR (DMSO- d_6 , 300 MHz): δ 11.21 (s, 1H, NH(A)), 9.60 (s, 1H, NH(B)), 8.73 (d, $J = 5.59$ Hz, 2H, H2, H6), 8.43 (d, $J = 6.99$ Hz, 1H, CH), 7.79 (d, $J = 5.78$ Hz, 2H, H3, H5), 7.60 (s, 1H), 7.42 (m, 1H), 7.21 (m, 1H), 7.07 (m, 1H). ^{13}C NMR (DMSO- d_6 , 75 MHz): 160.3, 150.4 (2C), 147.1, 142.6, 141.4, 131.2, 123.8, 122.4, 121.4 (2C), 118.7, 115.3. Anal. Calcd for $\text{C}_{13}\text{H}_{11}\text{BrN}_4\text{O}$ (319.16): C, 48.92; H, 3.47; N, 17.55. Found: C, 49.24; H, 3.86; N, 17.91.

N-(4-chloro-2-hydroxyphenyl)-*N'*-isonicotinoylformohydrazoneamide (**15j**) Yield 30.10 %; mp 191 °C (ethanol). IR (KBr): 3193, 1693, 1633, 1549, 1488, 1411, 1360, 1317, 1261, 1222, 1061, 1023, 1002, 848, 682 cm^{-1} . ^1H NMR (DMSO- d_6 , 300 MHz): δ 11.02 (s, 1H, NH(A)), 9.04 (s, 1H, NH(B)), 8.73 (d, $J = 2.77$ Hz, 2H, H2, H6), 8.36 (s, 1H, CH), 8.14 (s, 1H), 7.94 (s, 1H, OH), 7.76 (d, $J = 3.90$ Hz, 2H, H3, H5), 7.54 (m, 1H), 6.84 (m, 1H). ^{13}C NMR (DMSO- d_6 , 75 MHz): 160.9, 151.6 (2C), 147.8, 143.9, 141.2, 130.2, 122.7, 121.0 (2C), 119.2, 115.4, 107.3. Anal. Calcd for $\text{C}_{13}\text{H}_{11}\text{N}_4\text{O}_2\text{Cl}$ (291.72): C, 53.71; H, 3.81; N, 19.27. Found: C, 54.02; H, 4.06; N, 18.83.

N-(5-chloro-2-hydroxyphenyl)-*N'*-isonicotinoylformohydrazoneamide (**15k**) Yield 43.10 %; mp 207 - 208 °C (ethanol). IR (KBr): 3219, 1695, 1635, 1587, 1542, 1515, 1413, 1389, 1324, 1285, 1060, 1010, 848, 684 cm^{-1} . ^1H NMR (DMSO- d_6 , 300 MHz): δ 11.27 (s, 1H, NH(A)), 9.03 (s, 1H, NH(B)), 8.72 (d, $J = 4.72$ Hz, 2H, H2, H6), 8.31 (d, $J = 17.91$ Hz, 1H, CH), 8.15 (s, 1H), 7.77 (d, $J = 4.91$ Hz, 2H, H3, H5), 7.59 (d, $J = 5.50$ Hz, 1H), 7.54 (s, 1H, OH), 6.81 (m, 1H). ^{13}C NMR (DMSO- d_6 , 75 MHz): 160.6, 150.6 (2C), 147.8, 144.9, 141.5, 130.2, 122.9, 121.4

(2C), 118.2, 115.4, 108.3. Anal. Calcd for C₁₃H₁₁N₄O₂Cl (291.72): C, 53.71; H, 3.81; N, 19.27. Found: C, 53.39; H, 3.61; N, 19.55.

N-(3,4-dichlorophenyl)-*N'*-isonicotinoylformohydrazonamide (**15l**) Yield 32.60 %; mp 192 °C (acetonitrile). IR (KBr): 3443, 2988, 1693, 1633, 1549, 1487, 1411, 1360, 1316, 1262, 1061, 1023, 849, 684 cm⁻¹. ¹H NMR (DMSO-*d*₆, 300 MHz): δ 11.02 (s, 1H, NH(A)), 9.78 (s, 1H, NH(B)), 8.73 (d, *J* = 4.92 Hz, 2H, H2, H6), 8.54 (s, 1H, CH), 8.25 (s, 1H), 7.76 (s, 1H), 7.54 (d, *J* = 4.90 Hz, 2H, H3, H5), 7.02 (m, 1H). ¹³C NMR (DMSO-*d*₆, 75 MHz): 160.5, 150.7 (2C), 147.2, 142.3, 140.1, 131.8, 130.2, 122.9, 121.2 (2C), 116.9, 110.0. Anal. Calcd for C₁₃H₁₀N₄OCl₂ (309.16): C, 50.51; H, 3.26; N, 18.12. Found: C, 50.12; H, 3.66; N, 18.47.

N-(3,4-difluorophenyl)-*N'*-isonicotinoylformohydrazonamide (**15m**) Yield 24.15 %; mp 193 °C (ethanol). IR (KBr): 3189, 2915, 1694, 1633, 1557, 1487, 1411, 1361, 1261, 1183, 1151, 1061, 1023, 1003, 920, 848, 752, 682 cm⁻¹. ¹H NMR (DMSO-*d*₆, 300 MHz): δ 11.09 (s, 1H, NH(A)), 9.80 (s, 1H, NH(B)), 8.73 (d, *J* = 5.38 Hz, 2H, H2, H6), 8.54 (s, 1H, CH), 8.36 (m, 1H), 7.76 (s, 1H), 7.53 (d, *J* = 5.79 Hz, 2H, H3, H5), 7.10 (m, 1H). ¹³C NMR (DMSO-*d*₆, 75 MHz): 161.7, 151.2 (2C), 148.1, 141.9, 140.5, 132.2, 131.4, 122.6, 121.2 (2C), 117.9, 112.1. Anal. Calcd for C₁₃H₁₀N₄OF₂ (277.26): C, 56.52; H, 3.65; N, 20.28. Found: C, 56.12; H, 3.91; N, 19.89.

N-(3-chloro-4-fluorophenyl)-*N'*-isonicotinoylformohydrazonamide (**15n**) Yield 21.60 %; mp 193 - 195 °C (ethanol). IR (KBr): 3200, 2915, 1686, 1632, 1602, 1549, 1489, 1411, 1360, 1261, 1222, 1062, 905, 848, 682 cm⁻¹. ¹H NMR (DMSO-*d*₆, 300 MHz): δ 11.03 (s, 1H, NH(A)), 9.78 (s, 1H, NH(B)), 8.74 (d, *J* = 4.87 Hz, 2H, H2, H6), 8.38 (s, 1H, CH), 8.14 (m, 1H), 7.76 (s, 1H), 7.53 (d, *J* = 4.94 Hz, 2H, H3, H5), 6.99 (m, 1H). ¹³C NMR (DMSO-*d*₆, 75 MHz): 160.8, 158.1, 150.2 (2C), 147.0, 145.7, 140.4, 133.4, 126.8, 121.5 (2C), 115.8, 110.9. Anal. Calcd for C₁₃H₁₀N₄OCIF (293.71): C, 53.35; H, 3.44; N, 19.14. Found: C, 53.74; H, 3.09; N, 19.46.

N-(4-bromo-3-fluorophenyl)-*N'*-isonicotinoylformohydrazonamide (**15o**) Yield 11.60 %; mp 193 - 195 °C (ethanol). IR (KBr): 3201, 2989, 1686, 1631, 1602, 1548, 1489, 1411, 1359, 1261, 1222, 1062, 905, 848, 682 cm⁻¹. ¹H NMR (DMSO-*d*₆, 300 MHz): δ 11.03 (s, 1H, NH(A)), 9.80 (s, 1H, NH(B)), 8.74 (d, *J* = 4.46 Hz, 2H, H2, H6), 8.40 (d, *J* = 13.19 Hz, 1H, CH), 8.15 (s, 1H), 7.77 (d, *J* = 5.54 Hz, 2H, H3, H5), 7.54 (m, 1H), 7.00 (m, 1H). ¹³C NMR (DMSO-*d*₆, 75 MHz): 160.4, 157.4, 150.4 (2C), 146.7, 142.3, 141.1, 133.8, 121.4 (2C), 114.1, 105.0, 98.3.

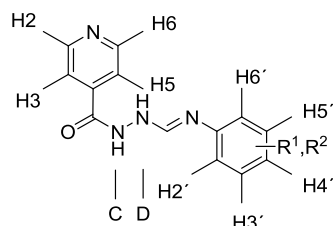
Anal. Calcd for C₁₃H₁₀N₄OBrF (338.17): C, 46.31; H, 2.99; N, 16.62. Found: C, 46.01; H, 3.39; N, 16.41.

General procedure for the synthesis of compounds **17a** – **17n**

Diethoxymethyl acetate (3 mmol) was added to a stirred solution of substituted aniline (2 mmol) in acetonitrile (20 mL) at 40 °C. The reaction mixture was stirred for 30 minutes at the same temperature. The crude product **16** was filtered off and without further purification was used for following reaction.

A solution of intermediate **16** (1 mmol) in acetonitrile (1 mL) was added to a stirred solution of isoniazid (1 mmol) in acetonitrile (10 mL) at 55 °C. The mixture was stirred for 6 hours at the same temperature and for 20 hours at room temperature. The precipitate was collected by filtration and recrystallized from appropriate solvent.

Data of compounds **17a** – **17n**



General structure for NMR evaluation

N'-[3-hydroxyphenylimino)methyl]isonicotinohydrazide (**17a**) Yield 56.90 %; mp 190-192 °C (methanol). IR (KBr): 3226, 3085, 3030, 2871, 2601, 2488, 1669, 1631, 1599, 1544, 1497, 1445, 1414, 1366, 1306, 1247, 1164, 1062, 1003, 964, 909, 849, 764, 697, 688 cm⁻¹. ¹H NMR (DMSO-*d*₆, 300 MHz): δ 11.15 (s, 1H, NH(C)), 9.42 (s, 1H, NH(D)), 8.69 (d, *J* = 6.12 Hz, 2H, H2, H6), 8.36 (s, 1H, CH), 7.81 (s, 1H, OH), 7.75 (d, *J* = 4.65 Hz, 1H), 7.72 (d, *J* = 6.10 Hz, 2H, H3, H5), 7.59 (m, 1H), 7.38 (m, 1H), 7.12 (t, *J* = 8.75 Hz, 1H). ¹³C NMR (DMSO-*d*₆, 75 MHz): 164.1, 160.3, 150.4 (2C), 147.7, 141.5, 140.5, 137.4, 121.4, 121.2 (2C), 118.2, 115.7. Anal. Calcd for C₁₃H₁₂N₄O₂ (256.26): C, 60.93; H, 4.72; N, 22.86. Found: C, 60.69; H, 5.04; N, 21.72.

N'-[4-hydroxyphenylimino)methyl]isonicotinohydrazide (**17b**) Yield 59.25 %; mp 190-192 °C (ethanol). IR (KBr): 3235, 3101, 3033, 2872, 1669, 1645, 1635, 1599, 1539, 1445, 1414, 1368,

1306, 1247, 1164, 1062, 849, 767, 697 cm^{-1} . ^1H NMR (DMSO- d_6 , 300 MHz): δ 11.05 (s, 1H, NH(C)), 9.88 (s, 1H, NH(D)), 8.71 (d, $J = 5.88$ Hz, 2H, H2, H6), 8.60 (s, 1H, CH), 7.79 (d, $J = 18.23$ Hz, 2H, H3, H5), 7.48 (s, 1H, OH), 7.10 (d, $J = 39.09$ Hz, 2H, H2', H6'), 6.71 (d, $J = 10.71$ Hz, 2H, H3', H5'). ^{13}C NMR (DMSO- d_6 , 75 MHz): 160.1, 152.9, 150.3 (2C), 148.4, 147.2, 140.8, 121.4 (2C), 118.5 (2C), 115.7 (2C). Anal. Calcd for $\text{C}_{13}\text{H}_{12}\text{N}_4\text{O}_2$ (256.26): C, 60.93; H, 4.72; N, 21.86. Found: C, 60.51; H, 4.45; N, 22.11.

N'-[(3-trifluoromethyl)phenylimino)methyl]isonicotinohydrazide (**17c**) Yield 70.91 %; mp 189-191 $^{\circ}\text{C}$ (acetonitril). IR (KBr): 3240, 3100, 3041, 1657, 1633, 1600, 1559, 1545, 1497, 1478, 1340, 1324, 1263, 1206, 1188, 1172, 1132, 1105, 1072, 999, 901, 881, 833, 791, 710, 697, 670, 639 cm^{-1} . ^1H NMR (DMSO- d_6 , 300 MHz): δ 11.25 (s, 1H, NH(C)), 9.78 (d, $J = 6.02$ Hz, 1H, NH(D)), 8.74 (d, $J = 5.83$ Hz, 2H, H2, H6), 8.52 (d, $J = 5.61$ Hz, 1H, CH), 7.84 (d, $J = 4.20$ Hz, 1H), 7.76 (d, $J = 5.70$ Hz, 2H, H3, H5), 7.52 (m, 2H), 7.24 (d, $J = 6.87$ Hz, 1H). ^{13}C NMR (DMSO- d_6 , 75 MHz): 160.3, 150.4 (2C), 147.1, 141.7, 141.3, 130.4, 130.0, 124.2 (q, $J = 259.6$ Hz, CF_3), 121.4 (2C), 120.1, 117.5, 112.5. Anal. Calcd for $\text{C}_{14}\text{H}_{11}\text{F}_3\text{N}_4\text{O}$ (308.27): C, 54.55; H, 3.60; N, 18.18. Found: C, 54.54; H, 3.25; N, 18.51.

N'-[(3-fluorophenylimino)methyl]isonicotinohydrazide (**17d**) Yield 79.90 %; mp 178-180 $^{\circ}\text{C}$ (ethanol). IR (KBr): 3212, 1668, 1634, 1643, 1575, 1496, 1460, 1320, 1218, 1152, 845, 776, 682 cm^{-1} . ^1H NMR (DMSO- d_6 , 300 MHz): δ 11.23 (s, 1H, NH(C)), 9.61 (d, $J = 5.99$ Hz, 1H, NH(D)), 8.70 (d, $J = 4.42$ Hz, 2H, H2, H6), 8.44 (d, $J = 5.84$ Hz, 1H, CH), 7.80 (d, $J = 3.55$ Hz, 1H), 7.72 (d, $J = 6.02$ Hz, 2H, H3, H5), 7.43 (m, 1H), 7.02 (d, $J = 6.75$ Hz, 1H), 6.79 (m, 1H). ^{13}C NMR (DMSO- d_6 , 75 MHz): 160.3, 150.4 (2C), 147.1, 142.8, 141.4, 130.9, 122.8, 121.4 (2C), 112.5, 107.5, 103.3. Anal. Calcd for $\text{C}_{13}\text{H}_{11}\text{N}_4\text{OF}$ (258.25): C, 60.46; H, 4.29; N, 21.69. Found: C, 60.16; H, 3.92; N, 21.99.

N'-[(4-fluorophenylimino)methyl]isonicotinohydrazide (**17e**) Yield 60.80 %; mp 183-185 $^{\circ}\text{C}$ (ethanol). IR (KBr): 3220, 1676, 1631, 1586, 1548, 1491, 1313, 1258, 1075, 1004, 846, 815, 693, 676 cm^{-1} . ^1H NMR (DMSO- d_6 , 300 MHz): δ 11.15 (s, 1H, NH(C)), 9.43 (s, 1H, NH(D)), 8.69 (d, $J = 6.12$ Hz, 2H, H2, H6), 8.36 (s, 1H, CH), 7.73 (d, $J = 6.10$ Hz, 2H, H3, H5), 7.37 (d, $J = 4.69$ Hz, 2H, H2', H6'), 7.14 (d, $J = 8.77$ Hz, 2H, H3', H5'). ^{13}C NMR (DMSO- d_6 , 75 MHz): 160.3, 150.4 (2C), 147.7, 141.5, 140.5 (2C), 137.4, 121.2 (2C), 118.1 (2C), 115.8 (q, $J =$

22.41 Hz, C-F). Anal. Calcd for C₁₃H₁₁N₄OF (258.25): C, 60.46; H, 4.29; N, 21.69. Found: C, 60.25; H, 3.96; N, 22.09.

N'-[(3-chlorophenylimino)methyl]isonicotinohydrazide (**17f**) Yield 76.95 %; mp 180-182 °C (ethanol). IR (KBr): 3212, 1673, 1633, 1597, 1549, 1484, 1314, 1220, 1166, 1097, 994, 907, 840, 775, 681 cm⁻¹. ¹H NMR (DMSO-*d*₆, 300 MHz): δ 11.23 (s, 1H, NH(C)), 9.64 (d, *J* = 6.29 Hz, 1H, NH(D)), 8.73 (d, *J* = 4.92 Hz, 2H, H2, H6), 8.49 (d, *J* = 5.99 Hz, 1H, CH), 7.75 (d, *J* = 6.12 Hz, 2H, H3, H5), 7.49 (s, 1H), 7.32 (m, 1H), 7.19 (d, *J* = 7.15 Hz, 1H), 6.95 (d, *J* = 7.22 Hz, 1H). ¹³C NMR (DMSO-*d*₆, 75 MHz): 160.3, 150.4 (2C), 147.1, 142.5, 141.4, 133.8, 130.9, 121.4 (2C), 120.9, 116.0, 115.0. Anal. Calcd for C₁₃H₁₁N₄OCl (274.71): C, 56.84; H, 4.04; N, 20.40. Found: C, 56.56; H, 3.92; N, 20.76.

N'-[(4-chlorophenylimino)methyl]isonicotinohydrazide (**17g**) Yield 33.60 %; mp 178-180 °C (ethanol). IR (KBr): 3234, 1634, 1586, 1494, 1407, 1314, 1289, 1262, 1093, 1011, 820, 675 cm⁻¹. ¹H NMR (DMSO-*d*₆, 300 MHz): δ 11.20 (s, 1H, NH(C)), 9.57 (d, *J* = 6.36 Hz, 1H, NH(D)), 8.73 (d, *J* = 4.44 Hz, 2H, H2, H6), 8.42 (d, *J* = 6.03 Hz, 1H, CH), 7.75 (d, *J* = 4.50 Hz, 2H, H3, H5), 7.34 (d, *J* = 4.40 Hz, 2H, H2', H6'), 7.20 (d, *J* = 8.69 Hz, 2H, H3', H5'). ¹³C NMR (DMSO-*d*₆, 75 MHz): 160.3, 150.4 (2C), 147.2, 141.4, 139.9, 129.1 (2C), 124.8, 121.4 (2C), 118.1 (2C). Anal. Calcd for C₁₃H₁₁N₄OCl (274.71): C, 56.84; H, 4.04; N, 20.40. Found: C, 56.90; H, 4.31; N, 20.49.

N'-[(3-bromophenylimino)methyl]isonicotinohydrazide (**17h**) Yield 79.70 %; mp 188-190 °C (ethanol). IR (KBr): 3201, 1675, 1632, 1547, 1481, 1407, 1315, 1219, 1071, 992, 909, 838, 763, 701, 680 cm⁻¹. ¹H NMR (DMSO-*d*₆, 300 MHz): δ 11.21 (s, 1H, NH(C)), 9.62 (d, *J* = 5.68 Hz, 1H, NH(D)), 8.73 (d, *J* = 4.72 Hz, 2H, H2, H6), 8.47 (d, *J* = 5.44 Hz, 1H, CH), 7.82 (d, *J* = 3.65 Hz, 1H), 7.71 (d, *J* = 6.10 Hz, 2H, H3, H5), 7.60 (s, 1H), 7.32 (d, *J* = 2.75 Hz, 1H), 7.09 (t, *J* = 2.03 Hz, 1H). ¹³C NMR (DMSO-*d*₆, 75 MHz): 160.3, 150.3 (2C), 147.1, 142.6, 141.3, 131.2, 123.8, 122.3, 121.4 (2C), 118.7, 115.3. Anal. Calcd for C₁₃H₁₁N₄OBr (319.16): C, 48.92; H, 3.47; N, 17.55. Found: C, 48.56; H, 3.72; N, 17.19.

N'-[(4-bromophenylimino)methyl]isonicotinohydrazide (**17i**) Yield 49.12 %; mp 186-188 °C (ethanol). IR (KBr): 3220, 1699, 1631, 1586, 1548, 1491, 1313, 1258, 1075, 1004, 846, 815, 693, 676 cm⁻¹. ¹H NMR (DMSO-*d*₆, 300 MHz): δ 11.21 (s, 1H, NH(C)), 9.58 (d, *J* = 7.07 Hz,

1H, NH(D)), 8.72 (d, $J = 6.07$ Hz, 2H, H2, H6), 8.42 (d, $J = 6.73$ Hz, 1H, CH), 7.74 (d, $J = 6.01$ Hz, 2H, H3, H5), 7.44 (d, $J = 8.85$ Hz, 2H, H2', H6'), 7.29 (d, $J = 8.86$ Hz, 2H, H3', H5'). ^{13}C NMR (DMSO- d_6 , 75 MHz): 160.4, 150.5 (2C), 147.2, 141.5, 140.3, 132.1 (2C), 121.5 (2C), 118.6 (2C), 112.7. Anal. Calcd for $\text{C}_{13}\text{H}_{11}\text{N}_4\text{OBr}$ (319.17): C, 48.92; H, 3.47; N, 17.55. Found: C, 49.20; H, 3.81; N, 17.89.

N'-[(3-nitrophenylimino)methyl]isonicotinohydrazide (**17j**) Yield 38.91 %; mp 190-191 °C (ethanol). IR (KBr): 3232, 3080, 1641, 1636, 1530, 1350, 1265, 1209, 1149, 1068, 998, 840, 736, 678 cm^{-1} . ^1H NMR (DMSO- d_6 , 300 MHz): δ 11.29 (s, 1H, NH(C)), 9.93 (d, $J = 7.29$ Hz, 1H, NH(D)), 8.74 (d, $J = 5.96$ Hz, 2H, H2, H6), 8.56 (d, $J = 7.19$ Hz, 1H, CH), 8.27 (s, 1H), 7.84 (d, $J = 5.27$ Hz, 1H), 7.77 (d, $J = 1.9$ Hz, 2H, H3, H5), 7.69 (d, $J = 7.59$ Hz, 1H), 7.58 (m, 1H). ^{13}C NMR (DMSO- d_6 , 75 MHz): 160.4, 150.4 (2C), 148.7, 146.8, 142.1, 141.3, 130.6, 122.7, 121.4 (2C), 115.8, 110.4. Anal. Calcd for $\text{C}_{13}\text{H}_{11}\text{N}_5\text{O}_3$ (285.26): C, 54.74; H, 3.89; N, 24.55. Found: C, 54.49; H, 4.12; N, 24.43.

N'-[(3,4-dichlorophenylimino)methyl]isonicotinohydrazide (**17k**) Yield 32.45 %; mp 207 - 209 °C (ethanol). IR (KBr): 3277, 3042, 1668, 1649, 1626, 1596, 1545, 1477, 1427, 1395, 1324, 1262, 1134, 1065, 840, 687 cm^{-1} . ^1H NMR (DMSO- d_6 , 300 MHz): δ 11.25 (s, 1H, NH(C)), 9.71 (s, 1H, NH(D)), 8.85 (s, 1H, CH), 8.74 (d, $J = 4.92$ Hz, 2H, H2, H6), 7.75 (d, $J = 5.90$ Hz, 2H, H3, H5), 7.50 (d, $J = 8.79$ Hz, 1H), 7.24 (d, $J = 8.81$ Hz, 1H), 7.19 (m, 1H). ^{13}C NMR (DMSO- d_6 , 75 MHz): 160.4, 150.4 (2C), 146.8, 141.3, 141.1, 131.6, 131.0, 122.5, 121.4 (2C), 117.8, 116.9. Anal. Calcd for $\text{C}_{13}\text{H}_{10}\text{N}_4\text{OCl}_2$ (309.16): C, 50.51; H, 3.26; N, 18.12. Found: C, 50.88; H, 3.43; N, 18.39.

N'-[(3,4-difluorophenylimino)methyl]isonicotinohydrazide (**17l**) Yield 29.60 %; mp 170 - 172 °C (ethanol). IR (KBr): 3204, 1686, 1633, 1601, 1549, 1484, 1412, 1337, 1261, 1111, 1061, 919, 848, 682 cm^{-1} . ^1H NMR (DMSO- d_6 , 300 MHz): δ 11.03 (s, 1H, NH(C)), 9.56 (s, 1H, NH(D)), 8.73 (d, $J = 4.34$ Hz, 2H, H2, H6), 8.66 (s, 1H, CH), 8.15 (m, 1H), 7.74 (d, $J = 4.34$ Hz, 2H, H3, H5), 7.54 (d, $J = 4.53$ Hz, 1H), 7.09 (m, 1H). ^{13}C NMR (DMSO- d_6 , 75 MHz): 164.1, 158.2, 156.9, 150.5 (2C), 143.0, 140.3, 134.5, 133.1, 130.5, 126.4, 121.5 (2C). Anal. Calcd for $\text{C}_{13}\text{H}_{10}\text{N}_4\text{OF}_2$ (277.26): C, 56.52; H, 3.65; N, 20.28. Found: C, 56.98; H, 3.38; N, 20.59.

N'-[(3-chloro-4-fluorophenylimino)methyl]isonicotinohydrazide (**17m**) Yield 44.90 %; mp 184 - 185 °C (ethanol). IR (KBr): 3046, 2879, 1669, 1634, 1552, 1504, 1427, 1404, 1369, 1318, 1263, 1222, 1065, 1001, 840, 684 cm⁻¹. ¹H NMR (DMSO-*d*₆, 300 MHz): δ 11.21 (s, 1H, NH(C)), 9.58 (s, 1H, NH(D)), 9.11 (d, *J* = 11.00 Hz, 1H), 8.73 (d, *J* = 4.25 Hz, 2H, H2, H6), 8.37 (d, *J* = 4.19 Hz, 1H, CH), 8.37 (d, *J* = 4.19 Hz, 2H, H3, H5), 7.34 (m, 2H). ¹³C NMR (DMSO-*d*₆, 75 MHz): 160.4, 152, 3, 150.5 (2C), 147.4, 141.4, 138.6, 135.0, 127.0, 121.4 (2C), 119.4, 117.0. Anal. Calcd for C₁₃H₁₀N₄OCIF (293.71): C, 53.35; H, 3.44; N, 19.14. Found: C, 52.94; H, 3.26; N, 19.43.

N'-[(4-bromo-3-fluorophenylimino)methyl]isonicotinohydrazide (**17n**) Yield 16.60 %; mp 186 - 187 °C (ethanol). IR (KBr): 3232, 1656, 1623, 1544, 1493, 1411, 1325, 1267, 1213, 1184, 1145, 1060, 842, 687 cm⁻¹. ¹H NMR (DMSO-*d*₆, 300 MHz): δ 11.26 (s, 1H, NH(C)), 9.74 (d, *J* = 6.58 Hz, 1H, NH(D)), 8.74 (d, *J* = 5.19 Hz, 2H, H2, H6), 8.42 (d, *J* = 6.36 Hz, 1H, CH), 7.75 (d, *J* = 5.21 Hz, 2H, H3, H5), 7.54 (d, *J* = 8.79 Hz, 1H), 7.03 (d, *J* = 8.74 Hz, 1H), 6.81 (m, 1H). ¹³C NMR (DMSO-*d*₆, 75 MHz): 160.4, 157, 1, 150.6 (2C), 146.7, 142.3, 141.3, 133.6, 121.4 (2C), 114.3, 104.6, 98.2. Anal. Calcd for C₁₃H₁₀N₄OBrF (338.17): C, 46.31; H, 2.99; N, 16.62. Found: C, 46.20; H, 2.54; N, 16.92.

4.4. Conclusion of the second part of thesis

Contemporary antituberculous drug modifications are one of the main approaches in the research of new antitubercotics. The connection of two active molecules by an easily released methine bridge was designed and synthesized. The work builds on the previous results of our research group.

The preparation of fluoro-containing hydrazone derivatives have been synthesized in the Faculty of Chemistry and Chemical Technology, University of Ljubljana as an international Erasmus and Contact program. The first or second line antitubercotics (PAS, CPX, NFX, PZA) were linked with fluorinated hydrazones for purpose of the increasing antimycobacterial activity of selected drugs (**11a-11l**, **13a**, **13b**). All evaluated compounds have shown higher activity against MDR-TB (0.5 µg/mL) than INH. Compounds containing CPX were the most active against *M. tbc.* H₃₇Rv and *M. kansasii* 235/80 and 6509/96. Hydrolysis stability measurement have exhibited that evaluated compound is stable at neutral pH and also in rat plasma, no significant decomposition was observed during 48 hours experiment. No formylciprofloxacin as putative metabolite was detected in the samples. It could improve the bioavailability to target site (Paper IV).

Unpublished experimental data of second serie of hydrazone derivatives of INH **15a-15o**, **17a-17n** (29 new compounds) are presented. The compounds with electron-acceptor substituents showed similar biological activity as a standard INH. In general, derivatives with halogenated substituents exhibited better MIC values. Several compounds exhibited the same inhibitory effect as INH against *M. tbc.* Compound **17n** with substituents 4-Br and 3-F was the most active against all tested strains *M. tbc.*, *M. avium* and *M. kansasii*, unluckily cytotoxicity on Hep G2 and PBMC of this derivative is relatively high. It is assumed that the methine bridge of derivatives is gradually hydrolyzed. Values of lipophilicity were higher than INH, it signifies more effective transport of the molecule through cellular membranes.

5. Biological testing of prepared compounds

In co-operation with Eötvös Lóránd University, Research Group of Peptide Chemistry, Hungarian Academy of Science in Budapest I have got the possibility to measure by myself the cytotoxicity of prepared compounds, eventually other biological assays which are suitable for further testing of promising compounds.

5.1. Cytotoxicity determination by MTT assay

MTT assay is quantitative colorimetric method which determines cell growth rate. Cell proliferation is controlled by growth factors that bind to cell surface receptors (integral transmembrane proteins). They are connected to signalling molecules. These molecules activate transcription factors which bind to DNA to modulate the production of proteins, resulting cell division. Dysfunction of any step in regulatory cascade causes abnormal cell proliferation. Determination of cell growth rates is widely used for the testing of drug action, cytotoxic agents and screening other biologically active compounds

The MTT assay^{129,130} is based on the reduction of the yellow tetrazolium salt MTT (3-(4,5-dimethylthiazol-2-yl)-2,5-diphenyltetrazolium bromide) by respiratory chain and other electron transport system.¹³¹ Non-water-soluble violet formazan crystals are formed in mitochondria of metabolic active cells.¹³²

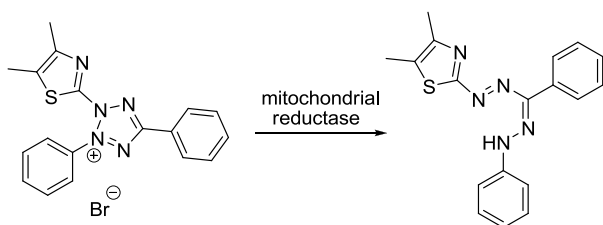


Fig. 23 Reduction of 3-(4,5-dimethylthiazol-2-yl)-2,5-diphenyltetrazolium bromide

The formazan is then solubilised usually in dimethyl sulfoxide and the concentration determined by optical density (OD) at $\lambda = 540$ and 620 nm using ELISA Reader. OD₆₂₀ values were subtracted from OD₅₄₀ values. The percent of cytotoxicity was calculated using the following equation:

$$\text{Cytotoxicity (\%)} = [1 - (\text{OD}_{\text{treated}}/\text{OD}_{\text{control}})] \times 100;$$

where OD_{treated} and OD_{control} correspond to the optical densities of the treated and the control cells, respectively.

The result is a sensitive assay with a colorimetric signal proportional to the cell number. This reduction occurs only when mitochondrial reductase enzymes are active, therefore conversion can be directly related to the number of living cells.¹³³ The 50% inhibitory concentration (IC_{50}) values were determined from the dose-response curves.

MTT assay was used for cytotoxicity determination of HepG2 human hepatoma cells (ATCC HB-8065), human PBMC (peripheral blood mononuclear cells)¹²⁸ and SH-SY5Y human neuroblastoma cell line. HepG2 and PBMC were cultured in RPMI-1640 medium without phenol red supplemented with 10% FCS (fetal calf serum), 2 mM L-glutamine and 160 $\mu\text{g}/\text{ml}$ gentamycin. SH-SY5Y was grown in DMEM (Dulbecco's Modified Eagle's Medium) medium without phenol red containing 10% FCS, 2 mM L-glutamine, 160 $\mu\text{g}/\text{mL}$ gentamycin and 1 % nonessential amino acids (NEAA).

5.1.1. Antituberculosis drug-induced hepatotoxicity

Human liver cell line Hep G2 was chosen as a model of hepatocytes. Cytotoxicity on HepG2 was determined due to toxic metabolites of antituberculosics which can develop drug-induced hepatotoxicity (DIH). Antituberculosis drug-induced hepatotoxicity can be fatal when is not recognized at an early stage, after which the therapy should be interrupted. Development of DIH depends on main risk factors as age, sex, ethnic, acetylator phenotype and HIV infection.¹³⁴

Isoniazid and its metabolites are considered as the most significant activators of DIH. Twenty-four hours of application of INH in concentrations > 26 mM led to a remarkable number of apoptotic cells positive for Annexin V.¹³⁵ Hydrazine, the metabolite of INH formed by amidase-catalysed hydrolysis, causes significant production of endogenous hydrogen peroxide which initiates processes of hydroxyl radical formation, that results in lysosomal damage and development of inflammation.¹³⁶ Incidence of drugs combination can have synergic hepatotoxic effect. It was proved that the *in vitro* hepatotoxicity of PZA is increased by pre-treatment of cells with INH.¹³⁷ On the other hand, INH is able to increase activity of CYP2E1, the enzyme

responsible for metabolism of xenobiotics to production of free radicals. Simultaneously, INH decreases activities of glutathione S-transferases (GSTs) function responsible for the protection of cytoplasm against free radicals, but RIF normalizes the production of ROS by CYP2E1 and GSTs. It indicates that RIF has antagonistic effect.¹³⁸

5.1.2. Immune response to *Mycobacterium tuberculosis*

Human PBMC (Peripheral blood mononuclear cells) are suitable cellular model of immunocompetent cells which are important for a local immune response and a destruction of mycobacteria.¹³⁹ PBMC are a preparation of blood cells which contains macrophages, monocytes and lymphocytes. Mostly, treatment of TB is based on the cellular immunity and chemotherapy. Protective immune response involves a phagocytosis of *Mycobacterium tuberculosis* by alveolar macrophages which are activated by antigen-specific CD 8 T lymphocytes.¹⁴⁰ The initial infection sets off a cascade of inflammatory molecules, including release of cytokines (INF- γ , TNF- α) and chemokines (CCL2, CCL3, CCL4, CCL5 – migration of macrophages to the lungs) from the infected macrophages¹⁴¹. Cells (macrophages, T and B cells) form a granuloma in the site of infection. Macrophages can differentiate into multinuclear giant cells. Necrosis can occur in granuloma. Apoptotic death of infected macrophages can be induced by 19 kDa glycoprotein of *M. tuberculosis*, TNF- α or Fas ligand.¹⁴²

Chemotherapy kills the majority of bacteria during few days, but subpopulation in stationary phase (granuloma) could persist in aerobic or anaerobic sites.¹⁴³ Therefore, administration of antituberculous drugs must be continued for at least 6 months. During this time an immune cell system should protect the body of patient. Therefore it is essential to find out if used drugs are not toxic for human PBMC which play important role in systemic immune response.

5.2. Flow cytometry

The basic principle of flow cytometry is to provide rapid analysis of multiple characteristics of single cells or particles including nuclei, microorganism, chromosome preparations and latex beads. They pass through a light source focused at a very small region. Usually there is an air-cooled argon gas laser in the instrument which emit a monochromatic beam of light fixed at 488 nm.¹⁴⁴ Emitted light is given off in all directions and is collected to series of filters and

dichroic mirrors that isolate particular wavelength bands. The light signals are detected by photomultiplier tubes and digitalized for computer analysis. The resulting information is usually displayed in histograms or two-dimensional dot-plot formats.¹⁴⁵ Generated optical signals represent the detection of various chemical or biological components. It is possible to separate particles or cells into populations. They based on statistical differences of 10 to 20 parameters that can be measured on each particle or cell. The most common detection system in flow cytometry uses fluorescent molecules which are attached to the particle of interest. The fluorescent probe might be bounded to membrane, cytoplasm or nuclear materials. Other common practice is application of monoclonal and polyclonal antibodies that recognize specific receptors on cells.

Fluorescent labeling of chitosan led us to try an experiment with the flow cytometry which was investigated to the uptake study of labeled chitosan by human PBMC (Fig. 21). Cellular uptake was observed on macrophages and monocytes. This ascertainment can be important for latent phase of TB. Chitosan connected with antituberculotics could be phagocytised by immunocompetent cells and destruct pathogenic mycobacteria.

6. References

- ¹ LOUVEAU, C.; DESCROIX, D.; GARNIER, L. et al. A nose-only apparatus for airborne delivery of *Mycobacterium tuberculosis* to mice: calibration of biological parameters. *Microbes and Infection*. 2005, vol 7, p 457-466.
- ² World Health Organization. *Global tuberculosis control 2009: surveillance, planning, financing*: WHO report 2009, http://whqlibdoc.who.int/publications/2009/9789241598866_eng.pdf
- ³ GANDY, M.; ZUMLA, A. The resurgence of disease: social and historical perspectives on the “new“ tuberculosis. *Social Science and Medicine*. 2002, vol 55, p 385-396.
- ⁴ FALKINHAM, J. O. Epidemiology of infection by nontuberculous mycobacteria. *Clinical Microbiology Reviews*. 1996, vol 9, p 177-215.
- ⁵ JOHNSON, R.; STREICHER, E. M.; LOUW, G. E. et al. Drug Resistance in *Mycobacterium tuberculosis*. *Current Issues in Molecular Biology*. 2006, vol 8, p 97-112.
- ⁶ World Health Organization. *Antituberculosis-drug resistance in the world*. Report No. 4, 2008, ISBN 978-92-4-156361.
- ⁷ BARRY 3rd, C. E.; BLANCHARD, J. S. The chemical biology of new drugs in the development for tuberculosis. *Current Opinion in Chemical Biology*. article in press.
- ⁸ VINŠOVÁ, J.; KRÁTKÝ, M. Nova Science Publishers. New York, 2009. In: Nguy, S., K'ung, Z., eds. Chap. Drug-Resistant Tuberculosis. ISBN 978-1-60876-055-8.
- ⁹ JANIN, Y. L. Antituberculosis drugs: Ten years of research. *Biorganic and Medicinal Chemistry*. 2007, vol 15, p 2479-2513.
- ¹⁰ PIDDOCK, L. J. V.; RICCI, V. Accumulation of five fluoroquinolones by *Mycobacterium tuberculosis* H37Rv. *Journal of Antimicrobial Chemotherapy*. 2001, vol 48, p 787-791.
- ¹¹ YEE, D.; VALLIQUETTE, C.; PELLETIER, M. et al. Incidence of serious side effects from first-line antituberculosis drugs among patients treated for active tuberculosis. *American Journal of Respiratory and Critical Care Medicine*. 2003, vol 167, p 1472-1477.
- ¹² SCHABERG, T.; REBHAN, K.; LODE, H.. Risk factors for side-effects of isoniazid, rifampin and pyrazinamide in patients hospitalized for pulmonary tuberculosis. *European Respiratory Journal*. 1996, vol 9, p 2026-2030.
- ¹³ BILLO, N.; CASTRO, J. L.; JONES, S. et al. The International Union against tuberculosis and lung disease: past, present and future. *International Health*. 2009, vol 1, p 117-123.
- ¹⁴ World Health Organization, *The Stop TB Strategy*, 2006, http://whqlibdoc.who.int/hq/2006/WHO_HTM_STB_2006.368_eng.pdf
- ¹⁵ LÖNNROTH, K.; JARRAMILLO, E.; WILLIAMS, B. G. et al. Divers of tuberculosis epidemics: The role of risk factors and social determinants. *Social Science and Medicine*. 2009, vol 68, p 2240-2246.

-
- ¹⁶ URAGANU, T.; TOKURA, S. Ed. Material science of chitin and chitosan. New York, Springer 2006
- ¹⁷ VINŠOVÁ, J.; VAVŘÍKOVÁ, E. Recent advances in drugs and prodrugs design of chitosan. *Current Pharmaceutical Design*. 2008, vol 14, p 1311-1326.
- ¹⁸ ZHENG, L. Y.; ZHU, J. F. Study on antimicrobial activity of chitosan with different molecular weights. *Carbohydrate Polymers*. 2003, vol 54, p 527-530.
- ¹⁹ QIN, C.; DU, Y.; XIAO, L. et al. Enzymic preparation of water-soluble chitosan and their antitumor activity. *International Journal of Biological Macromolecules*. 2002, vol 31, p 111-117.
- ²⁰ YEN, M. T.; YANG, J. H.; MAU, J. L. Antioxidant properties of chitosan from crab shells. *Carbohydrate Polymers*. 2008, vol 74, p 840-844.
- ²¹ AMIDI, M.; MASTROBATTISTA, E.; JISKOOT, W., et al. Chitosan-based delivery systems for protein therapeutics and antigens. *Advance Drug Delivery Review*. 2010, vol 62, p 59-82.
- ²² RAUW, F.; GARDIN, Y.; PALYA, V., et al. The positive adjuvant effect of chitosan on antigen-specific cell-mediated immunity after chicken vaccination with live Newcastle disease vaccine. *Veterinary Immunology and Immunopathology*. 2010, vol. 134, p 249-258.
- ²³ SHI, G.; CHEN, Y.; WAN, C., et al. Study of the preparation of chitosan-alginate complex membrane and the effects on adhesion and activation of endothelial cells. *Applied Surface Science*. 2008, vol 255, p 422-425.
- ²⁴ MINAGAWA, T.; OKAMURA, Y.; SHIGEMASA, Y., et al. Effects of molecular weight and deacetylation degree of chitin/chitosan on wound healing. *Carbohydrate Polymers*. 2007, vol 67, p 640-644.
- ²⁵ ONG, S. Y.; WU, J.; MOOCHHALA, S. M. et al. Development of a chitosan-based wound dressing with improved hemostatic and antimicrobial properties. *Biomaterials*. 2008, vol 29, p 4323-4332.
- ²⁶ TSAO, C. T.; CHANG, C. H.; LIN, Y. Y., et al. Evaluation of chitosan/ γ -poly (glutamic acid) polyelectrolyte complex for wound dressing materials. *Carbohydrate Polymers*. 2010, article in press.
- ²⁷ YANG, X.; YANG, K.; WU, S., et al. Cytotoxicity and wound healing properties of PVA/ws-chitosan/glycerol hydrogels made by irradiation followed by freeze-thawing. *Radiation Physics and Chemistry*. 2010, vol 79, p 606-611.
- ²⁸ VARMA, A. J.; DESHPANDE, S. V.; KENNEDY, J. F. Metal complexation by chitosan and its derivatives: a review. *Carbohydrate Polymers*. 2004, vol 55, p 77-93.
- ²⁹ MAO, S.; SUN, W.; KISSEL, T. Chitosan-based formulations for delivery of DNA and siRNA. *Advanced Drug Delivery Reviews*. 2010, vol 62, p 12-27.
- ³⁰ SHI, C.; ZHU, Y.; RAN, X., et al. Therapeutic potential of chitosan and its derivatives in regenerative medicine. *Journal of Surgical Research*. 2006, vol 133, p 185-192.

-
- ³¹ JAYAKUMAR, R.; CHENNAZHI, K. P.; MUZZARELLI, R. A. A. et al. Chitosan conjugated DNA nanoparticles in gene therapy. *Carbohydrate Polymers*. 2010, vol 79, p 1-8.
- ³² PARK, J. H.; SARAVANAKUMAR, G.; KIM, K., et al. Targeted delivery of low molecular drugs using chitosan and its derivatives. *Advanced Drug Delivery Reviews*. 2010, vol 62, p 28-41.
- ³³ BHATTARAI, N.; GUNN, J.; ZHANG, M. Chitosan-based hydrogels for controlled, localized drug delivery. *Advanced Drug Delivery Reviews*. 2010, vol 62, p 83-99.
- ³⁴ ARANAZ, I.; HARRIS, R.; HERAS, A. Chitosan amphiphilic derivatives. Chemistry and application. *Current Organic Chemistry*. 2010, vol 14, p 308-330.
- ³⁵ HUO, M.; ZHANG, Y.; ZHOU, J. et al. Synthesis and characterization of low-toxic amphiphilic chitosan derivatives and their application as micelle carrier for antitumor drugs. *International Journal of Pharmaceutics*. 2010, vol 394, p 162-173.
- ³⁶ LI, X. F.; FENG, X. Q.; YANG, S., et al. Chitosan kills *Escherichia coli* through damage to be of cell membrane mechanism. *Carbohydrate Polymers*. 2010, vol 79, p 493-499.
- ³⁷ CHUNG, Y. C.; CHEN, C. Y. Antibacterial characteristics and activity of acid-soluble chitosan. *Bioresource Technology*. 2008, vol 99, p 2806-2814.
- ³⁸ KONG, M.; CHEN, X. G.; LIU, C. S., et al. Antibacterial mechanism of chitosan microspheres in a solid dispersing system against *E. coli*. *Colloids and Surfaces B: Biointerfaces*. 2008, vol 65, p 197-202.
- ³⁹ ZHONG, Z.; LI, P.; XING, R., et al. Antimicrobial activity of hydroxybenzenesulfonanilides derivatives of chitosan, chitosan sulfates and carboxymethyl chitosan. *International Journal of Biological Macromolecules*. 2009, vol 45, p 163-168.
- ⁴⁰ LIN, S. B.; LIN, Y. C.; CHEN, H. H. Low molecular weight chitosan prepared with the aid cellulase, lysozyme and chitinase: Characterisation and antibacterial activity. *Food Chemistry*. 2009, vol 116, 47-53.
- ⁴¹ MASSON, M.; HOLAPPA, J.; HJALMARSODOTTIR, M. et al. Antimicrobial activity of piperazine derivatives of chitosan. *Carbohydrate Polymers*. 2008, vol 74, p 566-571.
- ⁴² SAJOMSANG, W.; TANTAYANON, S.; TANGPASUTHADOL, V. et al. Quaternization of *N*-aryl chitosan derivatives: synthesis, characterization and antibacterial activity. *Carbohydrate Research*. 2009, vol 344, p 2502-2511.
- ⁴³ SAJOMSANG, W.; TANTAYANON, S.; TANGPASUTHADOL, V. et al. Synthesis of methylated chitosan containing aromatic moieties: Chemoselectivity and effect on molecular weight. *Carbohydrate Polymers*. 2008, vol 72, p 740-750.
- ⁴⁴ MA, G.; ZHANG, X.; HAN, J. et al. Photo-polymerizable chitosan derivative prepared by Michael reaction of chitosan and polyethylene glycol diacrylate (PEGDA). *International Journal of Biological Macromolecules*. 2009, vol 45, p 499-503.
- ⁴⁵ JIN, X.; WANG, J.; BAI, J. Synthesis and antimicrobial activity of the Schiff base from chitosan and citral. *Carbohydrate Research*. 2009, vol 344, p 825-829.

-
- ⁴⁶ KONG, M.; CHEN, X. G.; LIU, C. S. et al. Antibacterial mechanism of chitosan microspheres in a solid dispersing system against *E. coli*. *Colloids and Surfaces B: Biointerfaces*. 2008, vol 65, p 197-202.
- ⁴⁷ XU, X.; ZHUANG, X.; CHENG, B. et al. Manufacture and properties of cellulose/*O*-hydroxyethyl chitosan blend fibers. *Carbohydrate Polymers*. 2010, doi: 10.1016/j.carbpol.2010.03.011.
- ⁴⁸ GINER, S. T.; OCIO, M. J.; LAGARON, J. M. Novel antimicrobial ultrathin structures of zein/chitosan blends obtained by electrospinning. *Carbohydrate Polymers*. 2009, vol 77, p 261-266.
- ⁴⁹ SABAA, M. W.; MOHAMED, N. A.; MOHAMED, R. R. et al. Synthesis, characterization and antimicrobial activity of poly (*N*-vinyl imidazole) grafted carboxymethyl chitosan. *Carbohydrate Polymers*. 2010, vol 79, p 998-1005.
- ⁵⁰ ANITHA, A.; DIVYA RANI, V. V.; KRISHNA, R. et al. Synthesis, characterization, cytotoxicity and antibacterial studies of chitosan, *O*-carboxymethyl and *N,O*-carboxymethyl chitosan nanoparticles. *Carbohydrate Polymers*. 2009, vol 78, p 672-677.
- ⁵¹ HAN, Y. S.; LEE, S. H.; CHOI, K. H. et al. Preparation and characterization of chitosan-clay nanocomposites with antimicrobial activity. *Journal of Physics and Chemistry of Solid*. 2010, vol 71, p 464-467.
- ⁵² SANPUI, P.; MURUGADOSS, A.; DURGA, P. V. et al. The antibacterial properties of a novel chitosan-Ag-nanoparticles composite. *International Journal of Food Microbiology*. 2008, vol 124, p 142-146.
- ⁵³ YOKSAN, R.; CHIRACHANCHAI, S. Silver nanoparticles dispersing in chitosan solution: Preparation by γ -ray irradiation and their antimicrobial activities. *Material Chemistry and Physics*. 2009, vol 115, p 296-302.
- ⁵⁴ NIU, M.; LIU, X.; DAI J., et al. Antibacterial activity of chitosan coated Ag-loaded nano-SiO₂ composites. *Carbohydrate Polymers*. 2009, vol 78, p 54-59.
- ⁵⁵ ONG, S. Y.; WU, J.; MOOCHHALA, S. M. et al. Development of a chitosan-based wound dressing with improved hemostatic and antimicrobial properties. *Biomaterials*. 2008, vol 29, p 4323-4332.
- ⁵⁶ ZHONG, Z.; XING, R.; LIU, S. et al. Synthesis of acyl thiourea derivatives of chitosan and their antimicrobial activities in vitro. *Carbohydrate Research*. 2008, vol 343, p 566-570.
- ⁵⁷ GUO, Z.; XING, R.; LIU, S. et al. The influence of molecular weight of quaternized chitosan on antifungal activity. *Carbohydrate Polymers*. 2008, vol 71, p 694-697.
- ⁵⁸ HERNANDEZ-LAUZARDO, A. N.; BAUTISTA-BANOS, S.; VELAZQUEZ-DEL VALLE, M. G. et al. Antifungal effects of chitosan with different molecular weights on *in vitro* development of *Rhizopus stolonifer* (Ehrenb.:Fr.) Vuill. *Carbohydrate Polymers*. 2008, vol 73, p 541-547.

-
- ⁵⁹ GIRI DEV, V. R.; VENUGOPAL, J.; SUDHA, S. et al. Dyeing and antimicrobial characteristics of chitosan treated wool fabrics with henna dye. *Carbohydrate Polymers*. 2009, vol 75, p 646-650.
- ⁶⁰ HIGAZY, A.; HASHEM, M.; ELSHAFEI, A. et al. Development of antimicrobial jute packaging using chitosan and chitosan-metal complex. *Carbohydrate Polymers*. 2010, vol 79, p 867-874.
- ⁶¹ SUN, S.; AN, Q.; LI, X. et al. Synergistic effects of chitosan-guanidine complexes on enhancing antimicrobial activity and wet-strength of paper. *Bioresource Technology*. 2010, doi: 10.1016/j.biortech.2010.02.046.
- ⁶² SANGSUWAN, J.; RATTANAPANONE, N.; RACHTANAPUN, P. Effect of chitosan/methyl cellulose films on microbial and quality characteristics of fresh-cut cantaloupe and pineapple. *Postharvest Biology and Technology*. 2008, vol 49, p 403-410.
- ⁶³ FERNANDEZ-SAIZ, P.; LAGARON, J. M.; HERNANDEZ-MUNOZ, P. et al. Characterization of antimicrobial properties on the growth of *S. aureus* of novel renewable blends of gliadins and chitosan of interest in food packaging and coating application. *International Journal of Food Microbiology*. 2008, vol 124, p 13-20.
- ⁶⁴ LUO, H.; LI, J.; CHEN, X. Antitumor effect of *N*-succinyl-chitosan nanoparticles on K562 cells. *Biomedicine and Pharmacotherapy*. 2009, doi:10.1016/j.biopha.2009.09.002.
- ⁶⁵ ZHANG, J.; CHEN, X. G.; SUN, G. Z. et al. Effect of molecular weight on the oleoyl-chitosan nanoparticles as carrier for doxorubicin. *Colloids and Surfaces B: Biointerfaces*. 2010, vol 77, 125-130.
- ⁶⁶ TAN, Y.L.; LIU, C. G. Self-aggregated nanoparticles from linoleic acid modified carboxymethyl chitosan: Synthesis, characterization and application *in vitro*. *Colloids and Surfaces B: Biointerfaces*. 2009, vol 69, p 178-182.
- ⁶⁷ KATO, Y.; ONISHI, H.; MACHIDA, Y. Evaluation of *N*-succinyl-chitosan as a systemic long-circulating polymer. *Biomaterials*. 2000, vol 21, p 1579-1585.
- ⁶⁸ JEONG, Y. I.; JIN, S. G.; KIM, I. Y. et al. Doxorubicin-incorporated nanoparticles composed of poly(ethylene glycol)-grafted carboxymethyl chitosan and antitumor activity against glioma cells *in vitro*. *Colloids and Surfaces B: Biointerfaces*. 2010, doi: 10.1016/j.colsurfb.2010.03.037.
- ⁶⁹ CHO, Y. I.; PARK, S.; JEONG, S. Y. et al. *In vivo* and *in vitro* anti-cancer activity of thermo-sensitive and photo-crosslinkable doxorubicin hydrogels composed of chitosan-doxorubicin conjugates. *European Journal of Pharmaceutics and Biopharmaceutics*. 2009, vol 73, p 59-65.
- ⁷⁰ HU, F. Q.; LIU, L. N.; DU, Y. Z. et al. Synthesis and antitumor activity of doxorubicin conjugates stearic acid-g-chitosan oligosaccharide polymeric micelles. *Biomaterials*. 2009, vol 30, p 6955-6963.
- ⁷¹ KIM, J. H.; KIM, Y. S.; PARK, K. et al. Antitumor efficacy of cisplatin-loaded glycol chitosan nanoparticles in tumor-bearing mice. *Journal of Controlled Release*. 2008, vol 127, p 41-49.

-
- ⁷² HUO, M.; ZHANG, Y.; ZHOU, J.; et al. Synthesis and characterization of low-toxic amphiphilic chitosan derivatives and their application as micelle carrier for antitumor drug. *International journal of Pharmaceutics*. 2010, doi:10.1016/j.ijpharm.2010.05.001.
- ⁷³ SARAVANAKUMAR, G.; MIN, K. H.; MIN, D. S. et al. Hydrotropic oligomer-conjugated glycol chitosan as a carrier of paclitaxel: Synthesis, characterization and *in vivo* biodistribution. *Journal of Controlled Release*. 2009, vol 140, p 210-217.
- ⁷⁴ LEE, E.; KIM, H.; LEE, I. H. et al. *In vivo* antitumor effects of chitosan-conjugated docetaxel after oral administration. *Journal of Controlled Release*. 2009, vol 140, p 79-85.
- ⁷⁵ HWANG, H. Y.; KIM, I. S.; KWON, I. C. et al. Tumor targetability and antitumor effect of docetaxel-loaded hydrophobically modified glycol chitosan nanoparticles. *Journal of Controlled Release*. 2008, vol 128, p 23-31.
- ⁷⁶ KATO, Y.; ONISHI, H.; MACHIDA, Y. Biological characteristics of lactosaminated *N*-succinyl chitosan as a liver-specific drug carrier in mice. *Journal of Controlled Release*. 2001, vol 70, p 295-307.
- ⁷⁷ WANG, Q.; ZHANG, L.; HU, Wei. et al. Norcantharidin-associated galactosylated chitosan nanoparticles for hepatocyte-targeted delivery. *Nanomedicine: Nanotechnology, Biology and Medicine*. 2010, vol 6, p 371-381.
- ⁷⁸ KONG, C. S.; KIM, J. A.; AHN, B. et al. Carboxymethylation of chitosan and chitin inhibit MMP expression and ROS scavenging in human fibrosarcoma cells. *Process Biochemistry*. 2010, vol 45, p 179-186.
- ⁷⁹ KIM, K. W.; THOMAS, R. L. Antioxidative activity of chitosan with varying molecular weights. *Food Chemistry*. 2007, vol 101, p 308-313.
- ⁸⁰ TOMIDA, H.; YASUFUKU, T.; FUJII, T. et al. Polysaccharides as potential antioxidative compounds for extended-release matrix tablets. *Carbohydrate Polymers*. 2010, vol 345, p 82-86.
- ⁸¹ FENG, T.; DU, Y.; LI, J. et al. Enhancement of antioxidant activity of chitosan by irradiation. *Carbohydrate Polymers*. 2008, vol 73, p 126-132.
- ⁸² YEN, M. T.; YANG, J. H.; MAU, J. L. Antioxidant properties of chitosan from crab shells. *Carbohydrate Polymers*. 2008, vol 74, p 840-844.
- ⁸³ ANRAKU, M.; FUJII, T.; FURUTANI, N. et al. Antioxidant effect of dietary supplement: reduction of indices of oxidative stress in normal subjects by water-soluble chitosan. *Food and Chemical Toxicology*. 2009, vol 47, p 104-109.
- ⁸⁴ SUN, T.; YAO, Q.; ZHOU, D. et al. Antioxidant activity of *N*-carboxymethyl chitosan oligosaccharides. *Bioorganic and Medicinal Chemistry Letters*. 2008, vol 18, p 5774-5776.
- ⁸⁵ XING, R.; LIU, S.; GUO, Z. et al. Relevance of molecular weight of chitosan-*N*-2-hydroxypropyl trimethyl ammonium chloride and their antioxidant activities. *European Journal of Medicinal Chemistry*. 2008, 43, 336-340.
- ⁸⁶ GUO, Z.; XING, R.; LIU, S. et al. Synthesis and hydroxyl radicals scavenging activity of quaternized carboxymethyl chitosan. *Carbohydrate Polymers*. 2008, vol 73, p 173-177.

-
- ⁸⁷ ZHONG, Z.; XING, R.; LIU, S. et al. The antioxidant activity of 2-(4(or 2)-hydroxyl-5-chloride-1,3-benzene-di-sulfanamide)-chitosan. *European Journal of Medicinal Chemistry*. 2008, vol 43, p 2171-2177.
- ⁸⁸ ZHONG, Z.; ZHONG, Z.; XING, R. et al. The preparation and antioxidant activity of 2-[phenylhydrazine (or hydrazine)-thiosemicarbazone]-chitosan. *Biological macromolecules*. 2010, doi:10.1016/j.ijbiomac.2010.05.016.
- ⁸⁹ PASANPHAN, W.; BUETTNER, G. R.; CHIRACHANCHAI, S. Chitosan gallate as a novel potential polysaccharide antioxidant: an EPR study. *Carbohydrate Research*. 2010, vol 345, p 132-140.
- ⁹⁰ PASANPHAN, W.; CHIRACHANCHAI, S. Conjugation of gallic acid onto chitosan: An approach for green and water-based antioxidant. *Carbohydrate Polymers*. 2008, vol 72, p 169-177.
- ⁹¹ SIRIPATRAWAN, U.; HARTE, B. R. Physical properties and antioxidant activity of an active film from chitosan incorporated with green tea extract. *Food Hydrocolloids*. 2010, doi:10.1016/j.foodhyd.2010.04.003.
- ⁹² SOUSA, F.; GUEBITZ, G. M.; KOKOL, V. Antimicrobial and antioxidant properties of chitosan enzymatically functionalized with flavonoids. *Process Biochemistry*. 2009, vol 44, p 749-756.
- ⁹³ RINAUDO, M.; MILAS, M.; LE DUNG, P. Characterization of chitosan. Influence of ionic strength and degree of acetylation on chain expansion. *International Journal of Biological Macromolecules*. 1993, vol 15, p 281-285.
- ⁹⁴ PENDELA, M.; DRAGOVIC, S.; BOCKX, L. et al. Development of a liquid chromatographic method for the determination of related substances and assay of D-cycloserine. *Journal of Pharmaceutical and Biomedical Analysis*. 2008, vol 47, p 807-811.
- ⁹⁵ DE SARRO, G.; GRATTERI, S.; NACCARI, F. et al. Influence of D-cycloserine on the anticonvulsant activity of some antiepileptic drugs against audiogenic seizures in DBA/2 mice. *Epilepsy Research*. 2000, vol 40, p 109-121.
- ⁹⁶ KAUFMAN, S. H. E.; RUBIN, E. Ed. Handbook of Tuberculosis. Molecular Biology and Biochemistry. Weinheim, Wiley-Vch 2008.
- ⁹⁷ ZHENG, W.; JIANG, Y. M.; ZHANG, Y. et al. Chelation therapy of manganese intoxication with para-aminosalicylic acid (PAS) in Sprague-Dawley rats. *NeuroToxicology*. 2009, vol 30, p 240-248.
- ⁹⁸ ABUO-RAHMA, G.; SARHAN, H. A.; GAD, G. Design, synthesis, antibacterial activity and physicochemical parameters of novel N-4-piperazinyl derivatives of norfloxacin. *Bioorganic and Medicinal Chemistry*. 2009, vol 17, p 3879-3886.
- ⁹⁹ NIWA, H.; HOBBO, S.; ANZAI, T. A nucleotide mutation associated with fluoroquinolone resistance observed in *gyrA* of in vitro obtained *Rhodococcus equi* mutants. *Veterinary Microbiology*. 2006, vol 115, p 264-268.

-
- ¹⁰⁰ RODRIGUEZ, J. C.; RUIZ, M.; CLIMENT, A. et al. In vitro activity of four fluoroquinolones against *Mycobacterium tuberculosis*. *International Journal of Antimicrobial Agents*. 2001, vol 17, p 229-231.
- ¹⁰¹ URBANIAK, B.; KOKOT, Z. J. Analysis of the factors that significantly influence the stability of fluoroquinolone-metal complexes. *Analytica Chimica Acta*. 2009, vol 647, p 54-59.
- ¹⁰² WIMER, S. M.; SCHOONOVER, L.; GARRISON, M. W. Levofloxacin: A therapeutic review. *Clinical Therapeutics*. 1998, vol 20, p 1049-1070.
- ¹⁰³ GOTTLIEB, P. L. Comparison of enoxacin versus trimethoprim-sulphamethoxazole in the treatment of patients with complicated urinary tract infection. *Clinical Therapeutics*. 1995, vol 17, p 493-502.
- ¹⁰⁴ NABER, K. G. Lomefloxacin versus ciprofloxacin in the treatment of chronic bacterial prostatitis. *International Journal of Antimicrobial Agents*. 2002, vol 20, p 18-27.
- ¹⁰⁵ SULTANA, N.; ARAYNE, M. S.; GUL, S. et al. Sparfloxacin metal-complexes as antifungal agents – Their synthesis, characterization and antimicrobial activities. *Journal of Molecular Structure*. 2010, doi:10.1016/j.molstruc.2010.04.038.
- ¹⁰⁶ MIYAMOTO, H.; UEDA, H.; OTSUKA, T. et al. Synthesis and antibacterial activities of substituted 1,4-dihydro-8-methyl-4oxoquinoline-3-carboxylic acids. *Chemical and Pharmaceutical Bulletin*. 1990, vol 38, p 2472-2475.
- ¹⁰⁷ REDDI, E.; CECCON, M.; VALDUGA, G. et al. Photophysical properties and antibacterial activity of meso-substituted cationic porphyrins. *Photochemistry and Photobiology*. 2002, vol 75, p 462-470.
- ¹⁰⁸ LANG, K.; MOSINGER, J.; WAGNEROVÁ, D. M. Photophysical properties of porphyrinoid sensitizers non-covalently bound to host molecules; model for photodynamic therapy. *Coordination Chemistry Reviews*. 2004, vol 248, p 321-350.
- ¹⁰⁹ LANG, K.; MOSINGER, J.; WAGNEROVÁ, D. M. Singletový kyslík v praxi - současnost a perspektiva. *Chemické Listy*. 2006, vol 100, p 169-177.
- ¹¹⁰ MOSINGER, J.; SLAVETINSKA, L.; LANG, K. et al. Cyclodextrin carriers of positively charged porphyrin sensitizers. *Organic and Biomolecular Chemistry*. 2009, vol 7, p 3797-3804.
- ¹¹¹ MOCZEK, L.; NOWAKOWSKA, M. Novel water-soluble photosensitizers from chitosan. *Biomacromolecules*. 2007, vol 8, p 433-438.
- ¹¹² LANG, K.; MOSINGER, J.; WAGNEROVÁ, D. M. Pokroky ve fotochemii singletového kyslíku. *Chemické Listy*. 2005, vol 99, p 211-221.
- ¹¹³ FINI, P.; LONGOBARDI, F.; CATUCCI, L. et al. Spectroscopic and electrochemical study of Rose Bengal in aqueous solutions of cyclodextrines. *Bioelectrochemistry*. 2004, vol 63, p 107-110.
- ¹¹⁴ MANNING, F. J.; WEHRLY, S. R.; FOULKES, G. N. Patient tolerance and ocular surface staining characteristics of lissamine green versus rose bengal. *Ophthalmology*. 1995, vol 102, p 1953-1957.

-
- ¹¹⁵ MOUSAVI, S. H.; AFSHARI, J. T.; BROOK, A.; et al. Direct toxicity of rose bengal in MCF-7 cell line: Role of apoptosis. *Food and Chemical Toxicology*. 2009, vol 47, p 855-859.
- ¹¹⁶ MOSINGER, J.; JIRSÁK, O.; KUBÁT, P. et al. Bactericidal nanofabrics based on photoproduction of singlet oxygen. *Journal of Material Chemistry*. 2007, vol 17, p 164-166.
- ¹¹⁷ MOSINGER, J.; LANG, K.; KUBÁT, P.; et al. Photofunctional polyurethane nanofabrics doped by zinc tetraphenylporphyrin and zinc phthalocyanine photosensitizers. *Journal of Fluorescence*. 2009, doi:10.1007/s10895-009-0464-0.
- ¹¹⁸ IMRAMOVSKÝ, A.; POLANC, S.; VINŠOVÁ, J. et al. A new modification of anti-tubercular active molecules. *Bioorganic and Medicinal Chemistry*. 2007, vol 15, p 2551-2559.
- ¹¹⁹ KOČEVAR, M.; SUŠIN, P.; POLANC, S. *N*-Acylethoxymethylene hydrazones as the source of a C₁ fragment. *Synthesis*. 1993, vol 8, p 773-774.
- ¹²⁰ <http://www.taacf.org/Process-text.htm>
- ¹²¹ KAUFMAN, S. H. E.; RUBIN, E. Ed. Handbook of Tuberculosis. *Molecular Biology and Biochemistry*. Weinheim, Wiley-Vch 2008.
- ¹²² VINSOVA, J.; IMRAMOVSKY, A.; JAMPILEK, J. et al. Recent advances on isoniazid derivatives. *Anti-Infective Agents in Medicinal Chemistry*. 2008, vol 7, p 12-31.
- ¹²³ STIGLIANI, J. L.; ARNAUD, P.; DELAINE, T. et al. Binding of the tautomeric forms of isoniazid-NAD adducts to the active site of *Mycobacterium tuberculosis* enoyl-ACP reductase (InhA): A theoretical approach. *Journal of Molecular Graphics and Modelling*. 2008, vol 27, p 536-545.
- ¹²⁴ HUANG, Y. S.; GE, J.; ZHANG, H. M. et al. Purification and characterization of the *Mycobacterium tuberculosis* FabD₂, a novel malonyl-CoA:AcpM transacylase of fatty acid synthase. *Protein Expression and Purification*. 2006, vol 45, p 393-399.
- ¹²⁵ SLAYDEN, R. A.; BARRY, C. E. The genetics and biochemistry of isoniazid resistance in *Mycobacterium tuberculosis*. *Microbes and Infection*. 2000, vol 2, p 659-669.
- ¹²⁶ HEYM, B.; COLE, S. T. Multidrug resistance in *Mycobacterium tuberculosis*. *International Journal of Antimicrobial Agents*. 1997, vol 8, p 61-70.
- ¹²⁷ KOŠMRLJ, B.; KOKLIČ, B.; POLANC, S. Transformation of hydrazine derivatives. Ethoxymethylene hydrazones as powerful reagents in organic synthesis. *Acta Chimica Slovenica*. 1996, vol 43, p 153-162.
- ¹²⁸ JURCEVIC, S.; HILLS, A.; PASVOL, G. et al. T cell responses to a mixture of *Mycobacterium tuberculosis* peptides with complementary HLA-DR binding profiles. *Clinical & Experimental Immunology*. 1996, vol 105, p 416-421.
- ¹²⁹ SLATER, T. F.; SAWYER, B.; STRAULI, U. Studies on succinate-tetrazolium reductase systems: III. Points of coupling of four different tetrazolium salts III. Points of coupling of four different tetrazolium salts. *Biochimica et Biophysica Acta*. 1963, vol 77, p 383-393.

-
- ¹³⁰ MOSMANN, T. J. Rapid colorimetric assay for cellular growth and survival: Application to proliferation and cytotoxicity assays. *Journal of Immunological Methods*. 1983, vol 65, p 55-63.
- ¹³¹ LIU, Y. B.; PETERSON, D. A.; KIMURA, H. et al. Mechanism of cellular 3-(4,5-dimethylthiazol-2-yl)-2,5-diphenyltetrazolium bromide (MTT) reduction. *Journal of Neurochemistry*. 1967, vol 69, p 581-593.
- ¹³² ALTMAN, F. P. Tetrazolium salts and formazans. *Progress in Histochemistry and Cytochemistry*, (9, 1-56) Gustav Fischer Verlag, Stuttgart 1976.
- ¹³³ DENIZOT, F.; LANG, R. Rapid colorimetric assay for cell growth and survival: Modifications to the tetrazolium dye procedure giving improved sensitivity and reliability. *Journal of Immunological Methods*. 1986, vol 89, p 271-277.
- ¹³⁴ SHARMA, S. K. Antituberculosis drugs and hepatotoxicity. *Infection, Genetics and Evolution*. 2004, vol 4, p 167-170.
- ¹³⁵ SCHWAB, C. E.; TUSCHL, H. In vitro studies on the toxicity of isoniazid in different cell lines. *Human and Experimental Toxicology*. 2003, vol 22, p 607-615.
- ¹³⁶ TAFAZOLI, S.; MASHREGI, M.; O'BRIEN, P. J. Role of hydrazine in isoniazid-induced hepatotoxicity in a hepatocyte inflammation model. *Toxicology and Applied Pharmacology*. 2008, vol 229, p 94-101.
- ¹³⁷ TOSTMANN, A.; BOEREE, M. J.; PETERS, W. H. M. et al. Isoniazid and its toxic metabolite hydrazine induce in vitro pyrazinamide toxicity. *International Journal of Antimicrobial Agents*. 2008, vol 31, p 577-580.
- ¹³⁸ YUE, J.; PENG, R.; CHEN, J. et al. Effect of rifampicin on CYP2E1-dependent hepatotoxicity of isoniazid in rats. *Pharmacological Research*. 2009, vol 59, p 112-119.
- ¹³⁹ ELLNER, J. J. Regulation of the human immune response during tuberculosis. *Journal of Laboratory and Clinical Medicine*. 1997, vol 130, p 469-475.
- ¹⁴⁰ COOPER, A. M.; FLYNN, J. A. The protective immune response to *Mycobacterium tuberculosis*. *Current Opinion in Immunology*. 1995, vol 7, p 512-516.
- ¹⁴¹ ALGOOD, H. M. S.; CHAN, J.; FLYNN, J. L. Chemokines and tuberculosis. *Cytokines and Growth Factor Reviews*. 2003, vol 14, p 467-477.
- ¹⁴² MACELA, A. et al. Infekční choroby a intracelulární parazitismus bakterií. Praha, Grada Publishing, a.s. 2006.
- ¹⁴³ ROOK, G. A. W.; SEAH, G.; USTIANOWSKI, A. *M. tuberculosis*: Immunology and vaccination. *European Respiratory Journal*. 2001, vol 17, p 537-557.
- ¹⁴⁴ NUNEZ, R. Flow cytometry: Principles and Instrumentation. *Current Issues in Molecular Biology*. 2001, vol. 3, p 39-45.
- ¹⁴⁵ BROWN, M.; WITTEWER, C. Flow cytometry: Principles and applications in hematology. *Clinical Chemistry*. 2000, vol 46, p 1221-1229.

7. Appendix

Paper I

Recent Advances in Drugs and Prodrugs Design of Chitosan

J. Vinsova* and E. Vavrikova

Faculty of Pharmacy, Charles University, Czech Republic, Heyrovskeho 1203, 500 05 Hradec Kralove

Abstract: The aim of this review is to outline the recent advances in chitosan molecular modeling, especially its usage as a prodrug or drug in a field of antibacterial, anticarcinogenic and antioxidant activity.

Polymeric materials like peptides, polysaccharides and other natural products have recently attracted attention as biodegradable drug carriers. They can optimize clinical drug application, minimize the undesirable drug properties and improve drug efficiency. They are used for the slow release of effective components as depot forms, to improve membrane permeability, solubility and site-specific targeting.

Chitosan is such a prospective cationic polysaccharide which has shown number of functions in many fields, including bio medicinal, pharmaceutical, preservative, microbial and others. This article discusses the structure characteristics of chitosan, a number of factors such as degree of polymerization, level of deacetylation, types of quarternisation, installation of various hydrophilic substituents, metal complexation, and combination with other active agents. Biodegradable, non-toxic and non-allergenic nature of chitosan encourages its potential use as a carrier for drug delivery systems in all above mentioned targets. The use of chitosan prodrug conjugates is aimed at the site-specific transport to the target cells use, for example, a spacer tetrapeptide Gly-Phe-Leu-Gly, promotion of drug incorporation into cells via endocytosis, hybridization or synergism of two types of drugs or a drug with a bioactive carrier. The design of chitosan macro-molecule prodrugs is also discussed.

Key Words: Chitosan, antibacterial activity, antitumor activity, antioxidant activity.

1. INTRODUCTION

Polymeric materials like peptides, polysaccharides and other natural products have recently attracted attention as biodegradable drug carriers. They can optimize clinical drug application, minimize the undesirable drug properties and improve drug efficiency. They are used for the slow release of effective components as depot forms, to improve membrane permeability, solubility and site-specific targeting.

Chitosan, (poly-D-glucosamine), is a natural polymer derived from chitin, the second most abundant polysaccharide after cellulose. Chitosan is produced by alkaline deacetylation of chitin, by treating with 50% hydroxide for several hours or by enzyme hydrolysis of *N*-deacetylase (EC3.5.1.41) [1] (Fig. 1). Degree of deacetylation of commercially prepared chitosan is usually in the range between 60-100%. In nature chitosan exists only in a small amount in several kinds of mushrooms *i.e.* *aspergillus* and *mucor* [2].

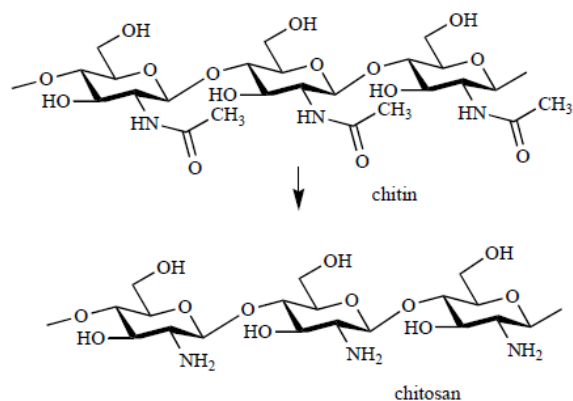


Fig. (1). Chitin deacetylation.

*Address correspondence to this author at the Faculty of Pharmacy, Charles University, Czech Republic, Heyrovskeho 1203, 500 05 Hradec Kralove; Tel: +420 495 067 343; Fax: +420 495 067 166; E-mail: jarmila.vinsova@faf.cuni.cz

Chitosan exhibits excellent biological properties; it is non-toxic, biocompatible and biodegradable [3-5]. For its exceptional features chitosan has received interest in various fields including antimicrobials, biomedical materials, cosmetics, food additives, separators, sewage disposal and agricultural material. Chitosan is used also as a dietary supplement to reduce and cut down weight. It binds itself to fats and cholesterol, and leads them away from the digestive tract before they are processed [6]. As fibrous material it improves activity of colon reduces the feeling of hunger and therefore is used for emaciation. Sometimes it gets higher affectivity that was not scientifically proved.

2. CHITOSAN STRUCTURE AND CRYSTAL FORMS

Chitosan, chemically poly[(1→4)-β-2-amino-2-deoxy-D-glucosane] is *N*-deacetylated derivative of chitin. In comparison with chitin it has better chemical and biochemical reactivity. It is composed from glukosamine units with free amino group on the second carbon. Its pK_a is 6.3-7 [7], and saltform it has cationic character. The amino group, which is rare in polysaccharides, can be used as the reactive site. Natural cationic polymers are less abundant than anionic; therefore chitosan attracts attention in various fields of use.

Four crystalline polymorphic forms of chitosan have been found by X-ray diffraction measurements, three hydrated and one anhydrous form. The first X-ray fiber pattern of chitosan prepared from lobster tendon chitin by solid state deacetylation was published by Clark and Smith in 1936 [8]. Sixty years later, Okuyama [9] analyzed the pattern of "tendon chitosan". Four chitosan chains and eight water molecules are packed in an orthorhombic unit cell. Each chitosan chain takes an extended two-fold helix, a "zigzag" structure which is stabilized by an O3 – O5 hydrogen bond with *gt* (*gauch-trans*) orientation of O6. Chitosan chains are packed together in an antiparallel fashion. The up-chain and lower-chain are bounded by N2-O6 hydrogen bonds to form a sheet structure, see (Fig. 2a, 2b). Water molecules form the column between the sheets and stabilize the crystal structure. This polymorph is the most abundant and commercially available chitosan has the same crystalline form.

Two other hydrated polymorphs are called Form II and L-2. In the L-2 crystal each chitosan chain takes an extended two-fold helix similar to that in tendon polymorph and is arranged in an antiparallel fashion as well [3]. Form II needs detailed characterization. The

fourth polymorph called an annelated was obtained by heating a tendon chitosan at 200 °C. Dehydration shortens the distance between zigzag tops and neighbouring sheets are more independent. This conformation is called relaxed two-fold helix and the change is an irreversible process [10] (Fig. 3).

3. SALTS AND COMPLEXES

Chitosan forms water soluble salts with both inorganic acids (hydrochloric acid, hydroiodic acid, phosphoric acid, phosphorous acid, sulfur acid and the others) and organic acids (formic acid, acetic acid, propionic acid, butyric acid, ascorbic acid and the oth-

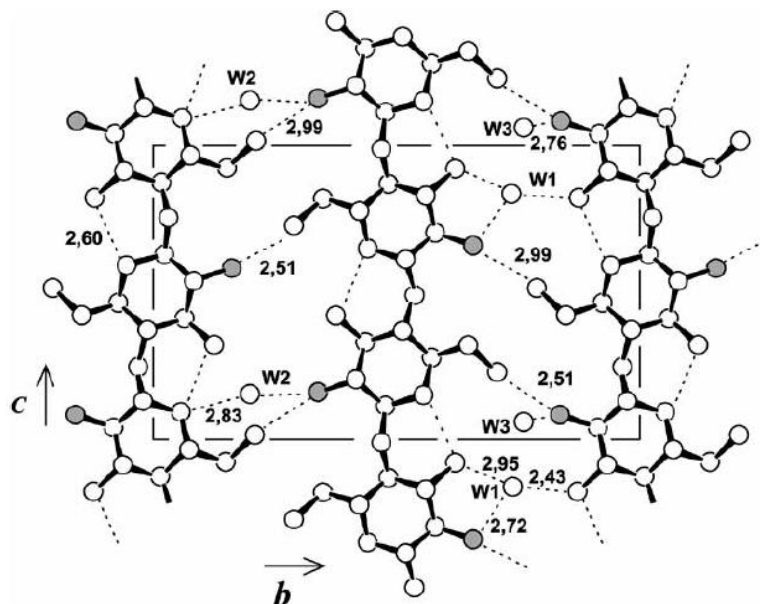


Fig. (2a). Tendon chitosan structure projected along the axe *a*. Filled circles denote nitrogen atoms [9].

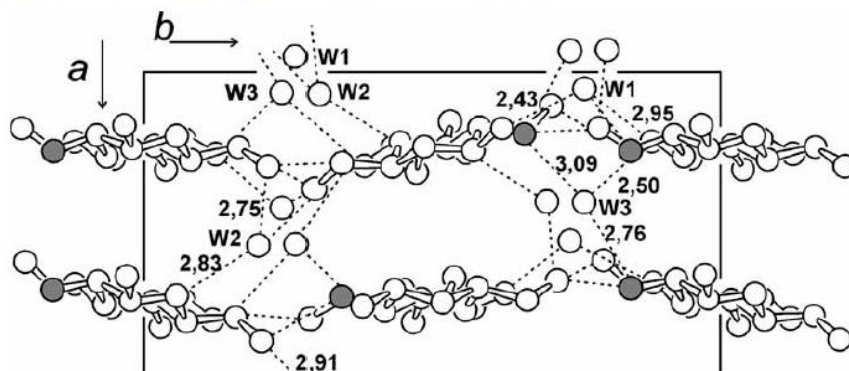


Fig. (2b). Tendon chitosan structure projected along the axe *c*. Filled circles denote nitrogen atoms [9].

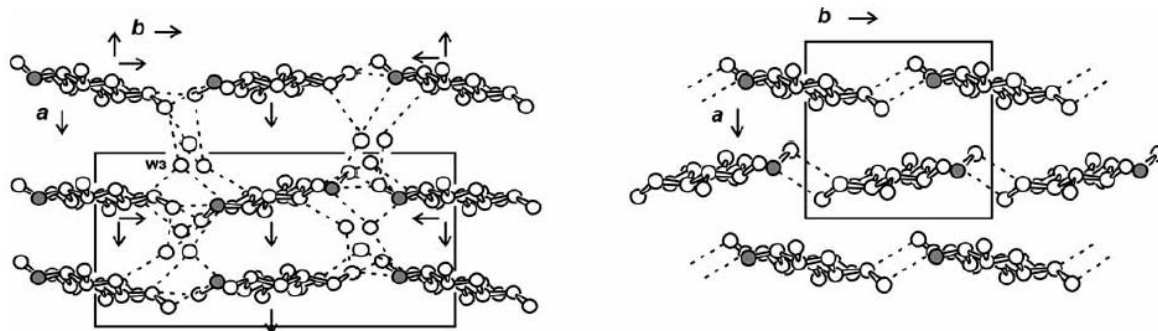


Fig. (3). Hydrated chitosan

Anhydrated chitosan.

ers). They are classified into four types depending on the kind of acid used, concentration and temperature at salt preparation [3], arrow direction show increase or decrease of temperature or concentration (Table 1).

For example, chitosan-hydrogen iodide salt crystallizes into both forms I and IIa depending on preparation condition. Type I form was obtained at laboratory temperature. Two polymer chains and four iodide ions are included in a monoclonic unit cell: $a = 0.946$; $b = 0.979$; c (fibre axes) = 1.033 nm; $\beta = 105.1^\circ$. Each chitosan chain takes an extended two-fold helix having fibre axis lengths similar to that of free chitosan. The corner chain is oriented up, while the other chain at the centre of the b axis is oriented down. These two chains are arranged in an antiparallel fashion, and they are linked along the b axis by two N2 – O6 hydrogen bonds to form a zigzag sheet. The iodide ions are on the top of the zigzag structure, they stabilize the salt structure similarly as water molecules by forming hydrogen bonds between N2 and O6. The columns of iodide ions also maintain the structure by electrostatic interactions between N2 and iodide ions [11] (Fig. 4).

The second crystalline iodide salt form IIa was obtained at low temperature. The crystalline unit cell is a tetragonal system with dimensions of $a = b = 1.068$; $c = 4.077$ nm. The molecular conformation is a 4/1 helix. The corner and center chains are arranged in an antiparallel fashion. Two iodide ions are packed between the corner chains, while the two other ions are located between the corner and center chain. One of the intramolecular O3 – O5 hydrogen bonds at glycoside linkage is weakened by interaction with iodide ions, see [12] (Fig. 5a, 5b).

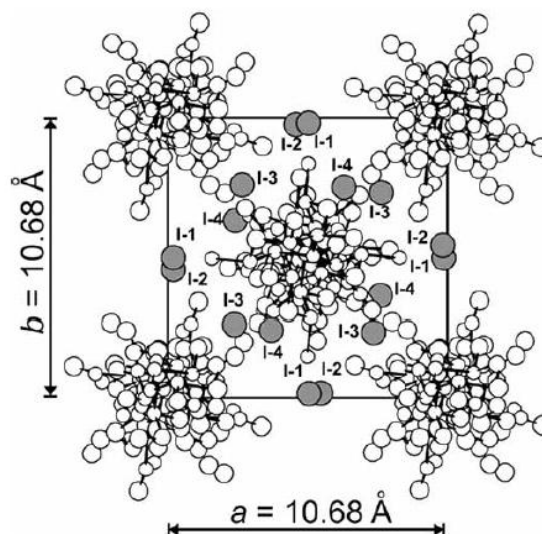


Fig. (5a). Chitosan HI salt type IIa projected along the c axis. Filled circles represent the iodide ions.

Chitosan has coordination behaviour and easily forms complexes with transition metals. Immersing a tendon chitosan in various metal salt solutions such as cadmium, zinc or cupric ions give

Table 1. Crystal Form of Chitosan Acid Salts

Crystal Form	Chitosan Conformation	Acid
I (anhydrous)	Extended 2-fold helix	HNO_3 (\uparrow conc.), HBr, HI (\uparrow T), HClO_4 , L- or D-lactic (\uparrow T), maleic acid, L-ascorbic acid, D-isoascorbic acid, salicylic acid (\downarrow T)
II (hydrated)	Relaxed 2-fold helix	HNO_3 (\downarrow conc.), H_2SO_4 , HCl, HF, HIO_4 , H_3PO_4 , L- or D-lactic (\downarrow T), succinic acid, fumaric acid, L-tartaric acid, monocarboxylic acids (formic, acetic, propionic, butyric)
IIa (hydrated)	4/1 helix	HI (\downarrow T)
III (anhydrous)	5/3 helix	Salicylic acid (\uparrow T), gentisic acid, acetylsalicylic acid

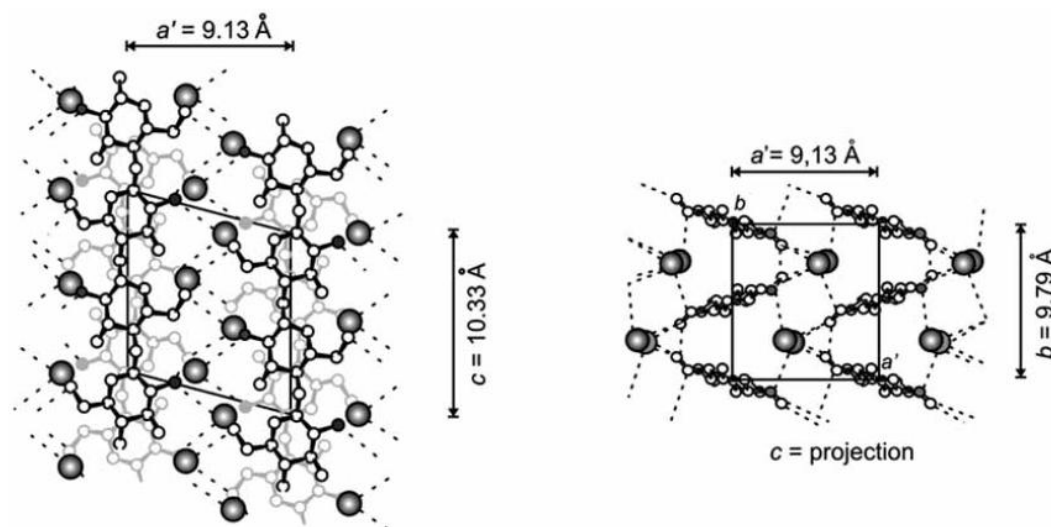


Fig. (4). Chitosan HI Type I salt; Dashed lines represent hydrogen bonds, big gray circles represent iodide ions.

X-ray diffraction patterns where the primary amino group is one of the ligands. The conformation pattern of chitosan chain in a solid phase was identical to the tendon form. All crystals were indexed with the orthorhombic unit cell. It is interesting that each metal was coordinated to every second amino group (Fig. 6).

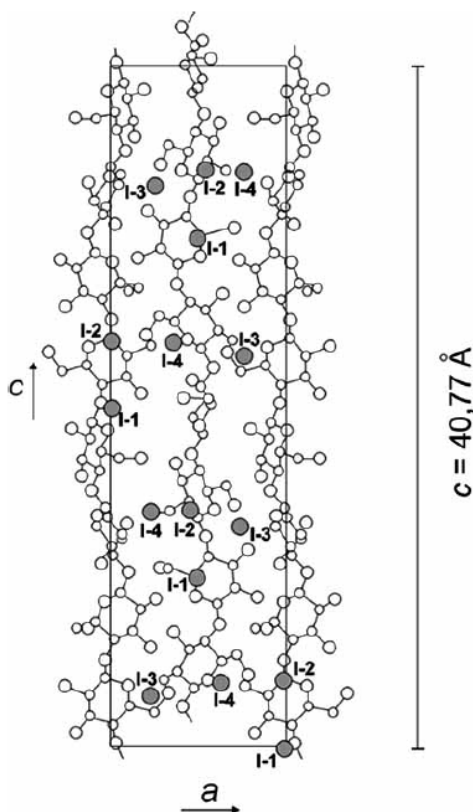


Fig. (5b). Chitosan HI salt type IIa projection along the *b* axis. Filled circles represent the iodide ions.

A single molecule of chitosan has three reactive centres: primary amino group, primary and secondary hydroxyl group. The amino group easily undergoes quarterisation, which leads to better solubility. Primary hydroxyl groups can be frequently substituted by a spacer chain usually carrying an active part of the molecule that is responsible for targeting or increasing water solubility. Secondary hydroxyl group is modified in order to increase water solubility. The anhydrous crystal does not dissolve in any aqueous acid solution or form complexes with any transition metal ions. However, the anhydrous crystal can be used as inert resin.

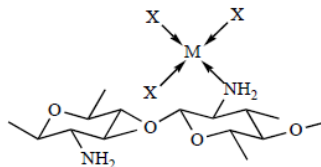


Fig. (6). Model of chitosan transition metal complex. M – Metal ion, X – electron donor other than amino group.

While storing acetic acid salt of chitosan at room temperature, the crystals change from relaxed two-fold helix into the annealed

extended two-fold helix conformation. This phenomenon is called spontaneous water removing by acid. The spontaneous change was observed with infrared spectra and increased the density of the sample [3].

4. PHARMACEUTICAL APPLICATIONS OF CHITOSAN

Chitosan has recently attracted more attention due to its significant biological functions such as biodegradability, biocompatibility, bioactivity and low toxicity [13,14]. These functions are becoming better understood in addition to chitosan's unique physicochemical properties. Chitosan is also bioactive agent useful in pharmaceutical and biomedical branches [5,15,16]. Chitosan could be useful especially as a supporter or carrier for biologically active species with control release of the drug in the target cell or tissue [17,18]. An optimal result should yield a minimum amount of side effects and prolonged activity.

The polymer can be used as a polymer drug when expressing its own pharmacological activity although the corresponding monomer unit is biologically inactive. The polymer prodrug is a macromolecular compound acting mainly as a drug carrier; it may or may not have biological activity. Polymer prodrug is usually composed of a polymer carrier, bonded via biodegradable covalent linkage with a therapeutic agent. Targeting moiety can be incorporated into the conjugate via a specific spacer arm that can improve physical properties and facilitate drug release in the receptor site.

The use of macromolecular prodrug conjugates of lower molecular weight drugs is aimed at a) improvement of its movement in the body by changing the solubility and molecular size b) retaining the appropriate concentration of a drug by means of slow release from carriers c) site-specific transport to target cells, d) promotion of drug incorporation into cells via endocytosis, e) hybridization or synergism of two types of drugs or a drug with a bioactive polymer carrier. The design of macromolecule drug conjugates must be in correlation with physical properties of conjugate and biochemical properties of the polymer carrier. Macromolecule carriers (their size, electrical charge, hydrophilic/lipophilic balance and specific transmembrane ability) can change pharmacological and immunological activity of drugs and their delivery.

To achieve the active patch macromolecular prodrug can pass after releasing the free drug by a diffusion route or by endocytosis as a polymer conjugate (Fig. 7). The most ideal is endocytosis, where the whole conjugate is incorporated into the cellular lysosomes where the active moiety is gradually liberated by lysosomal enzymes.

4.1. Antibacterial Activity

Chitosan itself possesses antimicrobial activity against many *G*⁺, (*Staphylococcus aureus*, *S. epidermis*, *Bacillus subtilis*) *G*⁻ bacteria, (*Pseudomonas aeruginosa*, *Escherichia coli*, *Klebsiella pneumoniae*, *Proteus vulgaris*) [19] and fungi at pH < 6. Although the exact mechanism by which chitosan exerts its antimicrobial activity is not fully known, it has been suggested that the positive amino group of glucosamine units interacts with negative charged components in microbial cell membranes, altering their barrier properties, thereby preventing the entry of nutrients or causing the leakage of intracellular contents [20,21], which leads to cell break up [22-24]. Another reported mechanism involves the penetration of low-molecular-weight chitosan in the cell, binding to deoxyribonucleic acid (DNA), and subsequent inhibition of ribonucleic acid (RNA) and protein synthesis [25]. Chitosan has also been shown to activate several defense processes in plant tissues and it inhibits the production of toxins and microbial growth because of its ability to chelate metal ions [26]. The biological activity of chitosan depends on many factors (its molecular weight, deacetylation degree, chitosan derivatization, and degree of substitution, length and position of a substituent in glucosamine units of chitosan, pH of

chitosan solution) that lead to the extensive study of modifications in an effort to prepare suitable applications and form with improved activity on the target organism.

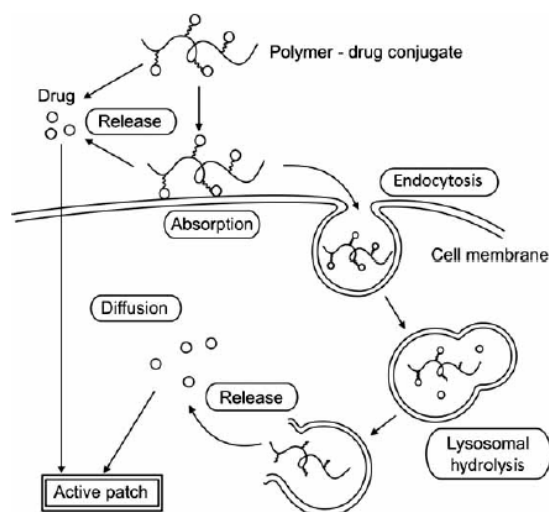


Fig. (7). Arrival routes of drugs toward the active site [3].

Water solubility and size of molecule play a very important role [27]. In general, the optimal size of an active molecule is 2-200 kDa. Following Table 2 shows minimal inhibition concentrations of various chitosane oligosaccharides and low molecular weight chitosans against various G⁺ and G⁻ bacterial strains.

Tokura et al. [32] have discovered that *E. coli* activity was inhibited almost completely by the high molecular weight of chitosan (9300), whereas low molecular weight (2200) was inactive.

To clarify this remarkable phenomenon FITC-labeled chitosan was used. It was found that high molecular weight chitosan stacked outside the cell to inhibit the permeation of nutrition, and low molecular weight chitosan accumulated inside the cell and was metabolized as nutrition.

Another important factor is pH. Antimicrobial activity of chitosan increases with decreasing pH [29,33,34] and this is done by ionization. Positively charged particles generate at pH < 6.5. Non-modified chitosan is insoluble at pH = 7 and antibacterially inactive [33,35], therefore a great attention is directed into the preparation of soluble chitosan salts. Water solubility increases by quaternization [19,36] and hydrophile substitution. For example, preparation of hydroxypropyl chitosan [37], *N*-carboxybutylchitosan [38], carboxymethylchitosan [39,40] and sulfate chitosan [41,42]. In addition, branched chitosan with *N*-acetyl-D-glucosamine and D-glucosamine at the C-6 position exhibited antimicrobial activities [43].

Amino group quaternization belongs to the most common chitosan modification. A free amino group was condensed with benzaldehyde (A) and salicylaldehyde (B) to produce a Schiff base (As, Bs), that was then reduced by sodium borohydride (to form An, Bn) and in the last step quaternized by methyl iodide (Aq, Bq) (Fig. 8). All products were tested for antifungal activity. As shown in (Fig. 9), the quaternized chitosan derivatives have better activity against *C. lagenarium* than Schiff bases and *N*-substituted chitosan derivatives [44].

A series of methylated chitosaccharide derivatives, possessing various degrees of methylation were synthesized with regard to their antibacterial effect against *Staphylococcus aureus*. By increasing the reaction time and reaction steps, a higher degree of *N*-quaternization was achieved. Using a solvent system with 50% water in DMF minimized *O*-methylation. Chito-oligomers and their methylated derivatives were inactive against *S. aureus*, whereas the chitosan polymer and its derivatives were active. The antibacterial activity measurements show that quaternization is vital for the derivatives to be active at pH 7.2 but has a negative effect on the

Table 2. Antibacterial Activity Against G⁺ and G⁻ Bacterium

Bacterial Strain	% of Deacetylation	MW (kDa)	MIC (%)	Ref.
Gram-negative Bacteria				
<i>Escherichia coli</i>	85	12	0.1	[28]
<i>Escherichia coli</i>	85	6	0.06	[28]
<i>Escherichia coli</i> O-157	90	5-10	0.12	[29]
<i>Vibrio parahaemolyticus</i>	75	1-10	0.4	[30]
<i>Salmonella typhimurium</i>	75-90	1-10	0.125	[31]
<i>Pseudomonas aeruginosa</i>	50-90	5-10	0.25	[31]
Gram-positive Bacteria				
<i>Micrococcus luteus</i>	90	5-10	0.031	[28]
<i>Streptococcus mutans</i>	90	5-10	0.008	[28]
<i>Streptococcus faecalis</i>	90	5-10	0.03	[28]
<i>Staphylococcus epidermis</i>	75-90	5-10	0.063	[31]
<i>Staphylococcus aureus</i>	50-90	1-10	0.125	[31]
<i>Bacillus subtilis</i>	75-90	5-10	0.125	[31]
<i>Bacillus cereus</i>	75-90	1-10	0.125	[31]
<i>Lactobacillus plantarum</i>	85	12	0.06	[28]
<i>Bifidobacterium bifidum</i>	85	12	0.0005	[28]

Minimal inhibitory concentration (MIC) is defined as the lowest concentration of chitosan at which the bacterial growth is completely inhibited.

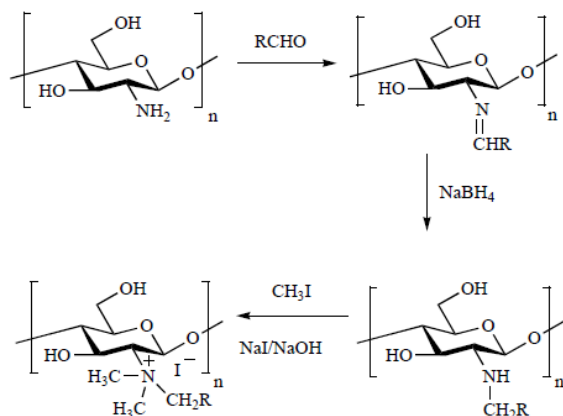
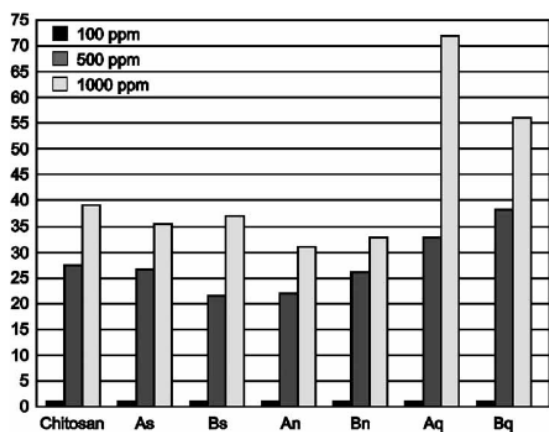


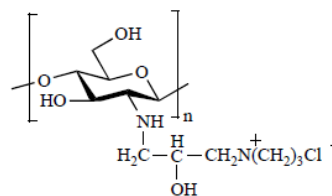
Fig. (8). Synthetic pathway for preparation of chitosan derivatives.

Fig. (9). The antifungal activity of chitosan and chitosan derivatives against *Colletotrichum lagenarium* (y axis = inhibition index (%)).

activity at pH 5.5. At acidic conditions the protonation of the free-, *N*-mono- and *N,N*-dimethylated amino groups is important for antibacterial activity. Surface activity does not contribute to antibacterial activity of these compounds. *N,N,N*-Trimethylchitosan is one of

the most promising chitoderivatives that has a fixed charge on the quaternized amino groups and is therefore soluble in the lower sections of the gastrointestinal tract. Trimethylated chitosan can act as an absorption enhancer at these conditions, whereas chitosan has no activity due to its limited solubility. The methylated derivatives can be produced in a one-step reaction of chitosan with methyl iodide in the presence of sodium hydroxide as a base using *N*-methyl-2-pyrrolidone as solvent [45]. A quaternized chitosan *N,N*-diethyl-*N*-methylchitosan (DEMC) has received attention as an oral drug delivery vehicle [46].

Quaternization can be done by the installation of a substituent having an amino group, e.i. chitosan-*N*-2-hydroxypropyltrimethylammonium chloride synthesis by the reaction of chitosan with glycidyltrimethylammonium chloride (Fig. 11), that showed bio-cidal activity on *Staphylococcus aureus*, *Bacillus subtilis*, *Staphylococcus epidermidis*, and *Candida albicans* [47].

Fig. (11). Chitosan-*N*-2-hydroxypropyltrimethylammonium chloride monomer.

Quaternary ammonium chitosan was also prepared by introduction of a quaternary ammonium group on a dissociative hydroxyl group and amino group. Aminoethyl hydroxyethyl chitosan hydrochloride was prepared by treating hydroxyethyl chitosan with chloroethylamine hydrochloride in sodium hydroxide solution [48] (Fig. 12). The derivate showed good solubility and inhibition effects against *Escherichia coli*.

Poly(*N*-vinylimidazole) is known as a good water soluble anti-bacterial active polymer [49]. It has been grafted onto chitosan in dilute acetic acid solution via ceric ion initiation. Their combination improved G+ and G- antibacterial activity and protonation of vinylimidazole led to an increase of water solubility [50].

To increase the numbers of amino groups, guanidinylated chitosan derivatives with different molecular weights have been synthesized by the guanidinylation reaction of chitosan with aminoimino-methanesulfonic acid (Fig. 13). Compared with chitosan, guanid-

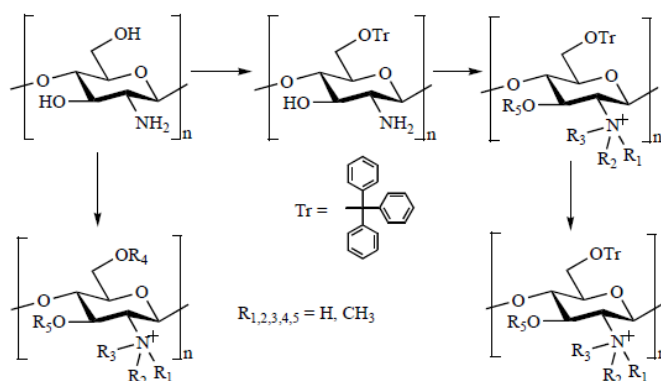


Fig. (10). Synthetic route of methylated chitosan derivatives.

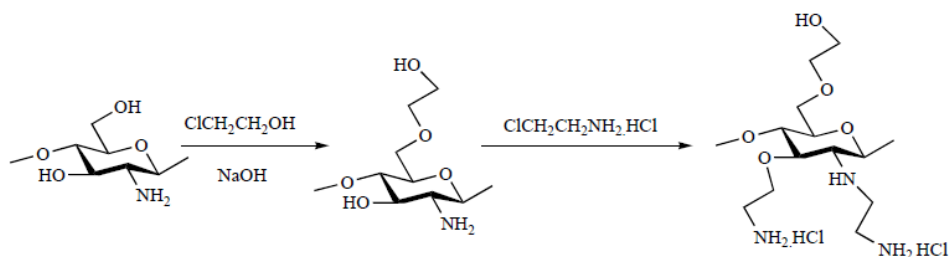


Fig. (12).

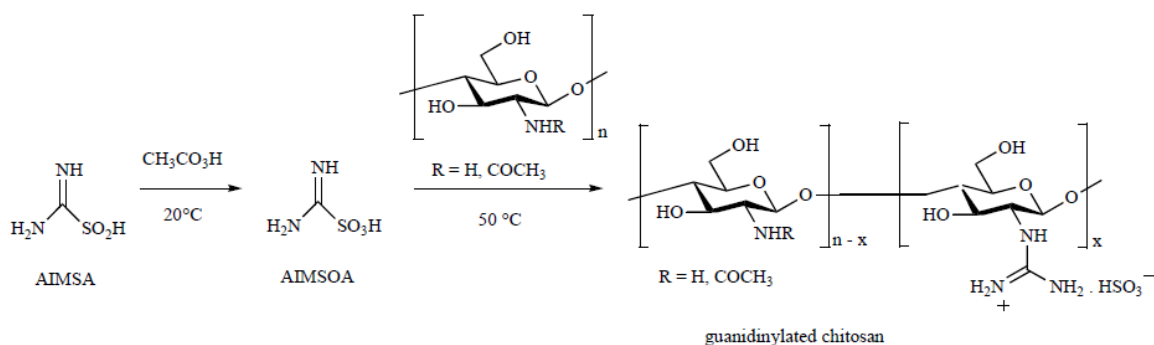


Fig. (13). Guanidinylated chitosan synthesis; AIMSA – aminoiminomethanesulfonic acid; AIMSOA – aminoiminomethanesulfonic acid.

inylated chitosan had much better antibacterial activity, whose minimum inhibitory concentrations in aqueous hydrochloric acid (pH 5.4) were 4 times lower than those of chitosan. Interestingly, guanidinylated chitosan inhibited the growth of *S. aureus* and *B. subtilis* at pH 6.6. The antibacterial activity of guanidinylated chitosan enhanced with decreasing pH.

When chitosan had been converted into a guanidine derivative, the positive charge density of the derivative increased, which led to the enhanced adsorption of polycation onto the negatively charged cell surface. Guanidinylated chitosan may be easier to associate with the cell surface and show higher antibacterial activity. For this reason, guanidinylated chitosan showed better antibacterial activity than chitosan against *Bacillus subtilis*, *Escherichia coli* and *Pseudomonas aeruginosa* [51].

A new galactosyl-lysyl-chitosan with high affinity to HepG2 (a liver cancer cell line) was reported. The novel glycoconjugated macromolecules using chitosan was grafted with branched galactose units. The branch-type of galactosylated chitosan was prepared by the introduction of L-lysine spacer arms to chitosan, followed by covalent coupling of lactobionic acid with a lysine spacer to provide chitosan with multivalent galactose units (Fig. 14). β -D-Galaktopyranosyl units are important for targeting drug-delivery system into liver cancer cells [52]. These conjugated molecules exposed activity against *Escherichia coli* and *Staphylococcus aureus*.

N-substitution by disaccharides was applied to increase solubility and antibacterial activity of chitosan. It was found that antibacterial activity of chitosan derivatives was affected by the degree of substitution (DS) with disaccharide and the kind of disaccharide present in the molecule. Regardless the kind of disaccharides linked to the chitosan molecule, a DS of 30–40%, in general, exhibited the most pronounced antibacterial activity against *E. coli* and *S. aureus*. Cellobiose chitosan derivative DS 30–40% was the most effective against *E. coli* and maltose chitosan derivative DS 30–40% was found the most active against *S. aureus*. The derivatives exhibited a higher activity than native chitosan at pH 7.0 [53].

Further, a series of low molecular weight *N*-2(3)-(dodec-2-enyl)succinoyl-/chitosan derivatives were prepared by the reaction of chitosane (4.6 kDa), and 2-(dodec-2-en-1-yl)succinamide (Fig. 15). These long aliphatic chain derivatives with different degrees of N-substitution have shown antimicrobial activity against *Escherichia coli*, *Pseudomonas aureofaciens*, *Enterobacter agglomerans*, *Bacillus subtilis*, *Candida krusei* and *Fusarium oxysporum* [54].

The silver ions can significantly enhance the antimicrobial properties of the chitosan fibers. Experimental results showed that when placed in contact with the silver containing chitosan fibers, the reduction in bacteria count was more than 98% [34]. Silver is widely applied in some medical fields for its high antimicrobial activity and low concentration [55] but the complex of chitosan with Ag^+ is unstable, therefore the complex of thiourea chitosan was prepared by the reaction of chitosan with ammonium thiocyanate in ethanol (Fig. 16). It is interesting that sulfur atoms were the major electron donors that coordinated to silver ions, not nitrogen or oxygen atoms. Thiourea chitosan- Ag^+ complex improved the instability of Ag^+ . The complex showed a wide spectrum of effective antimicrobial activities, MIC values were twenty times lower than those of chitosan. The complex had better antibacterial activity than antifungal activity [56].

The antimicrobial activity of water-soluble chitosan *N*-betainates [57] was measured against *E. coli* and *S. aureus* at pH 7.2 and also at acidic pH 5.5. The activities varied considerably depending on the different physical and chemical properties of the materials, e.g. their origin, molecular weight, degree of substitution, and solubility. However, the antimicrobial activity of chitosan *N*-betainates increased with a decreasing degree of substitution in acidic conditions, which suggests that the positive charge has to be situated on the amino group in the chitosan backbone if one wishes to achieve efficient antimicrobial activity. Antimicrobial activity against *E. coli* increased with decreasing molecular weight whereas activity against *S. aureus* increased with increasing molecular weight. The antimicrobial activity of chitosan also increases with increasing

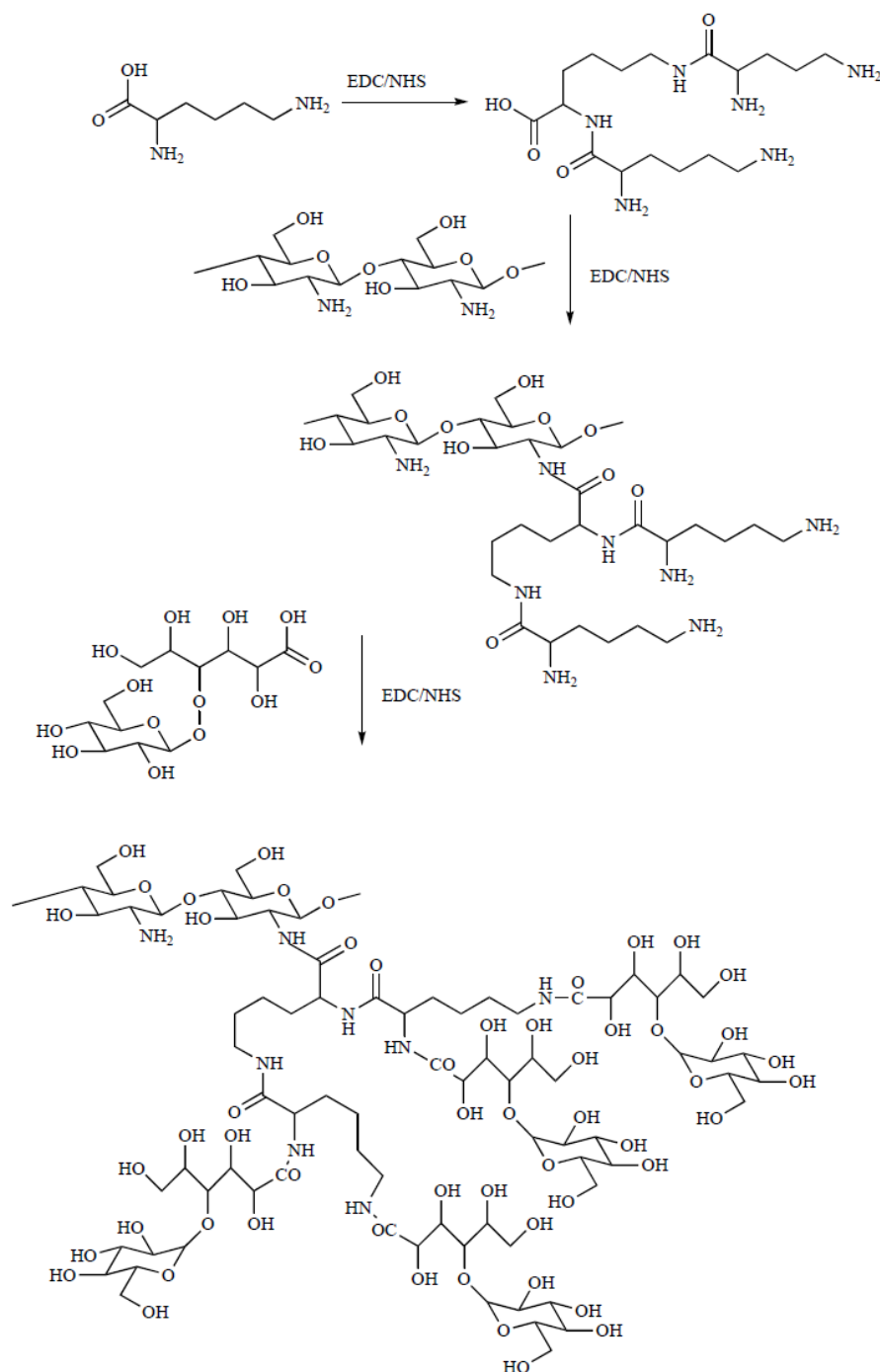


Fig. (14). Galactosyl-lysyl-chitosan synthesis, EDC (1-Ethyl-3-(3-dimethylaminopropyl)carbodiimide), NHS (*N*-hydroxylsuccinimide).

degree of deacetylation, due to the increasing number of ionisable amino groups. Free amino groups can be mono, di or trimethylated. Prolongation of alkyl chains can also increase the antimicrobial activity [58]. Co-administration of chitosan significantly prevents the antitubercular drugs induced hepatotoxicity. The overall hepatoprotective effect is probably due to a counteraction of free radi-

cals by its antioxidant nature and/or to its ability to inhibit lipid accumulation by its antilipidemic property [59].

Many research groups are engaged in combination of chitosan and other antibacterial agent. Thus conjugates with tetracycline and caminomycine have completely retained antibacterial activity [60].

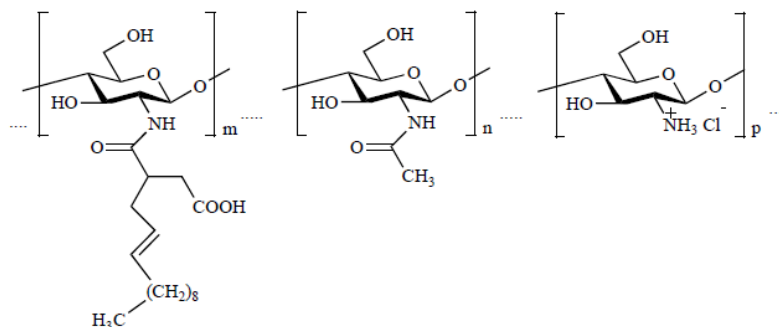


Fig. (15).

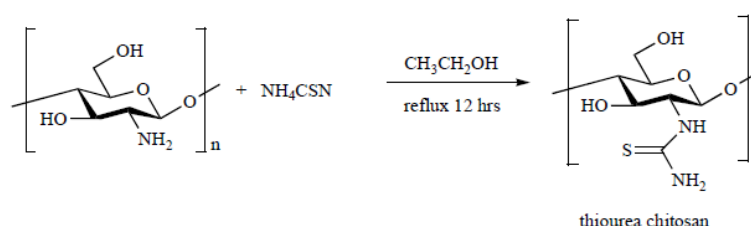


Fig. (16). Thiourea chitosan synthetic pathway.

Metronidazol tablets or capsules are used for the *Helicobacter pylori* treatment. For better releasing from the stomach, chitosan capsules with metronidazol were prepared [61].

The search for new therapeutic alternatives to the tuberculosis treatment by using a very potent drug in a single dose led, to the molecular modification of one of the first row antitubercotics isoniazid (INH) prodrug with prolonged action. Due to its hydro-solubility it can be easily handled and intravenously administrated. The *N*-methylene phosphonic chitosan was obtained by the reaction of chitosan with phosphorus acid in the presence of formaldehyde. Coupling with INH was carried out in two steps. Firstly, functionalization of the drug with a succinic spacer group was done and activation of the succinyl isoniazid through the cyclic 5- or 6-membered analog gave the hydrosoluble chitosan-isoniazid hemisuccinate prodrug [62] (Fig. 17).

Alginate/chitosan sponges were prepared by the gelation of sodium alginate followed by lyophilization, which created the porous structure, crosslinking with calcium chloride, and finally coating with chitosan to provide mechanical stability and accelerate the wound healing process. A polyionic complexation occurs between alginate and chitosan because of the polyanionic character of alginate and polycationic character of the chitosan. Sodium alginate was crosslinked with calcium chloride and finally coating with chitosan. This material is used for the treatment of wounds such as severe burns, trauma, diabetic, decubitus and venous stasis ulcers, and similar tissue damages. The healing response of tissues involves a complex interaction between cells, extracellular matrix molecules, and soluble mediators. Additionally, the presence of chitosan in a wound dressing is reported to promote fibroblast growth and affect macrophage activity, which accelerates the wound healing process [63]. Antibacterial agents ciprofloxacin [63], norfloxacin [64] and gatifloxacin [65] were loaded into this sponge. Some of the effective parameters (i.e., crosslinker concentration, drug content, alginate viscosity, chitosan molecular weight) on the water uptake and drug release rate were evaluated, the antimicrobial activity was increased with increasing ciprofloxacin release rate. This system seems a very promising alternative wound dressing to use in wound/burn dressing applications and wound healing.

When chitosan fibers were treated with AgNO_3 and ZnCl_2 solutions, the silver and zinc ions were chelated by chitosan through the amine groups in the fibers with three different chelate ratios (Fig. 18). These novel metal ions can be released into the solution when the silver- and zinc-containing fibers are placed in contact with normal saline. Results showed that the silver-containing chitosan fibers have good antimicrobial properties, while the zinc-containing fibers can be used to deliver zinc ions in wound care applications [66]. The complexes showed wide spectrum of effective antimicrobial activities, which were 2–8 times higher than those of chitosan and improved with increasing content of zinc ions. The complexes had a better antibacterial activity than antifungal activity, and showed excellent activity particularly against *E. coli* and *Corynebacteria* [67].

Coating materials with less hazardous and non-toxic properties are highly desirable. Incorporation of chitosan in polyethylene oxide (PEO) generates antimicrobial active films. The chitosan fraction contributes to antimicrobial effect of the films, decreases tendency to spherulitic crystallization of PEO, and enhances puncture and tensile strength of the films, while addition of the PEO results in thinner films with lower water vapor permeability [68]. Consequently, the quaternary ammonium derivative of chitosan was used as a coating binder to the acrylic resin emulsion. Furthermore, hybridized chitosan/acrylic resin films have excellent adsorption ability for formaldehyde [69].

4.2. Antitumor Activity

Antitumor activity of chitosan depends on the molecule size, solubility and partial acetylation. High molecular weight chitosan is inactive, that is why it is important to prepare low molecule weight chitosan. Lowering the molecular weight helps improve solubility in water. Chitinases and chitosanases are natural degrading enzymes capable to hydrolyse chitosan to low molecular weight products [3]. The number of cheaper enzymes as lysozyme [70], pectinase [71], hemicellulase [72] a papain [73], were found to catalyze the cleavage of the glycosidic linkage in chitosan. Chitinases have been known to produce by a number of microorganisms for example the chitinases produced by *Bacillus amyloliquefaciens* V656 were used to hydrolyze chitinous material [74]. Chitoooligosaccha-

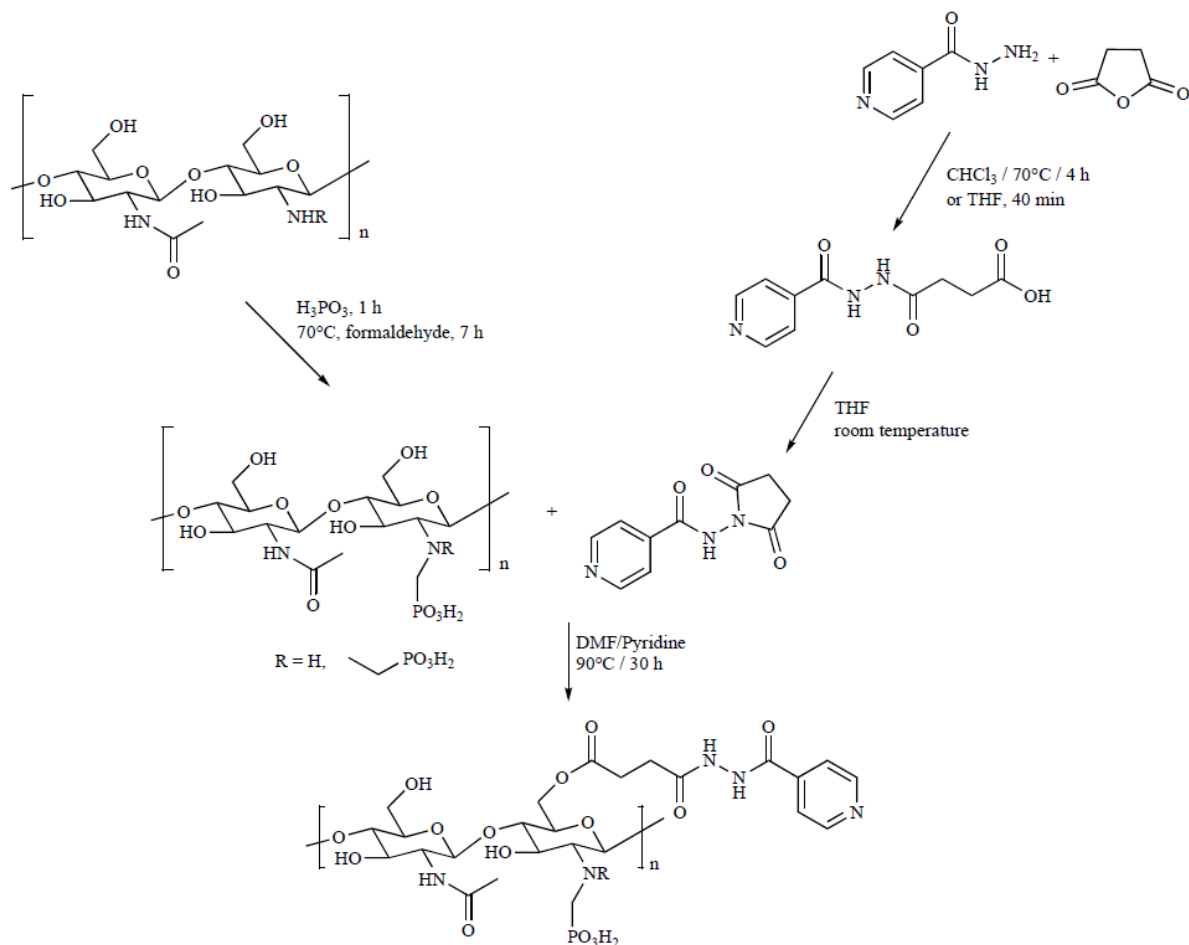


Fig. (17). Chitosan-isoniazid hemisuccinate prodrug synthesis.

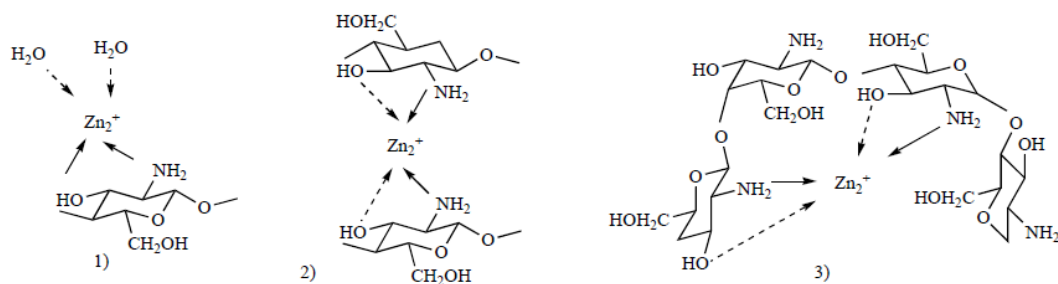


Fig. (18). Zinc complex structures with different chelate ratios.

ride hexamers are able to inhibit proliferation of CT26 cells and induce apoptosis in these cells. Three various chitinous materials induced DNA fragmentations of CT26 cells within 24 hours of treatment. Partially *N*-acetylated chitosan was hydrolysed with the cheap, commercially available and efficient cellulose [75]. The decrease of molecular weight led to the transformation of crystal structure, alteration of thermostability and increase of water-solubility, without chemical structure change. The total acetylation degree of chitosan was the same before and after degradation. This

water-soluble product inhibited the growth of sarcoma180 tumor cells in mice with maximum inhibitory rates of 50% by intraperitoneal injection and 31% by oral administration. The main objective of the research was to elucidate the structural features of low molecular weight/chitooligosaccharides obtained from chitosan (16% *N*-acetylation) and their effect in inhibiting angiogenesis and inducing apoptosis in Ehrlich ascites tumor (EAT) bearing mice. When injected intraperitoneally into mice, the ascites volume decreased to an extent of over 90% [76].

Complexes with different copper to chitosan ratios were tested *in vitro* as potential antitumor agents with 293 cells and HeLa cells. At the ratio of 0.11 mol of copper per one chitosan residue, the complex exhibited a higher antitumor activity and less toxicity than other copper-chitosan complexes tested. In addition, this study showed that the copper-chitosan complex inhibited tumor cell proliferation by arresting the cell cycle progression at the S phase in 293 cells. The copper complexes interact with DNA, leading to the chemically induced cleavage of DNA and, thus, antitumor activity. The mode of action is probably related to the binding of chitosan and copper, which is likely to leave some potential donor atoms free and these free donor atoms enhance the biological activity. All copper complexes of chitosan inhibited the proliferation of the two tumor cell lines, HeLa and 293 at 10^{-3} mol/L, but not the normal human lung fibroblast cell line HLF. Compared with HeLa cell lines, the copper complexes of chitosan were found to be more selective to 293 cell lines in this experiment [77].

In cancer chemotherapy, it is important that the antitumor drugs are delivered to the tumor sites efficiently in order to reduce the severity of side effects. Chitosan has been used as a novel drug delivery system for the well known anticancer drug, camptothecin. Camptothecin is a plant alkaloid that takes effect by inhibiting the enzyme topoisomerase I which is very important for DNA replication. Forming covalent enzyme-DNA complex results in single-strand breaks. Its clinical use has some practical disadvantages mainly due to the scarce water solubility and a number of toxic effects. To overcome these drawbacks, the aggregates of *O*-carboxymethylchitosan (OCMCS) were prepared as a biocompatible and amphiphilic controlled release delivery system [78] (Fig. 19).

Another known drug used for leukemia P388, leukemia L1210 and melanom B16 treatment is mitomycin C. It causes damage of DNA by the same way as alkylating cytostatics. *N*-Succinyl-chitosan has excellent characteristics as a drug carrier, with long-term retention in the systemic circulation and low toxicity. Water-soluble macromolecular prodrug of mitomycin C with highly succinylated *N*-succinyl-chitosan (Fig. 20) was prepared by activation of carboxylic group with water soluble carbodiimide. This water soluble prodrug form has got better possibility of administration [15,79,80].

5-Fluorouracil (5FU) is a pyrimidine analogue belonging to a group of antimetabolites. It has a strong antitumor activity which is accompanied by undesirable side effects. To provide a macromo-

lecular antitumor prodrug with reduced side effects and strong antitumor activity chitosan-5FU conjugates were synthesized. Conjugates attached through a hexamethylene spacer via urea bonds were synthesised. Thus chitosan-urea/C6/urea/5FU conjugate and chitosan-oligosaccharide/urea/C6/urea/5FU conjugates have exhibited stronger growth-inhibitory effect on Meth-A fibrosarcoma and MH-134Y hepatoma. These conjugates act as hybrid macromolecular prodrugs having immuno- and antitumor activities. Water soluble macromolecules are expected to be uptaken into cells by endocytosis or phagocytosis. Tumor cells show a higher degree of uptake efficiency than normal tissue cells. In the lysosomes of tumor cells there is a larger amount of cathepsin B. It was demonstrated that the tetrapeptide spacer Gly-Phe-Leu-Gly facilitates specific drug release in the lysosomal condition. Therefore 5FU was conjugated with the partly acetylated *O*-carboxymethylchitosan [81] (Fig. 21).

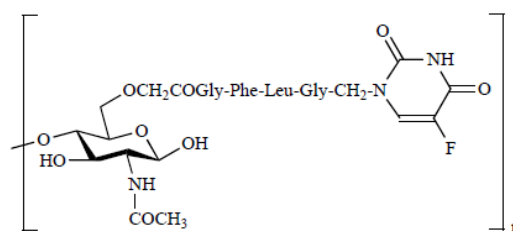


Fig. (21). *O*-carboxymethylchitosan-Gly-Phe-Leu-Gly-5FU conjugate.

Doxorubicin is one of the prominent clinical anthracycline ring antibiotics with a broad spectrum of antitumor activity. The mechanism of action resides on the inhibition of topoisomerase II enzyme that participates on three dimensional arrangement changes of DNA during its replication. To minimize undesirable side effects, such as cardiotoxicity, low stability, poor water solubility, chitosan alginate multilayer microcapsules were prepared (Fig. 22). The microcapsules were fabricated by deposition of oppositely charged chitosan and alginate onto carboxymethyl cellulose doped CaCO_3 colloidal particles [82]. Encapsulation of a drug effectively induces apoptose HepG2 tumor cells.

Cancer immunotherapy relies on the ability of the immune system to destroy tumor cells selectively and to elicit a long-lasting memory of such activity. Interleukin-12 (IL-12) is an immunomodulatory cytokine produced primarily by antigen-presenting

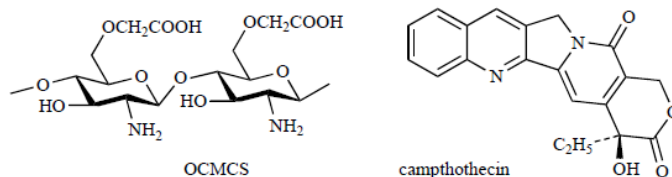


Fig. (19). Camptothecin chitosan aggregate.

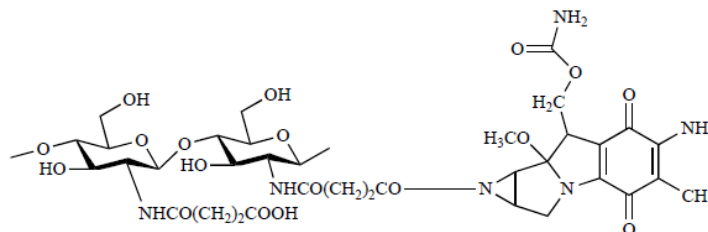


Fig. (20). *N*-succinyl-chitosan Mitomycin C.

cells, which play an important role in promoting Th1-type immune response and cell-mediated immunity. To augment the antitumor immune action by *in vivo* IL-12 gene delivery, mannosylated chitosan (MC) was prepared to induce mannose receptor-mediated endocytosis of IL-12 gene directly into dendritic cells which reside within the tumor. MC was prepared by the reaction of chitosan with mannopyranosylphenylisothiocyanate that was conjugated with DNA. Complexes were induced to self-assemble in phosphate buffer (pH 7.4) by mixing DNA plasmid with the appropriate polymer solution at the desired charge ratio. Complexes inhibit tumor growth in CT-26 and angiogenesis, and significantly induced cell cycle arrest and apoptosis [83].

4.3. Antioxidant Activity

Antioxidants are compounds that inhibit or delay an oxidation of cellular oxidizable substrates. Their main role is to help the body to protect itself against the damage, caused by reactive oxygen species (ROS) and degenerative diseases. ROS in a form of superoxide anion (O_2^-), hydroxyl radical ($\cdot OH$) and hydrogen peroxide (H_2O_2) are produced by sunlight, ultraviolet light, ionizing radiation, chemical reactions and metabolic processes which have a wide variety of pathological effects, such as cancer, cardiovascular diseases, diabetes, and atherosclerosis. These radicals are very unstable and react rapidly with other groups or substances in the body, leading to the cell or tissue injury. They exert their abilities against ROS production or activate a battery of detoxifying proteins.

Recently great attention is focused to the antioxidant activity of chitosan. Its antioxidant activity depends on the molecular weight as well as the degree of deacetylation [84-86]. Low molecular weight partly deacetylated chitosan is possible to consider as a natural antioxidant. Even if the exact mechanism of activity is unknown, it is assumed that amino group and hydroxyl groups bonded on C-2, C-3 and C-6 positions react with unstable free radicals to form more stable macromolecular radicals. This activity probably relates to chelating character of chitosan that leads to restrain lipid oxidation [87]. Chitosan exhibits high inhibition activity on linolenic acid peroxidation, 83.7% activity against hydroxyl radicals [88].

Xing *et al.* [89] have found, that all kinds of sulfated chitosans possessed antioxidant activities and free scavenging activities. Thus chitosan and chitosan sulfates with different molecular weight have been reacted with 4-acetamidobenzenesulfonyl chloride to obtain sulfanilamide derivatives of various molecule weight (Fig. 23). The results have indicated that the sulfanilamide group increased not only water solubility but also antioxidant activity [90].

Glutathione as the known native antioxidant peptide containing sulfur has inspired preparation of quite a number of sulfur modifications. Heterocyclic segment of 1,3,5-thiadiazine-2-thione substituted by aromate introduced two types of sulfur into the molecule (Fig. 24). Scavenging activity on hydroxyl radical was more pro-

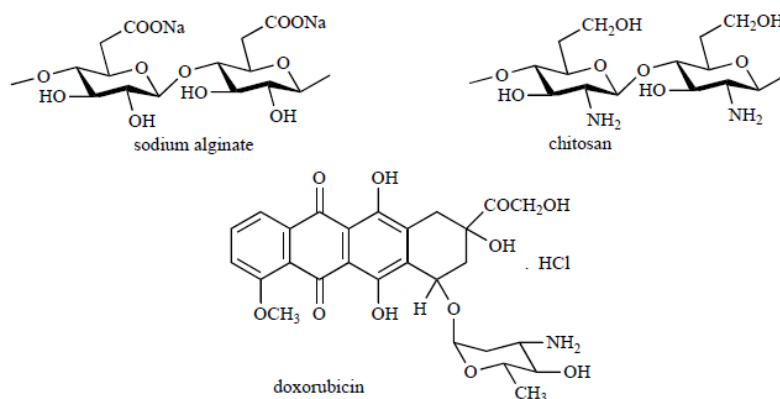


Fig. (22).

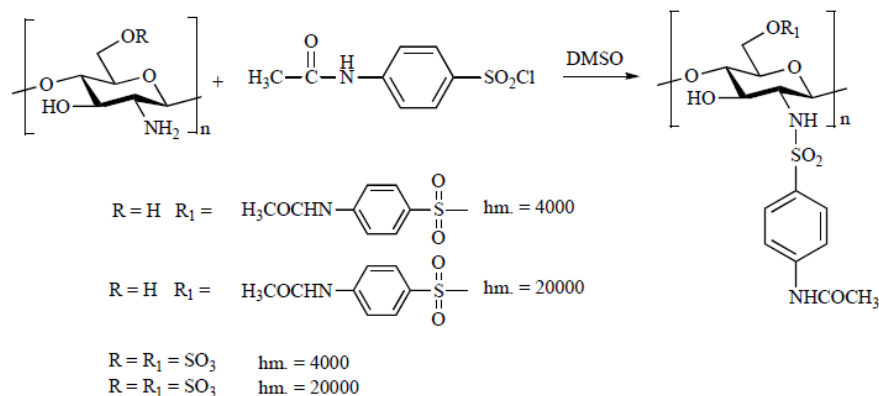


Fig. (23). Synthetic pathway of sulfanilamide derivatives of chitosan and chitosan sulfates.

nounced than that of chitosan. 1,3,5-Disubstituted-tetrahydro-2H-1,3,5-thiadiazine-2-thione derivatives can hydrolyze in water solutions, so their chitosan derivatives have SH groups after hydrolyzing that may induce stronger scavenging activity [91].

To enhance and sustain antioxidant activity, hydrogels composed from chitosan and eugenol were prepared. The allyl groups of eugenol monomer (2-methoxy-4-prop-2-enyl)-phenol) were directly bonded on the amino groups of chitosan using ceric ammonium nitrate (CAN) (Fig. 25). Scavenging activity increased with the graft yield of eugenol, because phenolic hydroxylic groups could play a major role as potent free-radical terminators. An introduction of bulky side chains leads to a faster thermal decomposition, decreased pH sensitivity and inhibition of initiation or propagation of oxidizing chain reactions [92].

Partly quarternized chitosan derivatives with gallic acid had much improved superoxide activity [93]. The superoxide anion O_2^- is formed in almost all cells and is a major agent in the mechanism of oxygen toxicity. Compared with other oxygen radicals, the superoxide anion has a longer life time, and thus is more dangerous.

In the same way as with antibacterial active chitosan derivatives, increasing antioxidant activity of amino or hydroxyl group of chitosan alkylated by ethyl, dimethylaminoethyl or diethylaminoethyl (Fig. 26) also occurs [94]. Antioxidant activity depends on the degree of deacetylation (50 and 90% was used) and on the type of substituted group. The most effective ROS scavenging effect found was 90% deacetylated *N*-aminoethyl chitosan (AEC90), which had the highest percentage of free amino groups. The results suggested that an amino group is a major factor for free radical scavenging activity; introduction of an amino group on the C-6 position did not cause any effect.

5-Chloro-2-hydroxy-benzaldehyde and 2-hydroxy-5-nitrobenzaldehyde were used for the preparation of a Schiff bases with free amino groups of chitosan and carboxymethylchitosan [95]

(Fig. 27). Although a free phenolic hydroxyl group was introduced into the molecule, antioxidant activity against the superoxide radical and hydroxyl radical did not increase. This is due to the fact that free amino group is fundamental for activity even if a hydroxyl group in previous derivatives stimulated the activity.

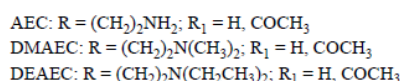
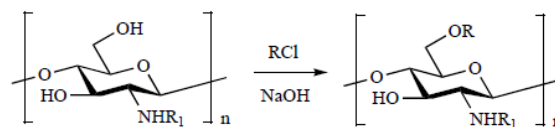


Fig. (26).

Among various reactive oxygen species, hydroxyl radicals have the strongest chemical activity, which can damage a wide range of essential biomolecules such as amino acids, proteins, and DNA. From four forms of chitosan having primary amino group, imino group (Schiff bases), secondary amino group and quarternised ammonium group the last one has shown the highest antioxidant activity against hydroxyl radicals. It was found that high positive charge density increases antioxidant activity [96].

5. CONCLUSION

Currently, chitosan has been attracting attention for its unique physico-chemical characters and bioactivities. According to the growing number of recently published scientific articles, it can be deduced, that chitosan is a perspective material of the extensive potential for various applications. Although there exist many scientific studies being engaged in various modifications, a detail

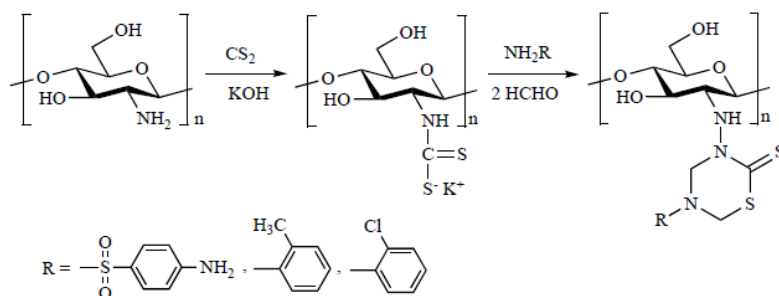


Fig. (24). Synthesis of 1,3,5-thiadiazine-2-thione derivatives of chitosan.

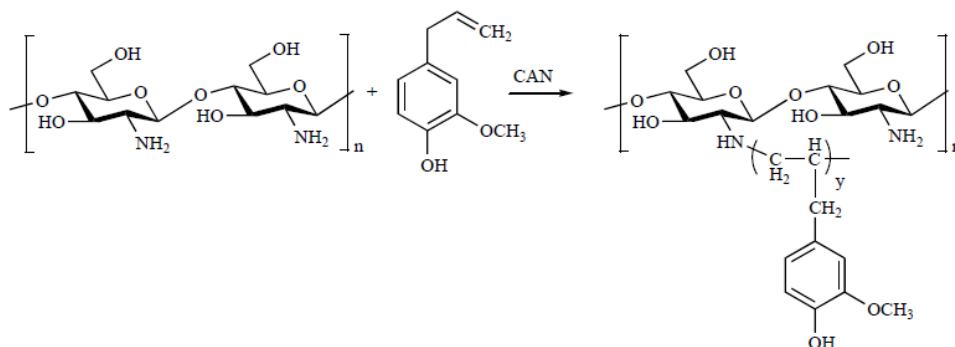


Fig. (25). CAN = diammonium cerium(IV)nitrate.

mechanism of activity on the molecular level has not yet been discovered. Therefore, future research should be directed towards understanding their molecular level details which may provide an insight into the unrevealed molecular level functions of chitosan and help to accelerate their future applications.

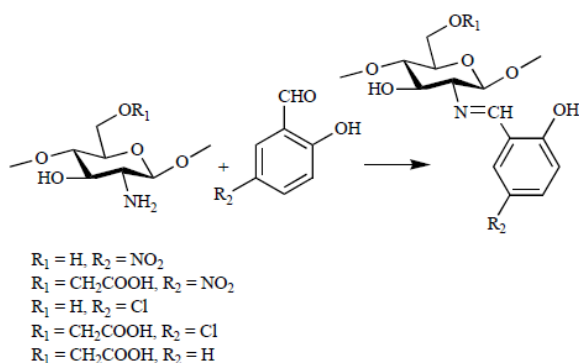


Fig. (27).

ACKNOWLEDGEMENT

This work was supported by MSM 0021620822 and GAUK 76807/2007.

REFERENCES

- [1] Tokuyasu K, Ohnishi-Kameyama M, Hayashi K. Purification and characterization of extracellular chitin deacetylase from *Colletotrichum lindemuthianum*. *Biosci Biotech Biochem* 1996; 60: 1598-603.
- [2] Hu KJ, Hu JL, Ho KP, Yeung KW. Screening of fungi for chitosan producers, and copper adsorption capacity of fungal chitosan and chitosanaceous materials. *Carbohydr Polym* 2004; 58: 45-52.
- [3] Uraganu T, Tokura S, Ed. *Material science of chitin and chitosan*. New York, Springer 2006.
- [4] Illum L. Chitosan and its use as a pharmaceutical excipient. *Pharm Res* 1998; 15: 1326-31.
- [5] Dodane V, Vilivalam VD. Pharmaceutical applications of chitosan. *Pharm Sci Technol Today* 1998; 1: 246-53.
- [6] Koide SS. Chitin-chitosan: Properties, benefits and risks. *Nutr Res* 1998; 18: 1091-101.
- [7] Schulz PC, Rodriguez MS, Del Blanco LF, Pistonesi M, Agullo E. Emulsification properties of chitosan. *Colloid Polym Sci* 1998; 276: 1159-65.
- [8] Clark GL, Smith AF. X-ray diffraction studies of chitin, chitosan and derivatives. *J Phys Chem* 1936; 40: 863-79.
- [9] Okuyama K, Noguchi K, Miyazawa T, Yui T, Ogawa K. Molecular and crystal structure of hydrated chitosan. *Macromolecules* 1997; 30: 5849-55.
- [10] Yui T, Imada K, Okuyama K, Obata Y, Suzuki K, Ogawa K. Molecular and crystal structure of the anhydrous form of chitosan. *Macromolecules* 1994; 27: 7601-5.
- [11] Lertworasirikul A, Yokoyama S, Noguchi K, Ogawa K, Okuyama K. Molecular and crystal structures of chitosan/HI type I salt determined by X-ray fiber diffraction. *Carbohydr Res* 2004; 339: 825-33.
- [12] Lertworasirikul A, Noguchi K, Ogawa K, Okuyama K. Plausible molecular and crystal structures of chitosan/HI type II salt. *Carbohydr Res* 2004; 339: 835-43.
- [13] Thanou M, Verhoef JC, Junginger HE. Oral drug absorption enhancement by chitosan and its derivatives. *Adv Drug Deliver Rev* 2001; 52: 117-26.
- [14] Yilmaz E. Chitosan: A versatile biomaterial. *Adv Exp Med Biol* 2004; 553: 59-68.
- [15] Kato Y, Onishi H, Machida Y. Application of chitin and chitosan derivatives in the pharmaceutical field. *Curr Pharm Biotechnol* 2003; 4:303-9.
- [16] Thanou M, Junginger HE. In: Dumitriu S Ed, *Polysaccharides*. New York, Marcel Dekker, Inc. 2005; 661-77.
- [17] Kumar MNVR, Hudson SM. In: Wnek GE, Bowlin GL Ed, *Encyclopedia of Biomaterials and Biomedical Engineering*. New York, Marcel Dekker, Inc. 2004; 310-23.
- [18] Felt O, Buri P, Gurny R. Chitosan: a unique polysaccharide for drug delivery. *Drug Dev Ind Pharm* 1998; 24: 979-93.
- [19] Chun HK, Jang WC, Heung JC, Kyu SC. Synthesis of chitosan derivatives with quaternary ammonium salt and their antibacterial activity. *Polym Bull* 1997; 38: 387-93.
- [20] Fernandez-Saizn P, Ocio MJ, Lagaron JM. Film-forming process and biocide assessment of high-molecular-weight chitosan as determined by combined ATR-FTIR spectroscopy and antimicrobial assay. *Biopolymers* 2006; 83: 577-83.
- [21] Tsai GJ, Su WH. Antibacterial activity of shrimp chitosan against *Escherichia coli*. *J Food Prot* 1999; 62: 239-43.
- [22] Liu H, Du Y, Wang X, Sun L. Chitosan kills bacteria through cell membrane damage. *Int J Food Microbiol* 2004; 95: 147-55.
- [23] Chen YL, Chou CC. Factors affecting the susceptibility of *Staphylococcus aureus* CCRC 12657 to water soluble lactose chitosan derivative. *Food Microbiol* 2005; 22: 29-35.
- [24] Helander IM, Nurmiaho-Lassila EL, Ahvenainen R, Rhoades J, Roller S. Chitosan disrupts the barrier properties of the outer membrane of Gram-negative bacteria. *Int J Food Microbiol* 2001; 71: 235-44.
- [25] Zheng LY, Zhu JF. Study on antimicrobial activity of chitosan with different molecular weights. *Carbohydr Polym* 2003; 54: 527-30.
- [26] Jia G, Wang HL, Wu JCG, Lin JG. Relationship between antibacterial activity of chitosan and surface characteristics of cell wall. *Acta Pharmacol Sin* 2004; 27: 932-6.
- [27] Liu N, Chen XG, Park HJ, Liu CG, Liu CS, Meng XH, *et al*. Effect of MW and concentration of chitosan on antibacterial activity of *Escherichia coli*. *Carbohydr Polym* 2006; 64: 60-5.
- [28] Gerasimenko DV, Avdienko ID, Bannikova GE, Zueva OY, Varlamov VP. Antibacterial effects of water-soluble low-molecular-weight chitosans on different microorganisms. *Appl Biochem Microbiol* 2004; 40: 253-7.
- [29] Jeon YJ, Park PJ, Kim SK. Antimicrobial effect of chitooligosaccharides produced by bioreactor. *Carbohydr Polym* 2001; 44: 71-6.
- [30] Park PJ, Lee HK, Kim SK. Preparation of hetero-chitooligosaccharides and their antimicrobial activity on *Vibrio parahaemolyticus*. *J Microbiol Biotechnol* 2004; 14: 41-7.
- [31] Park PJ, Je JY, Byun HG, Moon SH, Kim SK. Antimicrobial activity of hetero-chitosans and their oligosaccharides with different molecular weights. *J Microbiol Biotechnol* 2004; 14: 317-23.
- [32] Tokura S, Ueno K. Molecular weight-dependent antimicrobial activity by chitosan. *Macromol Symp* 1997; 120: 1-9.
- [33] Yang TC, Chou CC, Li CF. Antibacterial activity of N-alkylated disaccharide chitosan derivatives. *Int J Food Microbiol* 2005; 97: 237-45.
- [34] No HK, Park NY, Lee SH, Meyers SP. Antibacterial activity of chitosans and chitosan oligomers with different molecular weights. *Int J Food Microbiol* 2002; 74: 65-72.
- [35] Chung YC, Kuo CL, Chen CC. Preparation and important functional properties of water-soluble chitosan produced through Mailard reaction. *Bioresour Technol* 2005; 96: 1473-82.
- [36] Jia Z, Shen D, Xu W. Synthesis and antibacterial activities of quaternary ammonium salt of chitosan. *Carbohydr Res* 2001; 333: 1-6.
- [37] Xie W, Xu P, Wang W, Liu Q. Preparation and antibacterial activity of a water-soluble chitosan derivative. *Carbohydr Polym* 2002; 50: 35-40.
- [38] Muzzarelli R, Tarsi R, Filippini O, Giovanetti E, Biagini G, Varaldo PE. Antimicrobial properties of N-carboxybutyl chitosan. *Antimicrob Agents Chemother* 1990; 34: 2019-23.
- [39] Liu XF, Guan YL, Yang DZ, Li Z, Yao KD. Antibacterial action of chitosan and carboxymethylated chitosan. *J Appl Polym Sci* 2001; 79: 1324-35.
- [40] Wang LC, Chen XG, Zhong DY, Xu QC. Study on poly(vinyl alcohol)/carboxymethyl-chitosan blend films as local drug delivery system. *J Mater Sci: Mater Med* 2007; 18: 1125-33.

- [41] Jayakumar R, Nwe N, Tokura S, Tamura H. Sulfated chitin and chitosan as novel biomaterials. *Int J Biol Macromol* 2007; 40: 175-81.
- [42] Huang R, Du Y, Zheng L, Liu H, Fan L. A new approach to chemically modified chitosan sulfates and study of their influences on the inhibition of *Escherichia coli* and *Staphylococcus aureus* growth. *React Funct Polym* 2004; 59: 41-51.
- [43] Kurita K, Kojima T, Nishiyama Y, Shimojoh M. Synthesis and some properties of nonnatural amino polysaccharides: Branched chitin and chitosan. *Macromolecules* 2000; 33: 4711-6.
- [44] Guo Z, Xing R, Liu S, Zhong Z, Ji X, Wang L, Li P. Antifungal properties of Schiff bases of chitosan, N-substituted chitosan and quaternized chitosan. *Carbohydr Res* 2007; 342: 1329-32.
- [45] Runarsson OV, Holappa J, Nevalainen T, Hjalmsdottir M, Jarvinen T, Loftsson T, *et al.* Antibacterial activity of methylated chitosan and chito-oligomer derivatives: Synthesis and structure activity relationships. *Eur Polym J* 2007; 43: 2660-71.
- [46] Avadi MR, Sadeghi AMM, Tahzibi A, Bayati K, Pouladzadeh M, Zohuriaan-Mehr MJ, *et al.* Diethylmethyl chitosan as an antimicrobial agent: Synthesis, characterization and antibacterial effects. *Eur Polym J* 2004; 40: 1355-61.
- [47] Chi W, Qin C, Zeng L, Li W, Wang W. Microbiocidal activity of chitosan-N-2-hydroxypropyl trimethyl ammonium chloride. *J Appl Polym Sci* 2007; 103: 3851-6.
- [48] Xie Y, Liu X, Chen Q. Synthesis and characterization of water-soluble chitosan derivate and its antibacterial activity. *Carbohydr Polym* 2007; 69: 142-7.
- [49] Saravanan S, Selvan PS, Gopal N, Gupta JK, De B. Synthesis and antibacterial activity of some imidazole-5-(4H)one derivatives. *Arch Pharm* 2005; 338: 488-92.
- [50] Caner H, Yilmaz E, Yilmaz O. Synthesis, characterization and antibacterial activity of poly(N-vinylimidazole) grafted chitosan. *Carbohydr Polym* 2007; 69: 318-25.
- [51] Hu Y, Du Y, Yang J, Kennedy JF, Wang X, Wang L. Synthesis, characterization and antibacterial activity of guanidinylated chitosan. *Carbohydr Polym* 2007; 67: 66-72.
- [52] Mi FL, Yu SH, Peng CK, Sung HW, Shyu SS, Liang HF, *et al.* Synthesis and characterization of a novel glycoconjugated macromolecule. *Polymer* 2006; 47: 4348-58.
- [53] Yang TC, Chou CC, Li CF. Antibacterial activity of N-alkylated disaccharide chitosan derivatives. *Int J Food Microbiol* 2005; 97: 237-45.
- [54] Tikhonov VE, Stepanova EA, Babak VG, Yamskov IA, Palma-Guerrero J, Jansson HB, *et al.* Bactericidal and antifungal activities of a low molecular weight chitosan and its N-(2(3)-(dodec-2-enyl)succinoyl)-derivatives. *Carbohydr Polym* 2006; 64: 66-72.
- [55] Ma Y, Zhou T, Zhao C. Preparation of chitosan-nylon-6 blended membranes containing silver ions as antibacterial materials. *Carbohydr Res* 2008; 343: 230-7.
- [56] Chen S, Wu G, Zeng H. Preparation of high antimicrobial activity thiourea chitosan-Ag⁺ complex. *Carbohydr Polym* 2005; 60: 33-8.
- [57] Holappa J, Nevalainen T, Savolainen J, Soinen P, Elomaa M, Safin R. Synthesis and characterization of chitosan N-betainates having various degrees of substitution. *Macromolecules* 2004; 37: 2784-89.
- [58] Holappa J, Hjalmsdottir M, Masson M, Runarsson O, Asplund T, Soinen P, *et al.* Antimicrobial activity of chitosan N-betainates. *Carbohydr Polym* 2006; 65: 114-8.
- [59] Santhosh S, Sini TK, Anandan R, Mathew PT. Effect of chitosan supplementation on antitubercular drugs-induced hepatotoxicity in rats. *Toxicology* 2006; 219: 53-9.
- [60] Krysteva M, Todorova NP, Maneva K, Todorov D. Carminomycin-chitosan: a conjugated antitumor antibiotic. *J Bioact Comp Polym* 1999; 14: 178-84.
- [61] Ishak RAH, Awad GAS, Mortada ND, Nour SAK. Preparation, *in vitro* and *in vivo* evaluation of stomach-specific metronidazole-loaded alginate beads as local anti-*Helicobacter pylori* therapy. *J Control Release* 2007; 119: 207-14.
- [62] Rando DG, Brandt CA, Ferreira EI. Use of N-methylene phosphonic chitosan to obtain an isoniazid prodrug. *Brasillian J Pharm Sci* 2004; 40: 335-44.
- [63] Ozturk E, Agalar C, Kececi K, Denkbas EB. Preparation and characterization of ciprofloxacin-loaded alginate/chitosan sponge as a wound dressing material. *J Appl Polym Sci* 2006; 101: 1602-9.
- [64] Denkbas EB, Ozturk E, Ozdemir N, Kececi K, Agalar C. Norfloxacin-loaded chitosan sponges as wound dressing material. *J Biomater Appl* 2004; 18: 291-303.
- [65] Zhu A, Jin W, Yuan L, Yang G, Yu H, Wu H. O-Carboxymethyl-chitosan-based novel gatifloxacin delivery system. *Carbohydr Polym* 2007; 68: 693-700.
- [66] Qin Y, Zhu C, Chen J, Chen Y, Zhang C. The absorption and release of silver and zinc ions by chitosan fibers. *J Appl Polym Sci* 2006; 101: 766-71.
- [67] Wang X, Du Y, Liu H. Preparation, characterization and antimicrobial activity of chitosan-Zn complex. *Carbohydr Polym* 2004; 56: 21-6.
- [68] Zivanovic S, Li J, Davidson PM, Kit K. Physical, mechanical, and antibacterial properties of chitosan/PEO blend films. *Biomacromolecules* 2007; 8: 1505-10.
- [69] Wada T, Yasuda M, Yako H, Matoba Y, Urugami T. Preparation and characterization of hybrid quaternized chitosan/acrylic resin emulsions and their films. *Macromol Mater Eng* 2007; 292: 147-54.
- [70] Varum KM, Holme HK, Izume M, Stokke BT, Smidsrod X. Determination of enzymatic hydrolysis specificity of partially N-acetylated chitosans. *Biochim Biophys Acta* 1996; 1291: 5-15.
- [71] Shin-ya Y, Lee MY, Himode H, Kajuchi T. Effects of N-acetylation degree on N-acetylated chitosan hydrolysis with commercially available and modified pectinases. *Biochem Eng J* 2001; 7: 85-8.
- [72] Qin C, Du Y, Xiao L, Li Z, Gao X. Enzymic preparation of water-soluble chitosan and their antitumor activity. *Int J Bio Macromol* 2002; 31: 111-7.
- [73] Pantaleone D, Yalpani M, Scollar M. Unusual susceptibility of chitosan to enzymic hydrolysis. *Carbohydr Res* 1992; 237: 325-32.
- [74] Liang TW, Chen YJ, Yen YH, Wang SL. The antitumor activity of the hydrolysates of chitinous materials hydrolyzed by crude enzyme from *Bacillus amyloliquefaciens* V656. *Process Biochem* 2007; 42: 527-34.
- [75] Qin C, Zhou B, Zeng L, Zhang Z, Liu Y, Du Y, *et al.* The physicochemical properties and antitumor activity of cellulase-treated chitosan. *Food Chem* 2004; 84: 107-15.
- [76] Prashanth KVH, Tharanathan RN. Depolymerized products of chitosan as potent inhibitors of tumor-induced angiogenesis. *Biochim Biophys Acta* 2005; 1722: 22-9.
- [77] Zheng Y, Yi Y, Qi Y, Wang Y, Zhang W, Du M. Preparation of chitosan-copper complexes and their antitumor activity. *Bioorg Med Chem Lett* 2006; 16: 4127-9.
- [78] Aiping Z, Jianhong L, Wenhui Y. Effective loading and controlled release of camptothecin by O-carboxymethylchitosan aggregates. *Carbohydr Polym* 2006; 63: 89-96.
- [79] Song Y, Onishi H, Machida Y, Nagai T. Drug release and antitumor characteristics of N-succinyl-chitosan-mitomycin C as an implant. *J Control Rel* 1996; 42: 93-100.
- [80] Song Y, Onishi H, Nagai T. Conjugate of mitomycin C with N-succinyl-chitosan: In vitro drug release properties, toxicity and antitumor activity. *Int J Pharm* 1998; 98: 121-30.
- [81] Ouchi T, Tada M, Matsumoto M, Ohya Y, Hasegawa K, Arai Y, *et al.* Design of macromolecular prodrug of 5-fluorouracil using N-acetylpolygalactosamine as a targeting carrier to hepatoma. *React Funct Polym* 1998; 37: 235-44.
- [82] Zhao Q, Han B, Wang Z, Gao C, Peng C, Shen J. Hollow chitosan-alginate multilayer microcapsules as drug delivery vehicle: doxorubicin loading and in vitro and in vivo studies. *Nanomedicine* 2007; 3: 63-74.
- [83] Kim TH, Jin H, Kim HW, Cho MH, Cho CS. Mannosylated chitosan nanoparticle-based cytokine gene therapy suppressed cancer growth in BALB/c mice bearing CT-26 carcinoma cells. *Mol Cancer Ther* 2006; 5: 1723-32.
- [84] Kim KW, Thomas RL. Antioxidative activity of chitosans with varying molecular weights. *Food Sci* 2007; 101: 308-13.
- [85] Chien PJ, Sheu F, Huang WT, Su MS. Effect of molecular weight of chitosans on their antioxidative activities in apple juice. *Food Chem* 2007; 102: 1192-8.
- [86] Koryagin AS, Erofeeva EA, Yakimovich NO, Aleksandrova EA, Smirnova LA, Malkov AV. Analysis of antioxidant properties of chitosan and its oligomers. *Bull Exp Biol Med* 2006; 142: 461-3.

- [87] Peng C, Wang Y, Tang Y. Synthesis of crosslinked chitosan-crown ethers and evaluation of these products as adsorbents for metal ions. *J Appl Polym Sci* 1998; 70: 501-6.
- [88] Feng T, Du Y, Wei Y, Yao P. Antioxidant activity of half N-acetylated water-soluble chitosan in vitro. *Eur Food Res Technol* 2007; 225: 133-8.
- [89] Xing RE, Yu HH, Liu S, Zhang WW, Zhang QB, Li ZE, Li PC. Antioxidant activity of differently regioselective chitosan sulfates in vitro. *Bioorg Med Chem* 2005; 13: 1387-92.
- [90] Zhong Z, Ji X, Xing R, Liu S, Guo Z, Chen X, Li P. The preparation and antioxidant activity of the sulfanilamide derivatives of chitosan and chitosan sulfates. *Bioorg Med Chem* 2007; 15: 3775-82.
- [91] Ji X, Zhong Z, Chen X, Xing R, Liu S, Wang L, Li P. Preparation of 1,3,5-thiadiazine-2-thione derivatives of chitosan and their potential antioxidant activity in vitro. *Bioorg Med Chem Lett* 2007; 17: 4275-9.
- [92] Jung BO, Chung SJ, Lee SB. Preparation and characterization of eugenol-grafted chitosan hydrogels and their antioxidant activities. *J Appl Polym Sci* 2006; 99: 3500-6.
- [93] Sun T, Xie W, Xu P. Superoxide anion scavenging activity of graft chitosan derivatives. *Carbohydr Polym* 2004; 58: 379-82.
- [94] Je JY, Kim SK. Reactive oxygen species scavenging activity of aminoderivatized chitosan with different degree of deacetylation. *Bioorg Med Chem* 2006; 14: 5989-94.
- [95] Guo Z, Xing R, Liu S, Yu H, Wang P, Li C, *et al.* The synthesis and antioxidant activity of the Schiff bases of chitosan and carboxymethyl chitosan. *Bioorg Med Chem Lett* 2005; 15: 4600-3.
- [96] Guo Z, Liu H, Ji X, Li P. Hydroxyl radicals scavenging activity of N-substituted chitosan and quaternized chitosan. *Bioorg Med Chem Lett* 2006; 16: 6348-50.

Paper II

CHITOSAN A JEHO FARMACEUTICKÉ APLIKACE

EVA VAVŘÍKOVÁ A JARMILA VINŠOVÁ

Farmaceutická fakulta UK, Heyrovského 1203, 500 05
Hradec Králové
jarmila.vinsova@faf.cuni.cz

Došlo 11.10.07, přepracováno 3.6.08, přijato 11.9.08.

Klíčová slova: chitosan, antibakteriální aktivita, protinádorová aktivita, antioxidační aktivita

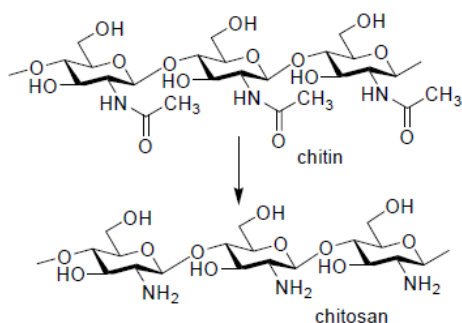
Obsah

1. Úvod
2. Charakteristika chitosanu
3. Farmaceutické aplikace chitosanu
 - 3.1. Antibakteriální aktivita
 - 3.2. Protinádorová aktivita
 - 3.3. Antioxidační aktivita
4. Závěr

1. Úvod

Polymery jsou v dnešní době stále častěji využívány jako vhodné biodegradabilní nosiče léčiv. Používají se k pomalému uvolňování účinné složky, tedy jako depotní formy, ke zvyšování rozpustnosti a lepší možnosti cíleného podání.

Mezi přírodní polymery typu polysacharidů patří chitosan (poly-D-glukosamin), odvozený od přírodního chitinu, druhého nejrozšířenějšího polysacharidu po celulóse. Získává se alkalickou deacetylací chitinu, několikahodinovým varem s 50% hydroxidem sodným nebo enzymaticky působením *N*-deacetylasy (EC 3.5.1.41)¹, (obr. 1).



Obr. 1. Deacetylace chitinu

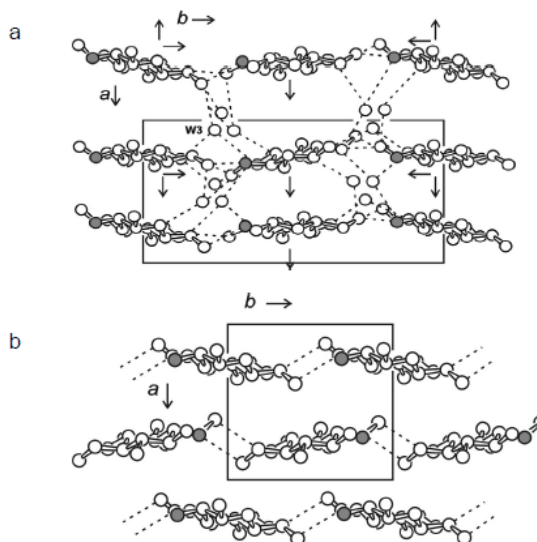
Stupeň deacetylace chitinu se udává v procentech, obvykle v rozmezí 60–100 %. Chitosan se v přírodě vyskytuje pouze v malém množství u několika typů hub rodu *Aspergillus* a *Mucor*².

Chitosan má vynikající biologické vlastnosti, je netoxický, biokompatibilní a biodegradabilní³. Pro své výjimečné vlastnosti se používá v různých oborech zahrnujících především biomedicínu, kosmetiku, agrochemii, fyzikální chemii, konzervaci potravin, čištění vody a impregnaci textilií⁴. Používá se také jako potravní doplněk pro snížení hladiny cholesterolu a redukci hmotnosti. Váže na sebe tuky a cholesterol a odvádí je ze zažívacího traktu dříve, než jsou zpracovány⁵. Jako vláknina zlepšuje činnost tlustého střeva a snižuje pocit hladu, proto se používá k hubnutí. Někdy se mu přičítá přílišný redukční účinek, který však nebyl vědecky prokázán.

2. Charakteristika chitosanu

Chitosan neboli (1→4)-2-amino-2-deoxy-β-D-glukan patří mezi méně časté kationové polymery. V porovnání s chitinem má větší chemickou a biochemickou reaktivitu.

Rentgenostrukturní analýzou^{6,7} byly objeveny 4 krystalické polymorfy chitosanu, tři hydratované (tendonová forma, forma II a L2), které snadno vytvářejí ve vodě rozpustné soli s organickými a minerálními kyselinami a jedna nehydratovaná forma, která vzniká zahříváním hydratovaného chitosanu na teplotu 200 °C (cit.³). Dehydrataci se



Obr. 2. a) Hydratovaný chitosan, b) nehydratovaný chitosan

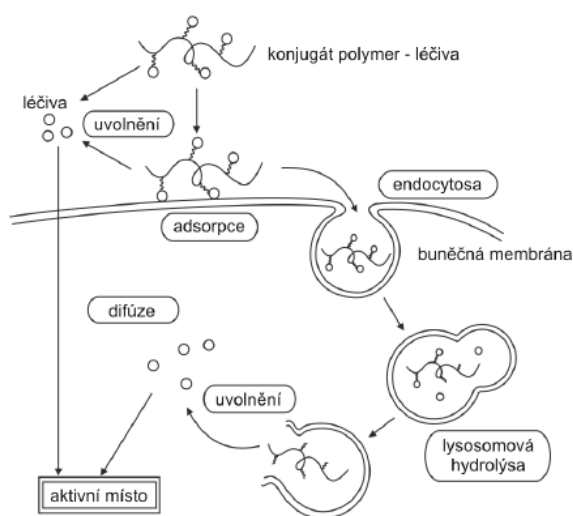
zkracují vzdálenosti vrcholů struktury „cik-cak“ a oddálení jednotlivých řetězců, (obr. 2, cit.⁸). Tato změna je ireversibilní. Nehydratované krystaly jsou nerozpustné v kyselinách, s kovovými ionty netvoří komplexy. Krystaly bezvodé formy ztrácí funkci biomateriálů a mohou být použity jako inertní pryskyřice.

Molekula chitosanu má tři reaktivní centra: primární aminoskupinu, primární a sekundární hydroxyskupinu. Aminoskupina snadno podléhá kvarternizaci, čímž lze zvýšit rozpustnost chitosanu ve vodě a tvoří komplexy s ionty kovů. Primární hydroxyskupina bývá nejčastěji substituována spojovacími články „spacery“, na které se váže aktivní složka – léčivo nebo skupina, která je zodpovědná za cílení léčiva nebo zvýšení rozpustnosti ve vodě. Sekundární hydroxyskupina je modifikována především za účelem zvýšení rozpustnosti ve vodě.

3. Farmaceutické aplikace chitosanu

Pro své výjimečné vlastnosti je chitosan velmi zajímavý materiál a bioaktivní činitel ve farmaceutických a biomedicínských odvětvích. Lze jej použít jako systém pro transport léčiv, jehož hlavním znakem je řízené uvolňování a cílení léčiva. Vyžaduje se též optimální odpověď receptoru, minimální vedlejší účinky a prodloužený efekt léčiva.

Polymer může být léčivem, pokud sám vykazuje farmakologickou aktivitu, i když jeho monomerní jednotky jsou neaktivní. Polymerní proléčivo je makromolekulární látka, která slouží nejčastěji jako nosič léčiva, sama může mít i nemusí biologickou aktivitu. Je obvykle složeno z polymerního nosiče, biodegradabilní vazby mezi nosičem a léčivem a mávající skupinu, která způsobuje cílení, např. specifický peptid pro cílovou buňku.



Obr. 3. Cesty léčivé látky k aktivnímu místu

Použití makromolekulárních proléčivových konjugátů s nízkou molekulovou hmotností je jednou z metod transportu léčiv, který je zaměřen na zlepšení pohybu látky změnou rozpustnosti a molekulární velikosti, udržení vhodných koncentrací léčiv pomalu se uvolňujících z nosičů, cílený transport léčiv do cílových buněk, podporu inkorporace léčiv do buněk endocytózou a hybridizaci dvou druhů léčiv nebo léčiva s bioaktivním polymerním nosičem. Design konečné molekuly konjugátu musí být také v souladu s fyzikálními vlastnostmi konjugátu a biochemickými vlastnostmi polymerního nosiče. Polymerní nosiče (jejich velikost, elektrický náboj, hydrofilnost nebo lipofilnost a specifická transmembránová transportní schopnost) mohou změnit farmakologické a imunologické aktivity látek, které roznášejí.

Průnik makromolekulárního proléčiva do buňky může probíhat difúzí uvolněného léčiva do buňky nebo endocytózou konjugátu polymer-léčivo (obr. 3). Nejdeálnější cestou pro polymery je endocytóza, kdy je celý konjugát vpraven do buňky a v lysosomech se z něho léčivo postupně uvolňuje působením lysosomových enzymů.

3.1. Antibakteriální aktivita

Samotný chitosan vykazuje antibakteriální účinnost vůči mnoha gram pozitivním (*Staphylococcus aureus*, *Staphylococcus epidermis*, *Bacillus subtilis*) i gram negativním bakteriím (*Pseudomonas aeruginosa*, *Escherichia coli*, *Klebsiella pneumoniae*, *Proteus vulgaris*)⁹ a houbám při pH < 6. Přesný mechanismus antimikrobiální účinnosti sice není plně znám, ale předpokládá se, že kladně nabitě aminoskupiny glukosaminových jednotek interagují s negativně nabitými komponentami mikrobiálních buněčných membrán, tím mění propustnost a způsobují únik intracelulárního obsahu^{10,11}, což vede k rozpadu buněk¹²⁻¹⁴. Další návrh mechanismu působení se týká penetrace nízkomolekulárního chitosanu do buňky, kde se váže na DNA a způsobuje částečnou inhibici RNA a proteinové syntézy¹⁵. Chitosan rovněž chelatuje s kovy potřebnými pro růst mikroorganismů¹⁶. Biologická aktivita chitosanu závisí na mnoha faktorech (molekulové hmotnosti, stupni deacetylace chitinu, derivatizaci, typu substituce, velikosti a poloze substituentů na chitosanovém skeletu, rozpustnosti, pH roztoku), které vedou k rozsáhlému studiu jeho modifikací ve snaze o přípravu vhodné aplikační formy, zlepšení účinku a cíleného působení.

Důležitým faktorem je velikost molekuly chitosanu a jeho koncentrace¹⁷. Obecně lze konstatovat, že optimální velikost aktivního chitosanu se pohybuje v rozmezí 2 až 200 kDa.

Tokura a spol.¹⁸ objevili, že chitosan s vyšší molekulovou hmotností (9300) téměř úplně inhibuje aktivitu *E. coli*, zatímco chitosan s nízkou molekulovou hmotností (2200) je inaktivní. K objasnění tohoto pozoruhodného faktu bylo použito chitosanu značeného pomocí fluorescein isothiokyanátu (FITC). Vysokomolekulární chitosan zaplní vnější stranu buněčné stěny a inhibuje pronikání živin dovnitř, zatímco chitosan s nízkou molekulovou

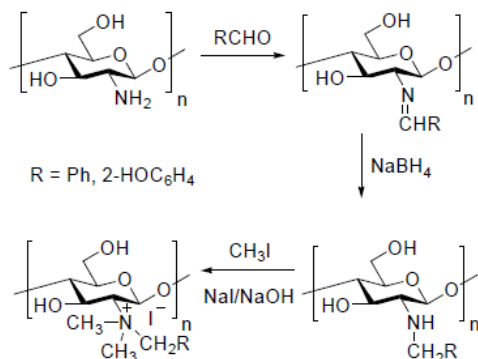
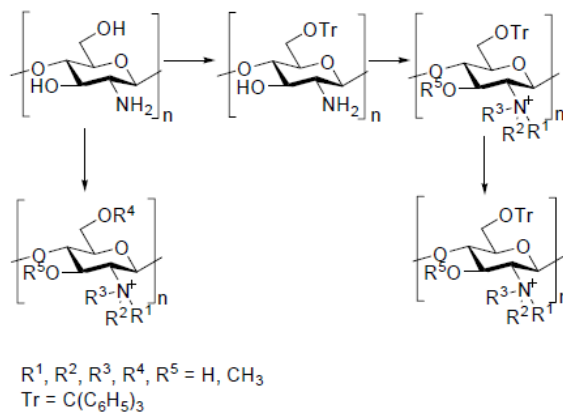


Schéma 1. Příprava Schiffových a kvarterních bázi

Schéma 2. *N*-methylace oligochitosanu a chitosanu

hmotností se akumuluje uvnitř buňky, což ukazuje na to, že *E. coli* metabolizuje tento chitosan jako potravu.

Další důležitou podmínkou je pH. Antimikrobiální účinnost chitosanu vzrůstá s klesajícím pH^{19,20}. Je-li pH < 6,5, dochází k ionizaci za vzniku pozitivně nabitě části. Nemodifikovaný chitosan je při pH 7 nerozpustný a antibakteriálně neúčinný^{19,21}, proto je velká pozornost směřována na přípravu jeho rozpustných solí. Rozpustnost se zvyšuje jak kvarternizací^{9,22}, tak hydrofilní substitucí, např. u (2-hydroxypropyl)chitosanu²³, *N*-(karboxybutyl)chitosanu²⁴, (karboxymethyl)chitosanu^{25,26} a sulfatovaného chitosanu^{27,28}, která navíc zvyšuje antibakteriální vlastnosti. Pro tento efekt se také syntetizují deriváty chitosanu větvené na uhlíku C6 monomerní jednotky²⁹.

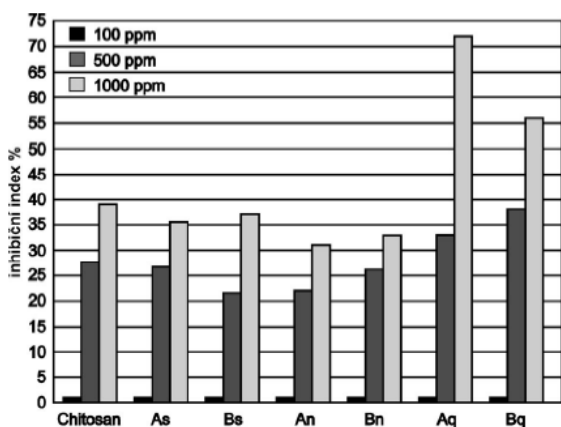
Kvarternizace dusíku aminoskupiny patří k nejčastějším modifikacím. Volná aminoskupina byla kondenzována s benzaldehydem (A) a salicylaldehydem (B) za vzniku Schiffových bázi, které byly dále redukovány tetrahydridoboritanem sodným a v posledním stupni kvarternizovány

methyljodidem (schéma 1). U všech produktů byla sledována antifungální účinnost. Nejúčinnější byly právě kvarterní báze³⁰ (viz obr. 4).

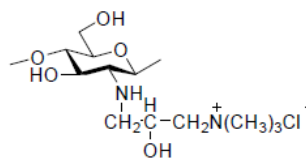
Methylace chitosanu vedla k syntéze *N,N,N*-trimethylchitosanu (schéma 2). Postupně byly methylovány vedle aminoskupin také hydroxyskupiny chitosanu a jeho oligomerů a sledována jejich antibakteriální účinnost vůči *Staphylococcus aureus* při pH 5,5 a 7,2. Oligomery chitosanu se ukázaly jako neaktivní, zatímco methylované deriváty chitosanu vykázaly jistou účinnost. Kvarternizace je potřebná pro účinnost při pH 7,2. Náboj kvarterní amoniové skupiny chitosanu umožňuje jeho rozpustnost v dolních částech gastrointestinálního traktu za neutrálních nebo alkalických podmínek³¹. Vedle *N*-methylovaných kvarterních amoniových solí byl připraven i analogický *N*-ethylderivát, který se používá jako perorální nosič³².

Kvarternizací lze zavést do chitosanu substituent s aminoskupinou, jako je např. při přípravě (2-hydroxypropyl)trimethylamoniového derivátu (obr. 5) reakcí chitosanu s glycidyltrimethylammonium-chloridem³³, který vykázal antioxidační a biocidní účinnost proti *Staphylococcus aureus*, *Bacillus subtilis*, *Staphylococcus epidermidis*, a *Candida albicans*.

Hydrochlorid (ethylamino)-2-(hydroxyethyl)chitosanu byl nejprve hydroxyethylován na primární hydroxyskupině a poté alkylován (2-chlorethyl)amin-hydrochloridem (schéma 3, cit.³⁴). Vznikl ve vodě lépe rozpustný, antibakteriálně účinný derivát proti *Escherichia coli*.



Obr. 4. Antifungální účinnost proti *Colletotrichum lagenarium*; As, Bs – Schiffovy báze; An, Bn – redukované formy; Aq, Bq – kvarterní báze



Obr. 5. Modifikovaný chitosan

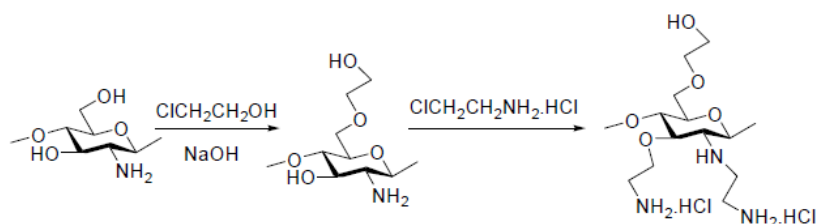


Schéma 3. Syntéza ethylamino(hydroxyethyl)chitosanu

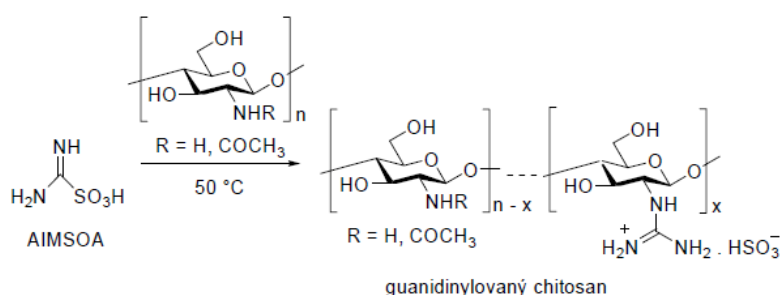


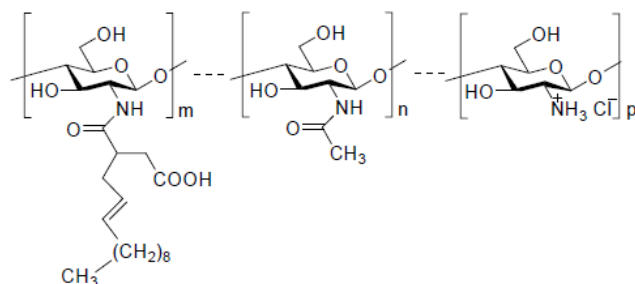
Schéma 4. Guanidinylace chitosanu

Poly(1-vinylimidazol) je znám jako ve vodě dobře rozpustný antibakteriálně účinný polymer³⁵. Byl připraven reakcí s chitosanem ve zředěné kyselině octové působením iontů ceru. Kombinace těchto sloučenin vedla k účinnosti proti grampozitivním i gramnegativním bakteriím. Protonace vinyloimidazolových jednotek zvyšuje rozpustnost ve vodě³⁶.

Guanidinylace chitosanu o různých molekulových hmotnostech vedla ke zvýšení počtu aminoskupin v molekule. Byla provedena aminoiminomethansulfonovou kyselinou (schéma 4). Tyto deriváty vykazaly čtyřikrát nižší hodnoty MIC než samotný chitosan. Zvýšená aktivita je způsobena vyšší hustotou pozitivního náboje guanidinových derivátů, které snadněji asociují na negativním povrchu buněk a vykazují vyšší antibakteriální účinnost proti *Staphylococcus aureus*, *Bacillus subtilis*, *Escherichia coli* a *Pseudomonas aeruginosa*³⁷.

Cílení do jaterních buněk vedlo k syntéze galaktosylovaného chitosanu s vysokou afinitou k HepG2 (buněčná linie rakovinných jaterních buněk). Po zavedení lysinového spojovacího článku na chitosan následovalo kovalentní spojení 4-*O*-β-D-galaktopyranosyl-D-glukonové kyseliny s více vaznými galaktosovými jednotkami. β-D-Galaktosové jednotky jsou významné právě pro cílenou dopravu do jaterních buněk³⁸. Tyto glykokonjugátové molekuly vykazaly aktivitu vůči *Escherichia coli* a *Staphylococcus aureus*.

N-Alkylace chitosanu disacharidy vedla ke zvýšení antibakteriální účinnosti proti *E. coli* a *S. aureus*. Typ disacharidu spojeného s molekulou chitosanu, stupeň substituce disacharidu a pH ovlivňovalo antibakteriální účinnost. Maltosové deriváty chitosanu (stupeň deacetylce chitinu 30–40 %) vykazaly nejvyšší antibakteriální účinnost proti *S. aureus*, zatímco proti *E. coli* byly neúčinnější cello-

Obr. 6. Příprava nízkomolekulárních *N*-[2-(dodec-2-en-1-yl)sukcinoyl]chitosanů

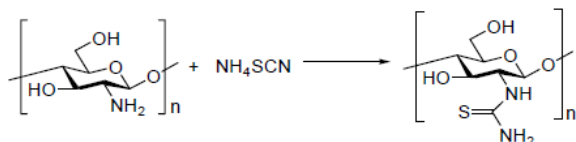


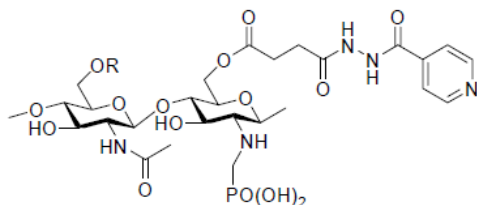
Schéma 5. Thiomočovinný derivát chitosanu

biosové deriváty (stupeň deacetylace chitinu 30–40 %). *N*-Alkylované disacharidové deriváty chitosanu vykazovaly vyšší aktivitu než samotný chitosan při pH 7,0 (cit.³⁹).

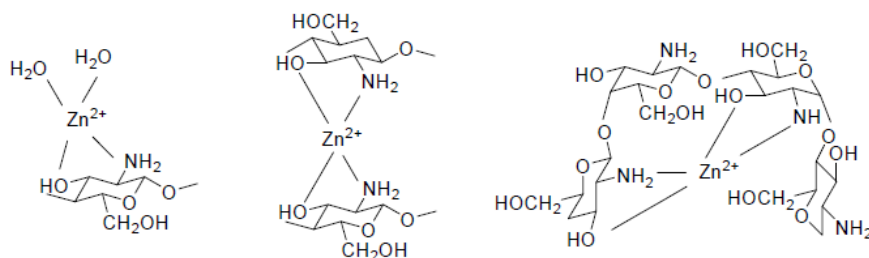
Dále byla připravena série nízkomolekulárních *N*-[2-(dodec-2-en-1-yl)sukcinoyl]chitosanů reakcí chitosanu (4,6 kDa), s 2-(dodec-2-en-1-yl)sukcinanhydridem (obr. 6). Tyto deriváty s dlouhým alifatickým řetězcem a různým stupněm *N*-substituce jsou účinné proti *Escherichia coli*, *Pseudomonas aureofaciens*, *Enterobacter agglomerans*, *Bacillus subtilis*, *Candida krusei* a *Fusarium oxysporum*⁴⁰.

Antibakteriální vlastnosti chitosanu mohou významně zvýšit stříbrné ionty, až o 98 % (cit.²⁰). Samotné stříbro a jeho ionty jsou známy svou antibakteriální účinností⁴¹. Proto byly připraveny komplexy thiomočovinného chitosanu připraveného reakcí chitosanu s thiokyanátem amonijným v ethanolu (schéma 5). Je zajímavé, že se stříbrem koordinuje svými volnými elektrony síra, nikoliv dusík. Tyto komplexy vykazovaly široké spektrum antimikrobiální účinnosti. Minimální inhibiční koncentrace byly 20× nižší než u samotného chitosanu, komplex měl vyšší antibakteriální než antifungální účinnost⁴².

Mnoho výzkumů se zabývá kombinací chitosanu a jiného antibakteriálního činidla. Např. konjugáty s tetra-



Obr. 7. Chitosan-isoniazid-hemisukcinát



Obr. 8. Struktury zinečnatých komplexů

cyklinem a karminomycinem si plně zachovaly antibakteriální účinnost⁴³. Tablety nebo tobolky metronidazolu se používají k léčbě *Helicobacter pylori*. Pro lepší uvolňování z žaludku byl zabudován do chitosanových tobolek⁴⁴.

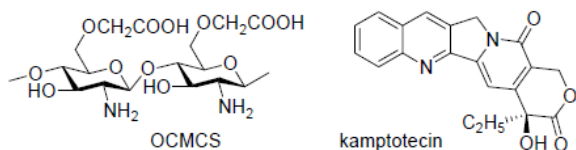
Chitosan byl použit k syntéze polymerního proléčiva isoniazidu (INH), důležitého antituberkulotika, pro prodloužení doby působení. Díky své rozpustnosti ve vodě se může podávat intravenózně. Kondenzace s INH vyžadovala dvoustupňovou syntézu. Nejprve byla provedena funkcionalizace chitosanu kyselinou fosforitou a částečná formylace volných aminoskupin. Isoniazid byl substituován sukcinanhydridem na sukcinyl isoniazid, který pak reakcí s chitosanem poskytl chitosan-isoniazid-hemisukcinát (obr. 7, cit.⁴⁵).

Monomerní alginát sodný byl pospojován chloridem vápenatým a poté pokryt chitosanem. Tento materiál se používá k léčbě ran i popálenin. Použití chitosanu při léčbě ran podporuje růst fibroblastů a působí na aktivitu makrofágů, což urychluje léčebný proces⁴⁶. Z dalších léčiv, která byla navázána na tento komplex, lze jmenovat ciprofloxacin⁴⁶, norfloxacin⁴⁷ a gatifloxacin⁴⁸.

Pokud chitosan reaguje s roztokem chloridu zinečnatého, vytváří cheláty s aminoskupinami různým způsobem (obr. 8). Tyto komplexy vykazují široké spektrum antimikrobiální účinnosti, jsou 2–8 krát účinnější než chitosan⁴⁹.

3.2. Protinádorová aktivita

Protinádorová účinnost chitosanu závisí na jeho molekulové hmotnosti, rozpustnosti a obsahu acetylových skupin. Vysokomolekulární chitosan je neúčinný, proto je třeba připravit chitosan o nižší molekulové hmotnosti. Ke štěpení polymerů chitosanu jsou nejčastěji používány přirozené enzymy chitosanasy a chitinasy³. Pro hydrolyzu lze využít i několika dalších levnějších hydrolytických enzymů, např. lysozymu⁵⁰, pektinasy⁵¹, hemicelulasy⁵² a papainu⁵³. Pro přípravu chitosanu rozpustného ve vodě byl použit také *Bacillus amyloliquefaciens* V656 obsahující chitinasu⁵⁴. Získané hexamery vykazovaly protinádorovou aktivitu, inhibovaly růst buněk adenokarcinomu CT26 u myši a indukovaly apoptózu. Hydrolyzáty indukují charakteristickou DNA fragmentaci buněk CT26. Po částečné hydrolyze *N*-acetylovaného chitosanu cellulasou⁵⁵ se změnila krystalová struktura, termostabilita a zvýšila se rozpustnost ve vodě bez změny chemické struktury. Částečně



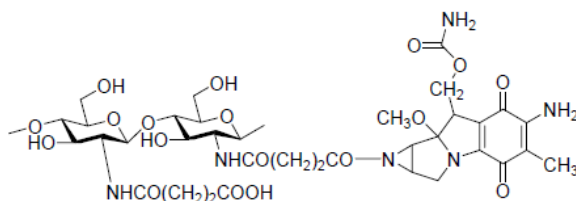
Obr. 9. Chitosan-kamptotecin

acetylovaný nízkomolekulární chitosan, hexamery a heptamery chitosanu a chitoooligosacharidy vykazují protinádorovou účinnost u sarkomu 180 po intraperitoneálním a perorálním podání. Hlavním cílem výzkumu v této oblasti je objasnění vlastností nízkomolekulárních chitosanů, jejich působení na inhibici angiogeneze a indukce apoptózy u Erichova ascitického tumoru u myši. Po intraperitoneální injekci buňky tohoto nádoru ztrácejí v důsledku indukce apoptózy až 90 % kapalné fáze⁵⁶.

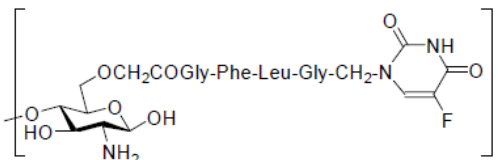
Na buněčné línii 293 a HeLa byly testovány různé poměry chitosanu a pentahydrátu síranu měďnatého (1:1.56, 1:0.8, a 1:0.4). Měďnatý komplex interaguje s DNA, což způsobí rozštěpení DNA a protinádorovou účinnost. Chelatace měďnatých iontů vede k zesílení pozitivního náboje na aminoskupině chitosanu. Komplex inhibuje rozmnožování buněk v S fázi růstového cyklu obou linií. K buňkám linie 293 byl komplex selektivnější než k buňkám HeLa; na normální plicní buněčné línii HLF nepůsobí. Nejvyšší aktivitu vykázal při poměru 1:0,4. Účinnost tedy závisí na koncentraci iontů v komplexu⁵⁷.

Chitosan se používá především jako nosič protinádorové látky na místo účinku. Kamptotecin je alkaloid a protirakovinné léčivo. Je velmi účinný při léčbě nádoru žaludku, tlustého střeva a močového měchýře, jeho nevýhodou je špatná rozpustnost a toxicita. Kamptotecinové alkaloidy blokuje topoisomerasu I, enzym důležitý pro replikaci DNA. Při inhibici topoisomerasy I je zablokováno rozpletení dvojitého vlákna DNA a řetězec DNA se rozpadá. Agregací s *O*-(karboxymethyl)chitosanem (OCMCS) byl připraven biokompatibilní a amfifilní systém pro řízené uvolňování látky v cílové tkáni, (obr. 9, cit.⁵⁸).

Dalším známým léčivem proti leukemii P388, leukemii L1210 a melanomu B16 je mitomycin C. Poškozuje DNA způsobem podobným alkylačním cytostatikům. Jako nosič byl použit *N*-sukcinylochitosan, který je netoxický při koncentraci 2 g kg⁻¹ i.p. a protinádorově neaktivní. Reakcí *N*-sukcinylochitosanu a mitomycinu C za použití vodného karbodiimidu byl připraven konjugát, který není nutné podávat i.p. (obr. 10, cit.^{59,60}).

Obr. 10. Konjugát *N*-sukcinylochitosanu a mitomycinu C

5-Fluoruracil (5FU) patří do skupiny antimetabolitů, který je používán již řadu let. Má však nepříjemné vedlejší účinky. Pro jejich snížení za zachování protinádorové aktivity byl navázán na chitosan přes hexamethylenový můstek a močovinnový zbytek. Konjugát chitosan/močovina/C6/močovina/5FU a chitosan-oligosacharid/močovina/C6/močovina/5FU konjugát vykazovaly silnou inhibiční aktivitu vůči Meth-A fibrosarkomu a MH-134Y hepatomu. Ve vodě rozpustné makromolekuly se do buňky dostávají endocytózou a fagocytózou. Nádorové buňky přijímají více těchto makromolekul. V lysosomech nádorových buněk je přítomno zvýšené množství lysosomové proteasy – kathepsinu B. Bylo zjištěno, že tetrapeptidový spojovací článek Gly-Phe-Leu-Gly umožňuje specifické uvolňování léčiva v lysosomech tímto enzymem, a proto byl 5FU konjugován s částečně acetylovaným *O*-(methoxykarbonyl)chitosanem (obr. 11, cit.⁶¹).

Obr. 11. Konjugát *O*-(karboxymethyl)chitosanu a Gly-Phe-Leu-Gly-5-fluoruracilu

Doxorubicin je antracyklinové protinádorové antibiotikum s širokým spektrem protinádorové aktivity. Působí blokádu enzymu topoisomerasy II, který se podílí na změnách v prostorovém uspořádání DNA při její replikaci před dělením buňky. Při blokáde topoisomerasy II se nespojují jednotlivé části DNA a ta se rozpadá. Pro velmi silné vedlejší účinky (kardiotoxicita), nízkou stabilitu a špatnou rozpustnost ve vodě byl připraven jako několikvrstvé mikrotobolky obsahující chitosan a alginát vázané na (karboxymethyl)celulóse dotované koloidními částicemi uhličitánu vápenatého⁶². Enkapsulace léčiva efektivně indukuje apoptózu HepG2 nádorových buněk.

3.3. Antioxidační aktivita

Antioxidanty jsou látky, které zpomalují nebo brání oxidaci oxidovatelných buněčných substrátů. Zachytávají radikály a ROS (reaktivní kyslíkové species) obsahující reaktivní kyslíkové atomy, zahrnující hydroxylový radikál $\cdot\text{OH}$, superoxidový radikál $\cdot\text{O}_2^-$ a peroxid vodíku H_2O_2 . Tyto radikály jsou velmi nestabilní a reagují rychle s jinými látkami v těle, což vede k poškození buněk a tkání. Antioxidanty působí proti tvorbě volných radikálů a ROS nebo aktivují celou řadu detoxikujících proteinů.

V posledních letech je věnována velká pozornost také antioxidační účinnosti chitosanu. Tato účinnost rovněž závisí na velikosti molekuly a stupni acetylace^{63–65}. Nízkomolekulární, částečně *N*-acetylovaný chitosan rozpustný ve vodě je možné považovat za přírodní antioxidant. I když přesný mechanismus jeho antioxidační účinnosti

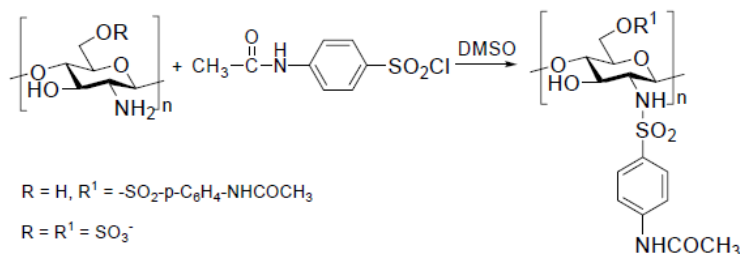


Schéma 6. Sulfatované deriváty chitosanu o molekulové hmotnosti 4000 Da a 20 000 Da

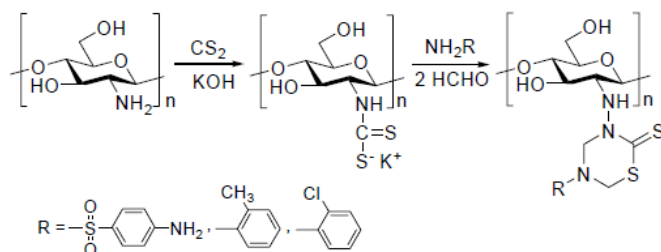


Schéma 7. Příprava 1,3,5-thiadiazin-2-thionových derivátů chitosanu

není znám, předpokládá se, že amino a hydroxyskupiny vázané na C-2, C-3 a C-6 pyranosového cyklu reagují s radikály za tvorby stabilnějších polymerních radikálů. Účinnost pravděpodobně souvisí s chelatačními vlastnostmi chitosanu, které vedou ke zpomalení oxidace lipidů⁶⁶. Chitosan inhibuje peroxidaci linolenové kyseliny, vykazuje vysokou aktivitu vůči hydroxylovým radikálům (83,7 %, cit.⁶⁷).

Xing a spol.⁶⁸ publikovali antioxidační aktivitu různých druhů sulfatovaných chitosanů při reakci s radikály. Byly připraveny sulfáty a sulfanilamidové deriváty chitosanu o různých molekulových hmotnostech (schéma 6). Výsledky ukázaly, že zavedení sulfanilamidové skupiny zvyšuje nejenom rozpustnost, ale i antioxidační aktivitu⁶⁹.

Glutathion jako známý přírodní antioxidační peptid obsahující síru inspiroval přípravu celé řady sirmých obměn. Do chitosanu byly zavedeny 1,3,5-thiadiazin-2-

-thionové deriváty obsahující dva typy síry s potenciální antioxidační aktivitou⁷⁰ (schéma 7).

Eugenol (4-allyl-2-methoxy-fenol) byl zabudován do molekuly chitosanu (schéma 8), aby zvýšil jeho antioxidační účinnost svými fenolickými hydroxyskupinami. Zavedením objemného substituentu se snížila citlivost na pH a zvýšila se inhibice iniciace a propagace oxidačních řetězových reakcí⁷¹.

Částečně kvartemizované deriváty chitosanu s kyselinou gallovou vykazovaly účinnost proti superoxidům⁷². Superoxidový anion $\cdot O_2^-$ vzniká téměř ve všech buňkách a je hlavní příčinou toxicity kyslíku. V porovnání s ostatními kyslíkovými radikály má superoxidový radikál dlouhou životnost a je tedy mnohem nebezpečnější.

Stejně jako u antibakteriálně účinných derivátů chitosanu byla kvůli zvýšení antioxidační účinnosti aminoskupina chitosanu alkylována ethylem, 2-(dimethylamino)

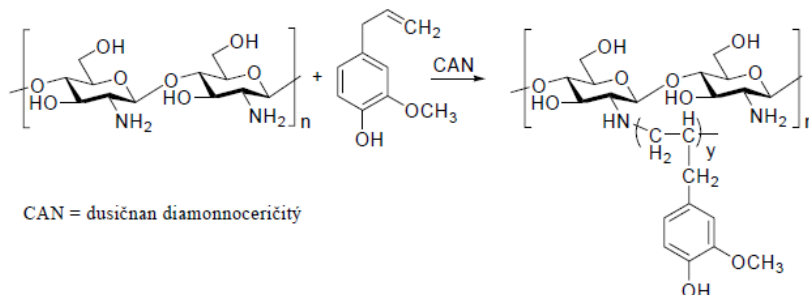


Schéma 8. Eugenolový polymer chitosanu

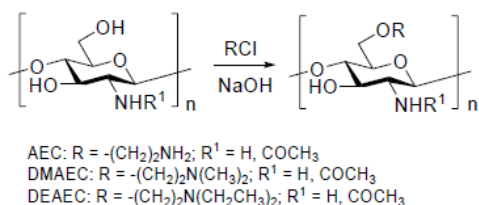


Schéma 9. Alkylace chitosanu

ethylem a 2-(diethylamino)ethylem⁷³. Antioxidační účinnost závisí na stupni deacetylace chitinu a typu substituce. Nejúčinnější lapač ROS volných radikálů se ukázal AEC90, což je 90% deacetylovaný N-aminoethylovaný chitosan mající nejvyšší procento volných aminoskupin (schéma 9).

5-Chlor-2-hydroxybenzaldehyd a 2-hydroxy-5-nitrobenzaldehyd byly použity pro přípravu Schiffových bází s aminoskupinami chitosanu a (karboxymethyl)chitosanu (schéma 10, cit.⁷⁴). Přestože byla do molekuly vnesena fenolická hydroxyskupina, antioxidační účinnost vůči superoxidovému a hydroxylovému radikálu se nezvýšila. Z toho vyplývá, že pro tuto účinnost je nezbytná především volná aminoskupina, i když hydroxyskupiny u předchozích derivátů působily stimulačně.

4. Závěr

Chitosan vykazuje celou řadu biologických aktivit. Podle narůstajícího počtu publikací v posledních letech lze usuzovat, že jde o velice perspektivní polykationtový polysacharid s širokým potenciálem využití v nejrůznějších aplikacích. V oblasti farmacie je jeho budoucnost především v roli biodegradabilního nosiče léčiv různých farmakologických skupin s možností jejich modifikace pro cílovou tkáň, odstranění některých nežádoucích vlastností léčiva a zvýšení biodostupnosti léčiva.

Tato práce byla podpořena projekty MSM 0021620822 a GAUK 76807/2007.

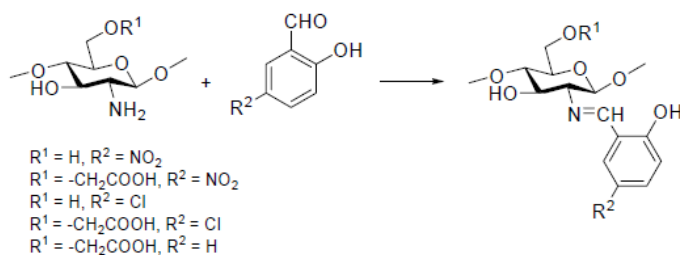


Schéma 10. Příprava Schiffových bází

LITERATURA

1. Tokuyasu K., Ohnishi-Kameyama M., Hayashi K.: *Biosci., Biotechnol., Biochem.* **60**, 1598 (1996).
2. Hu K. J., Hu J. L., Ho K. P., Yeung K. W.: *Carbohydr. Polym.* **58**, 45 (2004).
3. Uraganu T., Tokata S. (ed.): *Material Science of Chitin and Chitosan*. Springer, New York 2006.
4. Vinšová J., Vavříková E.: *Chem. Listy* **101**, 978 (2007).
5. Koide S. S.: *Nutr. Res. (N. Y.)* **18**, 1091 (1998).
6. Clark G. L., Smith A. F.: *J. Phys. Chem.* **40**, 863 (1937).
7. Okuyama K., Noguchi K., Miyazawa T., Yui T., Ogawa K.: *Macromolecules* **30**, 5849 (1997).
8. Yui T., Imada K., Okuyama K., Obata Y., Suzuki K., Ogawa K.: *Macromolecules* **27**, 7601 (1994).
9. Chun H. K., Jang W. C., Heung J. C., Kyu S. C.: *Polym. Bull.* **38**, 387 (1997).
10. Fernandez-Saizn P., Ocio M. J., Lagaron J. M.: *Biopolymers* **83**, 577 (2006).
11. Tsai G. J., Su W. H.: *J. Food Prot.* **62**, 239 (1999).
12. Liu H., Du Y., Wang X., Sun L.: *Int. J. Food Microbiol.* **95**, 147 (2004).
13. Chen Y. L., Chou C. C.: *Food Microbiol.* **22**, 29 (2005).
14. Helander I. M., Nurmiaho-Lassila E. L., Ahvenainen R., Rhoades J., Roller, S.: *Int. J. Food Microbiol.* **71**, 235 (2001).
15. Zheng L. Y., Zhu J. F.: *Carbohydr. Polym.* **54**, 527 (2003).
16. Jia G., Wang H. L., Wu J. C. G., Lin J. G.: *Acta Pharmacol. Sin.* **27**, 932 (2004).
17. Liu N., Chen X. G., Park H. J., Liu C. G., Liu C. S., Meng X. H., Yu L. J.: *Carbohydr. Polym.* **64**, 60 (2006).
18. Tokura S., Ueno K.: *Macromol. Symp.* **120**, 1 (1997).
19. Yang T. C., Chou C. C., Li C. F.: *Int. J. Food Microbiol.* **97**, 237 (2005).
20. No H. K., Park N. Y., Lee S. H., Meyers S. P.: *Int. J. Food Microbiol.* **74**, 65 (2002).
21. Chung Y. C., Kuo C. L., Chen C. C.: *Bioresour. Technol.* **96**, 1473 (2005).

22. Jia Z., Shen D., Xu W. *Carbohydr. Res.* 333, 1 (2001).
23. Xie W., Xu P., Wang W., Liu Q.: *Carbohydr. Polym.* 50, 35 (2002).
24. Muzzarelli R., Tarsi R., Filippini O., Giovanetti E., Biagini G., Varaldo P. E.: *Antimicrob. Agents Chemother.* 34, 2019 (1990).
25. Liu X. F., Guan Y. L., Yang D. Z., Li Z., Yao K. D.: *J. Appl. Polym. Sci.* 79, 1324 (2001).
26. Wang L. C., Chen X. G., Zhoni D. Y., Xu Q. C.: *J. Mater. Sci.: Mater. Med.* 18, 1125 (2007).
27. Jayakumar R., Nwe N., Tokura S., Tamura H.: *Int. J. Biol. Macromol.* 40, 175 (2007).
28. Huang R., Du Y., Zheng L., Liu H., Fan L.: *React. Funct. Polym.* 59, 41 (2004).
29. Kurita K., Kojima T., Nishiyama Y., Shimojoh M.: *Macromolecules* 33, 4711 (2000).
30. Guo Z., Xing R., Liu S., Zhong Z., Ji X., Wang L., Li P.: *Carbohydr. Res.* 342, 1329 (2007).
31. Runarsson O. V., Holappa J., Nevalainen T., Hjalmarsson M., Jarvinen T., Loftsson T., Einarsson J. M., Jonsdottir J., Valdimarsdottir M., Massona M.: *Eur. Polym. J.* 43, 2660 (2007).
32. Avadi M. R., Sadeghi A. M. M., Tahzibi A., Bayati Kh., Pouladzadeh M., Zohuriaan-Mehr M. J., Rafiee-Tehrani M.: *Eur. Polym. J.* 40, 1355 (2004).
33. Chi W., Qin C., Zeng L., Li W., Wang W.: *J. Appl. Polym. Sci.* 103, 3851 (2007).
34. Xie Y., Liu X., Chen Q.: *Carbohydr. Polym.* 69, 142 (2007).
35. Saravanan S., Selvan P. S., Gopal N., Gupta J. K., De B.: *Arch. Pharm.* 338, 488 (2005).
36. Caner H., Yilmaz E., Yilmaz O.: *Carbohydr. Polym.* 69, 318 (2007).
37. Hu Y., Du Y., Yang J., Kennedy J. F., Wang X., Wang L.: *Carbohydr. Polym.* 67, 66 (2007).
38. Mi F. L., Yu S. H., Peng C. K., Sung H. W., Shyu S. S., Liang H. F., Huang M. F., Wang C. C.: *Polymer* 47, 4348 (2006).
39. Yang T. C., Chou C. C., Li C. F.: *Int. J. Food Microbiol.* 97, 237 (2005).
40. Tikhonov V. E., Stepnova E. A., Babak V. G., Yamskov I. A., Palma-Guerrero J., Jansson H. B., Lopez-Llorca L. V., Salinas J., Gerasimenko D. V., Avdienko I. D., Varlamov V. P.: *Carbohydr. Polym.* 64, 66 (2006).
41. Kang H. Y., Jung M. J., Jeong Y. K.: *Korean J. Biotechnol. Bioeng.* 15, 521 (2000).
42. Chen S., Wu G., Zeng H.: *Carbohydr. Polym.* 60, 33 (2005).
43. Krysteva M., Todorova N. P., Maneva K., Todorov D., Dimnitrov C.: *Biotechnol. Biotechnol. Equip.* 14, 178 (1999).
44. Ishak R. A. H., Awad G. A. S., Mortada N. D., Nour S. A. K.: *J. Controlled Release* 119, 207 (2007).
45. Rando D. G., Brandt C. A., Ferreira E. I.: *Braz. J. Pharm. Sci.* 40, 335 (2004).
46. Ozturk E., Agalar C., Kececi K., Denkbaz E. B.: *J. Appl. Polym. Sci.* 101, 1602 (2006).
47. Denkbaz E. B., Ozturk E., Ozdemir N., Kececi K., Agalar C.: *J. Biomater. Appl.* 18, 291 (2004).
48. Zhu A., Jin W., Juan L., Yang G., Yu H., Wu H.: *Carbohydr. Polym.* 68, 693 (2007).
49. Wang X., Du Y., Liu H.: *Carbohydr. Polym.* 56, 21 (2004).
50. Varum K. M., Holme H. K., Izume M., Stokke B. T., Smidsrod X.: *Biochim. Biophys. Acta* 1291, 5 (1996).
51. Shin-ya Y., Lee M. Y., Hinode H., Kajiuchi T.: *Biochem. Eng. J.* 7, 85 (2001).
52. Qin C., Du Y., Xiao L., Li Z., Gao X.: *Int. J. Biol. Macromol.* 31, 111 (2002).
53. Pantaleone D., Yalpani M., Scollar M.: *Carbohydr. Res.* 237, 325 (1992).
54. Liang T. W., Chen Y. J., Yen Y. H., Wang S. L.: *Process Biochem.* 42, 527 (2007).
55. Qin C., Zhou B., Zeng L., Zhang Z., Liu Y., Du Y., Xiao L.: *Food Chem.* 84, 107 (2004).
56. Prashanth K. V. H., Tharanathan R. N.: *Biochim. Biophys. Acta* 1722, 22 (2005).
57. Zheng Y., Yi Y., Qi Y., Wang Y., Zhang W., Du M.: *Bioorg. Med. Chem. Lett.* 16, 4127 (2006).
58. Aiping Z., Jianhong L., Wenhui Y.: *Carbohydr. Polym.* 63, 89 (2006).
59. Song Y., Onishi H., Machida Y., Nagai T.: *J. Controlled Release* 42, 93 (1996).
60. Song Y., Onishi H., Nagai T.: *Int. J. Pharm.* 98, 121 (1998).
61. Ouch T., Tada M., Ohya Y., Hasegawa K., Arai Y., Kadowaki K., Akao S., Matsumoto T., Suzuki S., Suzuki M.: *React. Funct. Polym.* 37, 235 (1998).
62. Zhao Q., Han B., Wang Z., Gao C., Peng C., Shen J.: *Nanomedicine NBM* 3, 63 (2007).
63. Kim K. W., Thomas R. L.: *Food Sci.* 101, 308 (2007).
64. Chien P. J., Sheu F., Juany W. T., Su M. S.: *Food Chem.* 102, 1192 (2007).
65. Koryagin A. S., Erofeeva E. A., Yakimovich N. O., Aleksandrova E. A., Smirnova L. A., Malkov A. V.: *Pharmacol. Toxicol.* 142, 444 (2006).
66. Peng C., Wang Y., Tang Y.: *J. Appl. Polym. Sci.* 70, 501 (1998).
67. Feng T., Du Y., Wei Y., Yao P.: *Eur. Food Res. Technol.* 225, 133 (2007).
68. Xing R. E., Yu H. H., Liu S., Zhang W. W., Zhang Q. B., Li Z. E., Li P. C.: *Bioorg. Med. Chem.* 13, 1387 (2005).
69. Zhong Z., Ji X., Xing R., Liu S., Guo Z., Chen X., Li P.: *Bioorg. Med. Chem.* 15, 3775 (2007).
70. Ji X., Zhong Z., Chen X., Xing R., Liu S., Wang L., Li P.: *Bioorg. Med. Chem. Lett.* 17, 4275 (2007).
71. Jung B. O., Chung S. J., Lee S. B.: *J. Appl. Polym. Sci.* 99, 3500 (2006).
72. Sun T., Xie W., Xu P.: *Carbohydr. Polym.* 58, 379 (2004).
73. Je J. Y., Kim S. K.: *Bioorg. Med. Chem.* 14, 5989 (2006).
74. Guo Z., Xing R., Liu S., Yu H., Wang P., Li C., Li P.: *Bioorg. Med. Chem. Lett.* 15, 4600 (2005).

E. Vavříková and J. Vinšová (*Department of Inorganic and Organic Chemistry, Faculty of Pharmacy, Charles University, Hradec Králové*): **Chitosan and Its Pharmaceutical Applications**

Chitosan is a prospective cationic polysaccharide which shows a number of functions in many fields, including biomedical, pharmaceutical, preservation, microbial

and others. In this review, we have summarized three main areas of its biomedical applications due to its antimicrobial, anticancer, and antioxidant effects. The applications are influenced by a number of factors such as its polymerization degree, the degree of chitin deacetylation and some other physicochemical properties. The biodegradable, non-toxic and non-allergenic nature of chitosan suggests its use as a carrier in drug delivery systems.

Děkan přírodovědecké fakulty UK vypisuje konkurs na přijetí do doktorského studia

v následujících oborech:

analytická chemie, anorganická chemie, biochemie, fyzikální chemie, makromolekulární chemie, modelování chemických vlastností nano- a biostruktur, organická chemie a vzdělávání v chemii.

Studium bude zahájeno 1. 10. 2009. Podmínkou přijetí je absolvování VŠ ve shodném nebo blízkém studijním oboru. Přihlášky a podrobné informace jsou na adrese: PřF UK, oddělení doktorského studia, Albertov 6, 128 43 Praha 2, tel.. 221951162, 221951163. Přihlášky se přijímají do 30. 4. 2009.

Paper III

Cytotoxicity decreasing effect and antimycobacterial activity of chitosan conjugated with antituberculosic drugs

Eva Vavříková^a, Jana Mandíková^b, František Trejtnar^b, Kata Horváti^c, Szilvia Bösze^c, Jiřina Stolaříková^d and Jarmila Vinšová^{a*}

^a Charles University, Faculty of Pharmacy, Department of Inorganic and Organic Chemistry, Heyrovského 1203, 500 05 Hradec Králové, Czech Republic.

^b Charles University, Faculty of Pharmacy, Department of Pharmacology and Toxicology, Heyrovského 1203, 500 05 Hradec Králové, Czech Republic.

^c Eötvös Lóránd University, Research Group of Peptide Chemistry, Hungarian Academy of Science, Pázmány Péter Sétány 1/A, Budapest, H-1117, Hungary.

^d Laboratory for TBC, Regional Institute of Public Health in Ostrava, Partyzánské nám. 7, 702 00 Ostrava, Czech Republic.

*Corresponding author. Tel.: +420 495067343; fax: +420 495067166. E-mail address: vinsova@faf.cuni.cz (J. Vinšová)

Keywords:

Chitosan, isoniazid, pyrazinamide, ethionamide, in vitro antimycobacterial activity, cytotoxicity

Abstract

Water-soluble chitosan conjugates were prepared by connection with isoniazid, pyrazinamide and ethionamide across the *O*-carboxymethyl and *N*-succinyl bridge followed by phosphorylation. Their structures were characterized by FTIR and ¹H NMR spectroscopy. Degree of drug substitution and molecular weight of prepared compounds have been investigated. Antimycobacterial activity was determined against *Mycobacterium tuberculosis* and three non-tuberculosis strains. Chitosan derivatives showed significant MIC 125 µg/mL against all tested strains which can be explained by contribution of the presence of antituberculosic drugs and original structure of chitosan. Cytotoxicity of prepared compounds was evaluated in human liver cell line Hep G2 and human peripheral blood mononuclear cells

(PBMC). Toxicity of antituberculosic drugs on Hep G2 cells were compensated by connection with chitosan and tested compounds have not exhibited significant cytotoxic effect on PBMC cells. Chitosan conjugates with antituberculosic drugs could be potentially effective in the non-toxic chemotherapy of tuberculosis.

1. Introduction

Chitosan is known as a biological active polymer having many interesting properties, low toxicity, biocompatibility, biodegradability and low cost (Uraganu & Tokata, 2006; Vinsova & Vavrikova, 2008). Chitosan is a linear polysaccharide, derived from naturally abundant chitin, composed from D-glucosamine and *N*-acetyl-D-glucosamine units bonded by β -1,4-glycosidic linkages. Degree of deacetylation of commercially prepared chitosan is usually in the range between 60 – 100 % and has influence on the solubility, swelling index, wound dressing and antimicrobial properties (Qin et al., 2008). Potential pharmaceutical applications of chitosan seem to be promising. It is used as a carrier material in various drug delivery systems with a broad range of therapeutic application (Dodane & Vilivalam, 1998). The properties of chitosan make it a versatile excipient not only for controlled release applications but also as a bioadhesive polymer. Chitosan can act as a prodrug for targeting therapy composed of a polymer carrier, biodegradable covalent linkage and therapeutic agent. Targeting delivery of drugs improves their therapeutic efficacy and minimizes side effects. (Vinsova & Vavrikova, 2008)

Chitosan alone is completely soluble in both organic and inorganic acidic solutions at pH less than 6.5 due to the presence of free amino groups. Chemical modifications of chitosan molecule can also improve water solubility. Thus, an implementation of hydrophilic groups to the molecule of chitosan or quarterisation of amino group of chitosan is the most widely used. For introduction of carboxylic group there is very useful *O*-carboxymethylation or *N*-succinylation. Water solubility of *O*-carboxymethyl chitosan (OCMC) depends on reaction conditions of carboxymethylation, especially on reaction temperature and ratio of water/propan-2-ol as the reaction solvent (Chen & Park, 2003). In an attempt to improve antimicrobial activity of chitosan, OCMC was further quarternized. Quarternized carboxymethyl chitosan exhibited stronger antimicrobial activity against Gram-negative *Escherichia coli* and Gram-positive *Staphylococcus aureus*. (Sun et al., 2006) Graft copolymerization of poly(*N*-vinyl imidazole) onto carboxymethylchitosan has improved its antimicrobial activity (Sabaa et al., 2010). An inhibition effect of OCMC against fungal plant

pathogens was presented (Zhong et al., 2009) and against *C. albicans*, *C. krusei* and *C. glabrata* (Seyfarth et al., 2008) was documented also. In both cases, there was observed that antifungal activity depends on the size of molecule and polycationic character which is probably crucial for antifungal activity.

N-succinyl chitosan (NSCS) is well known as a drug carrier with a long circulating effect in the body (Kato et al., 2000). When the degree of acetylation is low (10%), it is completely soluble in water. Moreover, recently *N*-succinyl chitosan became a main component of micelles or nanoparticles used for delivery system. Sui et al. (2008) reported synthesis of *N*-succinyl chitosan with 2-(butoxymethyl)oxirane which decreased the surface tension and forms amphiphilic aggregates. Other study presented self-assembly formation of *N*-succinyl chitosan nanospheres in distilled water. Chitosan based drug matrix has a great potential in drug controlled release delivery. Hydrophobic domain as acetyl groups and glycosidic rings formed inside nanospheres which offer possibility for loading not only hydrophilic drugs but also hydrophobic drugs (Zhu et al., 2006). A work flowing from the previous experiment deals with the encapsulation of bovine serum albumin into nanoparticles of *N*-succinyl chitosan in molar ratio 30:1 by TEM technique (Zhu et al., 2007). Hence, these particles have a great potential to be used in controlled release delivery. Main utilisation of *N*-succinyl chitosan is in cancer therapy. A conjugate of mitomycin C (MMC) and *N*-succinyl chitosan exhibited good antitumor activities against various tumours (Kato et al., 2004). The conjugate had strong inhibition effect against the growing of a solid tumor Sarcoma 180 and MMC was gradually released over one week (Song et al., 1996). Lactosaminated *N*-succinyl-chitosan-mitomycin was examined against liver metastases of M5076 cells in the early and advanced stages. Lactosaminated part of molecule showed high accumulation in the liver and the conjugate functioned effectively in the early metastatic stage (Kato et al., 2001).

Tuberculosis (TB) is leading infection disease and serious world health problem due to which 1.3 million people died in 2008 (Global tuberculosis control, 2009). First line antituberculous drugs (isoniazid (INH), pyrazinamide (PZA), ethambutol, rifampicin (RIF), streptomycin) are used in combinations during the treatment of TB, administered daily or intermittently for several months to patients. Current anti-tuberculosis drugs INH, RIF and PZA are potentially hepatotoxic drugs. They are metabolized and detoxified in the liver. Toxic metabolites develop drug-induced hepatotoxicity (DIH). Antituberculosis drug-induced hepatotoxicity can be fatal when is not recognized at an early stage, after which the therapy should be

interrupted. Development of DIH depends on main risk factors as age, sex, ethnic, acetylator phenotype and HIV infection (Sharma, 2004). Twenty-four hours of application of INH in concentrations > 26 mM led to a remarkable number of apoptotic cells positive for Annexin V (Schwab & Tuschl, 2003). Hydrazine, the metabolite of INH formed by amidase-catalysed hydrolysis, causes significant production of endogenous hydrogen peroxide which initiates processes of hydroxyl radicals formation, that results in lysosomal damage and development of inflammation (Tafazoli et al., 2008). Incidence of drugs combination can have synergic hepatotoxic effect. It was proved that the *in vitro* hepatotoxicity of PZA is increased by pre-treatment of cells with INH (Tostmann et al., 2008). On the other hand, INH is able to increase activity of CYP2E1, the enzyme responsible for metabolism of xenobiotics to production of free radicals. Simultaneously, INH decreases activities of glutathione S-transferases (GSTs) function responsible for the protection of cytoplasm against free radicals, but RIF normalizes the production of ROS by CYP2E1 and GSTs. It indicates that RIF has antagonistic effect (Yue et al., 2009). Shantosh et al. (2006) presented that oral administration of RIF and INH significantly changed levels of diagnostic markers in serum and liver of rats. Co-administration of chitosan had a tendency to prevent antitubercular drug-induced hepatotoxicity in rats. The hepatoprotective effect of chitosan is probably due to a counteraction against free radicals by its antioxidant nature and/or to its ability to inhibit lipid accumulation due to its antilipidemic properties (Santhosh et al., 2007).

Mostly, treatment of TB is based on the cellular immunity and chemotherapy. Protective immune response involves a phagocytosis of *Mycobacterium tuberculosis* by macrophages which are activated by antigen-specific T cells (Cooper & Flynn, 1995). Chemotherapy kills the majority of bacteria during few days, but subpopulation in stationary phase could persist in aerobic or anaerobic sites (Rook et al., 2001). Therefore, administration of antituberculous drugs must be continued for at least 6 months. During this time immune cell system should protect body of patient. It is essential to find out if used drugs are not toxic for cells which play important role in immune response. PBMC are a preparation of blood cells which contains macrophages, monocytes and lymphocytes as an experimental model, PBMC may be used for this purpose.

In the current investigation, we have bonded first or second line antituberculous such as INH, PZA, ethionamide (ETA) on chitosan as a carrier through the short linkage by carboxymethyl group or succinyl-bridge with assumption of its hepatoprotective activity. The

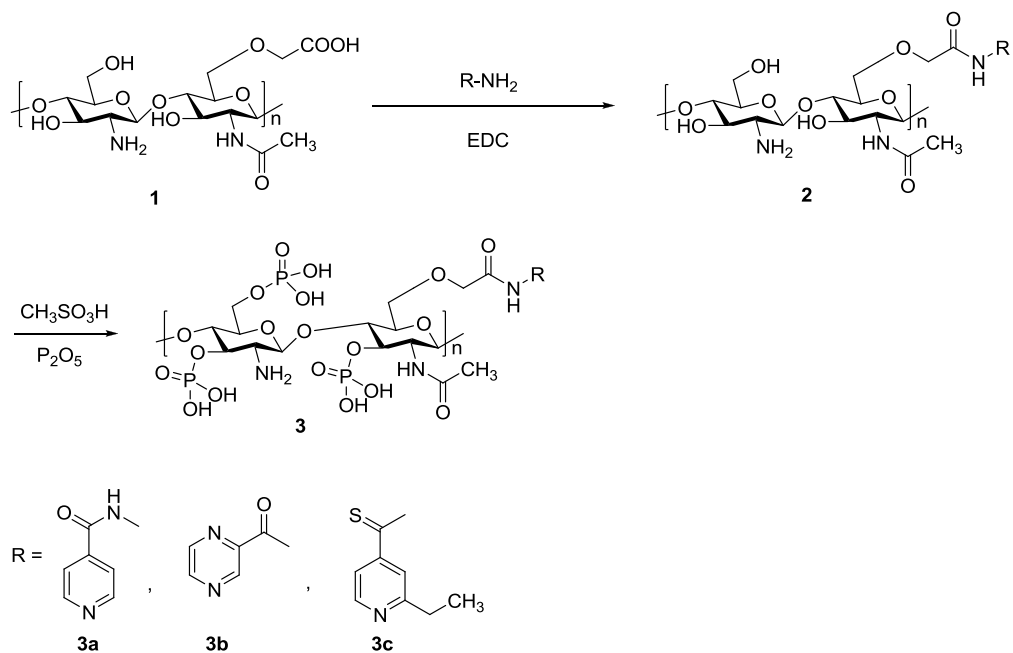
water solubility of prepared conjugates was increased by phosphorylation. Synthesis, characterization of derivatives, determination of antimycobacterial activity and evaluation of cytotoxicity are reported.

2. Experimental

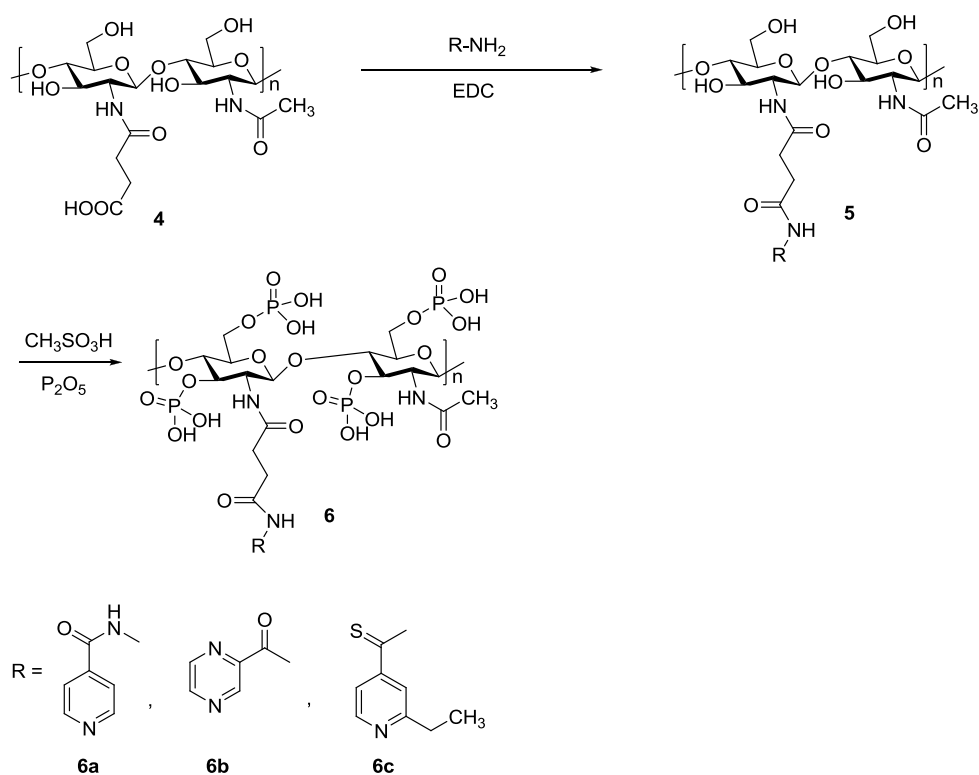
2.1 Synthesis

Two main approaches were used. First type of reaction was based on the formation of *O*-carboxymethylated chitosan (OCMC) **1**. The first step was the preparation of an intermediate product *O*-carboxymethyl chitosan by the reaction of chitosan and chloroacetic acid in propan-2-ol (Fan et al., 2006). The intermediate was precipitated in acetone. The following reaction was based on the linkage of OCMC with antituberculous drug. 500 mg of OCMC (**1**) was dissolved in water and 200 mg of appropriate drug (INH, PZA or ETA) was added. The mixture was cooled to 0-5 °C. The carboxylic group was activated with 220 mg of *N*-(3-dimethylaminopropyl)-*N'*-ethylcarbodiimide (Scheme 1) and the reaction mixture was stirred at 0 - 5 °C for 3 hours, then the temperature was gradually increased to the room temperature. After 24 hours without further isolation 2 ml of methanesulfonic acid and 300 mg of phosphorus pentoxide was added to the mixture (Nishi et al., 1984). The reaction mixture was stirred at 0 - 5 °C for 3 hours. The mixture was cooled overnight in a freezer and then the product **3** was precipitated with acetone.

Succinylation of amino group of chitosan was the second approach to the synthesis. Chitosan reacted with succinyl anhydride in dimethyl sulfoxide (Yan et al., 2006) to produce *N*-succinyl chitosan **4** (Scheme 2). The intermediate was precipitated in acetone. The following reaction was based on the linkage of NSCS with antituberculous drug. 500 mg of NSCS (**4**) was dissolved in water and 200 mg of appropriate drug (INH, PZA or ETA) was added. The mixture was cooled at 0-5 °C. The carboxylic group was activated with 220 mg of *N*-(3-dimethylaminopropyl)-*N'*-ethylcarbodiimide and the reaction mixture was stirred at 0 - 5 °C for 3 hours, then the temperature gradually increased to the room temperature. After 24 hours without isolation 2 ml of methanesulfonic acid and 300 mg of phosphorus pentoxide was added to the mixture. The reaction was stirred at 0 - 5 °C for 3 hours. The mixture was cooled overnight in a freezer and then the product **6** was precipitated with acetone.



Scheme 1. Conjugation of OCMC and antituberculosic drugs



Scheme 2. Conjugation of NSCS and antituberculosic drugs

2.2 Characterization

The chemicals were obtained from Sigma-Aldrich Co. Elemental analyses (C, H, N) were performed with a CHNS-O CE elemental analyzer (Fisons EA 1110). Infrared spectra were recorded on Nicolet Impact 400 IR spectrometer in ATR. NMR spectra were measured in D₂O on a Bruker Avance 300 (300 MHz for ¹H).

2.3 Determination of degree of deacetylation

Degree of deacetylation of chitosan was found out by calculation from ratio C/N of prepared compounds. The formula contains ratio C/N for completely *N*-deacetylated chitosan and for chitin, fully acetylated polymer (Kasaai et al., 2003).

2.4 Determination of molecular weight

Molecular weight (MW) of products was calculated from viscosity measurement. As an aqueous solution system was chosen 0.3 M acetic acid/0.2 M sodium acetate at 25 °C. Stock solutions were prepared from chitosan and prepared compounds **1**, **3a - 3c**, **4**, **6a - 6c**. Ubbelohde viscosimeter with average of capillary 0.64 ± 0.02 mm was used for the measurement.

2.5 Determination of degree of substitution

Degree of drug substitution on prepared compounds **3a - 3c**, **6a - 6c** was determined by UV spectrophotometric technique on the base of calibration curve method. Calibration curve was expressed for each antituberculous drug (INH, PZA, ETA). Degree of substitution was calculated as a percentage of drug from whole polymeric molecule of product.

2.6 Antimycobacterial activity

The prepared chitosan derivatives **1**, **3a - 3c**, **6a - 6c** were tested *in vitro* for antimycobacterial activity in the Laboratory for TBC, Health Institute in Ostrava, against *M. tuberculosis* 331/88 and some non-TB strains such as *M. avium* (330/88) and *M. kansasii* (235/80 and 6509/96). Antimycobacterial activity was measured in Sula's semisynthetic medium (SEVAC, Prague) at 37 °C. The compounds were dissolved in the same medium. The following concentrations were used: 500, 250, 125, 62, 32, 16, 8, 4, 2 and 1 µg/mL. MICs values were determined after incubation at 37 °C for 14 and 21 days, for *M. kansasii* for 7, 14, and 21 days. MIC was the lowest concentration of a substance, at which the inhibition of the growth of mycobacterium occurred.

2.7 *In vitro* cytotoxicity

2.7.1 *In vitro* cytotoxicity in PBMC

Human PBMC (Jurcevic et al., 1996) were cultured in RPMI-1640 medium without phenol red supplemented with 10% FCS, 2 mM of L-glutamine and 160 µg/ml of gentamycin. Cell cultures were maintained at 37 °C, 5% CO₂ in water-saturated atmosphere.

Cells were plated into 96-well plate with initial cell number of 5×10^3 per well (PBMC $1.5\text{--}2.0 \times 10^5$ cells/well). After 24 h incubation at 37 °C prior to the experiment, cells were treated with compounds **1**, **3a**, **3b**, **6a**, **6b** in 100 µL serum free medium overnight. Control cells were treated with serum free medium. Four parallel measurements were performed in all cases.

After overnight incubation at 37 °C, the cell viability was determined by 3-(4,5-dimethylthiazol-2-yl)-2,5-diphenyltetrazolium bromide (MTT)-assay (Slater et al., 1963; Mosmann, 1983). 45 µL MTT-solution (2 mg/mL) was added to each well. The respiratory chain (Slater et al., 1963) and other electron transport systems (Liu et al., 1997) reduce MTT and thereby form non-water-soluble violet formazan crystals within the cell (Altman, 1976). The amount of these crystals can be determined spectrophotometrically and serves as an estimate for the number of mitochondria and hence the number of living cells in the well (Denizot & Lang, 1986). After 4 hrs of incubation; cells were centrifuged for 5 min (2000 rpm) and supernatant was removed. The obtained formazan crystals were dissolved in 50 or 100 µL of DMSO and optical density (OD) of the samples was measured at $\lambda = 540$ and 620 nm using ELISA Reader (iEMS Reader, Labsystems, Finland). OD₆₂₀ values were subtracted from OD₅₄₀ values. The percent of cytotoxicity was calculated using the following equation: Cytotoxicity (%) = $[1 - (\text{OD}_{\text{treated}}/\text{OD}_{\text{control}})] \times 100$; where OD_{treated} and OD_{control} correspond to the optical densities of the treated and the control cells, respectively. In each case two independent experiments were carried out with 4–8 parallel measurements. The 50% inhibitory concentration (IC₅₀) values were determined from the dose-response curves. The curves were defined using Microcal™ Origin1 (version 6.0) software.

2.7.2 *In vitro* cytotoxicity in HepG2 cells

The synthesised compounds **1**, **3a** - **3c**, **4**, **6a** - **6c** were tested on cytotoxicity in human liver cell line Hep G2 (passage 26-28; ECACC, UK). A standard colorimetric method measuring a tetrazolium salt reduction (CellTiter 96 Aqueous One Solution Cell Proliferation Assay,

Promega, USA) was used for evaluation. 10000 cells per well were incubated at 37°C for 3 hours in 5% CO₂ atmosphere. The chitosan derivatives were dissolved in the cell medium without fetal bovine serum. Each compound was tested using six increasing concentrations. The treated cells were incubated together with controls at 37 °C for 24 hours in 5% CO₂ atmosphere. Than solution of MTS (3-(4,5-dimethylthiazol-2-yl)-5-(3-carboxymethoxyphenyl)-2-(4-sulfophenyl)-2H-tetrazolium) was added according to recommendation of the producer of the kit. The tested plate was incubated for 2 hours at 37°C and 5 % CO₂. The quantity of formazan formed in metabolically active cells was measured by the absorbance at 490 nm using a 96-well plate reader. Measured results were statistically evaluated in programs Microsoft Excel 2007 and GraphPad Prism 5.02. The standard cytotoxic parameter IC₅₀ was determined in each tested compound.

3. Results and discussion

3.1 Characterization of prepared compounds

Chitosan and its derivatives were confirmed by FT-IR ATR and ¹H NMR spectroscopy. Infrared spectra of chitosan and carboxymethyl derivateives **1**, **3a** - **3c** are compared in Fig. 1. and infrared spectra of chitosan and succinylated derivatives **4**, **6a** - **6c** are compared in Fig. 2.

Characteristic peaks for origin chitosan were 1650, 1588 and 1319 cm⁻¹ assigned to amides I, II and III. Umbrella vibration of methyl C-H bonds was presented by peak 1374 cm⁻¹. Assymmetrical stretching vibration of the C-O-C bridge was marked by 1149 cm⁻¹ (Chen & Park, 2003). Peak 1023 cm⁻¹ specified C-O secondary hydroxyl group stretch vibration. FTIR spectrum of **1** (OCMC) showed strong peak at 1436 cm⁻¹ which could be assigned to the symmetrical stretching vibration of COO⁻ group (Sabaa et al., 2010). Its asymmetrical stretching vibration occurred at 1558 cm⁻¹. Wide band around 1600 cm⁻¹ and sharp peak at 1506 cm⁻¹ assigned NH₂ group. The C-O absorption peak of the secondary hydroxyl group became weaker and moved to 1068 cm⁻¹. Infrared spectrum of **4** (NSCS) showed 1650 cm⁻¹ as amide I, decreasing of the amide II (1554 cm⁻¹) and increasing of the amide III (1400 cm⁻¹) in comparison with FTIR spectrum of chitosan. Peak 1432 cm⁻¹ indicated COO⁻ group of succinyl bridge.

FTIR spectra of prepared compounds **3a** – **3c** and **6a** - **6c** were similar. Small and wide absorption band between 1652 - 1620 cm⁻¹ indicated amides I. Amide II was occurred at 1570 – 1560 cm⁻¹ in case **6b** and **6c**. Peaks 1432 – 1406 cm⁻¹ assigned symmetrical stretching

vibration of COO^- group, which was in accordance with low degree of substitution of antitubercular drugs. Small peaks at $1248 - 1238 \text{ cm}^{-1}$ showed $\text{P}=\text{O}$ deformation vibration. Secondary amine N-H vibration was presented by absorption band at $1196 - 1184 \text{ cm}^{-1}$. Peaks $1061 - 1050 \text{ cm}^{-1}$ indicated secondary hydroxyl groups in chitosan structure. The sharp peaks at $789 - 786 \text{ cm}^{-1}$ presented deformation vibration of aromatic rings of connected antitubercular drugs.

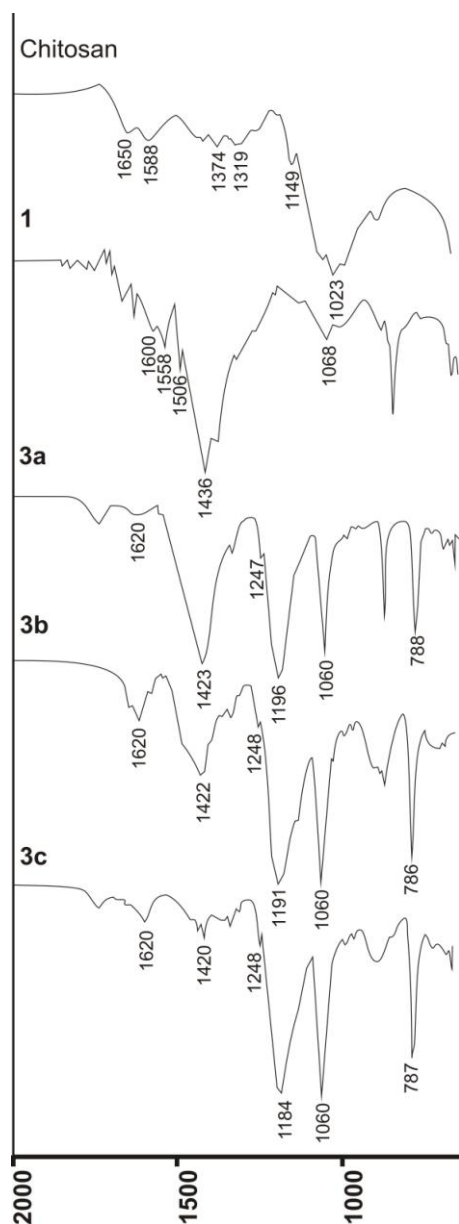


Fig. 1 FTIR spectra of chitosan, **1** and **3a – 3c**

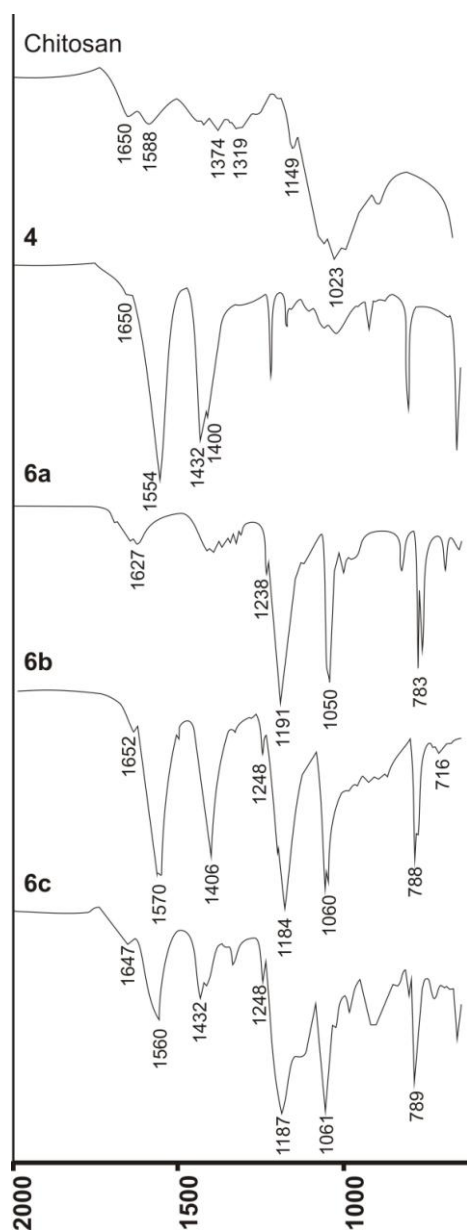


Fig. 2 FTIR spectra of chitosan, **4** and **6a – 6c**

^1H NMR spectrum of chitosan was measured in CF_3COOD and ^1H NMR spectra of **1**, **3a – 3c**, **4**, **6a – 6c** were measured in D_2O . An assignment of chemical shifts for proton of origin chitosan was ascertained in agreement with Kasaai (2010). *N*-acetyl glucosamine unit contained peak of H1 (4.68 ppm) and H2 (2.7 ppm). Glucosamine unit was presented by peaks H1 (4.95 ppm) and H2 (2.22 ppm). The resolution of H3, H4, H5 and H6 protons was low and chemical shifts occurred between 3.8 – 3.4 ppm. Methyl protons of acetyl group resonated at 1.92 ppm and its peak possess the highest resolution. In addition, spectrum of **1** (OCMC) showed a signal of carboxymethyl group at 3.93 ppm. Spectrum of **4** (NSCS)

contained a sharp peak at 2.53 ppm assigned to the methylene protons of succinyl group (Sui et al., 2008).

¹H NMR spectra of prepared products **3a** - **3c** and **6a** - **6c** contained characteristic peaks of chitosan, OCMC and NSCS, in addition, peaks of aromatic parts of molecules and amide bonds. Spectrum of compound **3a** exhibits two doublets at 8.61 and 7.73 ppm corresponded to hydrogens of pyridine ring. Peak at 8.45 ppm corresponded to hydrogens of hydrazide bond. Aromatic part of compound **3b** was characterized by 9.17 and 8.68 ppm of pyrazine ring, peak 8.68 was a multiplet, it corresponded also to amide bond of PZA. Pyridine ring of compound **3c** was characterized by peaks 8.36 and 7.51 ppm. 8.55 ppm corresponded to amide bond of ETA and NSCS.

¹H NMR spectrum of compound **6a** was characterized by 8.60 and 7.73 ppm which presented pyridine ring. Peak 8.36 ppm was multiplet assigned of chemical shift of pyrazine ring of compound **6b**. Compound **6c** had peak of pyridine ring at 6.77 ppm and 8.50 ppm corresponded to amide bond of ETA and NSCS.

3.2 Determination of degree of deacetylation

Elemental analysis of chitosan was measured and degree of acetylation was calculated according the formula based on the ratio carbon and nitrogen. $DA = ((C/N)-5.145)/(6.861-5.145) \times 100$. Number 5.145 corresponds to completely *N*-deacetylated chitosan and 6.861 exhibits fully acetylated chitosan. Resulting degree of deacetylation for origin chitosan is 20.04% which is in accordance with the information of provider.

3.3 Determination of molecular weight

The molecular weight of original chitosan and prepared derivatives were measured using viscosimetry. The Mark – Houwink equation formula was used for calculation of MW, $[\eta] = K \cdot M^a$; $[\eta]$ is intrinsic viscosity, M is molecular weight, K and a are viscometric constants depending on the degree of deacetylation of chitosan. Accordingly to Rinaudo et al. (2003), values for constants are $K = 0.074 \text{ cm}^3 \text{ g}^{-1}$ and $a = 0.76$. Resulting MW are summarized in Fig. 3. Original chitosan had MW 29972 Da but the synthetic procedure resulted in the significant degradation of the polymer backbone. This effect has been previously reported (Holappa et al., 2005; Masson et al., 2008). Prepared compounds **1**, **3a** - **3c**, **4**, **6a** - **6c** exhibited half values of MW.

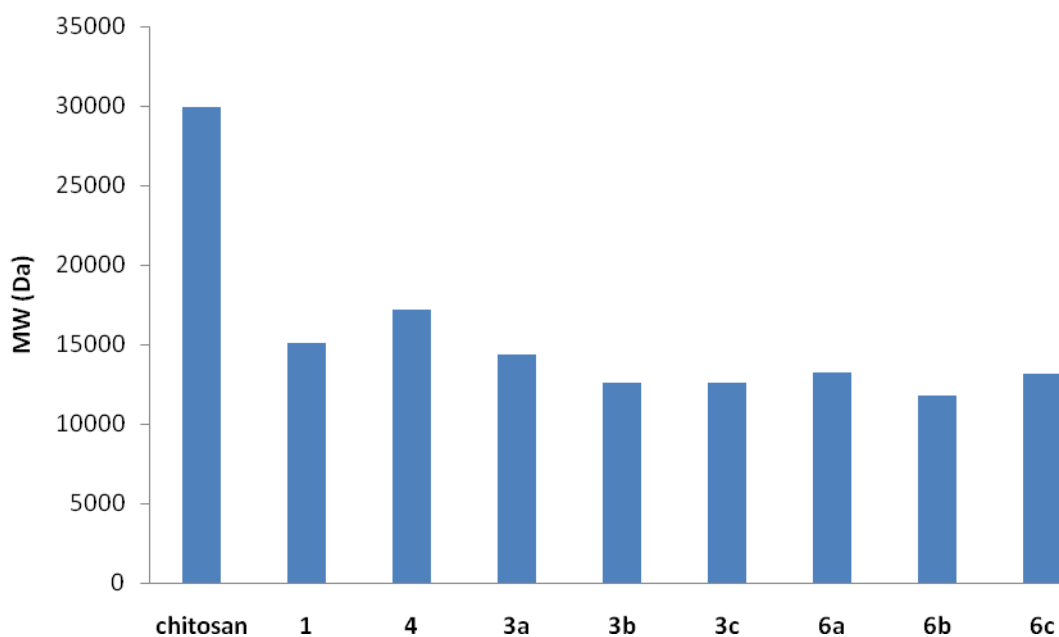


Fig. 3 Molecular weights of chitosan and prepared compounds

3.4 Determination of degree of substitution

Percentage of a content of antituberculosic drugs in molecules of chitosan derivatives **3a** - **3c**, **6a** - **6c** was determined by UV spectrophotometric technique on the base of calibration curve method. Calibration solutions of INH and PZA were dissolved in water, calibration solutions of ETA were dissolved in methanol. Samples of products were dissolved in water. Fig. 4 summarizes degree of substitution of each prepared compound. The highest values of substitution exhibited compounds **3b**, **6a** and **6b**. In general, percentage of a content of antituberculosic drugs was low. It was confirmed by reverse procedure of synthesis because of suspicion of degradation of amid bounds between antituberculosic drugs and **1** or **4** due to low pH during phosphorylation. The phosphorylation was made as the first step and the linkage of antituberculosic drugs was the following reaction. The degree of substitution was also between 0.6 – 1.5 %.

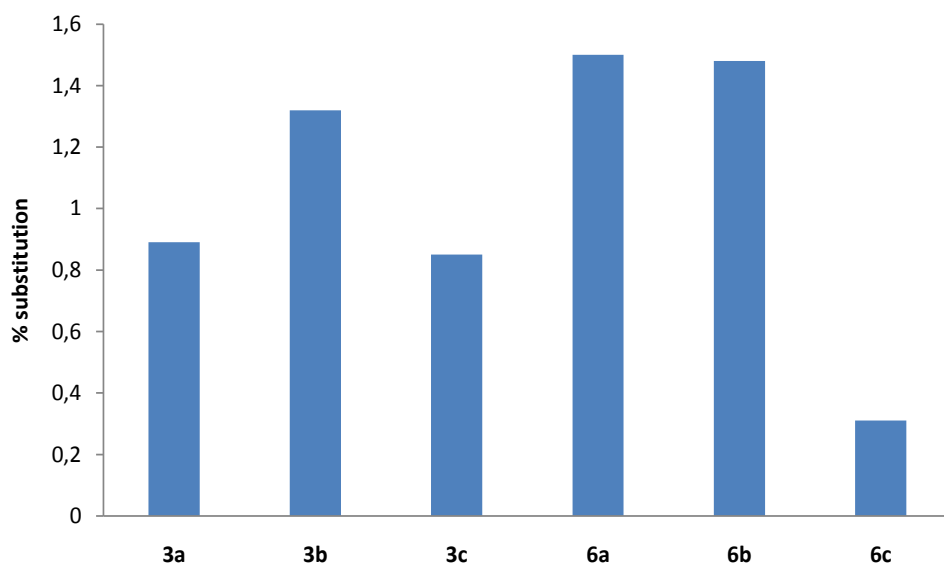


Fig. 4 Degree of substitution of prepared compounds

3.5 Antimycobacterial activity

Table 1 Values of antimycobacterial activity and *in vitro* cytotoxicity

	MIC [$\mu\text{g/mL}$]										[mg/mL]	
	<i>M. tbc</i> 331/88		<i>M. avium</i> 330/88		<i>M. kansasii</i> 235/80			<i>M. kansasii</i> 6509/96			HepG2 IC ₅₀	PBMC IC ₅₀
	14 d	21 d	14 d	21 d	7 d	14 d	21 d	7 d	14 d	21 d		
1	62.5	62.5	31.25	62.5	125	125	125	125	125	125	2.83	> 1.67
4	NT	NT	NT	NT	NT	NT	NT	NT	NT	NT	> 3	NT
3a	125	125	125	125	125	125	125	125	125	125	2.13	> 1.78
3b	125	125	125	125	125	125	125	125	125	125	> 3	> 9.35
3c	125	125	125	125	125	125	125	125	125	125	2.32	NT
6a	125	125	125	125	125	125	125	125	125	125	> 3	> 3.54
6b	125	125	125	125	125	125	125	125	125	125	2.72	> 8.86
6c	125	125	125	125	125	125	125	125	125	125	2.96	NT

NT = not tested

To the best of our knowledge no studies aimed to antimycobacterial activity of chitosan or chitosan derivatives against complex *M. tuberculosis* have not been published yet. The anti-TB screening results in the compounds **1**, **3a** - **3c**, **4**, **6a** - **6c** are summarized in Table 1. Compounds **3a** - **3c** and **6a** - **6c** have the same MIC of 125 µg/mL. Even if, **1** is without substitution of antituberculous drug, its MIC is lower – 62.5 µg/mL (*M. tuberculosis*) and 31.25 and 62.5 µg/mL (*M. avium*). In general, it seems that there are two factors influencing the activity of compounds. Firstly, presence of first or second line antituberculous drugs (INH, PZA, ETA) which is important in the inhibition of mycobacteria. Although, the degree of substitution is not high, products **3a** - **3c** and **6a** - **6c** have exhibited very good antimycobacterial activity. The second factor is probably an antibacterial activity of original chitosan structure which corresponds with the inhibition values against *M. tuberculosis* and *M. avium* of **1** and probably contributes to mycobacterial growth inhibition. The explication of this activity could be high degree of deacetylation of chitosan. It means that the amino group as the active functional group (chelating divalent cations) was found to be essential for the antibacterial activity of chitosan. MIC values of **3a** - **3c** and **6a** - **6c** are equal for all tested strains, this implies that amount of free amino groups in chitosan derivatives should be the same. It means that the degree of substitution of antituberculous drugs was very similar. It is in agreement with the low degree of substitution of linked drugs.

3.6 *In vitro* cytotoxicity

Results of the experiments on cytotoxicity are presented as inhibitory concentration which is necessary to decrease viability of the cell population to 50% from the maximal viability (IC₅₀). A comparison of the found cytotoxic concentrations and MIC values demonstrates that the prepared compounds in concentrations comparable to MICs exert very low toxicity for human hepatocytes and PBMC cells (Table 1).

3.6.1 *In vitro* cytotoxicity in PBMC

Current long duration treatment of TB is among others connected with immune cell system and its protective immune response. Using of antitubercular drugs which are toxic for lymphocytes can be an encumbrance. Resulting values of IC₅₀ PBMC toxicity on chitosan derivatives **1**, **3a**, **3b**, **6a**, **6b** were evaluated between 1.67 – 9.35 mg/mL. However, determined concentrations of prepared compounds were too low; toxicity curves have not

cross values IC_{50} . All tested compounds in examination range of concentrations have not exhibited obvious cytotoxic effect on PBMC cells.

3.6.2 *In vitro* cytotoxicity in HepG2 cells

5 – 10 % prevalence of DIH led us to the idea to prepare conjugates of antibacterial drugs with chitosan as a carrier that has supposed hepatoprotective activity. We have expected that the hepatotoxicity of products should be very low. The results on HepG2 toxicity were in accordance with our hypothesis. Since MW of all tested compounds are very similar, IC_{50} concentrations can be compared on mg/mL basis. IC_{50} values ranged from 2.13 to 2.96 mg/mL. In the cases of **4**, **3b** and **6a**, IC_{50} values were higher than 3 mg/mL. Toxicity curves did not reached values enabling calculation of IC_{50} .

4. Conclusions

Our main goal was to prepare a new carrier for antimycobacterial active drugs having lower hepatotoxic potential than original antituberculosics which could be used as a water-soluble antimycobacterial prodrug with a preventive action against antitubercular drug-induced hepatotoxicity. Thus we have synthesized chitosan derivatives with carboxymethylated and succinylated linkage used for the conjugation of some anti-tuberculosis drugs. For the first time, chitosan and its derivatives were evaluated as potential antimycobacterial agents. The performed tests have demonstrated powerful inhibitory effect against one TB strain and three non-TB strains. It is interesting that the lowest MIC has shown *O*-carboxymethylated chitosan (compound **1**). Toxicity studies showed that chitosan derivatives are toxic only in very high concentrations; both in case of hepatocytes and HepG2 toxicity was more pronounced and IC_{50} values were higher than 2.13 mg/mL. Chitosan and its derivatives may be a promising biomaterial which could be used for compensation of toxicity and for liver protection of hepatocytes during administration of antituberculosic drugs.

Acknowledgements

This work was financially supported by the Research project MSM 0021620822, IGA NS 10367-3, SVV-2010-261-001, by grants from the Hungarian National Science Fund (OTKA 68358) and National Office for Research and Technology (NKFP_07_1-TB_INTER-HU).

References

Altman, F. P. (1976). Tetrazolium salts and formazans. *Progress in Histochemistry and Cytochemistry*, (9, 1-56) Gustav Fischer Verlag, Stuttgart.

Chen, X. G., & Park, H. J. (2003). Chemical characteristics of *O*-carboxymethyl chitosans related on the preparation conditions. *Carbohydrate Polymers*, 53, 355-359.

Cooper, A. M., & Flynn, J. A. (1995). The protective immune response to *Mycobacterium tuberculosis*. *Current Opinion in Immunology*, 7, 512-516.

Denizot, F., & Lang, R. (1986). Rapid colorimetric assay for cell growth and survival: Modifications to the tetrazolium dye procedure giving improved sensitivity and reliability. *Journal of Immunological Methods*, 89, 271-277.

Dodane, V., & Vilivalam, V. D. (1998). Pharmaceutical applications of chitosan. *Pharmaceutical Science & Technology Today*, 1, 246-253.

Fan, L., Du, Y., Zhang, B., Yang, J., Zhou, J., & Kennedy, J. F. (2006). Preparation and properties of alginate/carboxymethyl chitosan blend fibers. *Carbohydrate Polymers*, 65, 447-452.

Global tuberculosis control (2009). WHO Library Cataloguing-in-Publication Data, ISBN 978 92 4 159886 6.

Holappa, J., Nevalainen, T., Soininen, P., Elomaa, M., Safin, R., Måsson, M., & Jarvinen, T. (2005). *N*-Chloroacyl-6-*O*-triphenylmethylchitosans: Useful intermediates for synthetic modifications of chitosan. *Biomacromolecules*, 6, 858-863.

Jurcevic, S., Hills, A., Pasvol, G., Davidson, R. N., Ivanyi, J., & Wilkinson, R. (1996). T cell responses to a mixture of *Mycobacterium tuberculosis* peptides with complementary HLA-DR binding profiles. *Clinical & Experimental Immunology*, 105, 416-421.

Kassai, M. R. (2010). Determination of the degree of *N*-acetylation for chitin and chitosan by various NMR spectroscopy techniques: A review. *Carbohydrate Polymers*, 79, 801-810.

Kasaai, M. R., Charlet, G., Paquin, P., & Arul, J. (2003). Fragmentation of chitosan by microfluidization process. *Innovative Food Science and Emerging Technologies*, 4, 403-413.

Kato, Y., Onishi, H., & Machida, Y. (2000). Evaluation of *N*-succinyl-chitosan as a systemic long-circulating polymer. *Biomaterials*, 21, 1579-1585.

Kato, Y., Onishi, H., & Machida, Y. (2001). Lactosaminated and intact *N*-succinyl-chitosans as drug carriers in liver metastasis. *International Journal of Pharmaceutics*, 226, 93-106.

Kato, Y., Onishi, H., & Machida, Y. (2004). *N*-succinyl- chitosan as a drug carrier: water-insoluble and water-soluble conjugates. *Biomaterials*, 25, 907-915.

Liu, Y. B., Peterson, D. A., Kimura, H., & Schubert, D. J. (1997). Mechanism of cellular 3-(4,5-dimethylthiazol-2-yl)-2,5-diphenyltetrazolium bromide (MTT) reduction. *Journal of Neurochemistry*, 69, 581-593.

Masson, M., Holappa, J., Hjalmsdóttir, M., Rúnarsson, Ö. V., Nevalainen, T., & Järvinen, T. (2008). Antimicrobial activity of piperazine derivatives of chitosan. *Carbohydrate Polymers*, 74, 566-571.

- Mosmann, T. J. (1983). Rapid colorimetric assay for cellular growth and survival: Application to proliferation and cytotoxicity assays. *Journal of Immunological Methods*, 65, 55-63.
- Nishi, N., Nishimura, S. I., Ebina, A., Tsutsumi, A., & Tokura, S. (1984). Preparation and characterization of water-soluble chitin phosphate. *International Journal of Biological Macromolecules*, 6, 53-54.
- Promega Corporation (1996). CellTiter 96® AQueous One Solution Cell Proliferation Assay. *US Patent Office*, Pat. No. 5 185 450.
- Qin, Y. (2008). The preparation and characterization of chitosan wound dressings with different degrees of acetylation. *Journal of Applied Polymer Science*, 107, 993-999.
- Rinaudo, M., Milas, M., & Le Dung, P. (1993). Characterization of chitosan. Influence of ionic strength and degree of acetylation on chain expansion. *International Journal of Biological Macromolecules*, 15, 281-285.
- Rook, G. A. W., Seah, G., & Ustianowski, A. (2001). *M. tuberculosis*: immunology and vaccination. *European Respiratory Journal*, 17, 537-557.
- Sabaa, M. W., Mohamed, N. A., Mohamed, R. R., Khalil, N. M., & Abd El Latif, S. M. (2010). Synthesis, characterisation and antimicrobial activity of poly(*N*-vinyl imidazole) grafted carboxymethyl chitosan. *Carbohydrate Polymer*, 79, 998-1005.
- Santhosh, S., Sini, T. K., Anandan, R., & Mathew, P. T. (2006). Effect of chitosan supplementation on antitubercular drugs-induced hepatotoxicity in rats. *Toxicology*, 219, 53-59.
- Santhosh, S., Sini, T. K., Anandan, R., & Mathew, P. T. (2007). Hepatoprotective activity of chitosan against isoniazid and rifampicin-induced toxicity in experimental rats. *European Journal of Pharmacology*, 572, 69-73.
- Schwab, C. E., & Tuschl, H. (2003). In vitro studies on the toxicity of isoniazid in different cell lines. *Human and Experimental Toxicology*, 22, 607-615.
- Seyfarth, F., Schliemann, S., Elsner, P., & Hipler, U. C. (2008). Antifungal effect of high- and low- molecular weight chitosan hydrochloride, carboxymethyl chitosan, chitosan oligosaccharide and *N*-acetyl-D-glucosamine against *Candida albicans*, *Candida krusei* and *Candida glabrata*. *International Journal of Pharmaceutics*, 353, 139-148.
- Sharma, S. K. (2004). Antituberculosis drugs and hepatotoxicity. *Infection, Genetics and Evolution*, 4, 167-170.
- Slater, T. F., Sawyer, B., & Sträuli, U. (1963). Studies on succinate-tetrazolium reductase systems: III. Points of coupling of four different tetrazolium salts III. Points of coupling of four different tetrazolium salts. *Biochimica et Biophysica Acta*, 77, 383-393.
- Song, Y., Onishi, H., Machida, Y., & Nagai, T. (1996). Drug release and antitumor characteristics of *N*-succinyl-chitosan-mitomycin C as an implant. *Journal of Controlled Release*, 42, 93-100.

Sui, W., Wang, Y., Dong, S., & Chen, Y. (2008). Preparation and properties of an amphiphilic derivative of succinyl-chitosan. *Colloids and Surfaces A: Physicochemical and Engineering Aspects*, 316, 171-175.

Sun, L., Du, Y., Fan, L., Chen, X., & Yang, J. (2006). Preparation, characterisation and antimicrobial activity of quaternized carboxymethyl chitosan and application as pulp-cap. *Polymer*, 47, 1796-1804.

Tafazoli, S., Mashregi, M., & O'Brien, P. J. (2008). Role of hydrazine in isoniazid-induced hepatotoxicity in a hepatocyte inflammation model. *Toxicology and Applied Pharmacology*, 229, 94-101.

Tostmann, A., Boeree, M. J., Peters, W. H. M., Roelofs, H. M. J., Aarnoutse, R. E., van der Ven, A. J. A. M., & Dekhuijzen, R. P. N. (2008). Isoniazid and its toxic metabolite hydrazine induce in vitro pyrazinamide toxicity. *International Journal of Antimicrobial Agents*, 31, 577-580.

Uraganu T., & Tokata S. (2006). *Material Science of Chitin and Chitosan*. (Eds.) New York, Springer.

Vinsova, J., & Vavrikova, E. (2008). Recent advances in drugs and prodrugs design of chitosan. *Current Pharmaceutical Design*, 14, 1311-1326.

Yan, Ch., Chen, D., Gu, J., Hu, H., Zhao, X., & Qiao, M. (2006). Preparation of *N*-succinyl-chitosan and their physical-chemical properties as a novel excipient. *Yakugaku Zasshi*, (The Pharmaceutical Society of Japan), 126, 789-793.

Yue, J., Peng, R., Chen, J., Liu, Y., & Dong, G. (2009). Effect of rifampicin on CYP2E1-dependent hepatotoxicity of isoniazid in rats. *Pharmacological Research*, 59, 112-119.

Zhong, Z., Li, P., Xing, R., & Liu, S. (2009). Antimicrobial activity of hydroxybenzenesulfonanilide derivatives of chitosan, chitosan sulfates and carboxymethyl chitosan. *International Journal of Biological Macromolecules*, 45, 163-168.

Zhu, A., Chen, T., Yuan, L., Wu, H., & Lu, P. (2006). Synthesis and characterization of *N*-succinyl-chitosan and its self-assembly of nanospheres. *Carbohydrate Polymers*, 66, 274-279.

Zhu, A., Yan, L., Chen, T., Wu, H., & Zhao, F. (2007). Interactions between *N*-succinyl-chitosan and bovine serum albumin. *Carbohydrate Polymers*, 69, 363-370.

Paper IV

New fluorine-containing hydrazones as potential antitubercular drugs

Eva Vavříková^{a,b,c}, Slovenko Polanc^b, Marijan Kočevár^b, Kata Horváti^c, Szilvia Bösze^c, Jiřina Stolaříková^d, Kateřina Vávrová^a and Jarmila Vinšová^{a,*}

^a Charles University, Faculty of Pharmacy, Department of Inorganic and Organic Chemistry, Heyrovského 1203, 500 05 Hradec Králové, Czech Republic

^b University of Ljubljana, Faculty of Chemistry and Chemical Technology, Department of Organic Chemistry, Aškerčeva 5, SI-1000 Ljubljana, Slovenia

^c Eötvös Lóránd University, Research Group of Peptide Chemistry, Hungarian Academy of Science, Pázmány Péter Sétány 1/A, Budapest, H-1117, Hungary

^d Institute of Public Health, Centre of Hygienic Laboratories, Partyzánské nám. 7, 702 00 Ostrava, Czech Republic

*Corresponding author. Tel.: +420 495067343; fax: +420 495067166. E-mail address: vinsova@faf.cuni.cz (J. Vinšová)

Keywords:

Tuberculosis, hydrazone, antitubercular drug, *in vitro* activity

Abstract

Several new fluorine-containing hydrazones were synthesized and screened for their *in vitro* antimycobacterial activity. Nine of these derivatives have shown a significant activity against MDR-TB strain with MIC 0.9-1.56 $\mu\text{mol/L}$ and high value of selectivity index (SI). Compound **3h** with the highest SI (1268.58) was used for stability evaluation with putative metabolites (ciprofloxacin and formylciprofloxacin) detection. Compound **3h** was stable at pH 7.4 of aqueous buffer and rat plasma, at acidic buffers (pH 3 and 5) slow decomposition was observed. Interestingly, no formylciprofloxacin was detected in the solution, and only slightly increased concentration of ciprofloxacin was observed instead. Trifluoromethyl hydrazones **3f** and **3g** exhibited the best activity against two strains of *Mycobacterium kansasii* (MIC 1 - 4 $\mu\text{mol/L}$). All evaluated compounds were found to be non-cytotoxic.

1. Introduction

Tuberculosis (TB) is still one of the major causes of bacterial infections and death in the world as 9.4 million incident cases of TB was estimated and 1.8 million of deaths from TB was determined in 2008.¹ These numbers are still alarming, hence, in 2006, WHO developed the Global plan named “The Stop TB Strategy”. Its goal is to reduce dramatically the global burden of TB till 2015 by ensuring all patients. The strategy also supports the development of new and effective tools to prevent, detect and treat TB. Other object is to achieve universal access to high-quality diagnosis and patient-centred treatment or to protect poor and vulnerable populations from TB, TB/HIV and MDR-TB. The main target is an elimination of TB as a public health problem till 2050.²

Modifications of first or second line antituberculous drugs are widely applied.³ A connection of two active parts is one of the possible approaches in the drug design giving a prodrug form.^{4,5} It is well known that the hydrazone group plays an important role for antimicrobial activity.⁶ Substituted carbohydrazone moiety has been found as a good pharmacophore group for many antituberculosis active molecules.^{7,8,9,10} In our previous study we described the possibilities of synergic effect of two components.¹¹ Namely, C₁ fragment that originated from hydrazones was found useful for the formation of C-N bond with the appropriate amines as nucleophiles.¹² It is assumed that the methine bridge as a linker of both parts is gradually hydrolyzed to release active molecule or molecules from their “depot” form. The combined molecule thus serves as a prodrug which can increase bioavailability, passing through the membrane, targeting to the active site and protecting against multidrug-resistance. Involvement of fluoroquinolones as second line antituberculous to the potential active molecule seems to be promising. Antimycobacterial activity of ciprofloxacin (CPX) or norfloxacin (NFX) connected with another active partner was proven as advantageous.⁴ Implementation of the fluorine atom to the molecule was also beneficial as it improves the antimycobacterial activity as well as the lipophilicity.⁶ The benzoic acid analogues of isoniazide was successfully applied to obtain the properly substituted 4,5-dihydro-1*H*-pyrazol-3-yl]-2-methylphenol derivatives showing activity against both susceptible and INH-resistant strains with a MIC value of 0.62 µg/mL.¹³

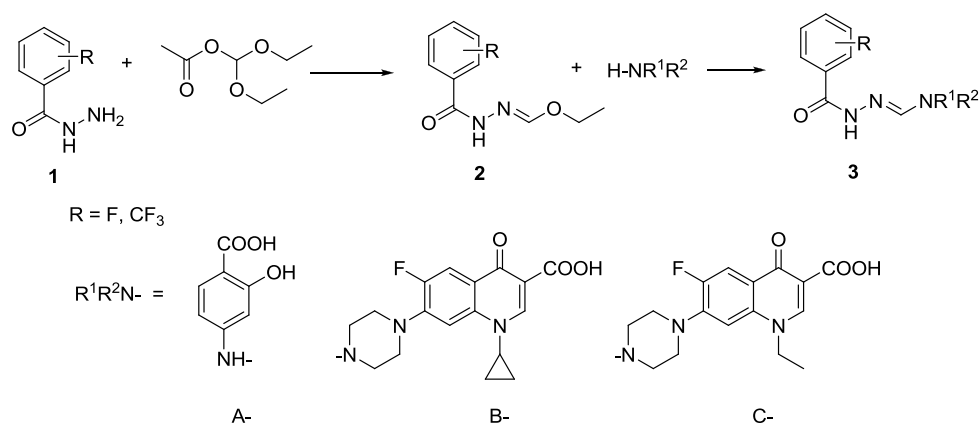
Thus, we have designed and synthesised other new kind of “double” active molecule having fluorinated hydrazone of benzoic acid as an isoniazide isostere, connected by methine linker with the first or second line antituberculous drugs. We expected possible enhanced activity

and slow release in the cell. All compounds were tested on mycobacterial inhibition against one tuberculosis strain *M. tuberculosis*, three non-tuberculosis strains and one MDR-TB strain.

2 Results and discussion

2.1 Chemistry

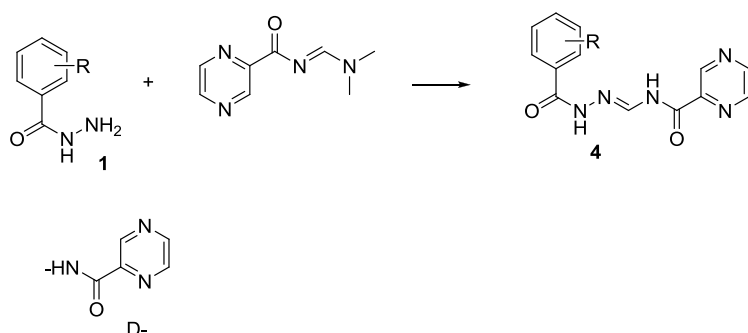
The synthesis of new potential antitubercular drugs involves two steps. The appropriate hydrazide of substituted benzoic acid (**1**) reacted with diethoxymethyl acetate in acetonitrile to give ethyl benzoylhydrazonoformate (**2**). The later was treated with *N*-nucleophile to afford (**3**) (Scheme 1). *p*-Aminosalicylic acid (PAS, A-H), ciprofloxain (CPX, B-H) and norfloxacin (NFX, C-H) were used as *N*-nucleophiles.



Scheme 1 Synthesis of PAS-, CPX- and NFX-derivatives

Isoniazid (INH) is not a suitable *N*-nucleophile for similar reactions as mentioned above. An attempt to substitute the ethoxy group in **2** with INH resulted in a partial transfer of the entire ethoxymethylene group from **2** to INH thus giving a mixture of two hydrazonoformates and two hydrazides.

Slightly different approach was applied for the synthesis of pyrazinecarboxamide (PZA, D-H) derivatives (Scheme 2). The starting carboxamide was first transformed with *N,N*-dimethylformamide dimethyl acetal to *N*-(dimethylaminomethylene)pyrazine-2-carboxamide,³ which reacted with a molecule of the appropriate hydrazide (**1**) to give *N*-(benzoylhydrazonomethyl)pyrazine-2-carboxamide (**4**).



Scheme 2 PZA-derivatives preparation

2.2 Antimycobacterial evaluation

In vitro antimycobacterial activity was evaluated against *Mycobacterium tuberculosis* H₃₇Rv (ATCC:27294), *Mycobacterium kansasii* CNTC My 235/80, *M. kansasii* 6509/96 and *Mycobacterium avium* CNTC 330/88. Minimal inhibitory concentration (MIC) is the lowest concentration of a substance at which the inhibition of the growth of *Mycobacterium* occurs. Compounds **3a-3l** were tested also against MDR-TB strain *Mycobacterium tuberculosis* A8 241 which is resistant to isoniazid and rifampicin (Table 1). MIC of compounds **3f** and **3g** (containing trifluoromethyl group and CPX) was found as the lowest against both strains of *Mycobacterium kansasii* in comparison to the other compounds and the standard INH (Table 2).

Table 1 Evaluation against *M. tbc.* strains

	R	R ¹ R ² N	MIC [μ g/mL]		SI for <i>M. tbc.</i> H ₃₇ Rv	SI for <i>M. tbc.</i>
			<i>M. tbc.</i>	<i>M. tbc.</i>		A8 241
			H ₃₇ Rv ATCC:27294	A8 241 MDR-TB		MDR-TB
3a	4-CF ₃	A	4	0.5	NT	NT
3b	3-CF ₃	A	4	0.5	NT	NT
3c	4-F	A	4	0.5	NT	NT
3d	3-F	A	2	0.5	148.25	592.64
3e	2-F	A	2	0.5	192.06	767.77
3f	4-CF ₃	B	1	0.5	189.21	378.41
3g	3-CF ₃	B	2	0.5	87.79	351.15

3h	4-F	B	1	0.5	634.29	1268.58
3i	3-F	B	1	0.5	402.38	804.76
3j	4-CF ₃	C	5	5	3.98	3.98
3k	4-F	C	NT	NT	NT	NT
3l	3-F	C	6	5	31.67	38
4a	4-CF ₃	D	NT	NT	NT	NT
4b	3-F	D	NT	NT	NT	NT
INH	-	-	0.01	1	NT	NT
CPX	-	-	0.5	NT	NT	NT
NFX	-	-	5	NT	NT	NT

NT – not tested

Table 2 Evaluation against non-tuberculous strains

			MIC [$\mu\text{mol/L}$]							
	R	R ¹ R ² N	<i>M. avium</i>		<i>M. kansasii</i>			<i>M. kansasii</i>		
			330/88		235/80		6509/96			
			14 d	21 d	7 d	14 d	21 d	7 d	14 d	21 d
3a	4-CF ₃	A	32	125	62.5	125	250	62.5	62.5	125
3b	3-CF ₃	A	250	500	32	125	125	62.5	62.5	62.5
3c	4-F	A	32	125	32	62.5	62.5	32	32	32
3d	3-F	A	32	62.5	32	62.5	62.5	32	32	32
3e	2-F	A	32	62.5	32	32	62.5	32	62.5	62.5
3f	4-CF ₃	B	32	62.5	2	2	4	1	1	2
3g	3-CF ₃	B	250	250	2	2	4	1	1	2
3h	4-F	B	62.5	125	4	4	8	8	8	16
3i	3-F	B	125	250	4	4	8	4	4	4
3j	4-CF ₃	C	500	500	2	4	8	2	4	8
3k	4-F	C	125	250	16	32	62.5	32	62.5	62.5
3l	3-F	C	125	250	16	32	62.5	16	16	32
4a	4-CF ₃	D	>1000	>1000	250	250	250	250	500	500
4b	3-F	D	>500	>500	250	250	>500	250	>500	>500
INH	-	-	>250	>250	>250	>250	>250	2	4	4

CPX	-	-	62.5	62,5	1	2	2	1	1	2
NFX	-	-	125	250	8	16	16	2	8	8
PAS	-	-	32	125	125	1000	>1000	32	125	500
PZA	-	-	500	>1000	500	>1000	>1000	125	1000	1000

NT – not tested

2.3 Cytotoxicity

Cytotoxicity of the most active compounds was determined on human hepatocellular liver carcinoma cells HepG2, PBMC (Peripheral Blood Mononuclear Cells) and human SH-Sy5y neuroblastoma cells by MTT assay for cellular toxicity. IC₅₀ values in mmol/L are presented in Table 3. Values of selectivity index (SI) indicate rate between IC₅₀ of HepG2 cytotoxicity and MIC *M. tuberculosis* are presented in Table 2. If the values of SI \geq 10, compounds are considered for further screening.¹⁴ IC₅₀ of tested compounds are within the range 0.0373-1.21 mmol/L. Selectivity index calculated for MDR-TB *M. tuberculosis* for compounds **3d-3i** exhibit high values.

Table 3 Cytotoxicity evaluation experimental data

	R	R ¹ R ² N	HepG2 IC ₅₀	PBMC IC ₅₀	Sy5y IC ₅₀
			[mmol/L]		
3a	4-CF ₃	A	NT	NT	NT
3b	3-CF ₃	A	NT	NT	NT
3c	4-F	A	NT	NT	NT
3d	3-F	A	0.934	0.934	NT
3e	2-F	A	1.210	1.210	NT
3f	4-CF ₃	B	0.347	0.347	NT
3g	3-CF ₃	B	> 0.322	> 0.322	NT
3h	4-F	B	> 1.280	> 0.763	NT
3i	3-F	B	> 0.812	> 0.305	NT
3j	4-CF ₃	C	> 0.0373	0.262	0.107
3k	4-F	C	> 0.797	> 0.331	NT
3l	3-F	C	> 0.393	> 0.393	> 0.430

4a	4-CF ₃	D	> 0.624	NT	NT
4b	3-F	D	> 0.130	> 0.305	NT
INH	NT	NT	NT	NT	NT

NT – not tested

2.4 Stability of **3h** in aqueous buffers and rat plasma

To get more information about the stability of compounds **3** we studied the ciprofloxacin-containing derivative **3h** as follows. First, an HPLC method for a simultaneous determination of **3h** and its putative metabolites, ciprofloxacin and formylciprofloxacin was developed. Due to a high lipophilicity of **3h** and its low solubility in aqueous environments, fluorescence detection was selected. The excitation/emission wavelengths were set according to those published for ciprofloxacin.¹⁵ Although it was possible to detect the second decomposition product, i.e. 4-fluorobenzoic hydrazide by simultaneous UV detection as well, the detector response was too low to detect it at the concentrations needed for dissolving the parent **3h** in the aqueous buffers. Nevertheless, a simple isocratic method using simple C18 reversed phase silica was able to separate **3h** and its putative metabolites, ciprofloxacin and formylciprofloxacin. To decrease the analysis time, we have used a monolithic column and a flow rate of 2.5 ml/min yielding retention times of 1.1, 3.8 and 4.8 min for ciprofloxacin, **3h** and formylciprofloxacin, respectively.

The stability of **3h** at different pH values is given in Figure 1. At pH 7.4, the compound was stable; no significant decomposition was observed during the 48 h experiment. In both acidic buffers (pH 3 and 5), the concentration of **3h** decreased, accompanied by a proportional increase in the concentration of ciprofloxacin. The half life values (with their 95% confidence intervals) were 2.9 (2.8 - 3.1) h and 11.8 (9.6 - 15.2) h at pH 3 and 5, respectively, and the plateau was reached at 0.5 (-1.1 - 2.0) % and 20.5 (14.0 - 27.1) % concentration. Interestingly, no formylciprofloxacin was detected in the samples.

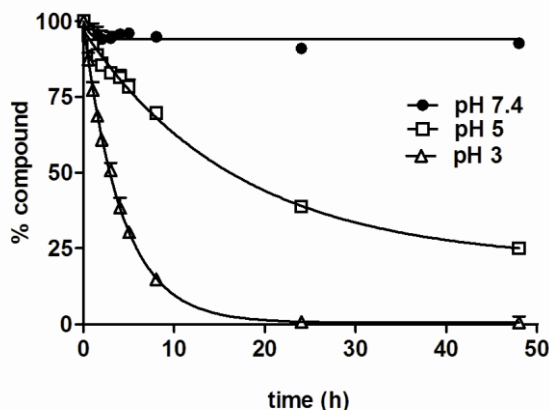


Figure 1. Stability of **3h** in aqueous buffers at pH 7.4, 5 and 3. Data are presented as means \pm S.D, $n = 3$. Where no error bars are visible, they are smaller than the symbol.

To be able to detect **3h**, ciprofloxacin and formylciprofloxacin in plasma, gradient analysis had to be employed to separate the most polar analyte ciprofloxacin from the endogenous plasma components. For this initial experiment, we used acetonitrile precipitation for the preparation of the sample, because we found satisfactory recovery values (more than 95%) for both **3h** and ciprofloxacin. For ciprofloxacin, this value is in accordance with a previous study.¹⁶ All three analytes were well separated from the endogenous plasma components with the retention times of ciprofloxacin, **3h** and formylciprofloxacin being 4.2, 6.2 and 6.7 min, respectively. Blank plasma samples were analysed and no interference peaks were found at the retention times of the analytes of interest. We did not find any interest of developing solid phase extraction to get cleaner plasma samples or to find a suitable internal standard, because after the initial experiments, we did not see any statistically significant decomposition of **3h**. After 48 h incubation, 87 ± 3 % of the parent compound was still present. One experiment (in triplicate) was prolonged to 96 h. At this time, 82 ± 3 % of **3h** was found, together with a proportional increase in ciprofloxacin concentration; again formylciprofloxacin was not detected. This slight decomposition in concentration of **3h** was not statistically different from that observed in the buffer at pH 7.4. Thus, no enzymatic decomposition occurs in rat plasma.

3. Conclusion

In this study, new fluorine-containing hydrazones with antimycobacterial properties were prepared and investigated. All evaluated compounds have shown higher activity against MDR-TB than INH. Prepared compounds are non-toxic in MIC concentrations for human hepatocytes, PBMC cells and human SH-Sy5y neuroblastoma cells. The highest selectivity

index for MDR-TB *M. tuberculosis* was found to be 1268.58 for 1-cyclopropyl-6-fluoro-4-oxo-7-{4-[[4-(trifluoromethyl)benzoyl]hydrazono]methyl}piperazin-1-yl}-1,4-dihydroquinoline-3-carboxylic acid (**3h**). An evaluation of its stability towards hydrolysis has shown that the compound is stable at neutral pH, thus improving the bioavailability to the target site. Compounds **3f** and **3g** (having trifluoromethylbenzoyl group and CPX in the molecule) were found as the most active against both strains of *Mycobacterium kansasii* in comparison to the other compounds as well as the standard INH.

4. Experimental

4.1 Synthesis

Chemicals were obtained from Sigma-Aldrich Co. Melting points were determined on a Kofler micro-hot-stage and are uncorrected. Elemental analyses (C, H, N) were performed with a Perkin-Elmer 2400 CHNS/O analyzer. Infrared spectra were recorded on a Bio-Rad FTS 3000 MX spectrometer in KBr pellets. NMR spectra were measured in CF₃CO₂D or DMSO-*d*₆ solutions on a Bruker Avance 300 (300 MHz for ¹H and 75.5 MHz for ¹³C). The chemical shifts δ , are given in ppm, related to tetramethylsilane (TMS) as an internal standard. The coupling constants (*J*) are reported in Hz. The reactions were monitored and the purity of the products was checked by TLC (Fluka silica gel/TLC cards 60 PF₂₅₄). Mass spectra were recorded with a VG-Analytical AutospecQ instrument.

4.1.1 General procedure for the synthesis of ethyl benzoylhydrazonoformate **2a-2e**

Diethoxymethyl acetate (243 mg, 1.5 mmol) was added at room temperature to the mixture of a substituted benzoic acid hydrazide **1** (1 mmol) in acetonitrile (10 mL). Reaction mixture was then stirred for 10 minutes at room temperature and evaporated to dryness. A crude product was recrystallized from the appropriate solvent.

4.1.1.1 **Ethyl [4-(trifluoromethyl)benzoyl]hydrazonoformate (2a)** Yield 93%; mp 148 – 150 °C (EtOH). IR (KBr): 3231, 1628, 1332, 1268, 1234, 1171, 1130, 1067, 976, 772 cm⁻¹. ¹H (DMSO-*d*₆, 300 MHz): δ 11.24 (s, 1H, NH), 8.37 (s, 1H, CH), 8.02 (d, *J* = 8.2 Hz, 2H, H₂, H₆), 7.85 (d, *J* = 8.1 Hz, 2H, H₃, H₅), 4.18 (q, *J* = 14.1, 5.4 Hz, 2H, CH₂), 1.29 (t, *J* = 7.1 Hz, 3H, CH₃). ¹³C NMR (DMSO-*d*₆, 75 MHz): 162.3, 157.2, 138.6, 124.8 (q, *J* = 819.3 Hz, CF₃), 129.5, 129.0, 126.2 (q, *J* = 11.2 Hz), 63.5, 15.0. MS (EI): 261 (*m/z* (M+H)⁺). Anal.

Calcd for $C_{11}H_{11}F_3N_2O_2$ (260.21): C, 50.77; H, 4.26; N, 10.77. Found: C, 50.90; H, 4.01; N, 10.81.

4.1.1.2 Ethyl [3-(trifluoromethyl)benzoyl]hydrazonoformate (2b) Yield 91%; mp 127 – 130 °C (ethyl acetate/hexane). IR (KBr): 3204, 3075, 1661, 1614, 1566, 1372, 1338, 1314, 1267, 1165, 1109, 1073, 814 cm^{-1} . 1H NMR (DMSO- d_6 , 300 MHz): δ 11.25 (s, 1H, NH), 8.37 (s, 1H, CH), 8.13 (d, $J = 8.1$ Hz, 2H), 7.92 (d, $J = 7.8$ Hz, 1H), 7.74 (t, $J = 7.6$ Hz, 1H), 4.17 (m, 2H), 1.29 (t, $J = 7.1$ Hz, 3H). MS (EI): 261 (m/z (M+H) $^+$). HRMS Calcd for ($C_{11}H_{11}F_3N_2O_2 + H$): 261.0851. Found: 261.0838. Anal. Calcd for $C_{11}H_{11}F_3N_2O_2$ (260.21): C, 50.77; H, 4.26; N, 10.77. Found: C, 49.90; H, 3.90; N, 12.20.

4.1.1.3 Ethyl 4-(fluorobenzoyl)hydrazonoformate (2c) Yield 88%; mp 138 – 139 °C (ethyl acetate/diethyl ether). IR (KBr): 3215, 3061, 2986, 1658, 1617, 1563, 1506, 1363, 1319, 1250, 1229, 1159, 1115, 1065, 1013, 848 cm^{-1} . 1H NMR (DMSO- d_6 , 300 MHz): δ 11.05 (s, 1H, NH), 8.37 (s, 1H, CH), 7.90 (m, 2H, H2, H6), 7.31 (m, 2H, H3, H5), 4.15 (q, $J = 7.0$ Hz, 2H, CH $_2$), 1.29 (t, $J = 7.1$ Hz, 3H, CH $_3$). ^{13}C NMR (DMSO- d_6 , 75 MHz): 163.8 (d, $J = 248.5$ Hz), 161.6, 155.9, 130.3 (d, $J = 3.0$ Hz), 129.8 (d, $J = 9.0$ Hz), 115.3 (d, $J = 21.8$ Hz), 67.2, 15.4. MS (EI): 211 (m/z (M+H) $^+$). Anal. Calcd for $C_{10}H_{11}FN_2O_2$ (210.20): C, 57.14; H, 5.27; N, 13.33. Found: C, 56.88; H, 5.11; N, 13.53.

4.1.1.4 Ethyl 3-(fluorobenzoyl)hydrazonoformate (2d) Yield 95%; mp 114 – 116 °C (acetonitrile). IR (KBr): 3203, 3074, 1655, 1616, 1559, 1479, 1442, 1364, 1312, 1248, 1221, 1127, 1069, 1015, 973, 849, 820 cm^{-1} . 1H NMR (DMSO- d_6 , 300 MHz): δ 11.10 (s, 1H, NH), 8.36 (s, 1H, CH), 7.67 (d, $J = 7.8$ Hz, 1H), 7.60 (m, 1H), 7.53 (m, 1H), 7.40 (m, 1H), 4.15 (q, $J = 7.0$ Hz, 2H, CH $_2$), 1.29 (dt, $J = 7.1, 2.0$ Hz, 3H, CH $_3$). MS (EI): 211 (m/z (M+H) $^+$). HRMS Calcd for ($C_{10}H_{11}FN_2O_2 + H$): 211.0883. Found: 211.0885. Anal. Calcd for $C_{10}H_{11}FN_2O_2$ (210.20): C, 57.14; H, 5.27; N, 13.33. Found: C, 56.71; H, 5.20; N, 13.85.

4.1.1.5 Ethyl 2-(fluorobenzoyl)hydrazonoformate (2e) Yield 93%; mp 101 – 105 °C (ethyl acetate/hexane). IR (KBr): 3220, 3079, 1655, 1612, 1562, 1476, 1365, 1318, 1251, 1217, 1100, 1065, 909, 753 cm^{-1} . 1H NMR (DMSO- d_6 , 300 MHz): δ 10.98 (s, 1H, NH), 8.28 (s, 1H, CH), 7.55 (m, 2H), 7.29 (m, 2H), 4.14 (q, $J = 7.2$ Hz, 2H), 1.28 (t, $J = 7.1$ Hz, 3H). MS (EI) 211 (m/z (M+H) $^+$). HRMS Calcd for ($C_{10}H_{11}FN_2O_2 + H$): 211.0883. Found: 211.0873. Anal. Calcd for $C_{10}H_{11}FN_2O_2$ (210.20): C, 57.14; H, 5.27; N, 13.33. Found: C, 56.93; H, 4.91; N, 13.98.

4.1.2 General procedure for the synthesis of derivatives of 4-amino-2-hydroxybenzoic acid **3a-3e**

4-Amino-2-hydroxybenzoic acid (1 mmol) was dissolved in acetonitrile (15 mL) at room temperature. Then, a solution of the corresponding ethyl benzoylhydrazonoformate (1 mmol) in acetonitrile (4 mL) was added. The reaction mixture was stirred at room temperature for 24 hours. The solid material was filtered off, dried in the air, suspended in acetonitrile (10 mL), refluxed for 5 minutes, and the product was filtered off from a hot suspension.

4.1.2.1 2-Hydroxy-4-[(4-trifluoromethylbenzoyl)hydrazonomethylamino]benzoic acid (3a) Yield 45%; mp 250 – 252 °C (acetonitrile). IR (KBr): 3214, 1657, 1616, 1562, 1328, 1250, 1171, 1121, 1072, 1021, 907, 854 cm^{-1} . ^1H NMR (DMSO- d_6 , 300 MHz): δ 11.23 (s, 1H, NH), 9.94 (s, 1H, OH), 8.60 (s, 1H, CH), 8.06 (d, $J = 8.1$ Hz, 3H, H2, H6), 7.88 (d, $J = 8.3$ Hz, 3H, H3, H5), 7.69 (t, $J = 7.6$ Hz, 1H), 6.86 (d, $J = 1.8$ Hz, 1H, OH), 6.66 (dd, $J = 8.7$, 1.9 Hz, 1H, NH). ^{13}C NMR (DMSO- d_6 , 75 MHz): 172.7, 163.7, 161.6, 148.2, 146.6, 138.7, 132.4, 128.9, 126.3 (q, $J = 10.7$ Hz), 124.8 (q, $J = 817.5$ Hz), 123.0, 108.3, 106.2, 102.8. MS (EI) 368 (m/z (M+H) $^+$). Anal. Calcd for $\text{C}_{16}\text{H}_{12}\text{F}_3\text{N}_3\text{O}_4$ (367.28): C, 52.32; H, 3.29; N, 11.44. Found: C, 52.04; H, 3.25; N, 11.27.

4.1.2.2 2-Hydroxy-4-[(3-trifluoromethylbenzoyl)hydrazonomethylamino]benzoic acid (3b) Yield 63%; mp 201 – 203 °C (acetonitrile). IR (KBr): 3415, 3216, 3069, 1638, 1583, 1555, 1336, 1279, 1237, 1161, 1128, 1072, 972, 773 cm^{-1} . ^1H NMR (DMSO- d_6 , 300 MHz): δ 11.24 (s, 1H, NH), 9.91 (s, 1H, OH), 8.60 (s, 1H, CH), 8.17 (d, $J = 8.9$ Hz, 3H), 7.93 (d, $J = 7.8$ Hz, 1H), 7.72 (d, $J = 7.7$ Hz, 3H), 6.84 (d, $J = 2.0$ Hz, 1H), 6.66 (dd, $J = 2.0$, 7.8 Hz, 1H, NH). ^{13}C NMR (DMSO- d_6 , 75 MHz): 172.7, 163.7, 161.3, 148.2, 146.6, 135.8, 132.3 (d, $J = 17.3$ Hz), 130.7, 128.5 (q, $J = 10.7$ Hz), 126.7, 124.5 (q, $J = 11.4$ Hz), 123.1, 119.5, 108.2, 106.3, 102.8. MS (EI) 368 (m/z (M+H) $^+$). Anal. Calcd for $\text{C}_{16}\text{H}_{12}\text{F}_3\text{N}_3\text{O}_4$ (367.28): C, 52.32; H, 3.29; N, 11.44. Found: C, 52.40; H, 3.18; N, 11.27.

4.1.2.3 4-[(4-Fluorobenzoyl)hydrazonomethylamino]-2-hydroxybenzoic acid (3c) Yield 60%; mp 194.9 – 195.5 °C (acetonitrile). IR (KBr): 3231, 3072, 1638, 1551, 1507, 1308, 1268, 1234, 1161, 971, 776 cm^{-1} . ^1H NMR (DMSO- d_6 , 300 MHz): δ 11.04 (s, 1H, NH), 9.86 (s, 1H, OH), 8.59 (s, 1H, CH), 7.93 (dd, $J = 8.7$, 5.6 Hz, 3H, H2, H6, H5'), 7.67 (d, $J = 8.7$ Hz, 1H, H6'), 7.34 (t, $J = 8.8$ Hz, 3H, H3, H5, H2'), 6.83 (d, $J = 1.7$ Hz, 1H, OH), 6.65 (d, $J = 8.7$ Hz, 1H, NH). ^{13}C NMR (DMSO- d_6 , 75 MHz): 167.3 (d, $J = 673.0$ Hz), 162.2, 160.9,

147.4, 131.5, 130.5, 129.7 (d, $J = 10.6$ Hz), 115.5, 115.2, 107.3, 105.2, 101.7, 100.6. MS (EI) 318 (m/z (M+H)⁺). Anal. Calcd for C₁₅H₁₂FN₃O₄ (317.27): C, 56.78; H, 3.81; N, 13.24. Found: C, 56.59; H, 3.89; N, 13.04.

4.1.2.4 **4-[(3-Fluorobenzoyl)hydrazonomethylamino]-2-hydroxybenzoic acid (3d)** Yield 71%; mp 178.3 – 179.2 °C (acetonitrile). IR (KBr): 3228, 1642, 1583, 1549, 1439, 1270, 1161, 972, 838, 774 cm⁻¹. ¹H NMR (DMSO-*d*₆, 300 MHz): δ 11.09 (s, 1H, NH), 9.89 (s, 1H, COOH), 8.59 (s, 1H, CH), 7.63 (m, 4H, H4, H5, H6, H5'), 7.56 (d, $J = 2.0$ Hz, 1H, H2), 7.40 (d, $J = 2.3$ Hz, 1H, H6'), 6.83 (d, $J = 1.9$ Hz, 1H, H2'), 6.76 (m, 1H, OH), 6.65 (d, $J = 2.0$ Hz, 1H, NH). ¹³C NMR (DMSO-*d*₆, 75 MHz): 171.8, 163.6, 162.9, 160.6, 147.4, 145.5, 136.5, 131.5, 130.5, 123.3, 118.1, 114.1, 107.3, 105.4, 101.9. MS (EI) 318 (m/z (M+H)⁺). Anal. Calcd for C₁₅H₁₂FN₃O₄ (317.27): C, 56.78; H, 3.81; N, 13.24. Found: C, 56.48; H, 3.54; N, 12.96.

4.1.2.5 **4-[(2-Fluorobenzoyl)hydrazonomethylamino]-2-hydroxybenzoic acid (3e)** Yield 54%; mp 195-196 °C (acetonitrile). IR (KBr): 3408, 3223, 3067, 2479, 1641, 1610, 1555cm⁻¹. ¹H NMR (DMSO-*d*₆, 300 MHz): δ 10.94 (s, 1H, NH), 9.88 (m, 1H, OH), 8.51 (s, 1H, CH), 7.67 (m, 3H), 7.55 (m, 1H), 7.32 (m, 3H), 6.87 (d, 1H, $J = 1.9$ Hz), 6.66 (dd, 1H, $J = 8.7, 2.0$ Hz, NH). ¹³C NMR (DMSO-*d*₆, 75 MHz): 172.7, 163.7, 159.93, 159.91 (d, $J = 248.4$ Hz), 148.2, 145.8, 133.2, 132.3, 131.0 (d, $J = 3.0$ Hz), 125.4 (d, $J = 3.4$ Hz), 124.5 (d, $J = 15.2$ Hz), 117.0 (d, $J = 22.2$ Hz), 108.3, 106.2, 102.8. MS (EI) 318 (m/z (M+H)⁺). Anal. Calcd for C₁₅H₁₂FN₃O₄ (317.27): C, 56.78; H, 3.81; N, 13.24. Found: C, 56.47; H, 3.52; N, 12.82.

4.1.3 General procedure for the synthesis of ciprofloxacin derivatives **3f-3i**

Ciprofloxacin (331 mg, 1 mmol) was dissolved in acetonitrile (15 mL) and glacial acetic acid (2.4 mL) at 50 °C. Then, ethyl benzoylhydrazonoformate **2** (1 mmol) was added and the reaction mixture was stirred at 50 °C for four hours. After this time the temperature was decreased to the room temperature and the reaction mixture was stirred for 30 minutes. The crystals were filtered off and washed with diethyl ether (20 mL). A solid material was refluxed in 5 mL of acetonitrile for 5 minutes and filtered off.

4.1.3.1 **1-Cyclopropyl-6-fluoro-4-oxo-7-{4-[4-(trifluoromethylbenzoyl)]hydrazonomethyl}-piperazin-1-yl}-1,4-dihydroquinoline-3-carboxylic acid (3f)** Yield 19%; mp 236 – 238 °C (acetonitrile). IR (KBr): 3513, 3469, 1709, 1663, 1622, 1495, 1463, 1320, 1261, 1238, 1133, 1062, 1014 cm⁻¹. ¹H NMR (DMSO-*d*₆, 300 MHz): δ 10.95 (s, 1H, NH), 8.68 (s, 1H, CH), 8.07

(s, 1H, CH), 8.01 (d, $J = 8.1$ Hz, 2H, H2, H6), 7.95 (d, $J = 13.2$ Hz, 1H), 7.85 (d, $J = 8.3$ Hz, 2H, H3, H5), 7.63 (d, $J = 7.5$ Hz, 1H), 3.85 (m, 1H), 3.55 (m, 4H, CH₂), 3.40 (m, 4H, CH₂), 1.34 (m, 2H), 1.20 (m, 3H). ¹³C NMR (DMSO-*d*₆, 75 MHz): 176.3, 165.9, 160.7, 154.6, 153.9, 151.3, 147.9, 145.0, 139.1, 138.3, 130.9, 127.9, 126.1 (q, $J = 10.9$ Hz), 122.2, 118.9, 111.1, 106.8, 49.1, 44.9, 35.9, 7.6. MS (EI) 545 (m/z (M)⁺). Anal. Calcd for C₂₆H₂₃F₄N₅O₄ (545.49): C, 57.25; H, 4.25; N, 12.84. Found: C, 55.29; H, 4.44; N, 12.30. C₂₆H₂₃F₄N₅O₄+H₂O calculated: C, 55.42; H, 4.47; N, 12.43.

4.1.3.2 **1-Cyclopropyl-6-fluoro-4-oxo-7-{4-[3-(trifluoromethylbenzoyl)hydrazonomethyl]piperazin-1-yl}-1,4-dihydroquinoline-3-carboxylic acid (3g)** Yield 51%; mp 238 – 239 °C (acetonitrile). IR (KBr): 3268, 3063, 1728, 1676, 1628, 1467, 1333, 1260, 1237, 1120, 1020, 937, 812, 747, 701 cm⁻¹. ¹H NMR (DMSO-*d*₆, 300 MHz): δ 10.98 (s, 1H, NH), 8.68 (s, 1H, CH), 8.12 (d, $J = 8.9$ Hz, 2H), 8.07 (s, 1H), 7.94 (d, $J = 13.2$ Hz, 1H), 7.89 (d, 7.9 Hz, 1H), 7.72 (t, $J = 7.7$ Hz, 1H), 7.63 (d, $J = 7.5$ Hz, 1H), 3.85 (m, 1H), 3.54 (d, $J = 5.0$ Hz, 4H, CH₂), 3.41 (d, $J = 4.9$ Hz, 4H, CH₂), 1.33 (m, 2H), 1.21 (m, 3H). ¹³C NMR (CF₃COOD, 75 MHz): 168.3, 167.7, 160.4, 155.7, 154.4, 151.0, 146.6, 138.9, 130.1, 128.2, 127.5, 126.9, 122.4 (q, $J = 10.5$ Hz), 119.0, 114.6, 110.9, 109.3, 102.6, 100.8, 49.7, 43.7, 36.0, 5.1. MS (EI) 546 (m/z (M+H)⁺). Anal. Calcd for C₂₆H₂₃F₄N₅O₄ (545.49): C, 57.25; H, 4.25; N, 12.84. Found: C, 57.12; H, 4.33; N, 13.13.

4.1.3.3 **1-Cyclopropyl-6-fluoro-4-oxo-7-{4-[4-(fluorobenzoyl)hydrazonomethyl]piperazin-1-yl}-1,4-dihydroquinoline-3-carboxylic acid (3h)** Yield 52%; mp 256 – 260 °C (acetonitrile). IR (KBr): 3279, 3047, 1725, 1675, 1627, 1505, 1468, 1335, 1260, 1237, 1020, 943, 848 cm⁻¹. ¹H NMR (DMSO-*d*₆, 300 MHz): δ 10.76 (s, 1H, NH), 8.69 (s, 1H, CH), 8.05 (s, 1H), 7.96 (d, $J = 13.2$, 1H), 7.88 (dd, $J = 2.9, 14.2$, 2H, H2, H6), 7.63 (d, $J = 7.6$, 1H), 7.30 (s, 2H, H3, H5), 3.85 (m, 1H), 3.53 (d, $J = 4.7$ Hz, 4H, CH₂), 3.40 (d, $J = 4.9$ Hz, 4H, CH₂), 1.33 (m, 2H), 1.21 (m, 3H). ¹³C NMR (CF₃COOD, 75 MHz): 172.5, 171.8, 167.7, 160.4, 159.0, 155.6, 151.3, 150.3, 143.5, 132.6, 126.5, 119.2, 117.2, 114.1, 107.2, 105.3, 54.2, 50.7, 40.6, 9.7. MS (EI) 496 (m/z (M+H)⁺). Anal. Calcd for C₂₅H₂₃F₂N₅O₄ (495.48): C, 60.60; H, 4.68; N, 14.13. Found: C, 60.30; H, 4.49; N, 13.97.

4.1.3.4 **1-Cyclopropyl-6-fluoro-4-oxo-7-{4-[3-(fluorobenzoylhydrazono)methyl]piperazin-1-yl}-1,4-dihydroquinoline-3-carboxylic acid (3i)** Yield 44%; mp 235-237 °C (acetonitrile). IR (KBr): 3297, 3050, 2823, 1722, 1677, 1629 cm⁻¹. ¹H NMR (DMSO-*d*₆, 300 MHz): δ 10.82 (s, 1H, NH), 8.66 (s, 1H, CH), 8.06 (s, 1H), 7.92 (d, 1H, $J = 13.2$ Hz), 7.58 (m,

5H), 7,36 (m, 1H), 3,85 (m, 1H, CH), 3,54 (m, 4H, CH₂), 3,39 (m, 4H, CH₂), 1,34 (m, 2H, CH₂), 1,21 (m, 2H, CH₂). ¹³C NMR (DMSO-*d*₆, 75 MHz): 177.2, 166.8, 164.5, 161.5, 161.2, 154.7, 148.9, 145.9, 140.0, 137.7, 137.7 (d, *J* = 7.0 Hz), 133.3, 131.3 (d, *J* = 8.2 Hz), 124.0 (d, *J* = 2.6 Hz), 114.8, 114.5, 112.1, 107.7, 50.0, 45.8, 36.8, 8.5. MS (EI) 496 (*m/z* (M+H)⁺). Anal. Calcd for C₂₅H₂₃F₂N₅O₄ (495.48): C, 60.60; H, 4.68; N, 14.13. Found: C, 60.39; H, 4.67; N, 14.05.

4.1.4 General procedure for the synthesis of norfloxacin derivatives **3j-3l**

Norfloxacin (319 mg, 1 mmol) was dissolved in acetonitrile (12 mL) and glacial acetic acid (2.5 mL) at 50 °C, followed by the addition of ethyl benzoylhydrazonoformate (1 mmol). The reaction mixture was stirred for 5 hours at 50 °C and after this time, the temperature was slowly decreased to the room temperature. After stirring at room temperature for 40 minutes, the solid was filtered off and washed with diethyl ether (25 mL). Crystals were dried in the air, suspended in acetonitrile (10 mL) and refluxed for 10 minutes. The product was filtered off from a hot suspension.

4.1.4.1 **1-Ethyl-6-fluoro-4-oxo-7-[4-[4-(trifluoromethylbenzoyl)hydrazonomethyl]piperazin-1-yl]-1,4-dihydroquinoline-3-carboxylic acid (3j)** Yield 56%; mp 259 – 260 °C (acetonitrile). IR (KBr): 3194, 1726, 1621, 1482, 1328, 1265, 1239, 1110, 1068, 1019, 860 cm⁻¹. ¹H NMR (DMSO-*d*₆, 300 MHz): δ 15.27 (s, 1H, COOH), 10.96 (s, 1H, NH), 8.96 (s, 1H, CH), 8.08 (s, 1H, CH), 8.01 (d, *J* = 8.1 Hz, 2H, H2, H6), 7.94 (d, *J* = 13.2 Hz, 1H), 7.85 (d, *J* = 8.3 Hz, 2H, H3, H5), 7.24 (d, *J* = 7.2 Hz, 1H), 4.61 (q, *J* = 6.9 Hz, 2H), 3.53 (d, *J* = 4.9 Hz, 4H, CH₂), 3.40 (d, *J* = 4.6 Hz, 4H, CH₂), 1.44 (t, *J* = 7.0 Hz, 3H, CH₃). ¹³C NMR (DMSO-*d*₆, 75 MHz): 176.1, 166.1, 160.7, 154.5, 154.0, 151.3, 148.5, 145.4, 138.3, 137.1, 130.5, 127.9, 126.1 (q, *J* = 10.7 Hz), 119.5, 111.4, 107.1, 106.4, 49.2, 49.1, 45.0, 14.4. MS (EI) 533 (*m/z* (M)⁺). Anal. Calcd for C₂₅H₂₃F₄N₅O₄ (533.47): C, 56.29; H, 4.35; N, 13.13. Found: C, 54.46; H, 4.64; N, 12.63. C₂₅H₂₃F₄N₅O₄+H₂O calculated: C, 54.45; H, 4.57; N, 12.70.

4.1.4.2 **1-Ethyl-6-fluoro-4-oxo-7-[4-[4-(fluorobenzoyl)hydrazonomethyl]piperazin-1-yl]-1,4-dihydroquinoline-3-carboxylic acid (3k)** Yield 44%; mp 270 – 272 °C (ethyl acetonitrile). IR (KBr): 3260, 3048, 1727, 1669, 1625, 1474, 1260, 1237, 1157, 1112, 1020, 852 cm⁻¹. ¹H NMR (DMSO-*d*₆, 300 MHz): δ 15.35 (s, 1H, COOH), 10.75 (s, 1H, NH), 8.97 (s, 1H, CH), 8.04 (s, 1H), 7.97 (d, *J* = 13.1, 1H), 7.88 (q, *J* = 3.1, 14.3, 2H, H2, H6), 7.28 (q, *J*

= 8.6, 24.2, 3H), 4.62 (m, 2H, CH₂), 3.51 (d, *J* = 5.3 Hz, 4H, CH₂), 3.39 (d, *J* = 5.4 Hz, 4H, CH₂), 1.43 (t, 3H, CH₃). ¹³C NMR (CF₃COOD, 75 MHz): 167.6, 164.8 (d, *J* = 257.4 Hz), 163.1, 160.4, 155.8, 154.3, 150.8, 145.7, 136.8, 128.1 (d, *J* = 9.9 Hz), 121.9 (d, *J* = 3.1 Hz), 114.2, 113.3, 109.4, 101.9, 101.1, 50.4, 49.7, 43.6, 10.5. MS (EI) 484 (*m/z* (M+H)⁺). Anal. Calcd for C₂₄H₂₃F₂N₅O₄ (483.47): C, 59.62; H, 4.80; N, 14.49. Found: C, 59.37; H, 4.67; N, 14.33.

4.1.4.3 1-Ethyl-6-fluoro-4-oxo-7-{4-[3-(fluorobenzoyl)hydrazonomethyl]piperazin-1-yl}-1,4-dihydroquinoline-3-carboxylic acid (3l) Yield 49%; mp 251 - 253 °C (acetonitrile). IR (KBr): 3267, 3055, 2875, 2817, 1724, 1670, 1628 cm⁻¹. ¹H NMR (DMSO-*d*₆, 300 MHz): δ 15.29 (s, 1H, COOH), 10.81 (s, 1H, NH), 8.97 (s, 1H, CH), 8.05 (s, 1H, CH), 7.69 (d, *J* = 13.2 Hz, 1H), 7.57 (m, 3H), 7.36 (m, 1H), 7.25 (d, *J* = 7.3 Hz, 1H), 4.61 (q, *J* = 7.2 Hz, 2H, CH₂), 3.53 (m, 4H, CH₂), 3.38 (m, 4H, CH₂), 1.44 (t, *J* = 7.2 Hz, 3H, CH₃). ¹³C NMR (CF₃COOD, 75 MHz): 168.4, 168.3, 163.2, 159.9, 156.5, 153.3 (d, *J* = 258.3 Hz), 146.8, 146.5 (d, *J* = 10.5 Hz), 137.5, 129.5 (d, *J* = 8.1 Hz), 128.7 (d, *J* = 7.3 Hz), 121.5 (d, *J* = 3.2 Hz), 120.2, 114.0, 113.0, 110.6, 102.7, 101.9, 51.2, 50.5, 44.4, 11.3. MS (EI) 484 (*m/z* (M+H)⁺). Anal. Calcd for C₂₄H₂₃F₂N₅O₄ (483.47): C, 59.62; H, 4.80; N, 14.49. Found: C, 59.33; H, 4.78; N, 14.44.

4.1.5 *N*-{2-[4-(Trifluoromethyl)benzoyl]hydrazonomethyl}pyrazine-2-carboxamide (4a) *N*-[(dimethylamino)methylene]pyrazine-2-carboxamide (178 mg, 1 mmol) was dissolved in acetonitrile (5 mL) at room temperature followed by the addition of a solution of 4-(trifluoromethyl)benzohydrazide **1** (204 mg, 1 mmol) in acetonitrile (5 mL). The reaction mixture was stirred for 4.5 hours at room temperature. The crystals were filtered off and dried in the air, suspended in methanol (10 mL) at room temperature, filtered off and dried in the air.

Yield 17%; mp 242 – 244 °C (methanol). IR (KBr): 3267, 1679, 1627, 1556, 1501, 1329, 1163, 1109, 1021, 921 cm⁻¹. ¹H NMR (DMSO-*d*₆, 300 MHz): 11.71 (s, 1H, NH), 11.35 (m, 1H, NH), 9.26 (d, *J* = 1.3 Hz, 1H, H3'), 9.08 (d, *J* = 3.9 Hz, 1H, CH), 8.94 (d, *J* = 2.4 Hz, 1H, H4'), 8.82 (m, 1H, H6'), 8.11 (d, *J* = 8.1 Hz, 2H, H2, H6), 7.91 (d, *J* = 8.3 Hz, 2H, H3, H5). ¹³C NMR (CF₃COOD, 75 MHz): 165.9, 162.9, 159.5, 145.8, 144.4, 138.7, 135.4, 128.3, 125.8, 123.8 (q, *J* = 11.1 Hz), 122.5, 116.6 (q, *J* = 878.0 Hz). MS (EI) 337 (*m/z* (M)⁺). Anal. Calcd for C₁₄H₁₀F₃N₅O₂ (337.26): C, 49.86; H, 2.99; N, 20.77. Found: C, 49.72; H, 3.09; N, 20.61.

4.1.6 ***N*-{[2-(3-fluorobenzoyl)hydrazinyl]methylene}pyrazine-2-carboxamide (4b)** *N*-[(Dimethylamino)methylene]pyrazine-2-carboxamide (267 mg, 1.5 mmol) was dissolved in acetonitrile (10 mL) at room temperature. The solution was warmed up to 50 °C. The catalyst (pyridinium *p*-toluenesulphonate polymer-bound, 427 mg, 1.5 mmol) was added to the solution, followed by the addition of 3-fluorobenzohydrazide (231 mg, 1.5 mmol). The reaction mixture was stirred for 4 hours at 50 °C, then the temperature was decreased to room temperature and stirring was continued for 16 hours at the same temperature. Then, the solid was filtered off and washed with methanol (4 x 10 mL). The filtrate was evaporated to dryness to afford **4b**.

Yield 16%; mp 200 – 202 °C (methanol). IR (KBr): 3293, 3245, 3082, 2360, 1683, 1625, 1552 cm⁻¹. ¹H NMR (DMSO-*d*₆, 300 MHz): δ 11.57 (s, 1H, NH), 11.32 (d, *J* = 9,6 Hz, 1H, NH), 9.26 (d, *J* = 1,3 Hz, 1H), 9.06 (d, *J* = 9,6 Hz, 1H, CH), 8.93 (d, *J* = 2,4 Hz, 1H), 8.81 (m, 1H), 7.72 (m, 2H), 7.58 (m, 1H), 7.43 (m, 1H). ¹³C NMR (DMSO-*d*₆, 75 MHz): 163.4, 162.3 (d, *J* = 244.4 Hz), 161.6, 149.1, 148.6, 144.5, 144.1, 141.4, 136.1, 131.0, 124.0 (d, *J* = 2.5 Hz), 118.8 (d, *J* = 21.0 Hz), 114.6 (d, *J* = 23.0 Hz). MS (EI) 288 (*m/z* (M+H)⁺). Anal. Calcd for C₁₃H₁₀FN₅O₂ (287.25): C, 54.36; H, 3.51; N, 24.38. Found: C, 53.89; H, 3.79; N, 23.98.

Procedure for the preparation of formylciprofloxacin

1-Cyclopropyl-6-fluoro-7-(4-formylpiperazin-1-yl)-4-oxo-1,4-dihydroquinoline-3-carboxylic acid A mixture of acetic anhydride (224 mg, 2.2 mmol) and formic acid (78 mg, 1.7 mmol) was heated at 50 °C for 20 minutes, then ciprofloxacin (351 mg, 1.1 mmol) was added and the mixture was heated at 80 °C for 2.5 hours. Upon cooling, a distilled water (2 mL) was slowly dropped to the reaction mixture, and crystals were filtered off.¹⁷

Yield 77%; mp 281 – 283 °C (methanol). IR (ATR): 2866, 1726, 1666, 1624, 1547, 1439, 1264, 1235, 1009, 937, 803 cm⁻¹. ¹H NMR (DMSO-*d*₆, 300 MHz): δ 8.92 (s, 1H), 8.23 (s, 1H), 7.96 (d, *J* = 12.3 Hz, 1H), 7.56 (d, *J* = 9.6 Hz, 1H), 4.15 (m, 1H), 3.81 (m, 1H), 3.62 (d, *J* = 4.3 Hz, 3H), 3.18 (d, *J* = 2.3 Hz, 1H), 2.46 (s, 4H), 1.38 (d, *J* = 2.6 Hz, 2H), 1.16 (s, 2H). ¹³C NMR (DMSO-*d*₆, 75 MHz): 176.6, 166.1, 161.2, 148.3, 145.2, 139.3, 119.3, 112.0, 107.3, 107.0, 50.4, 49.3, 44.6, 36.1, 7.8. Anal. Calcd for C₁₈H₁₈FN₃O₄ (359.35): C, 60.16; H, 5.05; N, 11.69. Found: C, 60.03; H, 5.17; N, 11.74.

4.2 Biological methods

4.2.1 *In vitro* Antimycobacterial activity against *M. avium* 330/88, *M. kansasii* 235/80 and *M. kansasii* 6509/96 strains.

In vitro antimycobacterial activity was evaluated against *Mycobacterium kansasii* CNTC My 235/80, *M. kansasii* 6509/96 and *Mycobacterium avium* CNTC 330/88. All strains were obtained from the Czech National Collection of Type Cultures (CNCTC) with exception of *M. kansasii* 6509/96, which is a clinical isolate. Antimycobacterial activity was measured in Sula's semisynthetic medium (SEVAC, Prague) at 37 °C. Compounds were dissolved in dimethyl sulfoxide solution (max 5% DMSO in water) and applied into the medium in concentration range 250, 125, 62, 31, 16, 8, 4,2 and 1 µmol/L. Minimal inhibitory concentration (MIC) was determined after incubation at 37 °C for 7, 14 and 21 days. The MIC is the lowest concentration of a substance at which the inhibition of the growth of mycobacterium occurs.

4.2.2 *In vitro* Antimycobacterial activity against *M. tuberculosis* H₃₇Rv and MDR *M. tuberculosis* A8 241.

In vitro antimycobacterial activity of the compound was determined on *M. tuberculosis* H₃₇Rv and *M. tuberculosis* MDR A8 (INH and RIF resistant strain) in Sula's semi-synthetic medium, which was prepared in-house^{18,19,20} at pH 6.5 by serial dilution. The test compounds were added to the medium as DMSO solutions. Minimal inhibitory concentration (MIC) was determined after incubation at 37 °C for 28 days. MIC was the lowest concentration of a compound at which the visible inhibition of the growth of *M. tuberculosis* MDR A8 occurred. The activities of the tested compounds were confirmed using a colony forming unit (CFU) determination by subculturing from the Sula's medium onto drug-free Löwenstein-Jensen solid medium. The samples were incubated for further 28 days.^{19,21,22} The experiments were repeated at least two times with similar results.

4.2.3 *In vitro* Cytotoxicity of compounds by MTT assay

HepG2 human hepatoma cells (ATCC HB-8065) and human PBMC (peripheral blood mononuclear cells)²³ were cultured in RPMI-1640 medium without phenol red supplemented with 10% FCS, 2 mM L-glutamine and 160 µg/mL gentamycin.^{24,25} SH-SY5Y human neuroblastoma cell line was grown in DMEM medium without phenol red containing 10% fetal calf serum (FCS), 2 mM L-glutamine, 160 µg/mL gentamycin and 1 % nonessential

amino acids (NEAA).^{26,27} Cell cultures were maintained at 37 °C, 5% CO₂ in water-saturated atmosphere.

Cells were plated into 96-well plate with initial cell number of 5 x 10³ per well (in the case of SH-SY5Y 7.5 x 10³, PBMC 2.0 x 10⁵ cells/well). After 24 h incubation at 37 °C prior to the experiment, cells were treated with compounds in 100 µL serum free medium overnight. Control cells were treated with serum free medium. Four parallel measurements were performed in all cases.

After overnight incubation at 37 °C, the cell viability was determined by 3-(4,5-dimethylthiazol-2-yl)-2,5-diphenyltetrazolium bromide (MTT)-assay.^{28,29} Then 45 µL MTT-solution (2 mg/mL) was added to each well. The respiratory chain¹²⁸ and other electron transport systems³⁰ reduce MTT and thereby form non-water-soluble violet formazan crystals within the cell.³¹ The amount of these crystals can be determined spectrophotometrically and serves to estimate the number of mitochondria and hence the number of living cells in the well.³² After 4 hrs of incubation, cells were centrifuged for 5 min (2000 rpm) and supernatant was removed. The obtained formazan crystals were dissolved in 50 or 100 µL DMSO and optical density (OD) of the samples was measured at $\lambda = 540$ and 620 nm using ELISA Reader (iEMS Reader, Labsystems, Finland). OD₆₂₀ values were subtracted from OD₅₄₀ values. The percent of cytotoxicity was calculated using the following equation:

$$\text{Cytotoxicity (\%)} = [1 - (\text{OD}_{\text{treated}}/\text{OD}_{\text{control}})] \times 100;$$

where OD_{treated} and OD_{control} correspond to the optical densities of the treated and the control cells, respectively. In each case two independent experiments were carried out with 4–8 parallel measurements. The 50% inhibitory concentration (IC₅₀) values were determined from the dose-response curves. The curves were defined using Microcal™ Origin1 (version 6.0) software.

4.3 Stability of **3h** in aqueous buffers and rat plasma

The hydrolytic stability of **3h** was first evaluated in aqueous buffers at pH 7.4, 5.0, and 3.0 as follows: 20 µL of stock solution of **3h** in dimethyl sulfoxide (0.15 µmol/mL) was added to 980 µL of 100 mM buffers (phosphate for pH 3 and 7 and acetate buffer for pH 5) yielding 3 nmol/mL solutions. Samples of the individual solutions were analyzed for the content of **3h**, ciprofloxacin and formylciprofloxacin at predetermined time intervals up to 48 h. The experiment was performed in triplicate.

For the determination of the stability of **3h** in rat plasma, 20 μL of the above stock solution of **3h** was added to 980 μL of rat plasma, yielding 3 nmol/mL concentrations of **3h**. At predetermined time intervals, 100 μL plasma samples were taken and precipitated by the addition of 100 μL acetonitrile. The sample was vortexed for 30 s and centrifuged at 10,000 rpm for 5 min. Then, 150 μL of the supernatant was transferred into a glass insert and analyzed for the content of **3h**, ciprofloxacin and formylciprofloxacin. The experiment was repeated six times (three times up to 48 h and three experiments were prolonged to 96 h). The recovery of the extraction procedure was determined in triplicate at the same concentrations as used in the experiment.

HPLC: The stability of **3h** was determined by HPLC using a Shimadzu Prominence (Kyoto, Japan) instrument consisting of LC-20AD pumps with DGU-20A3 degasser, SIL-20A HT autosampler, CTO-20AC column oven, SPD-M20A diode array detector, RF10AXL fluorescence detector and CBM-20A communication module. The data were analyzed using LC solutions 1.22 software.

For the determination of the stability of **3h** in aqueous buffers, a simple isocratic method using 20% acetonitrile in 50 mM phosphate buffer pH 2.0 as a mobile phase at a flow rate 2.5 mL/min and a monolithic Chromolith Performance column (RP-18e 100-4.6 mm, Merck, Darmstadt, Germany) with the same precolumn (RP-18e 10-4.6 mm) maintained at 30 °C was employed to separate **3h** from its putative metabolites ciprofloxacin and formylciprofloxacin. The compounds were detected by both UV at 280 nm (scanned from 230 to 350 nm) and fluorescence (excitation/emission set at 276/442 nm).¹⁵ Fluorescence was used for quantification. The retention times of ciprofloxacin, **3h** and formylciprofloxacin were 1.1, 3.8 and 4.8 min, respectively. The length of the analysis was 5.5 min.

For the determination of the stability of **3h** in rat plasma, a gradient method was employed. Solvent A was 50 mM phosphate buffer pH 2.0 and solvent B was acetonitrile. The mobile phase contained 11% B for 3 min, 25% B for 4 min and 11% B for 3 min with total analysis time of 10 min. The column and precolumn and the detection conditions were the same as above.

The calibration curves were constructed by spiking the buffers or plasma with known amounts of the analytes at the concentration levels from 0.1 to 5 nmol/mL. Both methods were

validated and were within the acceptance criteria for accuracy, precision and linearity recommended by the FDA Guidance for Industry for Bioanalytical Method Validation (2001).

Acknowledgements

This work was financially supported by the Research project MSM 0021620822, IGA NS 10367-3, by grants from the Hungarian National Science Fund (OTKA 68358) and National Office for Research and Technology (NKFP_07_1-TB_INTER-HU). The financial support from the Slovenian Research Agency (projects P1-0230-103 and BI-CZ/10-11-005) is also acknowledged. We would like to thank Dr. Bogdan Kralj and Dr. Dušan Žigon (Mass Spectrometry Center, Jožef Stefan Institute, Ljubljana, Slovenia) for recording the mass spectra. Dr. Zsolt Datki (Department of Medical Chemistry, University of Szeged, Szeged, Hungary) is acknowledged for a kind donation of SH-SY5Y human neuroblastoma cell line.

References

¹ Global tuberculosis control: a short update to the 2009 report, WHO Library Cataloguing-in-Publication Data, ISBN 978 92 4 159886 6.

http://www.who.int/tb/publications/global_report/2009/pdf/full_report.pdf

² The Stop TB Strategy, WHO.

http://whqlibdoc.who.int/hq/2006/WHO_HTM_STB_2006.368_eng.pdf

³ Vinšová, J.; Krátký, M. Drug-Resistant Tuberculosis: Causes, Diagnosis and Treatments; Nguy, S., K'ung, Z., Eds.; Nova Publishers: New York, 2009; Chapter. 2.

⁴ Sriram, D.; Yogeewari, P.; Devakaram, R. V. *Bioorg. Med. Chem.* **2006**, *14*, 3113.

⁵ Saraiva, M. F.; de Souza, M. V. N.; Tran Huu Dau, M. E.; Araújo, D. P.; de Carvalho, G. S. G.; de Almeida, M. V. *Carbohydr. Res.* **2010**, *345*, 761.

⁶ Bedia, K. K.; Elcin, O.; Seda, U.; Fatma, K.; Nathaly, S.; Sevim, R.; Dimoglo, A. *Eur. J. Med. Chem.* **2006**, *41*, 1253.

⁷ Eswaran, S.; Adhikari, A. V.; Pal, N. K.; Chowdhury, I. H. *Bioorg. Med. Chem. Lett.* **2010**, *20*, 1040.

⁸ Vinšová, J.; Imramovský, A.; Jampílek, J.; Monreal, J. F.; Doležal M. *Anti-Infective Agents in Medicinal Chemistry* **2008**, *7*, 1.

⁹ Nayyar, A.; Malde, A.; Coutinho, E.; Jain, R. *Bioorg. Med. Chem.* **2006**, *14*, 7302.

-
- ¹⁰ Pelttari, E.; Karhumaki, E.; Langshaw, J. *Zeitschrift fur Naturforschung C-A Journal of Biosciences* **2007**, *62*, 483.
- ¹¹ Imramovský, A.; Polanc, S.; Vinšová, J.; Kočevár, M.; Jampílek, J.; Rečková, Z. Kaustová, *Bioorg. Med. Chem.* **2007**, *15*, 2551.
- ¹² Košmrlj, B.; Koklič, B.; Polanc, S. *Acta Chim. Slov.* **1996**, *43*, 153.
- ¹³ Ali, M. A.; Yar, M. S. *Med. Chem. Res.* **2007**, *15*, 463.
- ¹⁴ <http://www.taacf.org/Process-text.htm>
- ¹⁵ De Smet, J.; Boussery, K.; Colpaert, K.; De Sutter, P.; De Paepe, P.; Decruyenaere, J.; Van Bocxlaer, J. *J. Chromatogr. B* **2009**, *877*, 961.
- ¹⁶ Vybíralová, Z.; Nobilis, M.; Zoulová, J.; Květina, J.; Petr, P. *J. Pharm. Biomed. Anal.* **2005**, *37*, 851.
- ¹⁷ Miyamoto, H.; Ueda, H.; Otsuka, T.; Aki, S.; Tamaoka, H.; Tominaga, M.; Nakagawa, K. *Chem. Pharm. Bull.* **1990**, *38*, 2472.
- ¹⁸ Sula, L. *Bull. World Health Organ.* **1963**, *29*, 589.
- ¹⁹ Sula, L.; Sundares, T. K. *Bull. World Health Organ.* **1963**, *29*, 607.
- ²⁰ Vinsova, J.; Cermakova, K.; Tomeckova, A.; Ceckova, M.; Jampilek, J.; Cermak, P.; Kunes, J.; Dolezal, M.; Staud, F. *Bioorg. Med. Chem.* **2006**, *14*, 5850.
- ²¹ Jensen, K. A. *Zentralb. Bakteriolog. Parasitenkd. Infektionskr. Hyg. Abt. I Orig.* **1932**, *125*, 222.
- ²² Löwenstein, E. *Zentralb. Bakteriolog. Parasitenkd. Infektionskr. Hyg. Abt. I Orig.* **1931**, *120*, 127.
- ²³ Jurcevic, S.; Hills, A.; Pasvol, G.; Davidson, R. N.; Ivanyi, J.; Wilkinson, R. J. *Clin. Exp. Immunol.* **1996**, *105*, 416.
- ²⁴ Knowles, B. B.; Aden, D. U.S. Patent 4,393,133, 1983.
- ²⁵ Knowles, B. B.; Howe, C. C.; Aden, D. P. *Science* **1980**, *209*, 497.
- ²⁶ Biedler, J. L.; Helson, L.; Spengler, B. A. *Cancer Res.* **1973**, *33*, 2643.
- ²⁷ Biedler, J. L.; Roffler-Tarlov, S.; Schachner, M.; Freedman, L. S. *Cancer Res.* **1978**, *38*, 3751.
- ²⁸ Slater, T. F.; Sawyer, B.; Sträuli, U. *Biochim. Biophys. Acta* **1963**, *77*, 383.
- ²⁹ Mosmann, T. *J. Immunol. Methods* **1983**, *65*, 55.
- ³⁰ Liu, Y. B.; Peterson, D. A.; Kimura, H.; Schubert, D. *J. Neurochem.* **1997**, *69*, 581.
- ³¹ Altman, F. P. *Prog. Histochem. Cytochem.* **1976**, *9*, 1.

³² Denizot, F.; Lang, R. J. *Immunol. Methods* **1986**, 89, 271.

CV

Curriculum Vitae

Eva Vavříková

Birth date: 19.07.1982

Marital status: single

Address: Zálešná II/3411, 760 01, Zlín

Tel: +420 732 742 733

Email: eva.vavrikova@faf.cuni.cz

EDUCATION

2006-present - Charles University in Prague, Faculty of Pharmacy, Hradec Králové, Czech Republic

Presently Ph.D. study at Department of Organic and Inorganic Chemistry, specialization Bioorganic Chemistry.

Concerned in research of substituted hydrazones and polysaccharide chitosan as prodrugs against *Mycobacterium tuberculosis*.

2004-2006 - University of Pardubice, Faculty of Chemical Technology, Pardubice

Mgr. - specialization Analysis of biological materials. Diploma thesis: Derivatization of Schizophyllane with Reactive Fluorescence Dyes.

2001-2004 - University of Pardubice, Faculty of Chemical Technology, Pardubice

Bc. - specialization Clinical biology and chemistry

1997-2001 - Grammar school, Zlín

Courses and Scholarships:

1. 29. 1. – 2. 2. 2007, Interpretation of Infrared Spectra Course, Prague, Czech Republic. Organizer: Jan Marek Marci Spectroscopic Society – finished with certificate.
2. 11. - 16. 11. 2007, Modern problems in NMR spectroscopy, Pec pod Sněžkou, Czech Republic. Organizer: Charles University, Faculty of Mathematics and Physics
3. 22. - 26. 9. 2008, School of mass spectroscopy, Seč, Czech Republic. Organizer: Jan Marek Marci Spectroscopic Society and University of Pardubice – finished with certificate.

International Fellowships

1. 01/2010-02/2010 Program of Fond mobility, Eötvös Lóránd University in Budapest, Research Group of Peptide Chemistry, Hungarian Academy of Science

(Hungaria).

2. 10/2008-02/2009 Program of Europe Union "Contact", University of Ljubljana, Faculty of Chemistry and Chemical Technology (Slovenia).

PUBLICATIONS

1. Vinsova, J.; Vavrikova, E.: Recent Advances in Drugs and Prodrugs Design of Chitosan. *Current Pharmaceutical Design*. 2008, vol 14, p 1311 – 1326.
2. Vavříková, E.; Vinšová, J.: Chitosan a jeho farmaceutické aplikace. *Chemické Listy*. 2009, vol 103, p 56-65.
3. Férriz, J. M.; Vávrová, K.; Kunc, F.; Imramovský, A.; Stolaříková, J.; Vavříková, E.; Vinšová, J.: Salicylanilide carbamates: Promising antitubercular agents active against multidrug resistant *Mycobacterium tuberculosis* strains. *Bioorganic and Medicinal Chemistry*. 2009, vol 18, p 1054-1061.
4. Vavříková, E.; Mandíková, J.; Trejtnar, F.; Horváti, K.; Bösze, S.; Stolaříková, J.; Vinšová, J.: Cytotoxicity decreasing effect and antimycobacterial activity of chitosan conjugated with antituberculous drugs. *Carbohydrate Polymers*. 2010, under revision.
5. Vavříková, E.; Polanc, S.; Horváti, K.; Bösze, S.; Stolaříková, J.; Vávrová, K.; Vinšová, J.: New fluorinated hydrazones as potential antitubercular drugs. *Bioorganic Medicinal Chemistry*. 2010, under revision.

ABSTRACTS OF CONFERENCE

1. Vavříková, E.; Vinšová, J.; Polanc, S.; Férriz, J. M.; Imramovský, A.: Preparation of new hydrazonoformamide derivatives of isoniazid. *Farmaceutski vestnik*. 2007, vol 58, p 202. 5th Joint Meeting on Medicinal Chemistry. Portorož, Slovenia, 17. - 21. 6. 2007. (poster)
2. Férriz, J. M.; Vinšová, J.; Imramovský, A.; Vavříková, E.: Synthesis of salicylanilide esters prodrugs form. *Farmaceutski vestnik*. 2007, vol 58, p 91. 5th Joint Meeting on Medicinal Chemistry. Portorož, Slovenia, 17. - 21. 6. 2007. (poster)
3. Férriz, J. M.; Vinšová, J.; Imramovský, A.; Vavříková, E.: Preparation and antimycobacterial activity of hydrazonoformamide derivatives of isoniazid. *Chemické zvesti*. 2007, vol 1/3, p 196. 59. zjazd chemikov. Tatranské Matliare, Slovensko, 2. – 6. 9. 2007. (poster)
4. Férriz, J. M.; Vinšová, J.; Imramovský, A.; Vavříková, E.: Synthesis and antimycobacterial activity evaluation of salicylanilide derivatives. *Zborník*. 2007, p 99. 36. konferencia Syntéza a analýza liečiv. Bratislava, Slovensko, 11. – 13. 9. 2007. (poster)
5. Vavříková, E.; Vinšová, J.; Polanc, S.; Férriz, J. M.; Imramovský, A.: Příprava nových hydrazonoformamidových derivátů isoniazidu. *Zborník*. 2007, p 139. 36. konferencia Syntéza a analýza liečiv. Bratislava, Slovensko, 11. – 13. 9. 2007.

(poster)

6. Vinšová, J.; Vavříková, E.: Chitosan a jeho farmaceutické aplikace. *Zborník*. 2007, p 16. 36. konferencia Syntéza a analýza liečiv. Bratislava, Slovensko, 11. – 13. 9. 2007. (lecture)
7. Vinšová, J.; Vavříková, E.: Farmaceutické aplikace chitosanu. *Chemické Listy*. 2007, vol 101, p 978-978. 42. Konference Pokroky v organické, bioorganické a farmaceutické chemii. Nymburk, 16. – 18. 11. 2007. (lecture)
8. Vavříková, E.; Vinšová, J.: Chitosan jako prodrug forma isoniazidu. *Chemické Listy*. 2008, vol 5, p 400. VIII. Mezioborové setkání mladých biologů, biochemiků a chemiků pořádané firmou Sigma – Aldrich. Devět skal – Žďárské vrchy, 10. – 13. 6. 2008. (poster)
9. Vavříková, E.; Vinšová, J.; Nový, Z.: Modifikované formy chitosanu ve spojení s isoniazidem. *Chemické Listy*. 2008, vol S, p s253. 37. Konference Syntéza a analýza léčiv. Brno, 8. – 10. 9. 2008. (poster)
10. Vavříková, E.; Vinšová, J.; Polanc, S.; Ferriz, J. M.; Imramovský, A.: Synthesis and antimycobacterial activity of new hydrazonoformamide derivatives of isoniazid. *Book of abstracts*. 2008, p 289. XXth International Symposium on Medicinal Chemistry. Vienna, Austria, 31. 8. – 4. 9. 2008. (poster)
11. Vavříková, E.; Vinšová, J.: Chitosan like prodrug form of isoniazide. *DVD of abstracts*. 2008. 2nd European Chemistry Congress. Torino, Italy, 16. – 20. 9. 2008. (poster)
12. Vavříková, E.; Vinšová, J.: Chitosan carrier of antituberculous drugs. *Book of abstracts*. 2009, p 180. Joint Meeting on Medicinal Chemistry. Budapest, Hungary, 24. – 27. 6. 2009. (poster)
13. Vavříková, E.; Vinšová, J.; Mandíková, J.; Stolaříková, J.: Vliv chitosanu na antimykobakteriální účinek a toxicitu isoniazidu. *Chemické Zvesti*. 2009, p 183. 61. zjazd chemikov. Tatranské Matliare, Slovensko, 7. – 11. 9. 2009. (poster)
14. Vavříková, E.; Vinšová, J.; Mandíková, J.; Stolaříková, J.: Nová antituberkulózní proléčiva na bázi chitosanu. *Sborník*. 2009, p 159. 38. Konference Syntéza a analýza léčiv, Hradec Králové, 14. – 16. 9. 2009. (poster)
15. Vavříková, E.; Vinšová, J.; Mandíková, J.; Stolaříková, J.: Chitosan coupling with antituberculous drugs. *Book of abstracts*. 2009, p 41. 6th Meeting of the European Network of Doctoral Studies in Pharmaceutical Sciences. Palermo, Italy, 16 - 18. 11. 2009. (lecture).

GRANTS (principal researcher)

Grant agency of Charles University: GAUK 76807/2007 Modelování a syntéza proléčiv antituberkulózní aktivních sloučenin

Ministry of Education of the Czech Republic: FRVŠ 92/2009 G6 Chitosan jako prodrug forma vybraných antituberkulózní

